DISSERTATION

CHARACTERIZATIONS OF CHROMOSOME ABERRATIONS, TELOMERE DYSFUNCTION, AND RADIOSENSITIVITY SIGNATURES IN CANINE CANCER CELL LINES

Submitted by

Junko Maeda

Graduate Degree Program in Cell and Molecular Biology

In partial fulfillment of the requirements

For the Degree of Doctor of Philosophy

Colorado State University

Fort Collins, Colorado

Summer 2015

Doctoral Committee:

Advisor: Takamitsu Kato

Joel Bedford
Susan Bailey
Douglas Thamm

ABSTRACT

CHARACTERIZATIONS OF CHROMOSOME ABERRATIONS, TELOMERE DYSFUNCTION, AND RADIOSENSITIVITY SIGNATURES IN CANINE CANCER CELL LINES

Cancer is now a leading cause of death in dogs as well as in humans due to longer life spans resulting from advances in nutrition and veterinary medicine, and the higher expectations of pet owners. Companion dogs share environmental influences with humans and spontaneously develop tumors with histopathologic and biologic behavior similar to tumors that occur in humans. Therefore, canine cancer research has much potential to benefit both dogs and humans.

Cancer cell lines have been widely used as *in vitro* experimental model systems and have proven to be useful for exploring the underlying biology of cancer. Canine cancer cell lines have increasingly been developed and utilized, but are not as fully characterized as human cell lines. In this thesis, we characterized canine cancer cell lines by examining: 1) chromosome aberrations, long appreciated as valuable biomarkers of carcinogenesis; 2) telomeres, chromosomal features with important implications for both aging and cancer; and 3) cellular radiosensitivity signatures, critical for evaluating individual response to radiation therapy. Such characterization of canine cancer cell lines will provide a better understanding of underlying canine cancer biology and provide new insights into improved clinical management, such as development of novel therapeutic targets and identification of radiation sensitivity markers, not only for dogs, but of potential relevance for humans as well.

First, we investigated chromosome and telomere aberrations in canine osteosarcoma (OSA) cell lines, a common primary bone tumor in both humans and dogs. Previously, malignant canine cancer cells have been reported to exhibit metacentric chromosomes (morphologically irregular chromosomes for canines) in a range of canine tumors including osteosarcoma. The metacentric chromosomes, which likely represent end-to-end chromosomal fusion events (Robertsonian translocations), may reflect telomere dysfunction, leading us to hypothesize that chromosome aberrations involving uncapped telomeres may be a common feature of canine OSA cells. Eight established canine OSA cell lines were evaluated; chromosome number and frequency of metacentric chromosomes were determined in metaphase spreads. Using fluorescence *in situ* hybridization (FISH) with a telomere specific probe, the contribution of dysfunctional telomeres was characterized. We also assessed telomere associated factors including telomerase activity, co-localization of DNA damage and telomere signals (telomere-dysfunction induced foci, TIFs), and expression of a DNA repair protein shown to be required for mammalian telomeric end-capping function, specifically the DNA-dependent protein kinase catalytic subunit (DNA-PKcs). Despite variable chromosome numbers, proliferation rates and radiosensitivities, all eight canine OSA cell lines displayed increased numbers of metacentric chromosomes and exhibited numerous telomere aberrations including interstitial telomeric signals and telomere fusions (telomere signals at the point of fusion, in this case in the centromeric regions). D17, the oldest canine OSA cell line used in the study, showed the highest frequency of telomere aberrations (51.4 per cell) and metacentric chromosomes (43.2 per cell). Furthermore, the cell lines were all telomerase positive and showed no correlations between their telomere aberrations and the other telomere associated factors analyzed. To better characterize the telomere dysfunction associated with canine OSA, we investigated telomere aberrations in primary cultures from ten spontaneous canine OSAs, as well

as the effects of long-term culture. Seven of the primary samples displayed no increase in frequency of metacentric chromosomes, while three of the samples did have elevated levels (11.5 per cell in the highest primary culture); however, no telomere signals were present at the involved centromeric regions. Telomere aberrations were observed in all of the primary cultures, but the number was small (1.87 per cell in the highest primary culture). Interestingly, we found that metacentric chromosome frequencies increased in one primary OSA culture with increasing passage in culture. In contrast, metacentric chromosomes did not accumulate with long-term culture of non-cancerous canine fibroblasts, or DNA repair deficient mouse fibroblasts (homozygous ataxia telangiectasia mutated (ATM) gene deficiency). Together, these results suggested that metacentric chromosomes and telomere dysfunction of are characteristics of canine OSA. Therefore, targeting of these unique telomere aberrations has potential for both improving diagnosis of canine OSA, as well as development of novel treatment strategies.

Lastly, we investigated radiosensitivity in a panel of canine cancer cell lines representing different cancer types. A human cancer cell line panel, NCI-60, consisting of different tumor types has been successfully utilized for *in vitro* anticancer drug screening, demonstrating the utility of such an approach in understanding cancer mechanisms; gene expression profiling and variable radiosensitivities facilitated development of informative markers regardless of tumor tissue type. A canine cancer cell line panel, called the ACC30, was recently developed at the Flint Animal Cancer Center (FACC), Colorado State University and includes microarray gene expression data. We aimed to test the hypothesis that identification of the determinants of response to ionizing radiation in the diverse canine cancer cell lines would provide additional information, some possibly specific to dogs, and some potentially supplementing those reported for human cancer. We obtained 27 canine cell lines derived from ten tumor types from the ACC30 panel. First,

radiosensitivity was determined using a clonogenic assay for adherent cell cultures, or a limiting dilution assay for suspension cell cultures. The 27 cell lines had varying radiosensitivities regardless tumor type (survival fraction at 2 Gy, SF2= 0.2–0.9). Based on the cellular characteristics analyzed in this study, there was a moderate correlation between radioresistance and better plating efficiency in the 27 cell lines. Next, we selected the six most radiosensitive cell lines as the radiosensitive group and the five most radioresistant cell lines as the radioresistant group. Then, we evaluated known parameters for cell killing by ionizing radiation (IR) including IR-induced DNA double strand break (DSB) repair and apoptosis, in the radiosensitive group as compared to the radioresistant group. However, the two groups were not distinguished by these parameters. Further, we investigated a possible common radiosensitivity signature using the basal gene expression profiling of the ACC panel for 20,000 genes. More than 550 genes were identified as being differentially expressed between the radiosensitive and radioresistant groups. Gene set enrichment analysis was used to inform potential pathways and functions involving the differentially expressed genes and indeed, several biological processes including cell adhesion, cell migration and apoptosis were related to radiosensitivity in the canine cancer cell lines. In support of our findings, cell adhesion was one of the signatures previously identified in the human microarray analysis. Together, our results suggest that cell adhesion related genes, rather than the more commonly regarded radiosensitivity associated apoptosis and DNA repair related genes, may provide beneficial radiosensitivity biomarkers for predicting individual response to radiotherapy, regardless of tumor type. Thus, the radiosensitivity signatures characterized here may help guide future development of intrinsic tumor radiosensitivity biomarkers for predictive assays in canine cancer, and has the potential to improve predicting radiosensitivity in human cancer as well.

ACKNOWLEDGEMENTS

I would like to start by first thanking the members of my graduate committee: Dr. Takamitsu Kato, Dr. Susan Bailey, Dr. Joel Bedford, and Dr. Douglas Thamm for their help and guidance throughout the project. I would especially like to thank my advisor Dr. Takamitsu Kato for his support, encouragement, and guidance over the last four years, without whom, none of the work would have been possible.

I would also like to thank all the lab members in the Kato lab. In particular, I would like to thank Colleen Brents, Coral Froning, Erica Roybal, Garret Phoonswadi and Garret Rota for the effort, time and energy they have committed to the completion of this project. I would like to thank Dr. Ian Cartwright for his previous support in Dr. Kato's lab.

A special thanks to Dr. Hatsumi Nagasawa and Barbara Rose for their help on the cell culture experiments.

Lastly, I would like to thank the faculty and staff of the Department of Cell and Molecular Biology, Environmental Radiological Health Sciences and Flint Animal Cancer Center. Especially I would like to thank Dr. Rodney Page and Dr. Stephen Withrow who gave me the opportunity to challenge this program in the United States. I would like to thank the Morris Animal Foundation for their generous support that provided funding for my Ph.D. studies.

TABLE OF CONTENTS

CHAPTER 1

INTRODUCTION

Canine cancer

Overview

Cancer is a major cause of death in dogs. In a study from necropsy data in the United States, cancer accounts for 23% of all deaths in dogs (Bronson, 1982). This is very similar to humans where one in four deaths is due to cancer (Siegel et al., 2014). The high population at risk highlights the importance of cancer in dogs. According to a 2013-2014 survey, approximately 43% of all households in the United States own a total of 83 million pet dogs (America Pet Products Association, 2014). More importantly, 63% of those dogs are regarded as a family member by their owners (U.S. Pet Ownership Statistics, 2012). It is estimated that the prevalence of cancer in dogs has increased over the last several decades (Dobson et al., 2002, Merlo et al., 2008). Advances in the care of companion dogs have allowed dogs to live longer due to better nutrition, vaccination for common infectious diseases and diagnostic methods and higher expectation of pet owners (Dobson et al., 2002, Paoloni and Khanna, 2007). This has resulted in an increase in age-related disease including cancer (Adams et al., 2010).

Dogs develop tumors spontaneously, and they are histologically and anatomically similar to human tumors (Figure 1.1) (Vail and MacEwen, 2000, Dobson et al., 2002). In reported data, common tumor types diagnosed in pet dogs consist of mammary carcinoma, skin cancer, melanoma and lymphoma (Vail and MacEwen, 2000, Bronden et al., 2007). It is important to note that the rates of certain tumor types, like osteosarcoma (OSA) and soft tissue sarcoma are

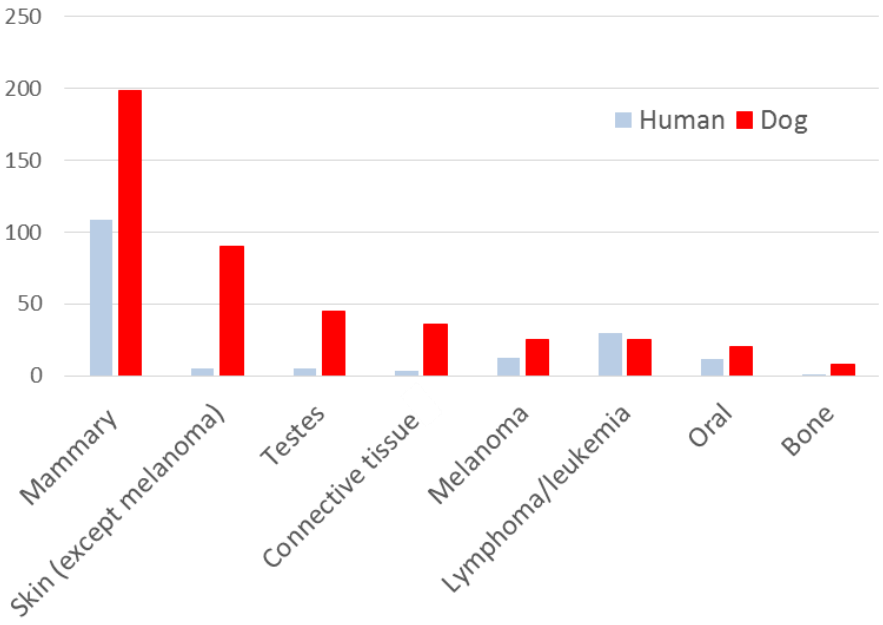

Figure 1.1: *Common cancer types in dogs and their annual incidence rates (per 100,000 at risk).* The data in dogs is based on a study in 1976. Both human and dog data are adapted from Vaile et al., 2000.

significantly higher in dogs than in humans, and some primary cancers in humans, predominantly prostate, gastrointestinal and lung carcinomas, are less common in dogs (Dobson et al., 2002, Siegel et al., 2014). The treatment options for pet dogs include surgery, radiation therapy and chemotherapy (Paoloni and Khanna, 2008, Withrow, 2007). Common human treatment methods are frequently chosen for cancer in pet dogs because the owner is motivated by prolonging the quality of their pet's life.

Canine Cancer as Models of Human Cancer

Cancer is a complex genetic disease and remains one of the most serious diseases in humans despite remarkable progress in cancer research (Siegel et al., 2014). That motivates extended research of the biology underlying cancer. Mouse models for various tumors have been developed using transgenic or knockout mice or xenograft techniques, and have provided effective in improving understanding of tumor biology (Politi and Pao, 2011, Sharpless and Depinho, 2006, Voskoglou-Nomikos et al., 2003). In contrast, dogs spontaneously develop cancer similar to that in humans. Canine cancer models have emerged as valuable resources in the study of human cancer (MacEwen 1990). Malignancies that have shown particular relevance as oncological models include OSA, non-Hodgkin's lymphoma, hemangiosarcoma, prostate carcinoma, lung carcinoma, mammary carcinoma, malignant melanoma, soft tissue sarcomas and bladder carcinoma (Porrello 2006, Paoloni 2007).

Human and canine cancers have similar characteristics such as anatomical and histopathological appearance, biological behavior, tumor genetics and response to conventional therapies (Paoloni and Khanna, 2007, MacEwen, 1990). Pet dogs share the same environment as their owners, and might help epidemiological studies of human cancers (MacEwen, 1990). Depending on the breed, dogs age five- to eight- fold faster than do humans (America Pet Products

Association, 2014). The most recently available data shows that the median age at death for a dog was 11 years and 3 months (Adams et al., 2010). Therefore, progression rates of tumors in dogs generally exceeds the typical rate observed in humans, which allows for rapid accrual of data to analyze (MacEwen, 1990, Hansen and Khanna, 2004). Some cancers, such as lymphoma and OSA, have higher rates in dogs than humans, so this relative abundance increases their model potential (Vail and MacEwen, 2000, Paoloni and Khanna, 2008). Dogs are relatively inbred compared to humans, and many of canine cancers exhibit an increased prevalence in particular breeds of dogs, providing an opportunity to identify genes linked to cancer development or its progression (Dobson, 2013). In the United States, 45% of pet dogs are estimated to be >6years old, which is the human equivalent of >42 (U.S. Pet Ownership Statistics, 2012). This, coupled with their large population size (>80 million in the US), results in a cancer rate sufficient to power clinical trials, including the assessment of new drugs (Rowell et al., 2011). Furthermore, in the genomic era the dog genome was found more homologous in sequence conservation to humans than mice, making it a valuable model organism for genetic study (Lindblad-Toh et al., 2005, O'Brien and Murphy, 2003, Khanna et al., 2006). These factors highlight a direct translational relevance of canine cancer to human cancer, compared to other animal models.

The greatest impediment to the use of companion dogs as tumor models is the relative lack of species-specific investigational tools, including antibodies. Until recently, these tools, although abundant for human and rodent investigations, have lagged in availability for application to the canine species (Khanna et at., 2006). Furthermore, the canine genome sequence was recently completed in 2005 (Lindblad-Toh et al., 2005). Due to technology advances, high-throughput methodologies in dogs have become possible as used to interrogate human cancer (Paoloni and Khanna, 2008). As more canine specific tools and genome approaches become available, canine

cancer shows promise as a model for therapeutic developments relating to human cancer (Paoloni and Khanna, 2008).

An early example of the use of pet dogs as model systems was OSA in large dog breeds for an assessment of techniques to optimize limb-sparing surgical procedures intended to use on human patients in 1989-1993 (LaRue et al., 1989, Withrow et al., 1993). The body size of a dog is important for the model because that could not have been recreated in mouse models. In addition to skeletal models, there are other studies that have also relied on the size of dogs, such as the respiratory size for assessment of novel anticancer inhalation therapies in dogs (Khanna and Vail, 2003, Hershey et al., 1999). From early on, cancer in pet dogs have been used in controlled and focused preclinical trials in the development of new cancer drugs (Paoloni and Khanna, 2008).

Canine Osteosarcoma

Canine OSA displays a striking resemblance to human OSA in tumor biology and behavior (Withrow, 2007): it affects heavy individuals, is preferentially located in the long bones, has high metastatic rate (90% for dogs, 80% for humans), and has similar metastatic sites and radioresistance (Table 1.1). Despite the strong similarities between canine and human OSA, there are a few differences. The incidence of spontaneous disease in canine populations has been estimated to be approximately ten times higher than that in humans (13.9/100,000 in dogs and 1.02/100,000 in humans) (Mirabello et al., 2009, Rowell et al., 2011). Canine OSA affects older dogs, while human OSA affects children and adolescents (Withrow, 2007). The relationship between bone growth and OSA formation is thought to be due to an increased chance of rapidly growing cells to be damaged (Gelberg et al., 1997). However, the exact etiologies of OSA in both species are unknown.

Table 1.1: Comparative aspect of canine and human OSA*.

Variable	Dog	Human
Incidence in United States	>8000/yr**	2000/yr
Mean age	7 years	14 years
Race/breed	Large or giant purebreds	None
Gender	1.5:1 male: female	1.5:1 male: female
Site	77% long bones Metaphyseal	90% long bones Methaphyseal
Etiology	Generally unknown	Generally unknown
% histologically high grade	95%	85-90%
DNA index	75% aneuploid	75% aneuploidy
Metastatic rate without chemotherapy	90% before 1 year	80% before 2 years
Metastatic sites	Lung>bone>soft tissue	Lung>bone>soft tissue
Improved survival with chemotherapy	Yes (1 year survival 50% from 10%)	Yes (5 year survival 60% from 20%)
Radiosensitivity	Generally poor	Generally poor

*Adapted from Dernell et al, 2007.
**13.9 per 100,000 in dogs vs 1.02 per 100,000 in humans (Rowell et al., 2011)

Similar molecular and genomic alterations between human and canine OSA have been recently recognized and have provided the opportunity for dogs with cancer to lend additional insight into the biology of human cancer (Rankin et al., 2012, Mueller et al., 2007). Alkaline phosphatase (ALP) levels have been identified as a negative prognostic factor in both humans and dogs with OSA (Ehrhart et al., 1998, Morello et al., 2011). The following genes; PTEN (phosphatase and tensin homolog), RB1 (retinoblastoma), EZR (villin-2), MET (meschymal-epithelial transition factor), ERBB2 (v-erb-b2 erythroblastic leukemia viral oncogene homolog 2), TP53 (tumor protein 53), and Myc were candidate genes because dysregulation of these has been found in both human OSA and canine OSA (Mueller et al., 2007, Rankin et al., 2012, Thomas et al., 2009). On the other hand, no clinical significance for most of these genes could be identified (Mendoza et al., 1998, Selvarajah and Kirpensteijn, 2010). A few genes have been linked to the onset, progression and prognosis of OSA; RUNX2 (runt-related transcription factor 2), a member of the RUNX gene family, is a mediator of differentiation expressed at different stages of osteoblast development, has been focused as an OSA associated gene in both humans and dogs (Angstadt et al., 2012, Martin et al., 2011). Survivin, which is an IAP (inhibitor of apoptosis) family has been shown as a negative prognostic factor for both human and canine OSA (Shoeneman et al., 2012, Trieb et al., 2003). Furthermore, in a previous study using global gene expression, human and canine OSA were indistinguishable on the basis of global gene expression signatures (Paoloni et al., 2009). They also identified two genes, IL-8 (interleukin-8) and SLCIA3 (solute carrier family 1 (glial high affinity glutamate transporter)), which were consistently overexpressed in canine OSA and associated with poor outcome in human OSA (Paoloni et al., 2009).

Despite the increasing investigations of genomic alterations in both human and canine OSA, no consistent molecular marker linked to the treatment strategies or the prognostic factors of OSA in the both species has been found (Rankin et al., 2012, Gorlick and Khanna, 2010). Studies have shown that human OSA typically presents with highly chaotic karyotypes (Sandberg, 2002). Among the multiple chromosomal changes in OSA, no specific chromosome aberration has been found (Smida et al., 2010). This in part hinders the identification of the genomic alterations with biological significance in the disease or suggests that multiple complex molecular pathways appear to be involved in the pathogenesis of OSA. Canine OSA is also characterized by a high degree of genomic rearrangements, showing similar characteristics to human OSA (Thomas et al., 2009).

Cancer Cell Line Panel for Cancer Research

Cancer cell lines have been widely used as in vitro experimental model systems and have proved to be useful for exploring the underlying biology of cancer (Domcke et al., 2013). Currently, well characterized numerous human cancer cell lines are available in cancer research. The Broad-Novaritis Cancer Cell Line Encyclopedia (CCLE), for example, contains genomic profiles of around 1,000 cell lines that are used as models for various tumor types (Barretina et al., 2012). Studies that use many cancer cell lines are able to have a general overview for diversity of cancer. While genomic differences between cancer cell lines and tissue samples have been pointed out in several studies (Ertel et al., 2006, Gillet et al., 2011), a study using a panel of 47 ovarian cell lines found that the ovarian cell lines closely represented tumor samples based on large set of molecular profiles with some extent of pronounced differences in several cell lines (Domcke et al., 2013).

The United States National Cancer Institute (NCI) 60 cell line panel, developed for drug screening in the late 1980s, is the most widely characterized panel (Shoemaker, 2006). It represents the first cell-based drug screening model which consists of 59 cell line (formerly 60) derived from cancers of nine different human organs: leukemias, melanomas, and cancers of breast, central nervous system (CNS), colon, lung, ovarian, prostate, and renal origin (Shoemaker, 2006). Since 1990, this screening model was rapidly introduced, and 100,000 chemical compounds and natural product extracts have been tested for anticancer activity with the panel (Shoemaker, 2006). The NCI-60 has also been the subject of numerous genomic, proteomic, and other profiling studies (Reinhold et al., 2012). Recently, its role has expanded to be a research tool to assist in the identification of mechanisms of drug action and basic advances in understanding of cancer mechanisms (Lorenzi et al., 2006, Weinstein, 2006).

Canine cancer cell lines have progressively been developed and utilized, but are not as fully characterized as human cell lines. To our knowledge, there are a few studies that have investigated their biology by characterizations in a large number of cell lines (Legare et al., 2011). Recently, a canine cancer cell line panel, called the ACC (Animal Cancer Center) 30, was developed in the Flint Animal Cancer Center (FACC) at Colorado State University as the canine counterpart to the NCI-60. Gene expression and drug sensitivity data for six chemotherapeutics in the ACC30 have been investigated and utilized for the study predicting chemosensitivity in dogs (Fowles et al., 2014).

Cytogenetics Studies in Canine Cancer

History of Cytogenetics in Canine Research

Chromosome aberrations, a hallmark of cancer, have profound effects on carcinogenesis and been appreciated as variable biomarkers of it (Albertson et al., 2003). Cytogenetic studies have

a long history in analyzing the role of numerical and structural chromosome aberrations in cancer statuses. In the 1880s, human chromosomes were observed by Flemming and Arnold, following Gregor Mendel's suggestion of the existence of biological elements called genes (Trask, 2002). In the 1890s, mitotic aberrations and chromosomal aberrations in tumor cells were observed and proposed as their causative role in cancer (Rowley, 2001). The power of cytogenetic analyses became evident in the late 1960s after the development of banding protocols for the production of highly reproducible patterns of dark and light bands along the length of each chromosome (Caspersson et al., 1969). In the 1960s, the Philadelphia chromosome was discovered, which results from a translocation between chromosomes 9 and 22 and is a common observation in chronic myeloid leukemia (CML) (Nowell and Hungerford, 1960). Identification of the genes involved in the translocations (BCR-ABL fusion gene) allowed for a better understanding of cancer development and more importantly developed targeted therapy for CML (An et al., 2010). Following the initial discovery, molecular cytogenetic techniques have since been improved and provided a variety of method, such as comparative genomic hybridization (CGH), spectral karyotyping (SKY), and multicolor FISH (mFISH) (Pandita et al., 1999). As a result, extensive information has been obtained concerning the regions with chromosomal aberrations and genes involved in cancers.

Chromosome Aberrations in Cancer

Chromosomal alterations found in tumors have been historically grouped into three categories: primary changes with importance for initiating the tumor, secondary changes that contribute to the tumor progression, and background that have no specific function. Furthermore, it is generally accepted that recurrent chromosomal aberrations affect genes important for tumor development. The vast majority of clinically relevant chromosomal aberrations that have been

identified include copy-neutral reciprocal translocations, deletions and amplifications. These chromosome aberrations contribute to altered expression of tumor suppressor genes and oncogenes following inhibition or activation, respectively (Hastings et al., 2009, Mitelman, 2000, Albertson et al., 2003). The BCR-ABL fusion protein, resulting from the Philadelphia chromosome in CML, for example, constitutively activates the tyrosine kinase of the ABL proto-oncogene, leading to deregulated cell proliferation (An et al., 2010, McWhirter et al., 1993). Recurrent chromosomal translocations are typically detected in hematological malignancies (Rabbitts, 1994, Rowley, 1998), and a number of recent studies have also shown that they are linked to the pathogenesis of solid tumors, such as prostate cancer and non-small-cell lung cancer (Meyerson, 2007, Shaffer and Pandolfi, 2006). Aneuploidy, which refers to gain or loss of individual chromosome from the normal chromosome number, is frequently seen in solid tumors (Albertson et al., 2003) and has been associated with poor patient prognosis for a variety of carcinomas, including breast (Pinto et al., 2006), colon (Araujo et al., 2007), endometrial (Suehiro et al., 2008, Susini et al., 2007) and renal cell carcinomas (Pinto et al., 2005). In contrast, some sarcomas (e.g. OSA and malignant fibrous histiocytoma) often are characterized by the gross rearrangement of chromosomes. Their high degree of aneuploidy, amplification, and multiple unbalanced chromosomal rearrangements make it difficult to define biologically significant changes (Bayani et al., 2003, Helman and Meltzer, 2003). In these sarcomas, no specific chromosome aberrations that play an important role in tumor progression of OSA have been identified.

Chromosome Instability in Cancer

Chromosome instability (CIN) is known as a form of genetic instability in which the rates of gain or loss of chromosomes (whole or fragments) is elevated, producing an evolving and unstable karyotype (Thompson et al., 2010). This is caused by aberrant chromosome segregation

during mitosis, resulting from many known mechanisms, including centromere dysfunction, centromere amplification, defective spindle check-point control and telomere dysfunction (Bakhoum and Compton, 2012). Chromosome instability is considered to induce aneuploidy and gross chromosomal rearrangement and a frequent event in solid tumors like OSA (Albertson et al., 2003). It is important to note that not all aneuploidy exhibit CIN, like stable aneuploidy karyotypes found in hematological malignancies (Receveur et al., 2004). It has been suggested that CIN causes intra-tumor heterogeneity and is positively correlated with poor patient prognoses in several cancers (Burrell et al., 2013). The mechanisms that cause CIN in solid tumors are not well understood yet (Bakhoum and Compton, 2012). Deregulations in cell cycle checkpoint and caretaker genes, such as ATM (Ataxia Telangiectasia mutated) genes and TP53, combined with defective chromosomal segregation during mitosis through the several mechanisms have been considered as the underlying mechanism of CIN in cancer (Bakhoum and Compton, 2012, Storchova and Pellman, 2004). There is not strict evidence that CIN is necessary for carcinogenesis. On the other hand, because CIN is known as a characteristic of numerous cancer predisposition syndromes linked to DNA repair pathways, including Ataxia Telangiectasia (AT), familial breast cancer, Werner syndrome and Nijmegen breakage syndrome (Canman et al., 1998), it has been suggested that CIN provides some benefit to tumor evolution.

Cytogenetic Study in Canine Cancer

Within 10 years of determining the accurate number of chromosomes in humans to be 46, which included two copies of 17 metacentric autosomes (Tjio and Levan, 1956), five acrocentric autosomes, and a pair of sex chromosomes, the canine karyotype was determined (Gustavsson, 1964). Canine cytogenetic studies have been challenging due to the difficult karyotype of the dogs with 76 small acrocentric autosomes and two metacentric sex chromosomes (Selden et al., 1975,

Reimann et al., 1999). Attempts to establish an accepted karyotype have been complicated by the similar size and banding morphology of many of the smaller chromosomes. The existing reports have shown that the numerical changes and increased abnormal metacentric chromosome were found frequently, and that a higher incidence of these abnormalities was found in sarcoma and lipoma than epithelial neoplasms (Reimann et al., 1999). Canine OSA has consistently been characterized by bizarre and irregular karyotypes and marked aneuploidy, including increased numbers of metacentric chromosomes (Taylor et al., 1975, Thomas et al., 2007).

The chromosome identification using whole chromosome paint probes (Langford et al., 1996, Yang et al., 1999) and single-locus bacterial artificial chromosomes (BACs) (Breen et al., 1999) improved chromosome analysis in dogs. Despite improvement based on FISH techniques to identify canine chromosomes, canine chromosome analysis was still hindered by the smaller autosomes and limited availability of spectrally resolvable fluorochromes for 78 chromosomes. Recently, canine molecular cytogenetics has significantly advanced with the comparative genomic hybridization (CGH) technique, which provides a global assessment of chromosome number variations (Dunn et al., 2000). Clones from the BAC library have been applied to generate panels of chromosome-specific FISH probes, enable identify all dog chromosomes within a metaphase spread (Courtay-Cahen et al., 2007, Thomas et al., 2007). Also from this library, panels of BAC clones have been used for CGH (Thomas et al., 2003). Presently, a high resolution CGH array (1 Mb) has been developed and applied for many canine cancers (Thomas et al., 2008). In studies using canine OSA, a wide range of recurrent DNA copy number aberrations in canine OSA have been reported with several similar aberrations to those in previous reported human OSA, emphasizing the canine OSA as the valuable model of human OSA (Angstadt et al., 2011).

Telomere Aberrations in Cancer

Discovery of Telomeres and Telomerase

The unique features of the ends of chromosomes were first described in the 1930s, by Muller, who found that chromosome repair after radiation-induced double strand breaks (DSBs) never involved the end of the chromosomes in Drosophila (Muller, 1938) and named the end a "telomere". McClintock observed that broken chromosomes in maize frequently fuse to their sister chromatids, but normal chromosome ends do not (McClintock, 1938). These two scientists were the first to understand the importance of telomeres in the maintenance of chromosome integrity. After the discovery of DNA structure and semiconservative replication, the concept of the "end replication problem" emerged (Watson, 1972, Olovnikov, 1973). It was based on the inability of conventional DNA polymerases to replicate the very end of the chromosome, resulting in shortening of telomeres in each cycle of DNA replication. Both Watson and Olvnikov suggested that mechanisms to maintain telomere length must exist. Furthermore, since a limited number of cell divisions of cultured human fibroblasts was previously observed by Hayflick ("Hayflick limit") (Hayflick and Moorhead, 1961, Hayflick, 1965), shortening of telomeres was believed to explain the underlying mechanism.

The first molecular characterization was completed in the 1970s, when Blackburn and Gall discovered that telomeres of *Tetrahymerna thermophila* were comprised of the tandem repeated motif TTGGGG (Blackburn and Gall, 1978). After the discovery, the human telomere sequence, conserved throughout vertebrate biology, has been found to consist of TTAGGG repetitive sequences (Moyzis et al., 1988, Meyne et al., 1989). Telomerase, an enzyme that can elongate telomeres and hence resolve the end replication problem, was discovered by Greider and Blackburn (Greider and Blackburn, 1985). At last, detecting telomere length become available

using the size of telomere repeat fragments (TRFs) obtained by restriction enzyme digestion of the DNA. It was shown that telomere length was shorter in older individuals (Hastie et al., 1990) and with increased cell division (Harley et al., 1990). Since then, the study of telomeres has rapidly expanded into research for cancer and aging.

Role of Telomeres

The principle function of telomeres is capping the ends of linear chromosomes and maintaining genomic integrity. It has been described that telomere structure serves to protect the end of the chromosome from DNA degradation and fusion, and, importantly, to prevent it from being interpreted as a double-strand break (DSB) (Bailey, 2008). The telomere cap structure consists of a telomere sequence associated with a set of proteins that are collectively termed as "Shelterin" (de Lange, 2005). It has been previously shown by electron microscopy that telomeres form a loop structure (Griffith et al., 1999) (Figure 1.2). The telomere loop (T-loop) is a large duplex lariat structure formed by folding back the telomeric DNA into itself (Griffith et al., 1999). The single stranded 3' overhang located on the ends of telomeric DNA invades the double stranded telomeric DNA to form displacement loop (known as the D-loop) (Griffith et al., 1999, Wright and Shay, 2005). The proteins belonging to the shelterin complex are Telomeric Repeat Factor 1 (TRF1), Telomeric Repeat Factor 2 (TRF2), Protection of Telomeres 1 (POT1), TRF1-Interacting Nuclear Factor 2 (TIN2), TPP1, and Replication Associated Protein 1 (RAP1). The complex shelterin is important to maintain telomere end capping structure and function (de Lange, 2005) (Figure 1.2). In addition, DNA repair proteins, including proteins involved in DNA DSB repair, are also found at telomeric ends and play a role to maintain telomere (Blasco, 2005, Bailey and Murnane, 2006). The role of the DNA repair proteins at telomeres is still puzzling since telomeres are normally protected from DNA DSB repair (Bailey and Murnane, 2006). Another vital function

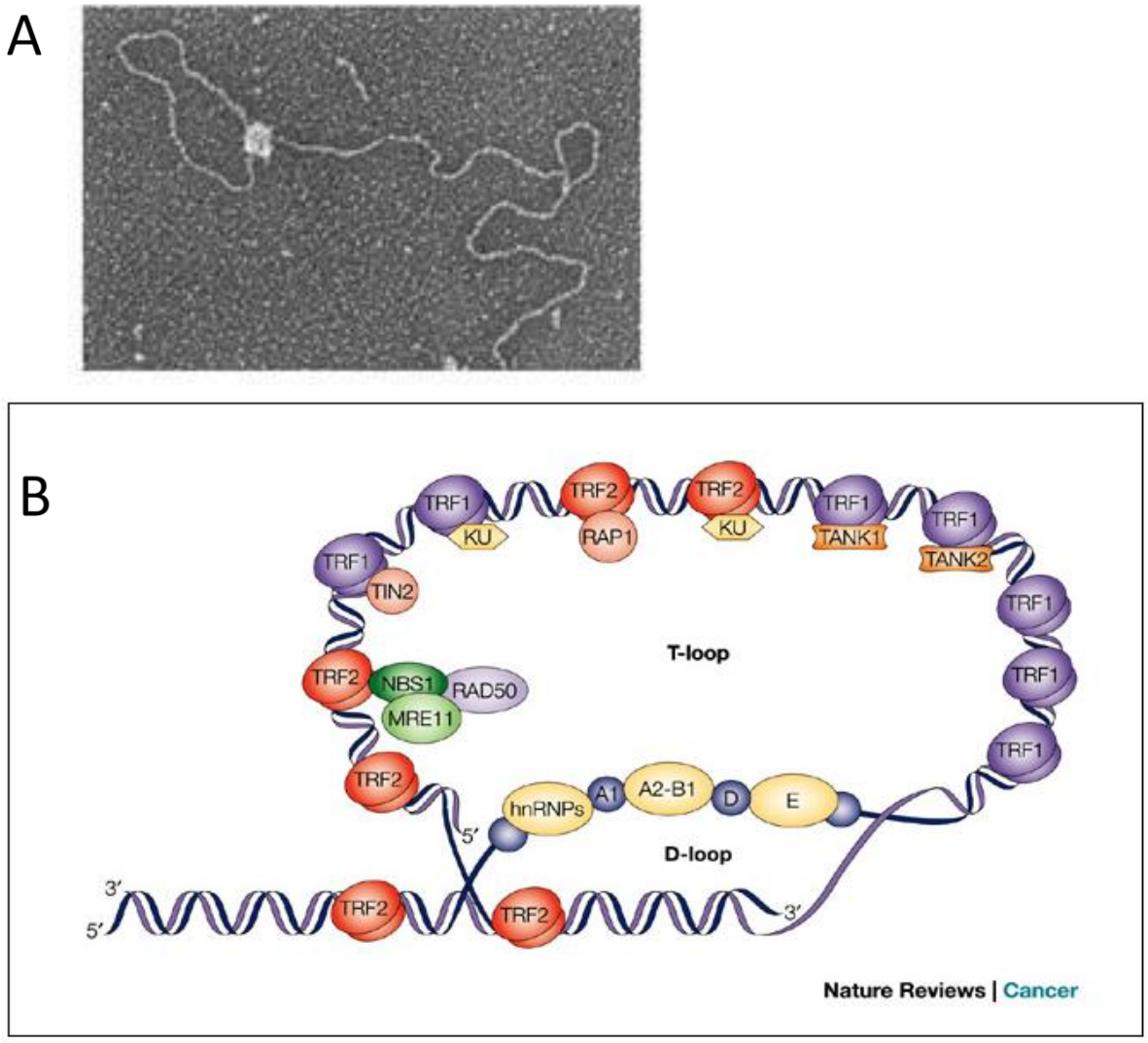

Figure 1.2: *T-loop structure of the telomeric 'cap'*. (A) T-loop structure of human telomere imaged by electron microscopy (Griffith et al., 1999). (B) The single-stranded portion of the 3' overhang of telomeric DNA folds into the double stranded DNA and forms a larger T-loop and smaller D-loop. (Neuman and Reddel, 2002).

of telomeres is to limit the lifespan of somatic cells, thus acting as tumor suppressor. In normal somatic cells, telomeres shorten with each cell cycle (approximately 50 to 200 base pairs) and causing cell senescence and apoptosis (Campisi, 1997). It has been shown that shortening telomeres to a critical length activates tumor suppressor proteins, p53 and p16, through DNA damage response and consequently p53-p21 and p16-pRB growth arrest pathways (Campisi, 2005, Kuilman et al., 2010). This point is referred to as the Hayflick limit or mortality stage 1 (M1) (Shay et al., 1993, Tlsty et al., 2001) (Figure 1.3). At the M1 stage, these cells stop dividing and enter the state of cell senescence. However, some cells bypass the M1 stage via inactivation of p53 and pRB pathways, and continue to divide with further decreasing telomere length (Tlsty et al., 2001, Shay et al., 1993). At the point when telomeres become dysfunctional, cells enter into the M2 stage or telomere crisis (Shay et al., 1993, Tlsty et al., 2001) (Figure 1.3). Progressive shortening and defects of telomere capping elicit chromosomal end-to-end fusions, and result in dicentric chromosomes and anaphase breakage-fusion-bridge (B/F/B) cycles, which lead to apoptosis and mitotic cell death (Greenberg, 2005). The two significant blockades, M1 and M2 have been postulated to inhibit normal cells transforming into cancerous cells (Campisi, 2005). In addition to the telomere shortening with cell division, the rate of shortening is influenced by several factors as reviewed by Lansdrop (Lansdorp, 2005), including oxidative stress and even psychological stress in humans (von Zglinicki, 2002, Epel et al., 2004).

Role of Telomerase

The enzyme telomerase consists of two core components: the catalytic telomerase reverse transcriptase (TERT), and the telomerase RNA component (TERC) that acts as a template for the synthesis of telomeric repeats, which together synthesize telomeric DNA (Meyerson et al., 1997, Harrington et al., 1997, Weinrich et al., 1997). Telomerase is only sufficiently active in human

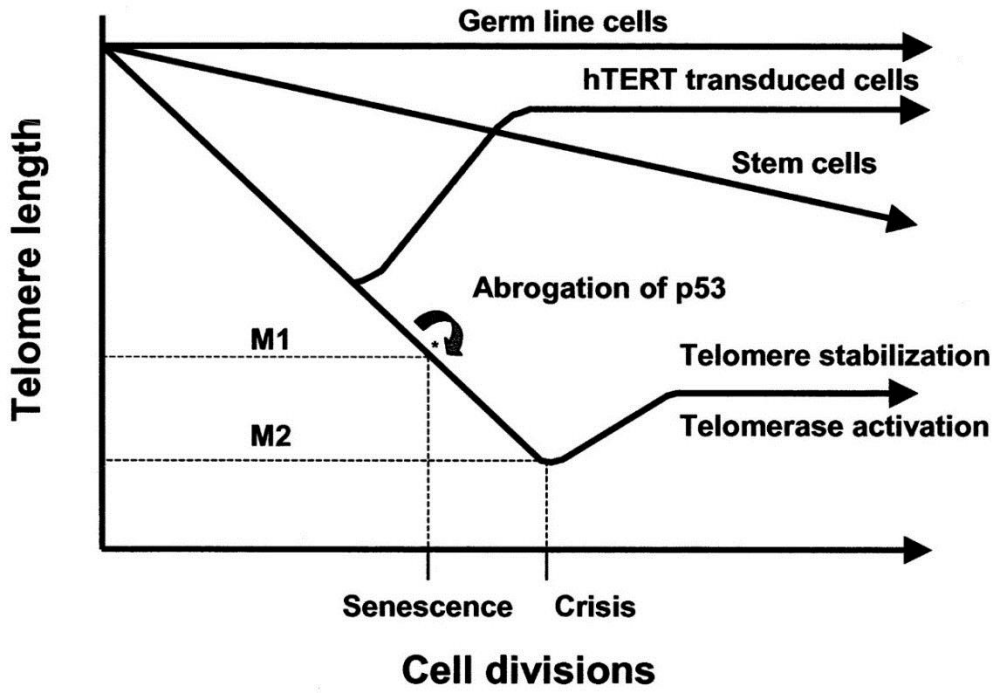

Figure 1.3: *Telomere shortening and M1 and M2 stage***.** Critically shortened telomeres may signals cells to enter the state of senescence at the Hayflick limit or M1 stage. Some cells are able to bypass the M1 stage via inactivation of p53 and pRB pathways. At the point when telomeres become dysfunctional, cells enter into the M2 stage or telomere crisis (Cong et al., 2002).

germ line and stem cells, being essentially inactive in most normal somatic human cells (Shay and Wright, 2011). It has been shown that hTERT (human TERT) is tightly regulated during cellular differentiation and is expressed at very low levels in normal human somatic cells, while hTERC (human TERC) is widely expressed in the majority of cell types, including those that are telomerase negative (Lopatina et al., 2003, Misiti et al., 2000). Therefore, this evidence has suggested that TERT serves as the major limiting agent for telomerase activity. Transfection of hTERT into human somatic cells extends the replicative lifespan, which is also evidence of the contribution of telomere shortening to cell senescence (Bodnar et al., 1998, Vaziri and Benchimol, 1998). It has been shown that hTERT expression also increase cell proliferation through Wnt/β-catenin signaling (Choi et al., 2008).

Cancer cells possessing the ability to bypass telomere-induced senescence must have a mechanism by which telomeres are maintained. In the vast majority of human tumors (approximately 90%), this is achieved by reactivation of the enzyme telomerase (Shay and Bacchetti, 1997, Kim et al., 1994). Typically, telomerase activation occurs late in tumorigenesis (Hackett and Greider, 2002). Some human tumor types that are telomerase negative can maintain their telomeres by an alternative mechanism known as alternative lengthening of telomeres (ALT) (Reddel et al., 2001). The differential expression of telomerase in cancer and normal cells makes it an attractive therapeutic target. Telomerase inhibitors for cancer patients are being investigated in human clinical trials. However, the existence of ALT and the efficacy delay remain important limitations to anti-telomerase therapy (Mokbel, 2003).

Telomere Biology in Dogs

Canine telomere biology is similar to that of humans and may fill the gap between human and murine animal model studies, as there are significant differences between mouse and human

telomere biology. The telomeres of mice are much longer than those of humans (40-60 kilo base pairs in mice versus 10-15 kilo base pairs in humans) (Moyzis et al., 1988). Telomerase is functionally active in most mouse somatic cells (Prowse and Greider, 1995), whereas telomerase activity is low or undetectable in many adult human somatic cells but present in germ cells, activated leukocytes and stem cells from a variety of organs (Kim et al., 1994). Furthermore, telomere shortening induces cell senescence in human somatic cells, while mouse cells lack a senescence checkpoint and immortalize spontaneously in culture (Todaro and Green, 1963). In contrast, dogs show parallels in telomere biology to humans in many respects. Telomere length is 12 to 23 kilo base pairs (Nasir et al., 2001), which is comparable to human length. Telomerase activity is absent in the somatic cells (Nasir et al., 2001), and telomere length decreases with age (McKevitt et al., 2002). The percentage of tumors with telomerase activity is 86% in human tumors and 92-95% in canine tumors (Biller et al., 1998, Yazawa et al., 1999, Kim et al., 1994). In addition, recent work has shown that both human and canine OSA display lower telomerase positivity relative to many other tumors. In human OSA, 32–44% are telomerase positive, were 73% of canine OSA (Ulaner et al., 2003, Sanders et al., 2004, Kow et al., 2008), again supportive of the shared telomere biology between two species.

Telomere Fusion in Cancer

Telomere fusion occurs when telomeres become dysfunctional either through excessive shortening (loss of sequence) or loss of end capping function (loss of structure) due to defects in the proteins that are associated with the shelterin complex (Frias et al., 2012, Bailey and Murnane, 2006). In subsequent cell divisions, the telomere fusion can trigger the anaphase breakage-fusion-bridge (B/F/B) cycles, and that fusion can lead to genomic arrangements of the type reflective of those frequently found in cancer (Frias et al., 2012). Altered function of various proteins of the

shelterin complex including TRF2, RAP1, and POT1 have shown to result in telomere fusion (van Steensel et al., 1998, Sarthy et al., 2009, Hockemeyer et al., 2006). It has also been shown that functional mammalian telomeres require the DNA-dependent protein kinase (DNA-PK), composed of a catalytic subunit (DNA-PKcs) and heterodimeric regulatory subunit (Ku70/Ku80), which are involved in DNA DSB repair (Bailey et al., 1999, Williams et al., 2009). In studies evaluating deficiencies in DNA-PKs, Ku70 and Ku80, dysfunctional telomeres also led to telomere fusion (Bailey and Murnane, 2006). Furthermore, DNA damage foci, such as phosphorylated histone, H2AX (γ-H2AX), were observed at the telomere uncapped by disruption of TRF2 in the telomere-dysfunction induced foci (TIFs) (Takai et al., 2003). The telomere-dysfunction induced foci also occur at dysfunctional telomeres resulting from loss of sequence, or in cancer cells (Nakamura et al., 2009, Herbig et al., 2004).

A study with mice has provided evidence that short dysfunctional telomeres can drive the earliest stages of cancer (Artandi et al., 2000). Tumors derived from terc-/- p53+/- mice contained high frequencies of telomere fusions. Recently, some reports using PCR-based techniques provided evidence that telomere fusions are present in human cancers, including breast cancer (Tanaka et al., 2012), chronic lymphocytic leukemia (CLL) (Lin et al., 2010), and sporadic colon cancer (Tanaka et al., 2014). These telomere fusions in breast cancer showed similar frequencies during early and later stages of breast carcinoma (Tanaka et al., 2012). In another study in colon cancer, telomere fusions were present in the early stages cancer regardless of either deficiency of p53 or the shortening of mean telomere length (Tanaka et al., 2014). From these studies, it has been proposed that telomere dysfunction may play a causal role in early carcinogenesis through a telomere fusion type chromosomal instability, leading to the promotion of neoplastic transformation (Murnane, 2012).

The presence of aberrant metacentric chromosomes has often been reported in cytogenetic studies of various canine cancers, including OSA, transmissible venereal tumor, hemangiopericytoma, hemangioendothelioma, spindle-cell sarcoma, mammary carcinoma, lymphoma and cutaneous mast cell tumors in dogs (Mayr et al., 1992, Mayr et al., 1994, Stone et al., 1991, Fujinaga et al., 1989). These metacentric chromosomes, which likely represent end-to-end chromosomal fusion events (Robertsonian translocations), may reflect telomere dysfunction. The Robertsonian translocation refers to a type of chromosome fusion to from one metacentric chromosome from two acrocentric chromosomes (Garagna et al., 2001). In a previous study in dogs, the conversion from normal to aberrant karyotype via telomeric fusions was reported using SV-40 transfection (Reimann et al., 1994). On the other hand, in the normal cells of other species that have only acrocentric autosomes in normal karyotypes, such as mouse (Todaro and Green, 1963) and cow (Lithner and Ponten, 1966, Murata et al., 2007), Robertsonian fusion events have been reported to increase with time in cultures. While the dog exhibits acrocentrics unlike humans, its telomere biology is known to be similar to human. Detailed characterizations of canine cancer cells should provide better understanding of the telomere dysfunctions in dogs.

Radiosensitivity signatures in cancer

Radiation Therapy and its Application in Veterinary Oncology

The primary goal of radiation therapy is to kill cancer cells while sparing normal, healthy tissue. This has been improved with recent advances in technologies and equipment in radiation therapy, such as advanced imaging, computerized treatment planning and advanced treatment techniques (Gordon, 2008). In veterinary oncology as well as in human oncology, the development of intensity modulated radiation therapy (IMRT), image guided radiation therapy (IGRT) and stereotactic body radiation therapy (SBRT) represent new advancements. These therapies allow

the precise delivery of radiation doses to tumors while simultaneously reducing doses delivered to normal surrounding organs (Gordon 2008). Additionally, charged particle radiation therapies, such as proton and carbon ion therapy, have gained interest in human radiation oncology (Schulz-Ertner et al., 2006). Particle radiotherapy takes advantage of the improved dose distribution to the tumor with almost no dose deposited in the normal tissue (Schulz-Ertner et al., 2006). There are only limited reports of the use of protons for treating dogs with brain tumors (Kaser-Hotz et al., 2002, Bley et al., 2005). Particle therapy can be expensive to implement, but potential applications have been discussed for veterinary oncology (Gordon 2008).

The Need for Predictive Assays and Canine Study

Tumors from individual patients with the same histological diagnosis can vary in their responsiveness to radiation. Thus, development of biologically guided personalized treatment strategies in radiation oncology is dependent on successful radiosensitivity predictive assays. Radiosensitivity can be determined by various means, including three important predictive assays; *ex vivo* tumor SF2 (survival fraction at 2Gy); tumor hypoxia; and tumor proliferative potential (Begg, 2009). However, these have yet to become routine in the clinic.

One of the most important elements that determines radioresponsiveness is intrinsic radiosensitivity resulting from genetic alterations in cellular response to radiation (Begg, 2009, Pawlik and Keyomarsi, 2004). Important biological pathways in radiation responses include apoptosis, cell cycle regulation, and DNA damage response and repair, which are often deficient in tumor cells due to mutations and other aberrations in these pathways (Pawlik and Keyomarsi, 2004, Begg, 2009). Therefore, the current study investigates molecular genetic events related to radiosensitivity with the potential of identifying gene regulatory pathways that may lead to development of improved radiosensitivity predictive assays.

As discussed above, companion dogs develop tumors similar to human malignancies (Vail and MacEwen, 2000, Dobson et al., 2002). The similarity is also seen in the response to radiation therapy. A relationship between histological type and radiation response exists, with hematological malignancies being sensitive, and OSA being relatively resistant in both human and veterinary oncology (MacEwen, 1990, Dernell, 2007). Expression profiles of important genetic alterations in human tumors have also been found in canine cancer models (Rowell et al., 2011). Therefore, canine tumors are potentially an excellent model to study response to radiation therapy. A recent review of canine studies involving the DNA damage response and repair, which play an important role in radiation response (Grosse et al., 2014), pointed out that very little is known about the DNA damage response in dogs. Further studies of canine DNA damage responses from basic biology to molecular and genetic studies are necessary in order to elucidate the similarities and differences as compared to human cancers and use canine tumors as models.

Radiation-induced DNA damage

Therapeutic radiation regimes utilize ionizing radiation (IR) (e.g. photons and particle radiation), which have sufficient energy to eject one or more orbital electrons from the atoms with which it interacts, thus causing the atom to be ionized (Hall, 2006). The deposition of energy in the tissues causes cell death principally by damaging DNA, the critical intracellular target (Hall, 2006). IR-induced DNA damage is caused by either direct or indirect effects. The electron ejected from the atom (called a fast electron) directly breaks chemical bonds that result in DNA strand breaks and distorts, or produces free radicals from surrounding water molecules that indirectly react with the DNA molecule (Hall, 2006). The quantity of radiation is expressed in Gray (Gy), which denotes the energy absorption of 1 J/kg.

IR produces a variety of damage types in DNA: following 1 Gy of gamma-rays, a cell will experience more than 1000 base damage, 1000 single strand breaks (SSBs), and 40 double strand breaks (DSBs) in a diploid human cell (Sutherland et al., 2000a, Sutherland et al., 2000b, Hall, 2006). DSBs are considered as the most critical DNA damage induced by IR (Hall 2006).

It is well established that the relative biological effectiveness (RBE) of a particular IR varies with its linear energy transfer (LET), which is the rate of deposition of energy per unit length along the radiation track. Photons and protons are low LET and heavy ions are high LET radiations (Hall, 2007). The same dose of high LET radiation is more effective than low LET for cell killing effect (Hall, 2007). In general, high-LET radiation induces a large number of complex clusters of DNA damage that are considerably more difficult to repair than damage induced by low LET (Loucas and Geard, 1994, George et al., 2001).

Biological effects induced by IR

Cells irradiated with IR undergo various responses to the consequent DNA damage. Cells attempt to repair the damage, delay cell division or die. DNA damage causes activation of DNA damage response (DDR), inducing activation of cell cycle checkpoint and DNA repair processes (Zhou and Elledge, 2000). Cell cycle arrest due to activating cell cycle checkpoints, is important in the response to IR (Zhou and Elledge, 2000). G2 arrest especially allows time for DNA damage to be repaired before mitosis. The ATM kinase, a major protein involving in sensing of DNA damage, phosphorylates numerous downstream targets, including p53, MDM2, CHK2, NBS1 and BRCA1 (Canman et al., 1998, Cortez et al., 1999, Pawlik and Keyomarsi, 2004, Gatei et al., 2000). The tumor suppressor p53 plays a central role in the cellular response to DNA-damaging agents, because it coordinates DNA repair with cell cycle progression and apoptosis (Fei and El-Deiry, 2003).

The DNA damage response also induces apoptosis in certain cells, such as lymphocytes (Hendry and West, 1997). Cell death by IR is generally explained by mitotic cell death; this occurs after mitosis, or after several rounds of cell divisions (Hall, 2006). In mitotic cell death, cells fail successful division due to persistent DNA damage, resulting in genomic loss and eventually cell death. Mitotic cell death may resemble features of apoptosis, necrosis, senescence and autophagy (Eriksson and Stigbrand, 2010). It has been shown that IR-induced apoptosis represents only a fraction of the total clonogenic cell kill, except in lymphocytes; therefore, mitotic cell death is thought to be the major mechanism of death by IR (Dewey et al., 1995).

Double strand breaks (DSBs) are considered to be the most dangerous of the different damage types induced by IR (Thompson, 2012). Unrepaired DSBs result in the loss of genetic material, or cell death. DSBs repaired improperly can lead to chromosomal rearrangements and mutations, and thereby contribute to tumorigenesis. Mammalian cells have developed several different repair mechanisms that are specialized in handling different kinds of damage (Jackson and Bartek, 2009). Cells can quickly and efficiently repair single-stranded DNA damage by base excision, nucleotide excision, and mismatch repair pathways (Jackson and Bartek, 2009). Cells have two significant pathways for DSB repair (Table 1.2): the error-prone non-homologous end-joining (NHEJ) pathway, which rapidly ligates the ends of broken DNA, and is the dominant pathway in mammalian cells active in the G1, S and G2 phase of the cell cycle; and the homologous recombination (HR) pathway, which uses a homologous template (sister chromatid or homologous chromosome) to conduct error-free, slow component of DSB repair (Thompson, 2012). Homologous recombination becomes active during S/G2 phases of the cell cycle in conjunction with NHEJ (Thompson, 2012).

Table 1.2: DNA double strand break repair and Fanconi anemia pathway.

	NHEJ	HR	FA
Function	DNA Repair	DNA Repair	Damage Response/Signaling
Primary Lesion	DSB	DSB	ICL, potentially DSB
Common response to IR in defective cell lines	Extreme sensitivity	Moderate sensitivity	Mild sensitivity
Major Proteins Associated	Ku 70/80, DNA-PKcs, XRCC4	MRN complex, Rad51, Rad51 paralogs, BRCA1/2, XRCC3	FA core complex (FANC A,B,C,E,F,G,L,M), FANCD2
Cell Cycle Stage Active	G1/G0, S, G2	Late S, G2	G1/G0, S, G2

Non-Homologous End-Joining

Non-homologous end-joining involves the simple re-ligation of the broken DNA ends and does not use homologous DNA as a template for repair (Thompson, 2012). NHEJ is referred to as an "error-prone" DNA repair pathway because the broken ends often trimmed by nucleases, resulting in mutation or deletion after repair. After the initial identification of the DSB by various proteins such as MRN complex (Mre11/Rad50/Nbs1), 53BP1, MDC1, the heterodimers Ku 70/80 are recruited to and bind to the free DSB ends (Thompson, 2012). Ku 70/80 then recruits DNA-PKcs and together they form the DNA-PK complex that holds the broken ends to allow ligases to fill the gap (Rivera-Calzada et al., 2007, Spagnolo et al., 2006). Damaged ends may have to be processed prior to ligation by nucleases such as Artemis (Thompson, 2012). XRCC4/LigIV finalizes the repair process (Smith et al., 2003). Numerous studies have shown that mutations in the genes associated to NHEJ increase hypersensitivity to radiation (Thacker and Zdzienicka, 2004).

Homologous Recombination

Homologous recombination is typically referred to as "error-free" because it repairs using homologous sequences. The pathway is initiated by resection at the DSB ends to create 3' single-strand overhangs, a process by the MRN complex and BRCA1 interaction (Thompson, 2012). The single-stranded 3' end is coated with replication protein A (RPA). BRCA1/2 along with RAD51 paralogs (XRCC2, XRCC3, Rad51B, Rad51C, and Rad51D) load Rad51 onto the RPA coated single-stranded DNA to form a nucleoprotein filament under the presence of BRCA2 (Thompson, 2012). The Rad51 coated single-strand DNA recruits both Rad52 and Rad54 and searches for homologous template. Then, the Rad51 coated single-stranded DNA invades the homologous sister chromatid and binds the homologous sequence to form heteroduplex DNA (Liang et al.,

1998). Strand invasion is followed by DNA synthesis for the missing sequence that was lost at the break end using the template. After synthesis, the invading strand is released and anneals to the other side of the break. A DNA ligase completes the repair by ligation of the gaps (Thompson, 2012). Deficiency in the HR pathway induces only mild sensitization to radiation (Thacker and Zdzienicka, 2004).

Fanconi Anemia DNA Repair Pathway

The Fanconi Anemia (FA) pathway, which is essential for repair of inter-strand DNA crosslinks (ICL), and potentially contributes to DNA DSB repair (Table 1.2) (Kee and D'Andrea, 2010). It has been noted that the loss of FA results in a mildly sensitive phonotype to IR, less severe than HR mutants (Duckworth-Rysiecki and Taylor, 1985, Niedernhofer et al., 2005). The FA pathway is driven by complexes of proteins; nine of FANC paralogs (FANCA, B, C, E, F, G, L, M and I) assemble in a complex required for FANCD2 activation by monoubiquitination in response to DNA damage or during S-phase progression (Moldovan and D'Andrea, 2009). The FA family that drives the repair of ICL is relatively unknown, however, it is believed that the FA family of proteins acts as a platform to recruit multiple nucleases for nucleolytic incision and promotes downstream of the ICL repair involving translesion DNA synthesis and HR (Thacker and Zdzienicka, 2004, Kim and D'Andrea, 2012).

Biological Factors Determining Tumor Response to Radiation

Many factors influence cellular response to radiation-induced damaged in cancer therapy. Primarily, there is a relationship between histological type and responsiveness to radiation therapy, with OSA being radioresistant and hematological malignancies being sensitive. As mentioned above, part of this difference is most likely attributable to the tendency of lymphomas to undergo

apoptosis in response to genotoxic treatment, whereas solid tumors appear to be relatively refractory to radiation induced apoptosis (Gewirtz, 2000). It is important to recognize differences between tumor types and that tumors from different patients with the same histological diagnosis can vary in their responsiveness to radiation. One factor that is important to determine radioresponsiveness is intrinsic radiosensitivity resulting from genetic alterations in cellular response to radiation, which is frequently found in cancer cells (Begg, 2009).

Also, vascular supply (hypoxia), tumor size and cell cycle phase are factors that affect radioresistance. Tumors in hypoxic states are regarded as resistant to radiation therapy (Hall, 2007). When molecular oxygen is present, DNA radicals generated by IR can react with oxygen producing chemically un-restorable DNA damage (oxygen fixation) (Ewing, 1998). Poorly vascularized areas frequently found in solid tumors, contribute to their radioresistance (Brown and Giaccia, 1998). In terms of cell cycle effect, cells are most sensitive to radiation in the M phase, less sensitive in the G1 phase (if cell cycle is long, early G1 is relatively resistant) and the least sensitive during the latter part of S-phase (Terasima and Tolmach, 1963, Sinclair and Morton, 1966) (Hall 2006). Dysregulated cell cycle checkpoint controls are often found in tumor cells. In solid tumors approximately half have mutations in p53, which is one of the key mediators of G1 cell cycle checkpoint (Mirzayans et al., 2013). Cells continue to progress into S phase following irradiation exposure in p53-deficient cells. The loss of p53 is generally associated with a more radioresistant phenotype (Mirzayans et al., 2013). The G2 cell cycle checkpoint control also plays an important role in radiation response. In tumor cells there are wide variations in G2 cell cycle checkpoint integrity, and in some cases, attenuated G2 checkpoint control is associated with a more radiosensitive phenotype (Pawlik and Keyomarsi, 2004).

Predictive Assay for Tumor Response to Radiation

Previous efforts to develop a predictive assay for tumor radioresponse have been reviewed (Table 1.3) (Begg, 2009, Torres-Roca and Stevens, 2008). Methods of measuring intrinsic radiosensitivity, hypoxia status, and tumor proliferative potential were developed. Intrinsic radiosensitivity was measured by *in vitro* colony formation assay (survival fraction at 2 Gy, SF2). Previous studies using head and neck cancer and cervix carcinoma showed that local control rates in patients following radiotherapy correlated with in vitro SF2 in primary culture (West et al., 1997, Bjork-Eriksson et al., 2000). However, clonogenic assays had relatively low yield due to the poor growth under *in vitro* conditions, and was time-consuming. Using electrodes to measure tumor pO2 could apply only for readily accessible tumors (Movsas et al., 2002). The proliferative potential with thymidine analogs was not predictive of clinical outcomes for studies in head and neck cancers (Begg et al., 1999). In order to estimate proliferation rate, flow cytometry analysis was performed in tumor biopsies in patients receiving a tracer dose of either iododeoxyuridine (IdU) or bromodeoxyuridine (BrdU) intravenously prior to treatment. Although SF2 and hypoxia could predict clinical outcome in radiation response in patients, these approaches are not practical for routine clinical application.

Approaches to Measurement of Intrinsic Radiosensitivity

Measurement of cellular intrinsic radiosensitivity is important to determine the radioresponsiveness of an individual tumor because tumors with same histopathological origin may show quite a wide range of sensitivity toward IR. The clonogenic assay, or colony formation assay has been utilized to evaluate intrinsic radiosensitivity. This measures the loss of clonogeneity, which is the ability of a single cell to grow into a colony. This assay was first used

Table 1.3: Predictive assays past and present*.

Process	Direct assays	Indirect assays (surrogates)	Disadvantages
Radiosensitivity	Colony formation (SF2) [a,d,e]	DNA breaks [b,e,f] Chromosome aberrations [b,e] Apoptosis [b,e] H2AX foci [b,d,e] IHC radiosensitive genes [b]	(a) Long assay time (b) Imperfect surrogate (c) Invasive assay (d) Technically difficult (reproducibility) (e) Little information on mechanisms to ease choice of alternative treatments (f) Injection of drug/tracer necessary
Hypoxia	Polarography (Eppendorf)[c]	Exogenous hypoxia markers (bioreductive drugs) [b,f] Vascular density [b,e] Vascular perfusion [b,e] IHC hypoxia genes [b]	
Proliferation	Thymidine analog labeling (BrdU) [b,f]	Mitotic index [b,e] IHC proliferation genes [b,e]	

*Adapted from Begg, 2009.

in 1956 by Puck and Marcus on HeLa cells in culture irradiated with X-rays to obtain radiation-dose survival curves (Puck and Marcus, 1956). The colony formation assay can detect reproductive cell death as a result of damage to chromosomes, apoptosis etc. (Brown and Attardi, 2005). Also, this can determine the effectiveness of anti-cancer drugs and treatments that can cause reproductive cell death. A dose of 2 Gy for intrinsic radiosensitivity is a dose per fraction commonly used in clinical radiotherapy. However, as mentioned above the colony formation assay is not clinically applicable. Other approaches to predict tumor intrinsic radiosensitivity have been developed (Table 1.3).

Measurements of chromosome damage resulting from DSBs by the G2 chromosomal assay has been successfully used to assess intrinsic radiosensitivity assessment in normal and pre-cancerous cells in human oncology (Parshad et al., 1983, Scott et al., 1996). An increase in chromatid type aberrations detected by this assay has been linked with cancer susceptibility. The G2 chromosomal assay has also shown good discrimination in radiation response to research chromosomal radiosensitivity in sporadic patients with low penetrance predisposition to cancer, such as breast cancer (Scott, 2004). Although there are a few reports using the G2 chromosome assay for tumor cells, a correlation between chromosome breaks and clonogenic survival has been shown in human squamous cell carcinoma using this assay (Schwartz, 1992).

Evidence suggests that intrinsic radiosensitivity results from alterations in the efficiency or deficiencies of repair of DNA DSBs. Early studies demonstrated a relationship between radiosensitivity and break rejoining (Schwartz 1998, West 1994), but no variations in the number of induced initial DSBs (Dikomey et al., 1998). Alterations in DNA break rejoining greatly affect chromosome aberration frequencies and thereby overall survival (Schwartz, 1998). Studies have shown that radiation sensitivity is correlated with residual levels of DNA DSBs (Schwartz, 1998).

Thus, both higher levels of residual breaks and slower overall rates of break rejoining are associated with a more radiosensitive phenotype. The correlation between cellular radiosensitivity and the efficiency of DNA DSB repair has been studied in various tumor cell lines. While early studies reported correlation between radiation sensitivity in tumor cells and initial break frequency, these were likely artifacts of the assays used to measure the DSBs themselves (McMillan et al., 2001). Previous studies also show that the correlation between tumor radioresistance and DNA DSB repair capacity is controversial (El-Awady et al., 2003, McMillan et al., 2001). In some of the studies, DSBs were measured by pulse-field gel electrophoresis (PGEF) or constant-field gel electrophoresis (CFGE), assays that require high doses (e.g. 40 Gy) to induce DSBs (McMillan et al., 2001). More recently, nuclear gamma- (γ-) H2AX focus formation at DSB sites has shown its efficiency to assess DSB repair efficiency (Rogakou et al., 1998). H2AX is a member of the histone protein H2A family and the phosphorylation at Ser139 is referred to as γ-H2AX (Rogakou et al., 1998). Previous studies have displayed rapid formation of γ-H2AX foci (within 20 minutes) and disappearance after DSB repair in human fibroblasts (Kato et al., 2006b). Currently, γ-H2AX is widely used as a sensitive marker of DNA DSBs, however, such measurements of γ-H2AX foci must be done with caution. It has been demonstrated that γ-H2AX foci occur in cell nuclei in the S phase of the cell cycle during replication stress (Ward and Chen, 2001). Further studies have suggested that endogeneous γ-H2AX foci are found in tumor cells besides those in S phase (Yu et al., 2006). Therefore, G1 synchronized cells (often through contact inhibition) have been used to assess IR-induced foci in normal cells (Kato et al., 2006a). However, even in asynchronous tumor cells, previous studies have shown that residual γ-H2AX foci can be used to evaluate radiosensitivity of cells or their ability to recover from damage (Banath et al., 2004, Mahrhofer et al., 2006).

The contribution of apoptosis in the response to clinical radiotherapy has been widely debated (Hendry and West, 1997, Dewey et al., 1995). Radiation readily induces apoptosis in tumors of hematopoietic origin, whereas it has been stated that DNA damage-induced apoptosis seem to be not common in solid tumors, such as breast cancer (Gewirtz, 2000, Steel, 2001). The results were not conclusive; some studies showed a correlation between SF2 and the frequency of apoptosis after irradiation (Hendry and West, 1997, Dunne et al., 2003), while others did not (Bromfield et al., 2003).

Molecular Pathway Analysis for Prediction of Intrinsic Radiosensitivity

Recently, an association between radiosensitivity and the expression of several genes has been demonstrated. Factors involved are in the two major DNA DSBs repair pathway, NHEJ and HR, and have been proposed as potential markers (e.g. Ku70, Ku80, DNA-PKcs, RAD51, ATM, MRE11) in various cancers, but clinical importance has not been validated (Sarbia et al., 2007, Sirzen et al., 1999). The variable expression of these genes, particularly overexpression of RAD51 is seen in many tumors and is linked to increased radioresistance (Klein, 2008). However, for the proteins involved in NHEJ, previous papers show inconsistent correlation between radiosensitivity and the level of expression of DNA-PKcs, Ku70 and Ku80 (Eriksson et al., 1999, Sirzen et al., 1999).

Cellular radioresponse has been suggested to be influenced by proteins that control apoptotic cell death, especially though the balance between anti- and pro-apoptotic members of the Bcl-2 family (Zhou et al., 2003). Anti-apoptotic proteins (e.g. Bcl-2 and Bcl-XL) and pro-apoptotic markers (e.g. Bad, Bak, Bax, and PUMA) have been studied as possible predictive factors in need of further evaluation (Lee et al., 1999). In addition, a study showed that

overexpression of survivin, one of the inhibitors of apoptosis (IAP) family members, was also suggested to be associated with radiosensitivity in a colon cancer cell line (Rodel et al., 2003).

There are more studies suggesting association between radioresistance and the expression of genes involved in various radiation response pathways or radiation related pathways, such as growth factor, signal transduction, cell cycle, cell adhesion and hypoxia (Ogawa et al., 2007). In the current knowledge, such signatures partially help prediction of the radiation response, but the relevance of these signatures remains to be determined.

Microarray predictive assay: NCI-60

The generation of novel high-throughput data sets has allowed simultaneous analysis of the expression levels of thousands of genes, which can be applied to the development of markers of clinical outcomes. For example, gene expression signatures have been developed for biomarkers to predict patient response to treatment shown to be prognostic in breast, lung and head-and neck cancers (van 't Veer et al., 2002, Beer et al., 2002, Chung et al., 2004). A significant amount of effort has been put into evaluating these microarray patterns for clinical use, especially in breast cancer, where markers for treatment decision derived from microarray are currently being tested in a clinical trial (MINDACT, TAILORx) (Cardoso et al., 2008, Sparano and Paik, 2008).

There is growing interest in generating a gene signature that reflects intrinsic radiosensitivity. Recently, there is a review paper about published studies identifying radiation sensitivity related genes from single tumor types, for example, cervical cancer, oral squamous cell carcinoma, colorectal cancer, or lung cancer (Ogawa et al., 2007). However, a study has suggested that a gene signature would be more robust and general if derived from heterogeneous cell lines involving multiple tissues of origin (Hall et al., 2014). For this purpose, the most comprehensive studies have used the NCI-60 panel of cell lines. Several groups have explored gene signatures to

predict radiosensitivity using the NCI-60 panel. The first study using NCI-60 panel identified 3 genes (RbAp48: retinoblastoma binding protein 4: R5PIA: ribose 5-phosphate isomerase A, and RGS19: G-protein signaling regulator 19) of which expression values are correlated with radiation sensitivity (Torres-Roca et al., 2005). In another study, the microarray data for NCI-60 cells were also analyzed by a meta-analysis using four platforms and identified a 31-gene radiosensitivity signature (Kim et al., 2012). In addition, a study suggested that basal expression patterns are possibly more informative than radiation response signatures because basal expression patterns discriminated well between radiosensitive and resistant lines than expression changes in response to IR (Amundson et al., 2008). On the other hand, the fact that there is relatively little overlap of genes between studies even with the same NCI-60 panel, is the current challenge to develop a predictive radiation sensitivity signature (Muyal et al., 2008).

The technology is promising at least for a better understanding of the molecular events implicated in radiation sensitivity, although the use of microarray for radiosensitivity has not yet achieved any significant impact at the clinical level. As mentioned above, the canine cancer cell line panel (ACC30) has been recently developed, and microarray profiling has been utilized for predictive assay for response to doxorubicin (Fowles et al., 2014). Genome-wide studies of canine cancer cell lines with different radiosensitivities in conjunction with biological endpoints can provide a framework for further elucidating profiles for prediction of radiotherapy response not only for dogs but also humans.

Objective of Dissertation

The main objective of this dissertation was to characterize sets of canine cancer cell lines by examining chromosome aberrations, telomere dysfunction and radiosensitivity signatures. Such

characterizations will provide a better understanding of underlying canine cancer biology. If there is a common characteristic, it will provide new insights into improved clinical managements, such as the development of novel therapeutic targets and identification of radiation sensitivity markers, not only for dogs, but with potential relevance for humans as well. The outline of this thesis is summarized in Figure 1.4.

In Chapter 2, we evaluated chromosome number, frequency of metacentric chromosomes in metaphase spreads, and characterized the contribution of dysfunctional telomeres using FISH with a telomere specific probe. All eight canine OSA cell lines displayed increased numbers of metacentric chromosome and exhibited numerous telomere aberrations including interstitial telomeric sequences and telomere fusions. In the eight canine OSA cell lines, we also assessed basic cellular characteristics, telomere associated factors including telomerase activity, co-localization of DNA damage and telomere signals (TIFs), and the expression of a DNA repair protein shown to be required for mammalian telomeric end-capping function, specifically the DNA-PKcs. To better characterize telomere dysfunction associated with canine OSA, we investigated telomere aberrations in primary cultures from ten spontaneous canine OSAs, as well as the effects of long-term culture in one of the cultures. We found that frequencies of telomere aberrations in these ten cultures were low, but could be increased with increasing passage in culture. In contrast, metacentric chromosomes did not accumulate with long-term culture of non-cancerous canine fibroblasts, or DNA repair deficient mouse fibroblasts (homozygous ATM gene deficiency).

In Chapter 3, we investigated radiosensitivity in a panel of canine cancer cell lines representing different cancer types. We obtained 27 canine cell lines derived from 10 tumor types from the ACC30 panel. First, radiosensitivity was determined using a clonogenic assay for

adherent cell cultures or from a limiting dilution assay for suspension cell cultures. The cellular characteristics were also analyzed. Based on the characteristics, there was a statistically significant correlation between radiosensitivity and plating efficiency. Next, we selected the six most radiosensitive cell lines as the radiosensitive group and the five most radioresistant cell lines as the radioresistant group. Then, we evaluated known parameters for cell killing by IR including IR-induced DNA DSB repair and apoptosis, in the radiosensitive group as compared to the radioresistant group. Furthermore, we investigated a possible common radiosensitivity signature using the basal gene expression profiling of the ACC panel for 20,000 genes. Our results suggest that cell adhesion related genes, rather than the more commonly regarded radiosensitivity associated apoptosis and DNA repair related genes, may provide the most beneficial radiosensitivity biomarkers for predicting individual response to radiotherapy, regardless of tumor type.

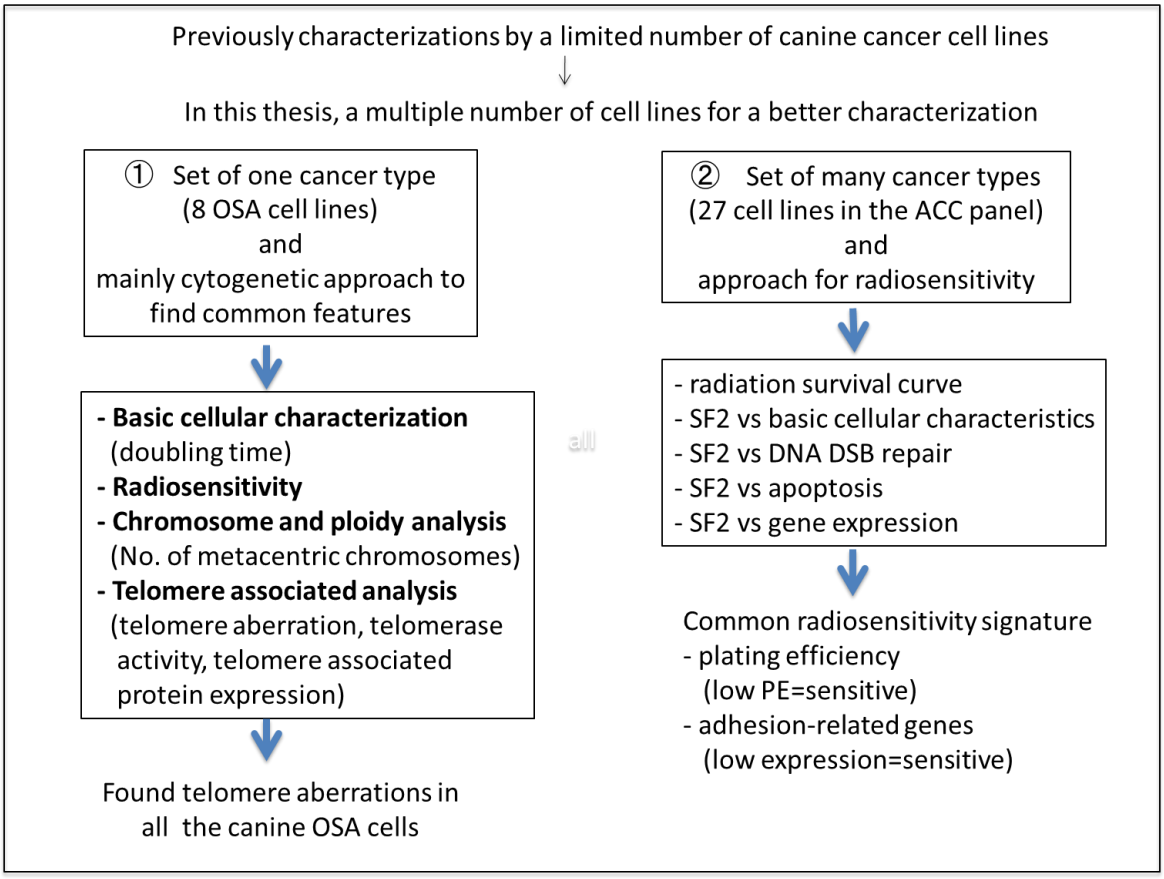

Figure 1.4: *The outline of this thesis.*

REFERENCES

ADAMS, V. J., EVANS, K. M., SAMPSON, J. & WOOD, J. L. 2010. Methods and mortality results of a health survey of purebred dogs in the UK. *J Small Anim Pract,* 51**,** 512-24.

ALBERTSON, D. G., COLLINS, C., MCCORMICK, F. & GRAY, J. W. 2003. Chromosome aberrations in solid tumors. *Nat Genet,* 34**,** 369-76.

AMUNDSON, S. A., DO, K. T., VINIKOOR, L. C., LEE, R. A., KOCH-PAIZ, C. A., AHN, J., REIMERS, M., CHEN, Y., SCUDIERO, D. A., WEINSTEIN, J. N., TRENT, J. M., BITTNER, M. L., MELTZER, P. S. & FORNACE, A. J., JR. 2008. Integrating global gene expression and radiation survival parameters across the 60 cell lines of the National Cancer Institute Anticancer Drug Screen. *Cancer Res,* 68**,** 415-24.

AN, X., TIWARI, A. K., SUN, Y., DING, P. R., ASHBY, C. R., JR. & CHEN, Z. S. 2010. BCR-ABL tyrosine kinase inhibitors in the treatment of Philadelphia chromosome positive chronic myeloid leukemia: a review. *Leuk Res,* 34**,** 1255-68.

ANGSTADT, A. Y., MOTSINGER-REIF, A., THOMAS, R., KISSEBERTH, W. C., GUILLERMO COUTO, C., DUVAL, D. L., NIELSEN, D. M., MODIANO, J. F. & BREEN, M. 2011. Characterization of canine osteosarcoma by array comparative genomic hybridization and RT-qPCR: signatures of genomic imbalance in canine osteosarcoma parallel the human counterpart. *Genes Chromosomes Cancer,* 50**,** 859-74.

ANGSTADT, A. Y., THAYANITHY, V., SUBRAMANIAN, S., MODIANO, J. F. & BREEN, M. 2012. A genome-wide approach to comparative oncology: high-resolution oligonucleotide aCGH of canine and human osteosarcoma pinpoints shared microaberrations. *Cancer Genet,* 205**,** 572-87.

APPA National Pet Owners Survey (2014). American Pet Products Manufacturers Association (APPMA) website: http://www.americanpetproducts.org/press_industrytrends.asp

ARAUJO, S. E., BERNARDO, W. M., HABR-GAMA, A., KISS, D. R. & CECCONELLO, I. 2007. DNA ploidy status and prognosis in colorectal cancer: a meta-analysis of published data. *Dis Colon Rectum,* 50**,** 1800-10.

ARTANDI, S. E., CHANG, S., LEE, S. L., ALSON, S., GOTTLIEB, G. J., CHIN, L. & DEPINHO, R. A. 2000. Telomere dysfunction promotes non-reciprocal translocations and epithelial cancers in mice. *Nature,* 406**,** 641-5.

BAILEY, S. M. 2008. Telomeres and double-strand breaks - all's well that "ends" well. *Radiat Res,* 169**,** 1-7.

BAILEY, S. M., MEYNE, J., CHEN, D. J., KURIMASA, A., LI, G. C., LEHNERT, B. E. & GOODWIN, E. H. 1999. DNA double-strand break repair proteins are required to cap the ends of mammalian chromosomes. *Proc Natl Acad Sci U S A,* 96**,** 14899-904.

BAILEY, S. M. & MURNANE, J. P. 2006. Telomeres, chromosome instability and cancer. *Nucleic Acids Res,* 34**,** 2408-17.

BAKHOUM, S. F. & COMPTON, D. A. 2012. Chromosomal instability and cancer: a complex relationship with therapeutic potential. *J Clin Invest,* 122**,** 1138-43.

BANATH, J. P., MACPHAIL, S. H. & OLIVE, P. L. 2004. Radiation sensitivity, H2AX phosphorylation, and kinetics of repair of DNA strand breaks in irradiated cervical cancer cell lines. *Cancer Res,* 64**,** 7144-9.

BARRETINA, J., CAPONIGRO, G., STRANSKY, N., VENKATESAN, K., MARGOLIN, A. A., KIM, S., WILSON, C. J., LEHAR, J., KRYUKOV, G. V., SONKIN, D., REDDY, A., LIU, M., MURRAY, L., BERGER, M. F., MONAHAN, J. E., MORAIS, P., MELTZER, J., KOREJWA, A., JANE-VALBUENA, J., MAPA, F. A., THIBAULT, J., BRIC-FURLONG, E., RAMAN, P., SHIPWAY, A., ENGELS, I. H., CHENG, J., YU, G. K., YU, J., ASPESI, P., JR., DE SILVA, M., JAGTAP, K., JONES, M. D., WANG, L., HATTON, C., PALESCANDOLO, E., GUPTA, S., MAHAN, S., SOUGNEZ, C., ONOFRIO, R. C., LIEFELD, T., MACCONAILL, L., WINCKLER, W., REICH, M., LI, N., MESIROV, J. P., GABRIEL, S. B., GETZ, G., ARDLIE, K., CHAN, V., MYER, V. E., WEBER, B. L., PORTER, J., WARMUTH, M., FINAN, P., HARRIS, J. L., MEYERSON, M., GOLUB, T. R., MORRISSEY, M. P., SELLERS, W. R., SCHLEGEL, R. & GARRAWAY, L. A. 2012. The Cancer Cell Line Encyclopedia enables predictive modelling of anticancer drug sensitivity. *Nature,* 483**,** 603-7.

BAYANI, J., ZIELENSKA, M., PANDITA, A., AL-ROMAIH, K., KARASKOVA, J., HARRISON, K., BRIDGE, J. A., SORENSEN, P., THORNER, P. & SQUIRE, J. A. 2003. Spectral karyotyping identifies recurrent complex rearrangements of chromosomes 8, 17, and 20 in osteosarcomas. *Genes Chromosomes Cancer,* 36**,** 7-16.

BEER, D. G., KARDIA, S. L., HUANG, C. C., GIORDANO, T. J., LEVIN, A. M., MISEK, D. E., LIN, L., CHEN, G., GHARIB, T. G., THOMAS, D. G., LIZYNESS, M. L., KUICK, R., HAYASAKA, S., TAYLOR, J. M., IANNETTONI, M. D., ORRINGER, M. B. & HANASH, S. 2002. Gene-expression profiles predict survival of patients with lung adenocarcinoma. *Nat Med,* 8**,** 816-24.

BEGG, A. C., HAUSTERMANS, K., HART, A. A., DISCHE, S., SAUNDERS, M., ZACKRISSON, B., GUSTAFFSON, H., COUCKE, P., PASCHOUD, N., HOYER, M., OVERGAARD, J., ANTOGNONI, P., RICHETTI, A., BOURHIS, J., BARTELINK, H., HORIOT, J. C., CORVO, R., GIARETTI, W., AWWAD, H., SHOUMAN, T., JOUFFROY, T., MACIOROWSKI, Z., DOBROWSKY, W., STRUIKMANS, H., WILSON, G. D. & ET AL. 1999. The value of pretreatment cell kinetic parameters as predictors for radiotherapy outcome in head and neck cancer: a multicenter analysis. *Radiother Oncol,* 50**,** 13-23.

BEGG, A. C. 2009. Predicting response to radiotherapy: evolutions and revolutions. *Int J Radiat Biol,* 85**,** 825-36.

BILLER, B. J., KITCHELL, B. E. & CADILE, C. D. 1998. Evaluation of an assay for detecting telomerase activity in neoplastic tissues of dogs. *Am J Vet Res,* 59**,** 1526-9.

BJORK-ERIKSSON, T., WEST, C., KARLSSON, E. & MERCKE, C. 2000. Tumor radiosensitivity (SF2) is a prognostic factor for local control in head and neck cancers. *Int J Radiat Oncol Biol Phys,* 46**,** 13-9.

BLACKBURN, E. H. & GALL, J. G. 1978. A tandemly repeated sequence at the termini of the extrachromosomal ribosomal RNA genes in Tetrahymena. *J Mol Biol,* 120**,** 33-53.

BLASCO, M. A. 2005. Telomeres and human disease: ageing, cancer and beyond. *Nat Rev Genet,* 6**,** 611-22.

BLEY, C. R., SUMOVA, A., ROOS, M. & KASER-HOTZ, B. 2005. Irradiation of brain tumors in dogs with neurologic disease. *J Vet Intern Med,* 19**,** 849-54.

BODNAR, A. G., OUELLETTE, M., FROLKIS, M., HOLT, S. E., CHIU, C. P., MORIN, G. B., HARLEY, C. B., SHAY, J. W., LICHTSTEINER, S. & WRIGHT, W. E. 1998. Extension of life-span by introduction of telomerase into normal human cells. *Science,* 279**,** 349-52.

BOGLIOLO, M., LYAKHOVICH, A., CALLEN, E., CASTELLA, M., CAPPELLI, E., RAMIREZ, M. J., CREUS, A., MARCOS, R., KALB, R., NEVELING, K., SCHINDLER, D. & SURRALLES, J. 2007. Histone H2AX and Fanconi anemia FANCD2 function in the same pathway to maintain chromosome stability. *EMBO J,* 26**,** 1340-51.

BREEN, M., LANGFORD, C. F., CARTER, N. P., HOLMES, N. G., DICKENS, H. F., THOMAS, R., SUTER, N., RYDER, E. J., POPE, M. & BINNS, M. M. 1999. FISH mapping and identification of canine chromosomes. *J Hered,* 90**,** 27-30.

BROMFIELD, G. P., MENG, A., WARDE, P. & BRISTOW, R. G. 2003. Cell death in irradiated prostate epithelial cells: role of apoptotic and clonogenic cell kill. *Prostate Cancer Prostatic Dis,* 6**,** 73-85.

BRONDEN, L. B., FLAGSTAD, A. & KRISTENSEN, A. T. 2007. Veterinary cancer registries in companion animal cancer: a review. *Vet Comp Oncol,* 5**,** 133-44.

BRONSON, R. T. 1982. Variation in age at death of dogs of different sexes and breeds. *Am J Vet Res,* 43**,** 2057-9.

BROWN, J. M. & ATTARDI, L. D. 2005. The role of apoptosis in cancer development and treatment response. *Nat Rev Cancer,* 5**,** 231-7.

BROWN, J. M. & GIACCIA, A. J. 1998. The unique physiology of solid tumors: opportunities (and problems) for cancer therapy. *Cancer Res,* 58**,** 1408-16.

BURRELL, R. A., MCGRANAHAN, N., BARTEK, J. & SWANTON, C. 2013. The causes and consequences of genetic heterogeneity in cancer evolution. *Nature,* 501**,** 338-45.

CAMPISI, J. 1997. The biology of replicative senescence. *Eur J Cancer,* 33**,** 703-9.

CAMPISI, J. 2005. Senescent cells, tumor suppression, and organismal aging: good citizens, bad neighbors. *Cell,* 120**,** 513-22.

CANMAN, C. E., LIM, D. S., CIMPRICH, K. A., TAYA, Y., TAMAI, K., SAKAGUCHI, K., APPELLA, E., KASTAN, M. B. & SILICIANO, J. D. 1998. Activation of the ATM kinase by ionizing radiation and phosphorylation of p53. *Science,* 281**,** 1677-9.

CARDOSO, F., VAN'T VEER, L., RUTGERS, E., LOI, S., MOOK, S. & PICCART-GEBHART, M. J. 2008. Clinical application of the 70-gene profile: the MINDACT trial. *J Clin Oncol,* 26**,** 729-35.

CASPERSSON, T., ZECH, L., MODEST, E. J., FOLEY, G. E., WAGH, U. & SIMONSSON, E. 1969. Chemical differentiation with fluorescent alkylating agents in Vicia faba metaphase chromosomes. *Exp Cell Res,* 58**,** 128-40.

CHOI, J., SOUTHWORTH, L. K., SARIN, K. Y., VENTEICHER, A. S., MA, W., CHANG, W., CHEUNG, P., JUN, S., ARTANDI, M. K., SHAH, N., KIM, S. K. & ARTANDI, S. E. 2008. TERT promotes epithelial proliferation through transcriptional control of a Myc- and Wnt-related developmental program. *PLoS Genet,* 4**,** e10.

CHUN, R. & DE LORIMIER, L. P. 2003. Update on the biology and management of canine osteosarcoma. *Vet Clin North Am Small Anim Pract,* 33**,** 491-516, vi.

CHUNG, C. H., PARKER, J. S., KARACA, G., WU, J., FUNKHOUSER, W. K., MOORE, D., BUTTERFOSS, D., XIANG, D., ZANATION, A., YIN, X., SHOCKLEY, W. W., WEISSLER, M. C., DRESSLER, L. G., SHORES, C. G., YARBROUGH, W. G. & PEROU, C. M. 2004. Molecular classification of head and neck squamous cell carcinomas using patterns of gene expression. *Cancer Cell,* 5**,** 489-500.

CONG, YU-SHENG, WOODRING E. WRIGHT & JERRY W. SHAY.2002. Human telomerase and its regulation. *Microbiology and molecular Biology Review 66.3: 4007-425*

CORTEZ, D., WANG, Y., QIN, J. & ELLEDGE, S. J. 1999. Requirement of ATM-dependent phosphorylation of brca1 in the DNA damage response to double-strand breaks. *Science,* 286**,** 1162-6.

COURTAY-CAHEN, C., GRIFFITHS, L. A., HUDSON, R. & STARKEY, M. 2007. Extensive coloured identification of dog chromosomes to support karyotype studies: the colour code. *Cytogenet Genome Res,* 116**,** 198-204.

DE LANGE, T. 2005. Shelterin: the protein complex that shapes and safeguards human telomeres. *Genes Dev,* 19**,** 2100-10.

DELANEY, G., JACOB, S., FEATHERSTONE, C. & BARTON, M. 2005. The role of radiotherapy in cancer treatment: estimating optimal utilization from a review of evidence-based clinical guidelines. *Cancer,* 104**,** 1129-37.

DERNELL WS, EHRHARDT NP, STAW RC, VAIL DM. 2007. Tumor of the skeletal system. In: Withrow SJ, Vail DM, editors. St Louis, MO:Saunders. 540-582

DEWEY, W. C., LING, C. C. & MEYN, R. E. 1995. Radiation-induced apoptosis: relevance to radiotherapy. *Int J Radiat Oncol Biol Phys,* 33**,** 781-96.

DIKOMEY, E., DAHM-DAPHI, J., BRAMMER, I., MARTENSEN, R. & KAINA, B. 1998. Correlation between cellular radiosensitivity and non-repaired double-strand breaks studied in nine mammalian cell lines. *Int J Radiat Biol,* 73**,** 269-78.

DOBSON, J. M. 2013. Breed-predispositions to cancer in pedigree dogs. *ISRN Vet Sci,* 2013**,** 941275.

DOBSON, J. M., SAMUEL, S., MILSTEIN, H., ROGERS, K. & WOOD, J. L. 2002. Canine neoplasia in the UK: estimates of incidence rates from a population of insured dogs. *J Small Anim Pract,* 43**,** 240-6.

DOMCKE, S., SINHA, R., LEVINE, D. A., SANDER, C. & SCHULTZ, N. 2013. Evaluating cell lines as tumour models by comparison of genomic profiles. *Nat Commun,* 4**,** 2126.

DUCKWORTH-RYSIECKI, G & TAYLOR, A. M. 1985. Effects on ionizing radiation on cells from Fanconi's anemia patients. *Cancer Res,* 45, 416-20.

DUNN, K. A., THOMAS, R., BINNS, M. M. & BREEN, M. 2000. Comparative genomic hybridization (CGH) in dogs--application to the study of a canine glial tumour cell line. *Vet J,* 160**,** 77-82.

DUNNE, A. L., PRICE, M. E., MOTHERSILL, C., MCKEOWN, S. R., ROBSON, T. & HIRST, D. G. 2003. Relationship between clonogenic radiosensitivity, radiation-induced apoptosis and DNA damage/repair in human colon cancer cells. *Br J Cancer,* 89**,** 2277-83.

EHRHART, N., DERNELL, W. S., HOFFMANN, W. E., WEIGEL, R. M., POWERS, B. E. & WITHROW, S. J. 1998. Prognostic importance of alkaline phosphatase activity in serum from dogs with appendicular osteosarcoma: 75 cases (1990-1996). *J Am Vet Med Assoc,* 213**,** 1002-6.

EL-AWADY, R. A., DIKOMEY, E. & DAHM-DAPHI, J. 2003. Radiosensitivity of human tumour cells is correlated with the induction but not with the repair of DNA double-strand breaks. *Br J Cancer,* 89**,** 593-601.

EPEL, E. S., BLACKBURN, E. H., LIN, J., DHABHAR, F. S., ADLER, N. E., MORROW, J. D. & CAWTHON, R. M. 2004. Accelerated telomere shortening in response to life stress. *Proc Natl Acad Sci U S A,* 101**,** 17312-5.

ERIKSSON, C., VAN DAM, A. M., LUCASSEN, P. J., BOL, J. G., WINBLAD, B. & SCHULTZBERG, M. 1999. Immunohistochemical localization of interleukin-1beta, interleukin-1 receptor antagonist and interleukin-1beta converting enzyme/caspase-1 in the rat brain after peripheral administration of kainic acid. *Neuroscience,* 93**,** 915-30.

ERIKSSON, D. & STIGBRAND, T. 2010. Radiation-induced cell death mechanisms. *Tumour Biol,* 31**,** 363-72.

ERTEL, A., VERGHESE, A., BYERS, S. W., OCHS, M. & TOZEREN, A. 2006. Pathway-specific differences between tumor cell lines and normal and tumor tissue cells. *Mol Cancer,* 5**,** 55.

EWING, D. 1998. The oxygen fixation hypothesis: a reevaluation. *Am J Clin Oncol,* 21**,** 355-61.

FEI, P. & EL-DEIRY, W. S. 2003. P53 and radiation responses. *Oncogene,* 22**,** 5774-83.

FOWLES, S 2014, "Canine COXEN: cross-species genomic applications for predicting chemosensitivity in dogs", in 15 th Annual Research Day at the Colorado State University

FRIAS, C., PAMPALONA, J., GENESCA, A. & TUSELL, L. 2012. Telomere dysfunction and genome instability. *Front Biosci (Landmark Ed),* 17**,** 2181-96.

FUJINAGA, T., YAMASHITA, M., YOSHIDA, M. C., MIZUNO, S., OKAMOTO, Y., TAJIMA, M. & OTOMO, K. 1989. Chromosome analysis of canine transmissible sarcoma cells. *Zentralbl Veterinarmed A,* 36**,** 481-9.

GARAGNA, S., MARZILIANO, N., ZUCCOTTI, M., SEARLE, J. B., CAPANNA, E. & REDI, C. A. 2001. Pericentromeric organization at the fusion point of mouse Robertsonian translocation chromosomes. *Proc Natl Acad Sci U S A,* 98**,** 171-5.

GATEI, M., SCOTT, S. P., FILIPPOVITCH, I., SORONIKA, N., LAVIN, M. F., WEBER, B. & KHANNA, K. K. 2000. Role for ATM in DNA damage-induced phosphorylation of BRCA1. *Cancer Res,* 60**,** 3299-304.

GELBERG, K. H., FITZGERALD, E. F., HWANG, S. & DUBROW, R. 1997. Growth and development and other risk factors for osteosarcoma in children and young adults. *Int J Epidemiol,* 26**,** 272-8.

GEORGE, K., WU, H., WILLINGHAM, V., FURUSAWA, Y., KAWATA, T. & CUCINOTTA, F. A. 2001. High- and low-LET induced chromosome damage in human lymphocytes: a time-course of aberrations in metaphase and interphase. *Int J Radiat Biol,* 77**,** 175-83.

GEWIRTZ, D. A. 2000. Growth arrest and cell death in the breast tumor cell in response to ionizing radiation and chemotherapeutic agents which induce DNA damage. *Breast Cancer Res Treat,* 62**,** 223-35.

GILLET, J. P., CALCAGNO, A. M., VARMA, S., MARINO, M., GREEN, L. J., VORA, M. I., PATEL, C., ORINA, J. N., ELISEEVA, T. A., SINGAL, V., PADMANABHAN, R., DAVIDSON, B., GANAPATHI, R., SOOD, A. K., RUEDA, B. R., AMBUDKAR, S. V. & GOTTESMAN, M. M. 2011. Redefining the relevance of established cancer cell lines to the study of mechanisms of clinical anti-cancer drug resistance. *Proc Natl Acad Sci U S A,* 108**,** 18708-13.

GILLETTE, E. L. 1997. History of veterinary radiation oncology. *Vet Clin North Am Small Anim Pract,* 27**,** 1-6.

GORDON, IRA K., & MICHAEL S. KENT. 2008."Veterinary radiation therapy: review and current state of the art. *Jounal of the Ameican Animal Hospital Association 42.2: 94-1009*

GORLICK, R. & KHANNA, C. 2010. Osteosarcoma. *J Bone Miner Res,* 25**,** 683-91.

GREENBERG, R. A. 2005. Telomeres, crisis and cancer. *Curr Mol Med,* 5**,** 213-8.

GREIDER, C. W. & BLACKBURN, E. H. 1985. Identification of a specific telomere terminal transferase activity in Tetrahymena extracts. *Cell,* 43**,** 405-13.

GRIFFITH, J. D., COMEAU, L., ROSENFIELD, S., STANSEL, R. M., BIANCHI, A., MOSS, H. & DE LANGE, T. 1999. Mammalian telomeres end in a large duplex loop. *Cell,* 97**,** 503-14.

GROSSE, N., VAN LOON, B. & ROHRER BLEY, C. 2014. DNA damage response and DNA repair - dog as a model? *BMC Cancer,* 14**,** 203.

GUSTAVSSON, I. 1975. The chromosome of the dogs. *Hereditas 51:* 187-189.

HACKETT, J. A. & GREIDER, C. W. 2002. Balancing instability: dual roles for telomerase and telomere dysfunction in tumorigenesis. *Oncogene,* 21**,** 619-26.

HALL, E. J., Giaccia, A. J. (2006). *Radiobiology for the Radiologist Sixth Edition*. Philadelphia, PA: Lippincott Williams and Wilkins.

HALL, J. S., IYPE, R., SENRA, J., TAYLOR, J., ARMENOULT, L., OGUEJIOFOR, K., LI, Y., STRATFORD, I., STERN, P. L., O'CONNOR, M. J., MILLER, C. J. & WEST, C. M. 2014. Investigation of radiosensitivity gene signatures in cancer cell lines. *PLoS One,* 9**,** e86329.

HANSEN, K. & KHANNA, C. 2004. Spontaneous and genetically engineered animal models; use in preclinical cancer drug development. *Eur J Cancer,* 40**,** 858-80.

HARLEY, C. B., FUTCHER, A. B. & GREIDER, C. W. 1990. Telomeres shorten during ageing of human fibroblasts. *Nature,* 345**,** 458-60.

HARRINGTON, L., ZHOU, W., MCPHAIL, T., OULTON, R., YEUNG, D. S., MAR, V., BASS, M. B. & ROBINSON, M. O. 1997. Human telomerase contains evolutionarily conserved catalytic and structural subunits. *Genes Dev,* 11**,** 3109-15.

HASTIE, N. D., DEMPSTER, M., DUNLOP, M. G., THOMPSON, A. M., GREEN, D. K. & ALLSHIRE, R. C. 1990. Telomere reduction in human colorectal carcinoma and with ageing. *Nature,* 346**,** 866-8.

HASTINGS, P. J., LUPSKI, J. R., ROSENBERG, S. M. & IRA, G. 2009. Mechanisms of change in gene copy number. *Nat Rev Genet,* 10**,** 551-64.

HAYFLICK, L. 1965. The Limited in Vitro Lifetime of Human Diploid Cell Strains. *Exp Cell Res,* 37**,** 614-36.

HAYFLICK, L. & MOORHEAD, P. S. 1961. The serial cultivation of human diploid cell strains. *Exp Cell Res,* 25**,** 585-621.

HELMAN, L. J. & MELTZER, P. 2003. Mechanisms of sarcoma development. *Nat Rev Cancer,* 3**,** 685-94.

HENDRY, J. H. & WEST, C. M. 1997. Apoptosis and mitotic cell death: their relative contributions to normal-tissue and tumour radiation response. *Int J Radiat Biol,* 71**,** 709-19.

HERBIG, U., JOBLING, W. A., CHEN, B. P., CHEN, D. J. & SEDIVY, J. M. 2004. Telomere shortening triggers senescence of human cells through a pathway involving ATM, p53, and p21(CIP1), but not p16(INK4a). *Mol Cell,* 14**,** 501-13.

HERSHEY, A. E., KURZMAN, I. D., FORREST, L. J., BOHLING, C. A., STONEROOK, M., PLACKE, M. E., IMONDI, A. R. & VAIL, D. M. 1999. Inhalation chemotherapy for macroscopic primary or metastatic lung tumors: proof of principle using dogs with spontaneously occurring tumors as a model. *Clin Cancer Res,* 5**,** 2653-9.

HOCKEMEYER, D., DANIELS, J. P., TAKAI, H. & DE LANGE, T. 2006. Recent expansion of the telomeric complex in rodents: Two distinct POT1 proteins protect mouse telomeres. *Cell,* 126**,** 63-77.

JACKSON, S. P. & BARTEK, J. 2009. The DNA-damage response in human biology and disease. *Nature,* 461**,** 1071-8.

JAFFE, N. 2009. Osteosarcoma: review of the past, impact on the future. The American experience. *Cancer Treat Res,* 152**,** 239-62.

KASER-HOTZ, B., SUMOVA, A., LOMAX, A., SCHNEIDER, U., KLINK, B., FIDEL, J. & BLATTMANN, H. 2002. A comparison of normal tissue complication probability of brain for proton and photon therapy of canine nasal tumors. *Vet Radiol Ultrasound,* 43**,** 480-6.

KATO, T. A., NAGASAWA, H., WEIL, M. M., GENIK, P. C., LITTLE, J. B. & BEDFORD, J. S. 2006a. gamma-H2AX foci after low-dose-rate irradiation reveal atm haploinsufficiency in mice. *Radiat Res,* 166**,** 47-54.

KATO, T. A., NAGASAWA, H., WEIL, M. M., LITTLE, J. B. & BEDFORD, J. S. 2006b. Levels of gamma-H2AX Foci after low-dose-rate irradiation reveal a DNA DSB rejoining defect in cells from human ATM heterozygotes in two at families and in another apparently normal individual. *Radiat Res,* 166**,** 443-53.

KEE, Y. & D'ANDREA, A. D. 2010. Expanded roles of the Fanconi anemia pathway in preserving genomic stability. *Genes Dev,* 24**,** 1680-94.

KHANNA, C., LINDBLAD-TOH, K., VAIL, D., LONDON, C., BERGMAN, P., BARBER, L., BREEN, M., KITCHELL, B., MCNEIL, E., MODIANO, J. F., NIEMI, S., COMSTOCK, K. E., OSTRANDER, E., WESTMORELAND, S. & WITHROW, S. 2006. The dog as a cancer model. *Nat Biotechnol,* 24**,** 1065-6.

KHANNA, C. & VAIL, D. M. 2003. Targeting the lung: preclinical and comparative evaluation of anticancer aerosols in dogs with naturally occurring cancers. *Curr Cancer Drug Targets,* 3**,** 265-73.

KIM, H. & D'ANDREA, A. D. 2012. Regulation of DNA cross-link repair by the Fanconi anemia/BRCA pathway. *Genes Dev,* 26, 1393-408.

KIM, H. S., KIM, S. C., KIM, S. J., PARK, C. H., JEUNG, H. C., KIM, Y. B., AHN, J. B., CHUNG, H. C. & RHA, S. Y. 2012. Identification of a radiosensitivity signature using integrative metaanalysis of published microarray data for NCI-60 cancer cells. *BMC Genomics,* 13**,** 348.

KIM, N. W., PIATYSZEK, M. A., PROWSE, K. R., HARLEY, C. B., WEST, M. D., HO, P. L., COVIELLO, G. M., WRIGHT, W. E., WEINRICH, S. L. & SHAY, J. W. 1994. Specific association of human telomerase activity with immortal cells and cancer. *Science,* 266**,** 2011-5.

KLEIN, H. L. 2008. The consequences of Rad51 overexpression for normal and tumor cells. *DNA Repair (Amst),* 7**,** 686-93.

KOW, K., THAMM, D. H., TERRY, J., GRUNERUD, K., BAILEY, S. M., WITHROW, S. J. & LANA, S. E. 2008. Impact of telomerase status on canine osteosarcoma patients. *J Vet Intern Med,* 22**,** 1366-72.

KUILMAN, T., MICHALOGLOU, C., MOOI, W. J. & PEEPER, D. S. 2010. The essence of senescence. *Genes Dev,* 24**,** 2463-79.

LANGFORD, C. F., FISCHER, P. E., BINNS, M. M., HOLMES, N. G. & CARTER, N. P. 1996. Chromosome-specific paints from a high-resolution flow karyotype of the dog. *Chromosome Res,* 4**,** 115-23.

LANSDORP, P. M. 2005. Major cutbacks at chromosome ends. *Trends Biochem Sci,* 30**,** 388-95.

LARUE, S. M., WITHROW, S. J., POWERS, B. E., WRIGLEY, R. H., GILLETTE, E. L., SCHWARZ, P. D., STRAW, R. C. & RICHTER, S. L. 1989. Limb-sparing treatment for osteosarcoma in dogs. *J Am Vet Med Assoc,* 195**,** 1734-44.

LEE, J. U., HOSOTANI, R., WADA, M., DOI, R., KOSIBA, T., FUJIMOTO, K., MIYAMOTO, Y., TSUJI, S., NAKAJIMA, S., NISHIMURA, Y. & IMAMURA, M. 1999. Role of Bcl-2 family proteins (Bax, Bcl-2 and Bcl-X) on cellular susceptibility to radiation in pancreatic cancer cells. *Eur J Cancer,* 35**,** 1374-80.

LEGARE, M. E., BUSH, J., ASHLEY, A. K., KATO, T. & HANNEMAN, W. H. 2011. Cellular and phenotypic characterization of canine osteosarcoma cell lines. *J Cancer,* 2**,** 262-70.

LIANG, F., HAN, M., ROMANIENKO, P. J. & JASIN, M. 1998. Homology-directed repair is a major double-strand break repair pathway in mammalian cells. *Proc Natl Acad Sci U S A,* 95**,** 5172-7.

LIN, T. T., LETSOLO, B. T., JONES, R. E., ROWSON, J., PRATT, G., HEWAMANA, S., FEGAN, C., PEPPER, C. & BAIRD, D. M. 2010. Telomere dysfunction and fusion during the progression of chronic lymphocytic leukemia: evidence for a telomere crisis. *Blood,* 116**,** 1899-907.

LINDBLAD-TOH, K., WADE, C. M., MIKKELSEN, T. S., KARLSSON, E. K., JAFFE, D. B., KAMAL, M., CLAMP, M., CHANG, J. L., KULBOKAS, E. J., 3RD, ZODY, M. C., MAUCELI, E., XIE, X., BREEN, M., WAYNE, R. K., OSTRANDER, E. A., PONTING, C. P., GALIBERT, F., SMITH, D. R., DEJONG, P. J., KIRKNESS, E., ALVAREZ, P., BIAGI, T., BROCKMAN, W., BUTLER, J., CHIN, C. W., COOK, A., CUFF, J., DALY, M. J., DECAPRIO, D., GNERRE, S., GRABHERR, M., KELLIS, M., KLEBER, M., BARDELEBEN, C., GOODSTADT, L., HEGER, A., HITTE, C., KIM, L., KOEPFLI, K. P., PARKER, H. G., POLLINGER, J. P., SEARLE, S. M., SUTTER, N. B., THOMAS, R., WEBBER, C., BALDWIN, J., ABEBE, A., ABOUELLEIL, A., AFTUCK, L., AIT-ZAHRA, M., ALDREDGE, T., ALLEN, N., AN, P., ANDERSON, S., ANTOINE, C., ARACHCHI, H., ASLAM, A., AYOTTE, L., BACHANTSANG, P., BARRY, A., BAYUL, T., BENAMARA, M., BERLIN, A., BESSETTE, D., BLITSHTEYN, B., BLOOM, T., BLYE, J., BOGUSLAVSKIY, L., BONNET, C., BOUKHGALTER, B., BROWN, A., CAHILL, P., CALIXTE, N., CAMARATA, J., CHESHATSANG, Y., CHU, J., CITROEN, M., COLLYMORE, A., COOKE, P., DAWOE, T., DAZA, R., DECKTOR, K., DEGRAY, S., DHARGAY, N., DOOLEY, K., DORJE, P., DORJEE, K., DORRIS, L., DUFFEY, N., DUPES, A., EGBIREMOLEN, O., ELONG, R., FALK, J., FARINA, A., FARO, S., FERGUSON, D., FERREIRA, P., FISHER, S., FITZGERALD, M., FOLEY, K., et al. 2005. Genome sequence, comparative analysis and haplotype structure of the domestic dog. *Nature,* 438**,** 803-19.

LITHNER, F. & PONTEN, J. 1966. Bovine fibroblasts in long-term tissue culture: chromosome studies. *Int J Cancer,* 1**,** 579-88.

LOPATINA, N. G., POOLE, J. C., SALDANHA, S. N., HANSEN, N. J., KEY, J. S., PITA, M. A., ANDREWS, L. G. & TOLLEFSBOL, T. O. 2003. Control mechanisms in the regulation of telomerase reverse transcriptase expression in differentiating human teratocarcinoma cells. *Biochem Biophys Res Commun,* 306**,** 650-9.

LORENZI, P. L., REINHOLD, W. C., RUDELIUS, M., GUNSIOR, M., SHANKAVARAM, U., BUSSEY, K. J., SCHERF, U., EICHLER, G. S., MARTIN, S. E., CHIN, K., GRAY, J. W., KOHN, E. C., HORAK, I. D., VON HOFF, D. D., RAFFELD, M., GOLDSMITH, P. K., CAPLEN, N. J. & WEINSTEIN, J. N. 2006. Asparagine synthetase as a causal, predictive biomarker for L-asparaginase activity in ovarian cancer cells. *Mol Cancer Ther,* 5**,** 2613-23.

LOUCAS, B. D. & GEARD, C. R. 1994. Kinetics of chromosome rejoining in normal human fibroblasts after exposure to low- and high-LET radiations. *Radiat Res,* 138**,** 352-60.

MACEWEN, E. G. 1990. Spontaneous tumors in dogs and cats: models for the study of cancer biology and treatment. *Cancer Metastasis Rev,* 9**,** 125-36.

MAHRHOFER, H., BURGER, S., OPPITZ, U., FLENTJE, M. & DJUZENOVA, C. S. 2006. Radiation induced DNA damage and damage repair in human tumor and fibroblast cell lines assessed by histone H2AX phosphorylation. *Int J Radiat Oncol Biol Phys,* 64**,** 573-80.

MARINA, N., GEBHARDT, M., TEOT, L. & GORLICK, R. 2004. Biology and therapeutic advances for pediatric osteosarcoma. *Oncologist,* 9**,** 422-41.

MARTIN, J. W., ZIELENSKA, M., STEIN, G. S., VAN WIJNEN, A. J. & SQUIRE, J. A. 2011. The Role of RUNX2 in Osteosarcoma Oncogenesis. *Sarcoma,* 2011**,** 282745.

MAYR, B., KRAMBERGER-KAPLAN, E., LOUPAL, G. & SCHLEGER, W. 1992. Analysis of complex cytogenetic alterations in three canine mammary sarcomas. *Res Vet Sci,* 53**,** 205-11.

MAYR, B., REIFINGER, M., WEISSENBOCK, H., SCHLEGER, W. & EISENMENGER, E. 1994. Cytogenetic analyses of four solid tumours in dogs. *Res Vet Sci,* 57**,** 88-95.

MCCLINTOCK, B. 1938. The Production of Homozygous Deficient Tissues with Mutant Characteristics by Means of the Aberrant Mitotic Behavior of Ring-Shaped Chromosomes. *Genetics,* 23**,** 315-76.

MCENTEE, M. C. 2006. Veterinary radiation therapy: review and current state of the art. *J Am Anim Hosp Assoc,* 42**,** 94-109.

MCKEVITT, T. P., NASIR, L., DEVLIN, P. & ARGYLE, D. J. 2002. Telomere lengths in dogs decrease with increasing donor age. *J Nutr,* 132**,** 1604S-6S.

MCMILLAN, T. J., TOBI, S., MATEOS, S. & LEMON, C. 2001. The use of DNA double-strand break quantification in radiotherapy. *Int J Radiat Oncol Biol Phys,* 49**,** 373-7.

MCWHIRTER, J. R., GALASSO, D. L. & WANG, J. Y. 1993. A coiled-coil oligomerization domain of Bcr is essential for the transforming function of Bcr-Abl oncoproteins. *Mol Cell Biol,* 13**,** 7587-95.

MENDOZA, S., KONISHI, T., DERNELL, W. S., WITHROW, S. J. & MILLER, C. W. 1998. Status of the p53, Rb and MDM2 genes in canine osteosarcoma. *Anticancer Res,* 18**,** 4449-53.

MERLO, D. F., ROSSI, L., PELLEGRINO, C., CEPPI, M., CARDELLINO, U., CAPURRO, C., RATTO, A., SAMBUCCO, P. L., SESTITO, V., TANARA, G. & BOCCHINI, V. 2008. Cancer incidence in pet dogs: findings of the Animal Tumor Registry of Genoa, Italy. *J Vet Intern Med,* 22**,** 976-84.

MEYERSON, M. 2007. Cancer: broken genes in solid tumours. *Nature,* 448**,** 545-6.

MEYERSON, M., COUNTER, C. M., EATON, E. N., ELLISEN, L. W., STEINER, P., CADDLE, S. D., ZIAUGRA, L., BEIJERSBERGEN, R. L., DAVIDOFF, M. J., LIU, Q., BACCHETTI, S., HABER, D. A. & WEINBERG, R. A. 1997. hEST2, the putative human telomerase catalytic subunit gene, is up-regulated in tumor cells and during immortalization. *Cell,* 90**,** 785-95.

MEYNE, J., RATLIFF, R. L. & MOYZIS, R. K. 1989. Conservation of the human telomere sequence (TTAGGG)n among vertebrates. *Proc Natl Acad Sci U S A,* 86**,** 7049-53.

MIRABELLO, L., TROISI, R. J. & SAVAGE, S. A. 2009. Osteosarcoma incidence and survival rates from 1973 to 2004: data from the Surveillance, Epidemiology, and End Results Program. *Cancer,* 115**,** 1531-43.

MIRZAYANS, R., ANDRAIS, B., SCOTT, A., WANG, Y. W. & MURRAY, D. 2013. Ionizing radiation-induced responses in human cells with differing TP53 status. *Int J Mol Sci,* 14**,** 22409-35.

MISITI, S., NANNI, S., FONTEMAGGI, G., CONG, Y. S., WEN, J., HIRTE, H. W., PIAGGIO, G., SACCHI, A., PONTECORVI, A., BACCHETTI, S. & FARSETTI, A. 2000. Induction of hTERT expression and telomerase activity by estrogens in human ovary epithelium cells. *Mol Cell Biol,* 20**,** 3764-71.

MITELMAN, F. 2000. Recurrent chromosome aberrations in cancer. *Mutat Res,* 462**,** 247-53.

MOKBEL, K. 2003. The evolving role of telomerase inhibitors in the treatment of cancer. *Curr Med Res Opin,* 19**,** 470-2.

MOLDOVAN, G. L. & D'ANDREA, A. D. 2009. FANCD2 hurdles the DNA interstrand crosslink. *Cell,* 139**,** 1222-4.

MORELLO, E., MARTANO, M. & BURACCO, P. 2011. Biology, diagnosis and treatment of canine appendicular osteosarcoma: similarities and differences with human osteosarcoma. *Vet J,* 189, 268-77.

MOVSAS, B., CHAPMAN, J. D., HANLON, A. L., HORWITZ, E. M., GREENBERG, R. E., STOBBE, C., HANKS, G. E. & POLLACK, A. 2002. Hypoxic prostate/muscle pO2 ratio predicts for biochemical failure in patients with prostate cancer: preliminary findings. *Urology,* 60**,** 634-9.

MOYZIS, R. K., BUCKINGHAM, J. M., CRAM, L. S., DANI, M., DEAVEN, L. L., JONES, M. D., MEYNE, J., RATLIFF, R. L. & WU, J. R. 1988. A highly conserved repetitive DNA sequence, (TTAGGG)n, present at the telomeres of human chromosomes. *Proc Natl Acad Sci U S A,* 85**,** 6622-6.

MUELLER, F., FUCHS, B. & KASER-HOTZ, B. 2007. Comparative biology of human and canine osteosarcoma. *Anticancer Res,* 27**,** 155-64.

MULLER, H. J. 1938. The remarking of chromosomes. *Net 13, 181-198*

MURATA, K., HANZAWA, K., KASAI, F., TAKEUCHI, M., ECHIGOYA, T. & YASUMOTO, S. 2007. Robertsonian translocation as a result of telomere shortening during replicative senescence and immortalization of bovine oviduct epithelial cells. *In Vitro Cell Dev Biol Anim,* 43**,** 235-44.

MURNANE, J. P. 2012. Telomere dysfunction and chromosome instability. *Mutat Res,* 730**,** 28-36.

MUYAL, J. P., SINGH, S. K. & FEHRENBACH, H. 2008. DNA-microarray technology: comparison of methodological factors of recent technique towards gene expression profiling. *Crit Rev Biotechnol,* 28**,** 239-51.

NAKAMURA, A. J., REDON, C. E., BONNER, W. M. & SEDELNIKOVA, O. A. 2009. Telomere-dependent and telomere-independent origins of endogenous DNA damage in tumor cells. *Aging (Albany NY),* 1**,** 212-8.

NASIR, L., DEVLIN, P., MCKEVITT, T., RUTTEMAN, G. & ARGYLE, D. J. 2001. Telomere lengths and telomerase activity in dog tissues: a potential model system to study human telomere and telomerase biology. *Neoplasia,* 3**,** 351-9.

NIEDERNHOFER, L. J., LAILAI, A. S. & HOEIJMAKERS, J. H. 2005. Fanconi anemia (cross) linked to DNA repair. *Cell,* 123, 1191-8.

NEUMAN, A. A., & REDDE, R. R. (2002). Telomere maintenance and cancer -- look, no telomerase. [Research Support, Non-U.S. Gov't Review]. *Nat Rev Cancer, 2*(11), 879-884. doi: 10.1038/nrc929

NOWELL, P. C. & HUNGERFORD, D. A. 1960. Chromosome studies on normal and leukemic human leukocytes. *J Natl Cancer Inst,* 25**,** 85-109.

O'BRIEN, S. J. & MURPHY, W. J. 2003. Genomics. A dog's breakfast? *Science,* 301**,** 1854-5.

OGAWA, K., MURAYAMA, S. & MORI, M. 2007. Predicting the tumor response to radiotherapy using microarray analysis (Review). *Oncol Rep,* 18**,** 1243-8.

OLOVNIKOV, A. M. 1973. A theory of marginotomy. The incomplete copying of template margin in enzymic synthesis of polynucleotides and biological significance of the phenomenon. *J Theor Biol,* 41**,** 181-90.

PANDITA, A., ZIELENSKA, M., THORNER, P., BAYANI, J., GODBOUT, R., GREENBERG, M. & SQUIRE, J. A. 1999. Application of comparative genomic hybridization, spectral karyotyping, and microarray analysis in the identification of subtype-specific patterns of genomic changes in rhabdomyosarcoma. *Neoplasia,* 1**,** 262-75.

PAOLONI, M., DAVIS, S., LANA, S., WITHROW, S., SANGIORGI, L., PICCI, P., HEWITT, S., TRICHE, T., MELTZER, P. & KHANNA, C. 2009. Canine tumor cross-species genomics uncovers targets linked to osteosarcoma progression. *BMC Genomics,* 10**,** 625.

PAOLONI, M. & KHANNA, C. 2008. Translation of new cancer treatments from pet dogs to humans. *Nat Rev Cancer,* 8**,** 147-56.

PAOLONI, M. C. & KHANNA, C. 2007. Comparative oncology today. *Vet Clin North Am Small Anim Pract,* 37**,** 1023-32; v.

PARSHAD, R., SANFORD, K. K. & JONES, G. M. 1983. Chromatid damage after G2 phase x-irradiation of cells from cancer-prone individuals implicates deficiency in DNA repair. *Proc Natl Acad Sci U S A,* 80**,** 5612-6.

PAWLIK, T. M. & KEYOMARSI, K. 2004. Role of cell cycle in mediating sensitivity to radiotherapy. *Int J Radiat Oncol Biol Phys,* 59**,** 928-42.

PINTO, A. E., ANDRE, S., PEREIRA, T., SILVA, G. & SOARES, J. 2006. DNA flow cytometry but not telomerase activity as predictor of disease-free survival in pT1-2/N0/G2 breast cancer. *Pathobiology,* 73**,** 63-70.

PINTO, A. E., MONTEIRO, P., SILVA, G., AYRES, J. V. & SOARES, J. 2005. Prognostic biomarkers in renal cell carcinoma: relevance of DNA ploidy in predicting disease-related survival. *Int J Biol Markers,* 20**,** 249-56.

POLITI, K. & PAO, W. 2011. How genetically engineered mouse tumor models provide insights into human cancers. *J Clin Oncol,* 29**,** 2273-81.

PROWSE, K. R. & GREIDER, C. W. 1995. Developmental and tissue-specific regulation of mouse telomerase and telomere length. *Proc Natl Acad Sci U S A,* 92**,** 4818-22.

PUCK, T. T. & MARCUS, P. I. 1956. Action of x-rays on mammalian cells. *J Exp Med,* 103**,** 653-66.

RABBITTS, T. H. 1994. Chromosomal translocations in human cancer. *Nature,* 372**,** 143-9.

RANKIN, K. S., STARKEY, M., LUNEC, J., GERRAND, C. H., MURPHY, S. & BISWAS, S. 2012. Of dogs and men: comparative biology as a tool for the discovery of novel biomarkers and drug development targets in osteosarcoma. *Pediatr Blood Cancer,* 58**,** 327-33.

RECEVEUR, A., ONG, J., MERLIN, L., AZGUI, Z., MERLE-BERAL, H., BERGER, R. & NGUYEN-KHAC, F. 2004. Trisomy 4 associated with double minute chromosomes and MYC amplification in acute myeloblastic leukemia. *Ann Genet,* 47**,** 423-7.

REDDEL, R. R., BRYAN, T. M., COLGIN, L. M., PERREM, K. T. & YEAGER, T. R. 2001. Alternative lengthening of telomeres in human cells. *Radiat Res,* 155**,** 194-200.

REIMANN, N., BARTNITZKE, S., NOLTE, I. & BULLERDIEK, J. 1999a. Working with canine chromosomes: current recommendations for karyotype description. *J Hered,* 90**,** 31-4.

REIMANN, N., NOLTE, I., BARTNITZKE, S. & BULLERDIEK, J. 1999b. Re: Sit, DNA, sit: cancer genetics going to the dogs. *J Natl Cancer Inst,* 91**,** 1688-9.

REIMANN, N., ROGALLA, P., KAZMIERCZAK, B., BONK, U., NOLTE, I., GRZONKA, T., BARTNITZKE, S. & BULLERDIEK, J. 1994. Evidence that metacentric and submetacentric chromosomes in canine tumors can result from telomeric fusions. *Cytogenet Cell Genet,* 67**,** 81-5.

REINHOLD, W. C., SUNSHINE, M., LIU, H., VARMA, S., KOHN, K. W., MORRIS, J., DOROSHOW, J. & POMMIER, Y. 2012. CellMiner: a web-based suite of genomic and pharmacologic tools to explore transcript and drug patterns in the NCI-60 cell line set. *Cancer Res,* 72**,** 3499-511.

RIVERA-CALZADA, A., SPAGNOLO, L., PEARL, L. H. & LLORCA, O. 2007. Structural model of full-length human Ku70-Ku80 heterodimer and its recognition of DNA and DNA-PKcs. *EMBO Rep,* 8**,** 56-62.

RODEL, C., HAAS, J., GROTH, A., GRABENBAUER, G. G., SAUER, R. & RODEL, F. 2003. Spontaneous and radiation-induced apoptosis in colorectal carcinoma cells with different intrinsic radiosensitivities: survivin as a radioresistance factor. *Int J Radiat Oncol Biol Phys,* 55**,** 1341-7.

ROGAKOU, E. P., PILCH, D. R., ORR, A. H., IVANOVA, V. S. & BONNER, W. M. 1998. DNA double-stranded breaks induce histone H2AX phosphorylation on serine 139. *J Biol Chem,* 273**,** 5858-68.

ROWELL, J. L., MCCARTHY, D. O. & ALVAREZ, C. E. 2011. Dog models of naturally occurring cancer. *Trends Mol Med,* 17**,** 380-8.

ROWLEY, J. D. 1998. The critical role of chromosome translocations in human leukemias. *Annu Rev Genet,* 32**,** 495-519.

ROWLEY, J. D. 2001. Chromosome translocations: dangerous liaisons revisited. *Nat Rev Cancer,* 1**,** 245-50.

SANDBERG, A. A. 2002. Cytogenetics and molecular genetics of bone and soft-tissue tumors. *Am J Med Genet,* 115**,** 189-93.

SANDERS, R. P., DRISSI, R., BILLUPS, C. A., DAW, N. C., VALENTINE, M. B. & DOME, J. S. 2004. Telomerase expression predicts unfavorable outcome in osteosarcoma. *J Clin Oncol,* 22**,** 3790-7.

SARBIA, M., OTT, N., PUHRINGER-OPPERMANN, F. & BRUCHER, B. L. 2007. The predictive value of molecular markers (p53, EGFR, ATM, CHK2) in multimodally treated squamous cell carcinoma of the oesophagus. *Br J Cancer,* 97**,** 1404-8.

SARTHY, J., BAE, N. S., SCRAFFORD, J. & BAUMANN, P. 2009. Human RAP1 inhibits non-homologous end joining at telomeres. *EMBO J,* 28**,** 3390-9.

SCHULZ-ERTNER, D., JAKEL, O. & SCHLEGEL, W. 2006. Radiation therapy with charged particles. *Semin Radiat Oncol,* 16**,** 249-59.

SCHWARTZ, J. L. 1992. The radiosensitivity of the chromosomes of the cells of human squamous cell carcinoma cell lines. *Radiat Res,* 129**,** 96-101.

SCHWARTZ, J. L. 1998. Alterations in chromosome structure and variations in the inherent radiation sensitivity of human cells. *Radiat Res,* 149**,** 319-24.

SCOTT, D. 2004. Chromosomal radiosensitivity and low penetrance predisposition to cancer. *Cytogenet Genome Res,* 104**,** 365-70.

SCOTT, D., SPREADBOROUGH, A. R., JONES, L. A., ROBERTS, S. A. & MOORE, C. J. 1996. Chromosomal radiosensitivity in G2-phase lymphocytes as an indicator of cancer predisposition. *Radiat Res,* 145**,** 3-16.

SELDEN, J. R., MOORHEAD, P. S., OEHLERT, M. L. & PATTERSON, D. F. 1975. The Giemsa banding pattern of the canine karyotype. *Cytogenet Cell Genet,* 15**,** 380-7.

SELVARAJAH, G. T. & KIRPENSTEIJN, J. 2010. Prognostic and predictive biomarkers of canine osteosarcoma. *Vet J,* 185**,** 28-35.

SHAFFER, D. R. & PANDOLFI, P. P. 2006. Breaking the rules of cancer. *Nat Med,* 12**,** 14-5.

SHARPLESS, N. E. & DEPINHO, R. A. 2006. The mighty mouse: genetically engineered mouse models in cancer drug development. *Nat Rev Drug Discov,* 5**,** 741-54.

SHAY, J. W. & BACCHETTI, S. 1997. A survey of telomerase activity in human cancer. *Eur J Cancer,* 33**,** 787-91.

SHAY, J. W. & WRIGHT, W. E. 2011. Role of telomeres and telomerase in cancer. *Semin Cancer Biol,* 21**,** 349-53.

SHAY, J. W., WRIGHT, W. E. & WERBIN, H. 1993. Toward a molecular understanding of human breast cancer: a hypothesis. *Breast Cancer Res Treat,* 25**,** 83-94.

SHELDEN, JR..,MOORHEAD. PS., OEHLERT. ML., PATTERSON. DF.1975. The gimesa banding pattern of the canine karyotype. *Cytogenet Cell Genet 15:* 380-387

SHOEMAKER, R. H. 2006. The NCI60 human tumour cell line anticancer drug screen. *Nat Rev Cancer,* 6**,** 813-23.

SHOENEMAN, J. K., EHRHART, E. J., 3RD, EICKHOFF, J. C., CHARLES, J. B., POWERS, B. E. & THAMM, D. H. 2012. Expression and function of survivin in canine osteosarcoma. *Cancer Res,* 72**,** 249-59.

SIEGEL, R., MA, J., ZOU, Z. & JEMAL, A. 2014. Cancer statistics, 2014. *CA Cancer J Clin,* 64**,** 9-29.

SINCLAIR, W. K. & MORTON, R. A. 1966. X-ray sensitivity during the cell generation cycle of cultured Chinese hamster cells. *Radiat Res,* 29**,** 450-74.

SIRZEN, F., NILSSON, A., ZHIVOTOVSKY, B. & LEWENSOHN, R. 1999. DNA-dependent protein kinase content and activity in lung carcinoma cell lines: correlation with intrinsic radiosensitivity. *Eur J Cancer,* 35**,** 111-6.

SMIDA, J., BAUMHOER, D., ROSEMANN, M., WALCH, A., BIELACK, S., POREMBA, C., REMBERGER, K., KORSCHING, E., SCHEURLEN, W., DIERKES, C., BURDACH, S., JUNDT, G., ATKINSON, M. J. & NATHRATH, M. 2010. Genomic alterations and allelic imbalances are strong prognostic predictors in osteosarcoma. *Clin Cancer Res,* 16**,** 4256-67.

SMITH, J., RIBALLO, E., KYSELA, B., BALDEYRON, C., MANOLIS, K., MASSON, C., LIEBER, M. R., PAPADOPOULO, D. & JEGGO, P. 2003. Impact of DNA ligase IV on the fidelity of end joining in human cells. *Nucleic Acids Res,* 31**,** 2157-67.

SPAGNOLO, L., RIVERA-CALZADA, A., PEARL, L. H. & LLORCA, O. 2006. Three-dimensional structure of the human DNA-PKcs/Ku70/Ku80 complex assembled on DNA and its implications for DNA DSB repair. *Mol Cell,* 22**,** 511-9.

SPARANO, J. A. & PAIK, S. 2008. Development of the 21-gene assay and its application in clinical practice and clinical trials. *J Clin Oncol,* 26**,** 721-8.

STEEL, G. G. 2001. The case against apoptosis. *Acta Oncol,* 40**,** 968-75.

STONE, D. M., JACKY, P. B. & PRIEUR, D. J. 1991. Cytogenetic evaluation of four canine mast cell tumors. *Cancer Genet Cytogenet,* 53**,** 105-12.

STORCHOVA, Z. & PELLMAN, D. 2004. From polyploidy to aneuploidy, genome instability and cancer. *Nat Rev Mol Cell Biol,* 5**,** 45-54.

SUEHIRO, Y., OKADA, T., ANNO, K., OKAYAMA, N., UENO, K., HIURA, M., NAKAMURA, M., KONDO, T., OGA, A., KAWAUCHI, S., HIRABAYASHI, K., NUMA, F., ITO, T., SAITO, T., SASAKI, K. & HINODA, Y. 2008. Aneuploidy predicts outcome in patients with endometrial carcinoma and is related to lack of CDH13 hypermethylation. *Clin Cancer Res,* 14**,** 3354-61.

SUSINI, T., AMUNNI, G., MOLINO, C., CARRIERO, C., RAPI, S., BRANCONI, F., MARCHIONNI, M., TADDEI, G. & SCARSELLI, G. 2007. Ten-year results of a prospective study on the prognostic role of ploidy in endometrial carcinoma: dNA aneuploidy identifies high-risk cases among the so-called 'low-risk' patients with well and moderately differentiated tumors. *Cancer,* 109**,** 882-90.

SUTHERLAND, B. M., BENNETT, P. V., SIDORKINA, O. & LAVAL, J. 2000a. Clustered damages and total lesions induced in DNA by ionizing radiation: oxidized bases and strand breaks. *Biochemistry,* 39**,** 8026-31.

SUTHERLAND, B. M., BENNETT, P. V., SIDORKINA, O. & LAVAL, J. 2000b. Clustered DNA damages induced in isolated DNA and in human cells by low doses of ionizing radiation. *Proc Natl Acad Sci U S A,* 97**,** 103-8.

TAKAI, H., SMOGORZEWSKA, A. & DE LANGE, T. 2003. DNA damage foci at dysfunctional telomeres. *Curr Biol,* 13**,** 1549-56.

TANAKA, H., ABE, S., HUDA, N., TU, L., BEAM, M. J., GRIMES, B. & GILLEY, D. 2012. Telomere fusions in early human breast carcinoma. *Proc Natl Acad Sci U S A,* 109**,** 14098-103.

TANAKA, H., BEAM, M. J. & CARUANA, K. 2014. The presence of telomere fusion in sporadic colon cancer independently of disease stage, TP53/KRAS mutation status, mean telomere length, and telomerase activity. *Neoplasia,* 16**,** 814-23.

TAYLOR, N., SHIFRINE, M., WOLF, H. G. & TROMMERSHAUSEN-SMITH, A. 1975. Canine osteosarcoma karyotypes from an original tumor, its metastasis, and tumor cells in tissue culture. *Transplant Proc,* 7**,** 485-93.

TERASIMA, T. & TOLMACH, L. J. 1963. Variations in several responses of HeLa cells to x-irradiation during the division cycle. *Biophys J,* 3**,** 11-33.

THACKER, J. & ZDZIENICKA, M. Z. 2004. The XRCC genes: expanding roles in DNA double-strand break repair. *DNA Repair (Amst),* 3**,** 1081-90.

THOMAS, R., DUKE, S. E., BLOOM, S. K., BREEN, T. E., YOUNG, A. C., FEISTE, E., SEISER, E. L., TSAI, P. C., LANGFORD, C. F., ELLIS, P., KARLSSON, E. K., LINDBLAD-TOH, K. & BREEN, M. 2007. A cytogenetically characterized, genome-anchored 10-Mb BAC set and CGH array for the domestic dog. *J Hered,* 98**,** 474-84.

THOMAS, R., DUKE, S. E., KARLSSON, E. K., EVANS, A., ELLIS, P., LINDBLAD-TOH, K., LANGFORD, C. F. & BREEN, M. 2008. A genome assembly-integrated dog 1 Mb BAC microarray: a cytogenetic resource for canine cancer studies and comparative genomic analysis. *Cytogenet Genome Res,* 122**,** 110-21.

THOMAS, R., FIEGLER, H., OSTRANDER, E. A., GALIBERT, F., CARTER, N. P. & BREEN, M. 2003. A canine cancer-gene microarray for CGH analysis of tumors. *Cytogenet Genome Res,* 102**,** 254-60.

THOMAS, R., WANG, H. J., TSAI, P. C., LANGFORD, C. F., FOSMIRE, S. P., JUBALA, C. M., GETZY, D. M., CUTTER, G. R., MODIANO, J. F. & BREEN, M. 2009. Influence of genetic background on tumor karyotypes: evidence for breed-associated cytogenetic aberrations in canine appendicular osteosarcoma. *Chromosome Res,* 17**,** 365-77.

THOMPSON, L. H. 2012. Recognition, signaling, and repair of DNA double-strand breaks produced by ionizing radiation in mammalian cells: the molecular choreography. *Mutat Res,* 751**,** 158-246.

THOMPSON, S. L., BAKHOUM, S. F. & COMPTON, D. A. 2010. Mechanisms of chromosomal instability. *Curr Biol,* 20**,** R285-95.

TJIO, J. H. 1978. The chromosome number of man. *Am J Obstet Gynecol,* 130**,** 723-4.

TLSTY, T. D., ROMANOV, S. R., KOZAKIEWICZ, B. K., HOLST, C. R., HAUPT, L. M. & CRAWFORD, Y. G. 2001. Loss of chromosomal integrity in human mammary epithelial cells subsequent to escape from senescence. *J Mammary Gland Biol Neoplasia,* 6**,** 235-43.

TODARO, G. J. & GREEN, H. 1963. Quantitative studies of the growth of mouse embryo cells in culture and their development into established lines. *J Cell Biol,* 17**,** 299-313.

TORRES-ROCA, J. F., ESCHRICH, S., ZHAO, H., BLOOM, G., SUNG, J., MCCARTHY, S., CANTOR, A. B., SCUTO, A., LI, C., ZHANG, S., JOVE, R. & YEATMAN, T. 2005. Prediction of radiation sensitivity using a gene expression classifier. *Cancer Res,* 65**,** 7169-76.

TORRES-ROCA, J. F. & STEVENS, C. W. 2008. Predicting response to clinical radiotherapy: past, present, and future directions. *Cancer Control,* 15**,** 151-6.

TRASK, B. J. 2002. Human cytogenetics: 46 chromosomes, 46 years and counting. *Nat Rev Genet,* 3**,** 769-78.

TRIEB, K., LEHNER, R., STULNIG, T., SULZBACHER, I. & SHROYER, K. R. 2003. Survivin expression in human osteosarcoma is a marker for survival. *Eur J Surg Oncol,* 29**,** 379-82.

ULANER, G. A., HUANG, H. Y., OTERO, J., ZHAO, Z., BEN-PORAT, L., SATAGOPAN, J. M., GORLICK, R., MEYERS, P., HEALEY, J. H., HUVOS, A. G., HOFFMAN, A. R. & LADANYI, M. 2003. Absence of a telomere maintenance mechanism as a favorable prognostic factor in patients with osteosarcoma. *Cancer Res,* 63**,** 1759-63.

US pet ownership & demographics sourcebook. (2012). American Veterinary Medical Association. Web site: https://www.avma.org/KB/Resources/Statistics/Pages/Market-research-statistics-US-pet-ownership.aspx

VAIL, D. M. & MACEWEN, E. G. 2000. Spontaneously occurring tumors of companion animals as models for human cancer. *Cancer Invest,* 18**,** 781-92.

VAN 'T VEER, L. J., DAI, H., VAN DE VIJVER, M. J., HE, Y. D., HART, A. A., MAO, M., PETERSE, H. L., VAN DER KOOY, K., MARTON, M. J., WITTEVEEN, A. T., SCHREIBER, G. J., KERKHOVEN, R. M., ROBERTS, C., LINSLEY, P. S., BERNARDS, R. & FRIEND, S. H. 2002. Gene expression profiling predicts clinical outcome of breast cancer. *Nature,* 415**,** 530-6.

VAN STEENSEL, B., SMOGORZEWSKA, A. & DE LANGE, T. 1998. TRF2 protects human telomeres from end-to-end fusions. *Cell,* 92**,** 401-13.

VAZIRI, H. & BENCHIMOL, S. 1998. Reconstitution of telomerase activity in normal human cells leads to elongation of telomeres and extended replicative life span. *Curr Biol,* 8**,** 279-82.

VON ZGLINICKI, T. 2002. Oxidative stress shortens telomeres. *Trends Biochem Sci,* 27**,** 339-44.

VOSKOGLOU-NOMIKOS, T., PATER, J. L. & SEYMOUR, L. 2003. Clinical predictive value of the in vitro cell line, human xenograft, and mouse allograft preclinical cancer models. *Clin Cancer Res,* 9**,** 4227-39.

WARD, I. M. & CHEN, J. 2001. Histone H2AX is phosphorylated in an ATR-dependent manner in response to replicational stress. *J Biol Chem,* 276**,** 47759-62.

WATSON, J. D. 1972. Origin of concatemeric T7 DNA. *Nat New Biol,* 239**,** 197-201.

WEINRICH, S. L., PRUZAN, R., MA, L., OUELLETTE, M., TESMER, V. M., HOLT, S. E., BODNAR, A. G., LICHTSTEINER, S., KIM, N. W., TRAGER, J. B., TAYLOR, R. D., CARLOS, R., ANDREWS, W. H., WRIGHT, W. E., SHAY, J. W., HARLEY, C. B. & MORIN, G. B. 1997. Reconstitution of human telomerase with the template RNA component hTR and the catalytic protein subunit hTRT. *Nat Genet,* 17**,** 498-502.

WEINSTEIN, J. N. 2006. Spotlight on molecular profiling: "Integromic" analysis of the NCI-60 cancer cell lines. *Mol Cancer Ther,* 5**,** 2601-5.

WEST, C. M., DAVIDSON, S. E., ROBERTS, S. A. & HUNTER, R. D. 1997. The independence of intrinsic radiosensitivity as a prognostic factor for patient response to radiotherapy of carcinoma of the cervix. *Br J Cancer,* 76**,** 1184-90.

WILLIAMS, E. S., KRINGLER, R., PONNAIYA, B., HARDT, T., SCHROCK, E., LEES-MILLER, S., MEEK, K., ULLRICH, R. & BAILEY, S. M. 2009. Telomere dysfunction and DNA-PKcs deficiency: characterization and consequence. *Cancer Res,* 69, 2100-7.

WITHROW, S. J., THRALL, D. E., STRAW, R. C., POWERS, B. E., WRIGLEY, R. H., LARUE, S. M., PAGE, R. L., RICHARDSON, D. C., BISSONETTE, K. W., BETTS, C. W. & ET AL. 1993. Intra-arterial cisplatin with or without radiation in limb-sparing for canine osteosarcoma. *Cancer,* 71**,** 2484-90.

WITHROW, S.J.,& Vail, D. M. WITHROW&MacEwen's Small Aminal Clinical Oncology 846 (Saunders Elesevier, St. Louis, 2007)

WRIGHT, W. E. & SHAY, J. W. 2005. Telomere-binding factors and general DNA repair. *Nat Genet,* 37**,** 116-8.

YANG, F., O'BRIEN, P. C., MILNE, B. S., GRAPHODATSKY, A. S., SOLANKY, N., TRIFONOV, V., RENS, W., SARGAN, D. & FERGUSON-SMITH, M. A. 1999. A complete comparative chromosome map for the dog, red fox, and human and its integration with canine genetic maps. *Genomics,* 62**,** 189-202.

YAZAWA, M., OKUDA, M., SETOGUCHI, A., NISHIMURA, R., SASAKI, N., HASEGAWA, A., WATARI, T. & TSUJIMOTO, H. 1999. Measurement of telomerase activity in dog tumors. *J Vet Med Sci,* 61**,** 1125-9.

YU, T., MACPHAIL, S. H., BANATH, J. P., KLOKOV, D. & OLIVE, P. L. 2006. Endogenous expression of phosphorylated histone H2AX in tumors in relation to DNA double-strand breaks and genomic instability. *DNA Repair (Amst),* 5**,** 935-46.

ZHOU, B. B. & ELLEDGE, S. J. 2000. The DNA damage response: putting checkpoints in perspective. *Nature,* 408**,** 433-9.

ZHOU, L., YUAN, R. & SERGGIO, L. 2003. Molecular mechanisms of irradiation-induced apoptosis. *Front Biosci,* 8**,** d9-19.

CHAPTER 2

CHARACTERIATIONS OF CHROMOSOME ABERRATIONS AND TELOMERE DYSFUNCTION IN CANINE OSTEOSARCOMA CELLS

Summary

Due to its high mortality rate, canine OSA needs new treatment strategies, such as molecular target therapy. Identifying common characteristics in canine OSA cell lines may provide new insight and facilitate development of novel therapeutic targets. Previously, malignant canine cancer cells were reported to exhibit aberrant metacentric chromosomes, likely representing end-to-end chromosomal fusion events (Robertsonian translocations). Telomeres play an important role in the maintenance of chromosome integrity, and their dysfunction can result in chromosome fusions. Here, we hypothesized that chromosome aberrations involving uncapped telomeres may be a common feature of canine OSA cells. To test this hypothesis, we used a set of canine OSA cell lines, including eight established cell lines and ten primary cell cultures to evaluate chromosome number and frequency of metacentric chromosome in metaphase spreads, as well as FISH with a telomere specific probe. We also assessed factors associated with telomere maintenance and function, including telomerase activity, telomere-dysfunction induced foci (TIFs), and expression of a DNA repair protein required for mammalian telomeric end-capping (specifically DNA-PKcs). Despite variable chromosome numbers, proliferation rates and radiosensitivities, all eight canine OSA cell lines displayed increased frequencies of metacentric chromosomes and exhibited numerous telomere aberrations which included interstitial telomeric sequences and telomere fusions (telomere signals at the point of fusion, in this case in the centromeric regions). D17, the oldest canine OSA cell line used in the study, showed the highest

frequency of telomere aberrations (51.4 per cell) and metacentric chromosomes (43.2 per cell; 55% of average chromosome of 79). Further, all OSA cell lines were telomerase positive and showed no correlation between telomere aberrations and other telomere associated factors analyzed. To better characterize the telomere dysfunction associated with canine OSA, we investigated telomere aberrations in primary cultures from ten spontaneous canine OSAs, as well as the effects of long-term culture. Seven of the ten primary samples displayed no increase in frequency of metacentric chromosomes, while three of the ten samples did have elevated levels (11.5 per cell in the highest primary culture). However, no telomere signals were present at the involved centromeric regions. Telomere aberrations were observed in all of the primary cultures, but the number was relatively small (1.87 per cell in the highest primary culture). Interestingly, we found that metacentric chromosome frequencies increased in one primary OSA culture with increasing passage in culture. In contrast, metacentric chromosomes did not accumulate with long-term culture of non-cancerous canine fibroblasts, or DNA repair deficient mouse fibroblasts (homozygous ATM gene deficiency). Together, these results suggested that metacentric chromosomes and telomere dysfunction are characteristics of canine OSA. Therefore, targeting of these unique telomere aberrations has the potential for both improving diagnosis of canine OSA and developing novel treatment strategies.

Introduction

Canine OSA is the most common malignant bone tumor that serves as model for human OSA because the two are remarkably similar (Vail and MacEwen, 2000). High metastasis rate and aggressive local behavior remain poor indicators of the prognosis for this cancer type (Jaffe, 2009, Mueller et al., 2007). Even with aggressive treatments, 72% of dogs die as a result of metastasis

within the first two years of diagnosis (Dernell, 2007). Due to the high mortality rate related to OSA, new and more effective treatment strategies have been discussed, such as molecular targeted therapy which is necessary to improve the prognosis in canine patients with OSA. The study of naturally occurring OSA in dogs is increasingly considered as an approach to identify novel relevant tumor targets that have been missed through the study of the human OSA alone (Rankin et al., 2012, Paoloni and Khanna, 2008).

Chromosome aberrations have been appreciated as valuable biomarkers of carcinogenesis (Albertson et al., 2003). The correlation of chromosomal aberrations with clinical behavior of human cancer is widely recognized as an approach for developing novel means for diagnosis, prognosis, and therapeutic design. In human OSA, the high degree of aneuploidy, amplification, and multiple unbalanced chromosomal rearrangements characterized as chromosomal instability have been shown, which is known as the hallmarks of most solid tumors (Albertson et al., 2003). Unfortunately, no specific chromosome aberrations that play an important role in tumor progression of human OSA have been identified. Aneuploidy and increased number of metacentric chromosomes, which are morphologically irregular chromosome types in the normal acrocentric chromosomes of the dog, have been found in various canine cancer cell lines including OSA (Taylor et al., 1975, Thomas et al., 2009, Reimann et al., 1999). The metacentric chromosomes likely represent end-to-end chromosomal fusion events (Robertsonian translocations). Despite its recurrent observation in canine cancer cells, the biological and clinical significance of the observed cytogenetic abnormalities have not been thoroughly investigated.

Chromosomal instability has been shown to be induced by aberrant chromosome segregation during mitosis, resulting from many known mechanisms, including centromere dysfunction, centromere amplification, defective spindle check-point control and telomere

dysfunction (Bakhoum and Compton, 2012, Storchova and Pellman, 2004). However, the mechanisms that cause chromosome instability in solid tumors are currently not well understood. Chromosome instability is a well-known characteristic of numerous cancer predisposition syndromes linked to DNA repair pathways, such as Ataxia Telangiectasia (AT) (van Gent et al., 2001). The Ataxia Telangiectasia mutated (ATM) gene, which is responsible for AT, plays a major role in the network of signal transduction initiated by DNA double strand breaks (DSBs) (Cornforth and Bedford, 1985, Shiloh, 2001). Cells derived from AT individuals are known to be extremely sensitive to ionizing radiation and display chromosome abnormalities with the form of end-end associations involving telomeres, which is also seen in ATM deficient mouse cells (Kojis et al., 1991, Hande et al., 2001).

Telomeres, elongated by the enzyme telomerase, are nucleoprotein structures that protect the ends of linear chromosomes from DNA degradation and fusion and importantly, prevent them from being interpreted as DSBs (Bailey, 2008). Telomere dysfunction resulting from critically eroded or unprotected telomeres can lead to telomere fusion and chromosome instability (Bailey and Murnane, 2006, Desmaze et al., 2003). Defects in the proteins required for telomeric end capping structure and function, such as TRF2 and DNA-PK, are known to result in unprotected telomeres and telomere fusions (van Steensel et al., 1998, Bailey et al., 1999). In subsequent cell divisions, telomere fusion can trigger cycles of breakage-fusion-bridge (B/F/B) that can lead to chromosome instabilities and reflect those frequently found in cancer (Frias et al., 2012). In addition, recently, some reports showed evidence that telomere fusions are present in human cancers, including breast cancer, chronic lymphocytic leukemia (CLL), and sporadic colon cancer (Tanaka et al., 2012, Lin et al., 2010).

The Robertsonian translocation has also been observed in specific strains during evolution in mice (e.g. *Mus musculus domesticus*) and cows (e.g. *Japanese black*), which have only acrocentric autosomes in normal karyotypes (Nachman and Searle, 1995, Geshi et al., 1996). It has been also described that mouse embryonic fibroblasts and bovine fibroblasts showed increased number of the Robertsonina tralnslocations during long term culture (Todaro and Green, 1963, Lithner and Ponten, 1966). These chromosomes are known to result from centric fusions, where no detectable telomere signals by telomere FISH are present at the centromeric regions of fused chromosomes (Catalan et al., 2000, Garagna et al., 2001, Murata et al., 2007). In contrast, there are no reports showing the Robertsonian fusion in any specific breeds of dogs. In a previous study on dogs, SV-40 transfection increased aberrant karyotype of telomeric fusions, suggesting under p53 and Rb suppression the chromosome aberrations are caused by telomere dysfunctions in dogs (Reimann et al., 1994). However, no report has demonstrated that the telomere fusions are present in canine cancer. Detailed characterizations of canine cancer cells should provide better understanding of the telomere dysfunctions in dogs.

In this study, we hypothesized that chromosome aberrations involving uncapped telomeres may be a common feature of canine OSA cells. Common characteristics will provide insights into improved clinical management, such as the development of novel therapeutic targets, not only for dogs, but with a potential relevance for humans as well. Recently, a study reported the significant differences in cellular characteristics such as anchorage-independent growth in soft agar among canine OSA cell lines (Legare et al., 2011). This indicates that a set of the cell lines are necessary to understand its biology. Therefore, to test this hypothesis, we selected a panel of eight canine OSA cell lines and primary cultures from ten spontaneous canine OSAs and evaluated chromosome number, frequency of metacentric chromosomes, and telomere aberrations in canine

OSA cell. As other potential common features, basic characteristics including growth rates, radiosensitivity, and ploidy patterns in the eight canine OSA cell lines were also evaluated. Furthermore, we assessed telomere associated factors including telomerase activity, co-localization between DNA damage and telomere signals (TIFs), and expression of DNA-PKcs in the eight canine OSA cell lines. Finally, long-term culture effects on aberrant metacentric chromosomes with one of the canine OSA cultures, non-cancerous canine fibroblasts, or DNA repair deficient mouse fibroblasts (homozygous ATM gene deficiency) were examined.

Materials and Methods

Cell Culture

The canine OSA cell lines Abrams, D17, Grey, Hughes, and Moresco were supplied as previously described (Legare et al., 2011), and Gracie, MacKinley, and Vogel were kindly supplied by Flint Animal Cancer Center of Colorado State University (Fort Collins, CO, USA). All OSA cell lines were grown in Minimum Essential Medium (MEM, Thermo Fisher Scientific, Waltham, MA) supplemented with 10% fetal bovine serum (FBS; Sigma-Aldrich, St Louis, MO), 1% MEM vitamins, non-essential amino acids, sodium pyruvate, penicillin, streptomycin and fungizone. Cell lines were maintained at 37°C, humidified with 5% CO_2.

Ten tumor samples from dogs diagnosed with OSA, presenting with disease limited to the limb and the scapular region, were collected with the approval of Institutional Animal Care and Use Committee protocol with informed owner consent. The primary cultures were maintained in Minimum Essential Medium with 15% fetal bovine serum, 1% MEM vitamins, non-essential amino acids, sodium pyruvate, penicillin, streptomycin and fungizone at 37°C, humidified with 5% CO_2. Experiments were carried out using less than three passage cell cultures.

One of the primary canine OSA culture (OSA2), a normal primary canine fibroblast culture and four mouse primary fibroblast cultures were used for long time cultures. Normal canine skin fibroblasts were established from six-year-old female Beagle previously (Fujii et al., 2013), with approvals from the Committee for Animal Research and Welfare of Gifu University, Japan. Mouse fibroblast cultures were kindly provided from Dr. Nagasawa and Dr. Weil of Colorado State University. Four mouse skin fibroblast cell cultures were utilized in this study derived from two mouse strains both with and without ATM homozygous mutation; B6 ATM+/+, B6 ATM-/-, BALB/c ATM+/+ and BALB/c ATM-/-. ATM-/- were generated by introducing a truncation mutation into the gene at nucleotide 5790 (Barlow et al., 1996). Briefly, the cell strains were derived from ear punch biopsies. Ears were treated with collagenase for 40 min at 37 ºC and cultured in Minimum Essential Medium with 15% fetal bovine serum, penicillin, streptomycin and fungizone. For long time culture, cells were cultured in T-25 flasks. When the cells became 80% to 90% confluent, they were trypsinized, counted by coulter counter (Beckman Coulter, Brea, CA), and allocated to four parts; two new flasks and two frozen stocks. Two new flasks were placed back in culture for further passage and processing for chromosome analysis.

Chromosome Analysis

Cells were cultured with 0.1 mg/mL colcemid (GIBCO, Invitrogen, Carlsbad, CA) for 6 hours in order to harvest metaphase chromosomes. Samples were treated in hypotonic 75 mM KCl solution for 20 minutes at 37°C and fixed in 3:1 (methanol: acetic acid) fixation solution three times. Spread metaphase chromosomes were stained with Giemsa solution, and the chromosome number was observed under a BX51 microscope (Olympus, Tokyo, Japan). A minimum of 150 metaphase cells were analyzed for two separate experiments. At least 75 metaphase cells were

analyzed to count metacentric chromosomes per cell. For primary cell cultures, 100 metaphase cells were analyzed for a single experiment.

Cell Proliferation

In order to determine proliferation rates of the various cell lines, a five-day proliferation trial was performed. Five thousand cells were plated in T12.5 flasks. The number of cells was counted every 24 hours for five days by coulter counter (Beckman Coulter, Brea, CA). Cellular doubling times were then calculated by Graph Pad Prism 5 software (Graph Pad Software, La Jolla, CA) with the following formula;

$$Y(t) = A \times e^{K \times t}, Doubling\ time = 0.6932/K$$

Where A is initial number of cells and Y(t) is the number of cells at time t. Three independent experiments were carried out.

Gamma-ray Irradiation and Colony Formation Assay

Randomly dividing log phase cultures were irradiated with ^{137}Cs gamma-rays delivered at a dose rate of approximately 2.5 Gy per minute at room temperature (using a J.L. Shepherd Model Mark I-68 6000Ci ^{137}Cs irradiator). Sensitivity to radiation was evaluated by colony formation assays. Cells were exposed to gamma-rays, treated with trypsin-EDTA, and plated onto triplicate 100 mm culture dishes at appropriate cell density. After incubating for 7–14 days to allow colony formation, surviving colonies were rinsed with 0.9% NaCl, fixed with 100% ethanol, and stained by 0.1% crystal violet. Each colony consisting of more than 50 cells was scored as a survivor. At least three independent experiments were carried out. Survival curves were drawn using linear or linear-quadratic regression equations using Prism 5 software (Graph Pad Software). Survival fraction at 2 Gy was calculated using the Prism 5 software.

Particle Irradiation

The canine OSA cell lines Abrams, D17, Grey and Moresco were used for particle-irradiation experiments. Experiments were carried out at the National Institute of Radiological Science (NIRS) in Chiba, Japan. For heavy ion exposure, accelerated ions were irradiated using the Heavy Ion Medical Accelerator in Chiba (HIMAC) at room temperature. The details concerning the beam characteristics of the particle radiation, biological irradiation procedures, and dosimetry have been described elsewhere (Suzuki et al., 2000, Kamada et al., 2002). Briefly, accelerated monoenergetic iron ions have 500 MeV/nucleon of initial energy and 200 keV/μm of LET at the irradiated position. Carbon-ions were accelerated at 290 MeV/nucleon of initial energy and spread out with a ridge filter for 6 cm width of spread-out Bragg peak (SOBP). The monolayer cell culture was irradiated at the center (50 keV/μm of average LET) within the SOBP. Monoenergetic 70 MeV/n protons that were accelerated using the NIRS-930 cyclotron delivery port in C-8 have a LET value of 1.0 at the irradiated position. Dose rates for heavy ions and protons were set at 1 Gy/min. Colony formation assays were carried out as described above. We calculated relative biological effectiveness (RBE), which is defined as the ratio of dose of photons and charged particles inducing the same biological effects, based on D10 values. The D10 values represent doses required to achieve 10% survival, and were obtained from each survival curve using the Prism 5 software (Graph Pad Software).

Flow Cytometry

Cells were trypsinized, washed once with PBS and fixed in 70% ethanol. The fixed cells were collected by centrifugation and resuspended in 20 mg/mL propidium iodide and 500 mg/mL RNase A. The DNA contents were measured using FacsCalibur Flow Cytometer and the Cell Quest Pro program (BD Biosciences, Franklin Lakes, NJ). The ploidy levels of the eight canine

OSA and CHO (Chinese hamster ovary) cells were defined by the DNA peak value of the cells. G1 peak of CHO cells were used as the standard of 2N signal. Each of the cell lines were gated at 10,000 events via the flow cytometer.

Fluorescence in situ Hybridization (FISH) for Telomeres

Cells were synchronized in metaphase by 0.1 mg/mL colcemid treatment. Samples were incubated at 37°C in a hypotonic solution of 75 mM KCl for 20 minutes and fixed three times in 3:1(methanol: acetic acid) fixation solution. Cells dropped on slides were treated with 100 mg/mL RNAse A for ten minutes at 37°C, fixed in 4% formaldehyde, and rinsed in PBS. The slides were denatured by 70% formamide/2X saline sodium citrate (SCC) buffer (3 M NaCl, 0.3 M sodium citrate, pH 7.0) at 75°C for 2 minutes, followed by dehydration in ethanol series. Peptide-nucleicacid (PNA) telomere probes (DAKO, Carpinteria, CA) were denatured at 75°C for 5 minutes. The denatured probes were added to the fixed cells on slides and kept in a humidified dark chamber at 37°C for 3 hours. Slides were then washed in 70% formamide/2X saline sodium citrate (SCC) buffer at 32°C for 15 minutes and in sodium phosphate (PN) buffer (0.1 M NaH2PO4, 0.1 M Na2HPO4, pH 8.0 and 0.1% NP40) for 5 minutes. Lastly, slides were counterstained with Prolong Gold Antifade reagent (Invitrogen) with 4',6-diamidino-2-phenylindole, dihydrochloride (DAPI), and photographed using a BX61 microscope and a cooled CCD Exi Aqua camera (Q-imaging, BC, Canada).

Telomere Fusions

Telomere fusions from (a minimum of) 27 metaphase cells were scored for the presence of marker aberrations. Four types of telomere fusions; ITS^{1}, a single interstitial telomeric sequence, ITS^{2+}, multiple interstitial telomeric sequences, Rb^{1}, Robertsonian translocation with a telomere

signal in the centromere, and Rb^{2+}, Robertsonian translocation distinguished by more than one telomere signal in centromere region, were used for telomere fusion scoring. The telomere signal strength was measured by the line measurement function of Q-capture Pro software (Q-imaging). The diameter of telomeric signal was measured and the mean ratio (fusion points/chromosome ends) was obtained. At least 30 fusion points and 100 chromosome ends were analyzed.

Immuno-Telomere FISH with Phosphorylated Histone H2AX Immunocytochemistry

Cells were cultured for 24 hours on plastic chamber slides and then washed with PBS followed by fixation with 4% paraformaldehyde for 15 minutes. Following a second wash with PBS, cells were then permeabilized with 0.2% Triton X 100 in PBS for 10 minutes. Cells were then blocked in PBS with 10% goat serum overnight at 4°C. Following overnight incubation, the cells were incubated with a mouse monoclonal phosphorylated histone H2AX (γ-H2AX) antibody (Ser139) (Millipore, Billerica, MA) in 10% goat serum with PBS for one hour at 37°C. The cells were then washed three times for ten minutes each in PBS, followed by incubation for 1 hour at 37°C with Alexa 488 Fluor-conjugated goat antimouse antibody (Molecular Probes, Eugene, OR). The slides were then washed three times for ten minutes each in PBS. After 15 minutes of paraformaldehyde treatment, PNA-FISH was carried out as described above. The cells were cover slipped and visualized with Olympus BX51 equipped with a cooled CCD Exi Aqua camera (Q-imaging). Q-Capture Pro software (Q-imaging) was utilized to obtain images. Numbers of the colocalizations of telomere signals and H2AX were counted for a minimum of 50 cells.

Telomerase Activity

Telomerase activity was measured by the commercially available TRAPeze® Telomerase Detection Kit (Millipore) according to the manufacturer's instructions with the minor

modification. After further incubation at 30°C for 30 minutes, an additional step was held at 90°C for three minutes. The resulting mixture was subjected to PCR for 34 cycles of 30 seconds at 94°C, 30 seconds at 59°C, and one minute at 72°C. Final elongation was performed at 72°C for 3 minutes. PCR products were run on NOVEX 15% nondenaturing TBE-PAGE gels (Invitrogen), stained with 1:10,000 ethidium bromide in deionized water for 30 minutes, and destained in deionized water for an additional 30 minutes at room temperature. Visualization of PCR products was performed with a ChemiDocTM XRS Imager (Bio-Rad, Hercules, CA).

Western Blotting

Cells were lysed with M-PER Mammalian Protein Extraction Reagent (Thermo Fisher Scientific) and protease inhibitors, Halt Protease Inhibitor Cocktail Kit (Thermo Fisher Scientific). Protein extracts (20 mg per sample) were size-fractionated on NuPage® 4–12% Bis-Tris gels (Invitrogen), electro-transferred to nitrocellulose membranes (Bio-Rad) in a buffer (25 mM Tris, 192 mM glycine, 20% (v/v) methanol, and 0.01% SDS) at a current density of 3.0 mA/cm^2 for 16 hours at 4°C. The filters were blocked with Tris-buffered saline with 0.05% Tween 20 containing 2% (w/v) skim milk and reacted with the mouse anti-DNA-PKcs monoclonal antibody (Ab-4; Neomarkers, Fremonti, CA) (1:1000) for 2 hours at room temperature, followed by an incubation with goat anti-mouse IgG HRP conjugated antibody (1:10,000) for 1 hour at room temperature (Santa Cruz Biotechnology, Inc., Santa Cruz, CA). The immunoreactive signals were detected using SuperSignal Western Blotting Detection Kit (Thermo Fisher Scientific) and ChemiDocTM XRS+ System (Bio-Rad). Protein expression from band strength was analyzed by Image Lab software (Bio-Rad).

ATM Genotyping

ATM genotyping was performed on DNA extracted from the 30th passage of mice fibroblast cultures. PCR amplification of genomic DNA using a protocol described previously (Liao et al., 1999) with some modification in the PCR condition. The three-primer set; GACTTCTGTCAGATGTTGCTGCC (ATM-F), CGAATTTGCAGGAGTTGCTGAG (ATM-B), and GGGTGGGATTAGATAAATGCCTG (ATM-Neo) and genomic DNA with ATM heterozygous mutation were used. This set yields a 161-bp amplimer from the wild-type ATM allele and a 441-bp amplimer from the knockout allele. The conditions of PCR was 94°C for 4 min, 35 cycles at 94°C for 45sec and 57°C for 45 sec, 1 min and 72°C for 45sec, and 72°C 7 min. PCR products were gel electrophoresed on a 2.0% agarose gel and stained with 1:10,000 ethidium bromide. Visualization of PCR products was performed with a ChemiDocTM XRS Imager (Bio-Rad).

Statistical Analysis

For statistical analysis, Graph Pad Prism 5 software (Graph Pad Software) was used. To test the long culture effects, the comparisons of telomere aberrations and numbers of metacentric chromosomes between the lowest and highest passages in canine and mouse fibroblasts were carried out using an unpaired t-test with Welch's correction with a two sided levels. The comparisons of those among different passages in canine OSA cultures were carried out using non-parametric Kruskal-Wallis test. The D'Agostino-Pearson test was used to test if the values are normal distribution. P values of less than 0.05 were considered statistically significant.

Results

Cellular Doubling Times and Chromosome Abnormality in Canine OSA Cell Lines

Eight canine OSA cell lines were characterized first with a cell proliferation assay, a chromosome analysis and a DNA ploidy pattern (Table 2.1). The doubling times were approximately 18 hours for Grey, Gracie and Hughes, 22 hours for D17, 27 hours for Abrams and MacKinley, and 36 hours for Vogel. Wide ranges of chromosome numbers were seen in Abrams and D17, and bimodal distributions were observed. The cell lines Grey, Hughes and Moresco displayed relatively large average numbers of chromosomes, with modal numbers of 120, 130, and 80 respectively. Alternatively, Gracie, MacKinley and Vogel had stable numbers of chromosomes with smaller averages. The frequency and distribution of chromosome numbers in hypodiploidy (less than 78 chromosomes) and hyperploidy (more than 78 chromosomes) are presented in Figure 2.1. All canine OSA cell lines showed increased numbers of metacentric chromosomes resulting from centric fusion events (Table 2.1). Frequencies of metacentric chromosomes were especially high in D17 (55%) compared to the other cell lines: 24% for Abrams, 13% for Grey, 6% for Gracie, 14% for Hughes, 38% for Moresco, 27% for MacKinley, and 12% for Vogel. We determined the DNA content of the cell populations by flow cytometry (Table 2.1). A comparison between flow cytometry and chromosome number distribution by a metaphase analysis was made, and we found a relationship between abnormal ploidy and increased chromosome numbers.

Cellular Radiosensitivity in Canine OSA Cell Lines with Photon, Proton, and Heavy ion

Figure 2.2 shows dose-response survival curves for the cell-killing effect on exponentially growing the eight kinds of canine OSA cell lines irradiated with gamma-rays. Radionsensitivities among the cell lines were not uniform (Figure 2.2). Abrams, D17, Gracie and

Table 2.1: Characteristics in eight canine OSA cell liens.

OSA Cell Line	No. of Chromosomes per cell*	No. of Metacentric Chromosomes per cell**	Radio-sensitivity (SF2)***	Cell Doubling Time (hours)	Ploidy Pattern by Flow Cytometry
Abrams	85.8±25.2	20.9±8.6	0.65	27.2	Triploid
D 17	79.1±25.4	43.2±14.2	0.70	22.2	Triploid
Grey	112.1±26.8	14.8±5.1	0.21	18.1	Tetraploid
Gracie	74.7±4.8	4.3±2.5	0.84	19.2	Diploid
Hughes	126.0±18.0	18.2±3.4	0.07	17.9	Tetraploid
Moresco	82.4±15.9	30.9±4.9	0.81	22.1	Triploid
MacKinley	58.2±5.1	15.7±3.2	0.49	27.6	Diploid
Vogel	71.7±6.3	8.5±2.9	0.22	35.9	Diploid

*Mean ± SD of chromosome number per cell from more than 150 metaphases
**Mean ± SD of metacentrics per cell from more than 75 metaphases.
***SF2: The survival fraction after 2 Gy. Calculated by Graph Pad Prism 5 with linear or linear quadratic regression.

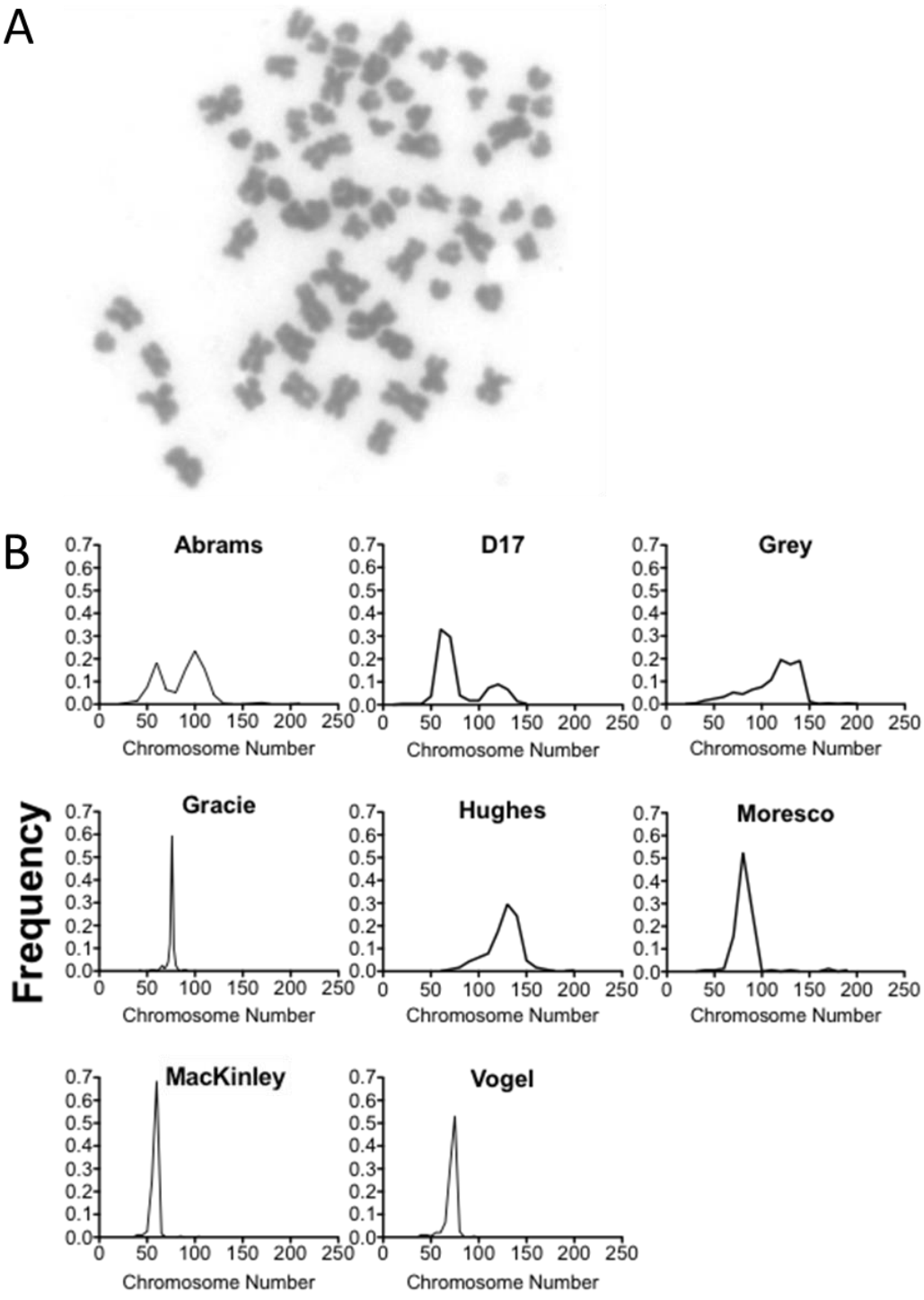

Figure 2.1: *Chromosome analysis by a classical cytogenetic assay in the eight canine OSA cell lines.* (A) Representative image of metaphase spread from D17. (B) Distribution of chromosome number. The data given is derived from the analysis of at least 150 metaphase chromosomes. Chromosome modes for the canine OSA cell lines are as follows; Abrams: (60, 100), D17: (60, 120), Grey: (120), Gracie: (75), Hughes: (130), Moresco: (80), MacKinley: (60), and Vogel: (75).

Moresco were quite resistant to ionizing radiation, while Grey, Hughes, MacKinley and Vogel were relatively more radiosensitive. The SF2 values (survival fraction at 2 Gy) of each cell line ranged from 0.07 to 0.84 (Table 2.1).

Four canine OSA cell lines, Abrams, D17, Moresco and Grey were further used to investigate cell killing effects by particle radiations, as well as gamma-rays. The responses to high LET radiations were different between the radioresistant cell lines (Abrams, D17 and Moresco) and the radiosensitive cell line (Grey) (Figure 2.3). For the clinical setting heavy ion beam, it was observed that the carbon ion beam (LET at 50 keV/μm) significantly decreased cell survival fractions of the four canine OSA cell lines compared to gamma-rays. Iron-ion beams which have higher LET values (200 keV/μm) than carbon ion beams decreased the cell survivals further than the carbon ions in the three radioresistant cell lines (Abrams, D17 and Moresco). However, the radiosensitive cell line Grey showed similar cell survival for carbon and iron-ion irradiation. The proton cell survival curves showed similar profiles to those of gamma-rays for the four cell lines. In order to describe the increased effects of particle radiation, we calculated relative biological effectiveness (RBE) based on D10 value (the dose resulted in 10% cell survival) relative to gamma-rays (Figure 2.3b). The RBE values ranged 0.90-1.26 for proton, 1.56-2.10 for carbon-ion and 2.22-3.69 for iron-ion among the cell lines. The RBEs for iron ions in radiosensitive Grey was smaller than those in the three radioresistant cell lines (Figure 2.3b).

Telomere Aberrations in Canine OSA

Fluorescence in situ hybridization (FISH) with a PNA telomere probe revealed that all eight canine OSA cell lines exhibited numerous telomere fusions at the Robertsonian centric fusion points (Rb) and interstitial telomere sequences (ITSs) (Figure 2.4). Frequency distribution plots regarding the four types of telomere abnormalities in the eight cell lines is presented in

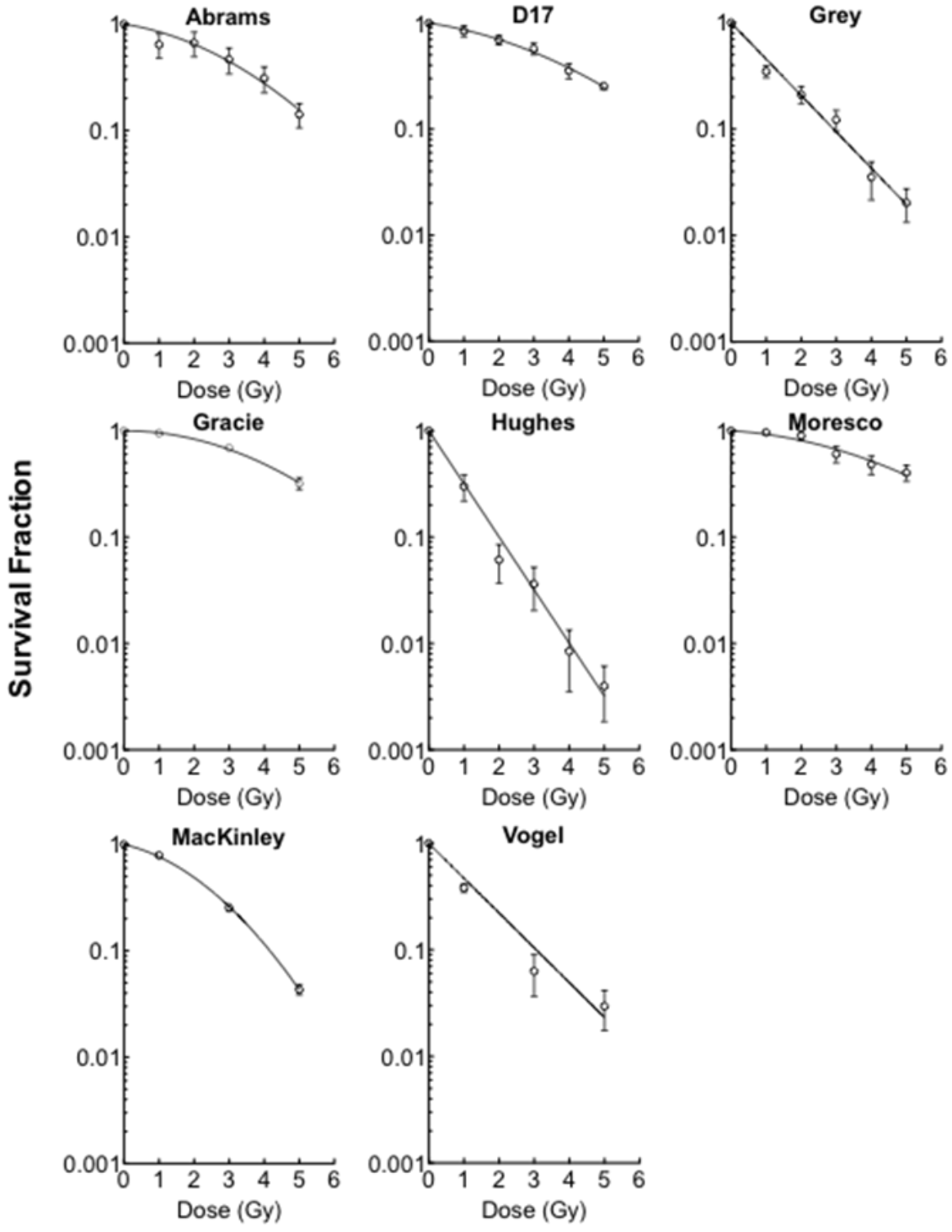

Figure 2.2: *Radiation induced survival curves in eight canine OSA cell lines.* Experiments were carried out at least three times and error bars indicate the standard error of the means.

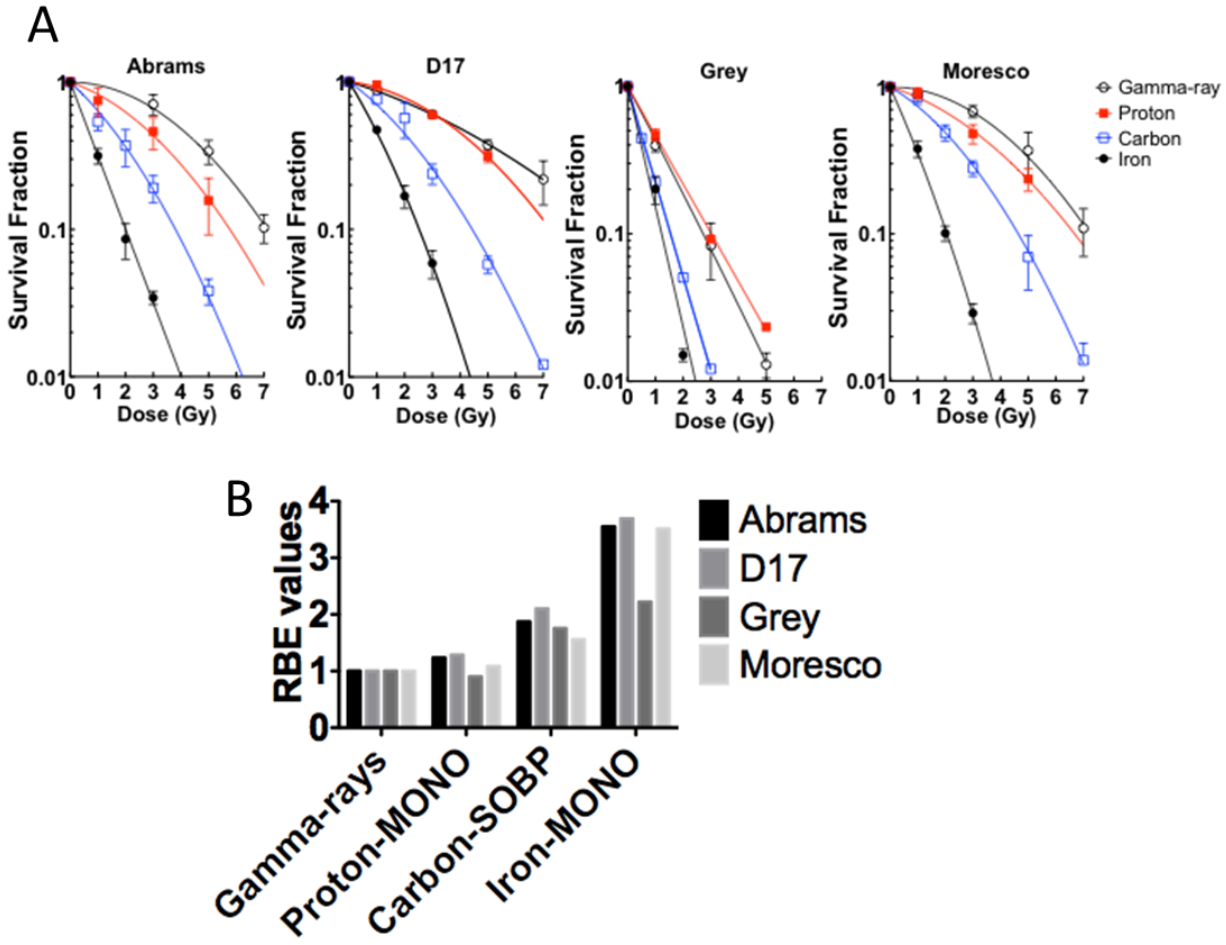

Figure 2.3: *Radiosensitivity by gamma-rays, proton, carbon ion irradiation in four canine OSA cell lines.* Survival curves for ionizing radiation exposures. Cells were irradiated to ionizing radiation having different LET. Black open circle: gamma-rays 0.2 keV/μm, red closed square: proton, LET 1 keV/μm, blue open square: carbon, LET 50 keV/μm; and black closed circle: iron LET 200 keV/μm. Experiments were carried out at least three times and error bars indicate the standard error of the means. (B) Relative biological effectiveness (RBE) values calculated from dose to get 10% survival fractions.

Figure 2.5. Notable differences in the distribution of telomere fusion types were observed within the eight OSA cell lines. In this analysis, maximum telomere fusions were 36 per cell for D17 representing a Rb^{2+} translocation. D17, Hughes and MacKinley lines were also characterized by the Rb^{2+} telomere fusions, while Gracie and Vogel tended to have ITS^{1} and ITS^{2+} translocations. The numbers of telomere fusions in Abrams, Grey and Moresco lines were small, with these cell lines primarily exhibiting an Rb^{-}, Robertsonian translocation with no telomere signal in centromeres. We observed different strengths of telomeric signals between fusion points and regular telomeric ends of chromosomes. In D17, Hughes, Moresco, and MacKinley, the telomere signals were stronger in fusion points than in telomeric ends (Table 2.2); however, those values in fusion points were less than two.

Telomere and H2AX Co-localization: TIFs

To assess whether telomere aberrations were elevated in nuclear foci of phosphorylated histone H2AX (γ-H2AX) resulting from DNA damage, we utilized γ-H2AX and FISH to assess co-localization. Figure 2.6a illustrates co-localization of telomere signals and γ-H2AX foci in interphase nuclei. In each canine OSA cell line, the average numbers of co-localizations were approximately 1.5 to 4.8 per nucleus (Table 2.2). The appearance of co-localization of telomere signals and γ-H2AX foci clearly shows DNA damage associated with these telomere fusions, and that the canine OSA cell lines have unstable telomeres.

DNA-PKcs Protein Expression in Canine OSA

We measured DNA-PKcs expression by western blot analysis (Figure 2.6b). Expressions of DNA-PKcs were not uniform among the cell lines. We observed less expression of DNA-PKcs protein in Hughes (20% of average) and Vogel (12% of average) cells. The expression of DNA-

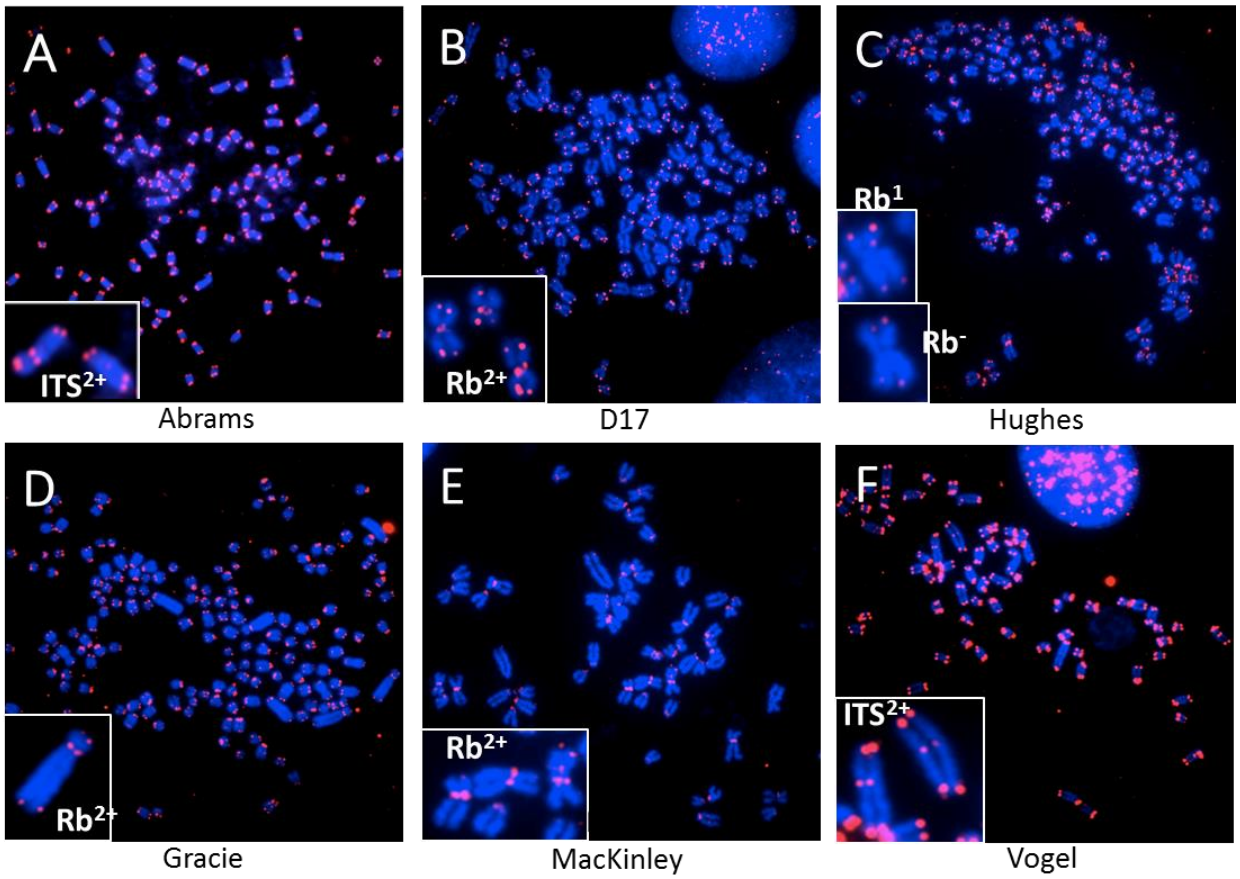

Figure 2.4: *Telomere abnormalities*. Representative FISH images of the eight canine OSA cell lines' metaphase chromosomes hybridized with probes against telomeres. Blue represents DNA staining by DAPI and red represents a telomere signal by Cy3. Note the abnormal telomere signals in the magnification box; interstitial telomere signals (A and F), more than one telomere signal in centromere regions (B, D and E), and one or no telomere signal (C) is observed. Note that at the end of chromosomes, there is no telomere signal present (B and E).

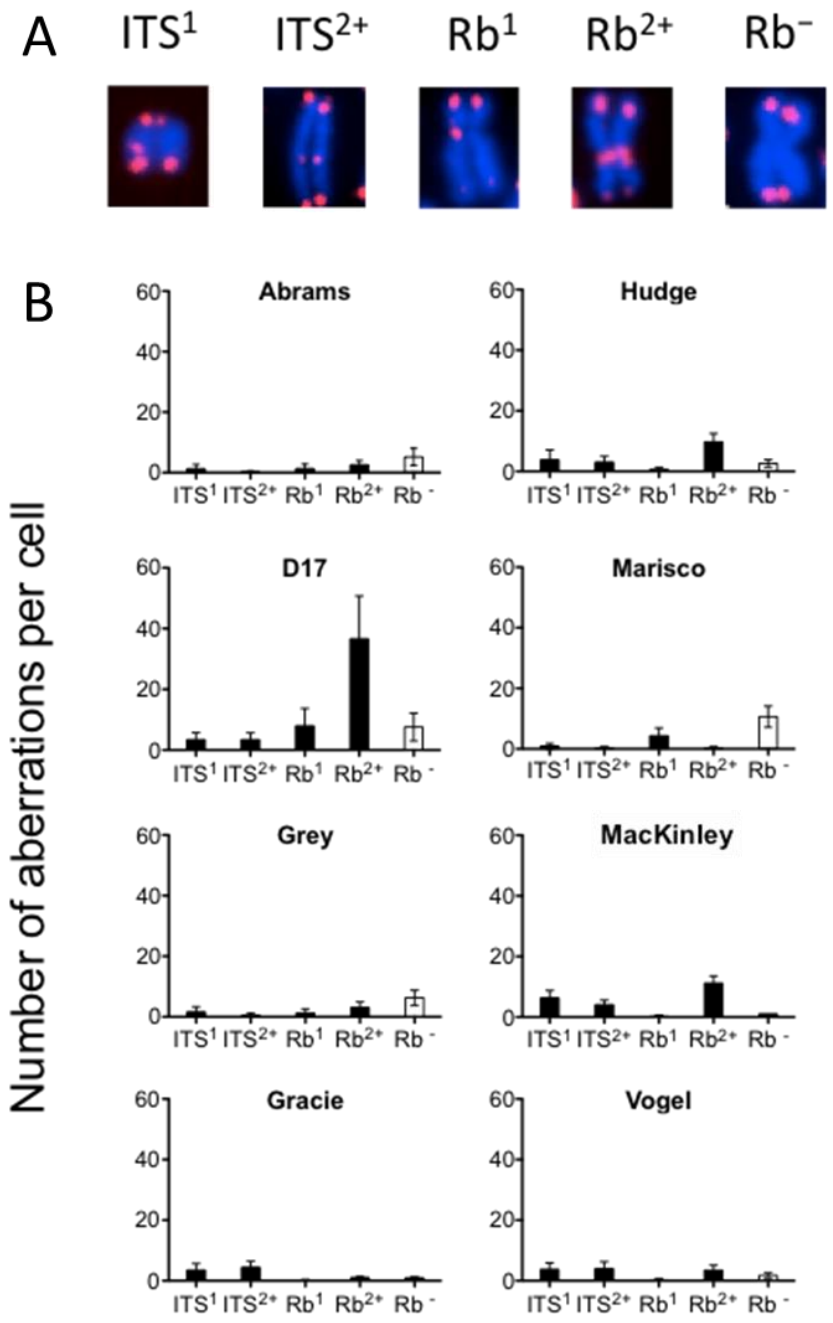

Figure 2.5: *Telomere abnormalities distinguished by Rb fusions and interstitial signals in OSA cells.* (A) Four types of telomere abnormalities; ITS^{1}, one interstitial telomeric sequence, ITS^{2+}, more than one interstitial telomeric sequences, Rb^{1}, Robertsonian translocation with one telomere signal in the centromere region, and Rb^{2+}, Robertsonian translocation with more than one telomere signals in the centromere region. Rb^{-} represents Robertsonian translocation with no telomere signal in the centromere region. (B) The number of telomere aberrations per each metaphase cell. Error bars indicate the standard error of the means.

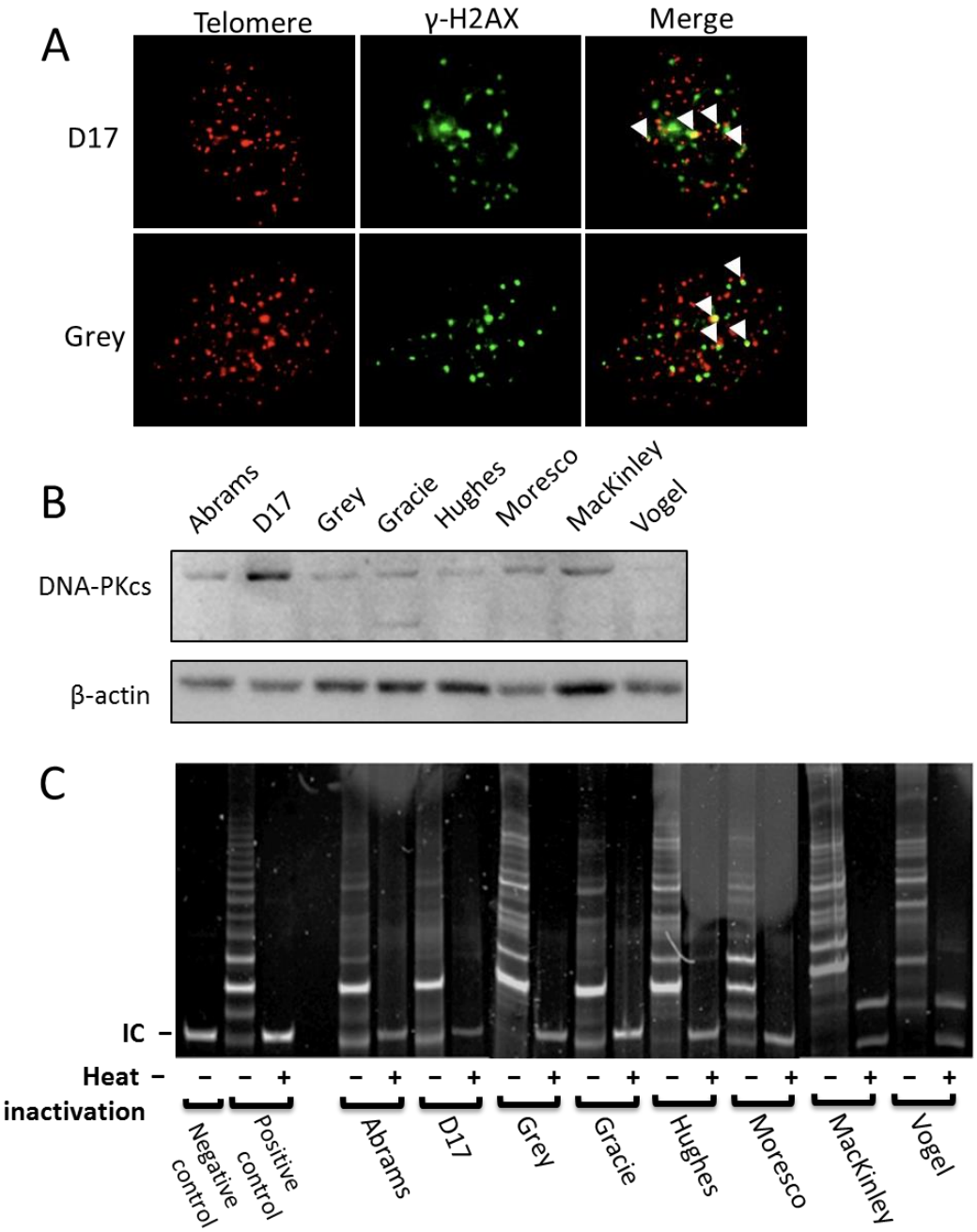

Figure 2.6: *Telomere associated factors in canine OSA cell lines.* (A) TIFs: representative images for colocalization of telomere signals and γ-H2AX foci in interphase nuclei of OSA cells. Telomere signals, and γ-H2AX, and the merged images in D17 and Grey cell lines. Arrows denote co-localizations. (B) Western blot analysis of DNA-PKcs in the eight canine OSA cells. ß-actin expression was used as a normalization control. DNA-PKcs is estimated from molecular weight (460 kDa). (C) Telomerase activity in canine OSA cell lines. TRAP assay confirmed all cell lines expressed enzymatically active TERT. Positive controls were provided by the manufacturer. Non–heated extract, (+) heated extract, IC: internal PCR control.

Table 2.2: Summary of telomere abnormalities and other telomere associated factors in eight canine OSA cell lines.

OSA Cell Line	Sum of Telomere Abnormalities per cell[1]	Telomerase Activity by TRAP assay	DNA-PKcs Expression by Western blotting[2]	No. of Colocalizations for telomere and γ-H2AX foci[3]	Signal Ratio of Telomeres[4]
Abrams	5.4	Positive	1.55	3.15	0.71±0.36
D17	51.4	Positive	2.88	3.26	1.12±0.63
Grey	6.4	Positive	0.60	4.82	0.92±0.38
Gracie	9.1	Positive	0.68	2.80	0.89±0.41
Hughes	17.2	Positive	0.20	3.10	1.61±0.96
Moresco	10.0	Positive	0.73	2.27	1.48±0.89
MacKinley	17.5	Positive	1.22	1.76	1.20±0.85
Vogel	11.4	Positive	0.13	1.48	0.83±0.35

[1] Sum of four types of telomere abnormalities ± SD per cell from more than 27 cells.
[2] The values are arbitrary unit. Average value of 8 cell lines is 1.
[3] Mean ± SD of numbers per cell from more than 50 cells.
[4] Telomere signal ratio (at fusion area/at telomere area) ± SD.

PKcs in D17 was approximately three times more than the average of the eight canine OSA cell lines. Abrams and MacKinley showed 50% and 20% more expression of DNA-PKcs compared to the average of eight cell lines. DNA-PKcs was estimated from molecular weight (460 kDa) and confirmed by the same size of human samples (see in chapter 3).

Telomerase Activity by TRAP Assay

To further investigate the involvement of telomere fusion, we measured telomerase activity by TRAP assay in canine OSA cell lines. All eight of the OSA cell lines were determined to be telomerase positive. Heat inactivation was used for negative controls of each sample for telomerase activity. (Figure 2.6c).

Telomere Aberrations in Spontaneous canine OSA Assay

To better characterize telomere dysfunction associated with canine OSA, we analyzed telomere fusions in ten primary canine OSA cell cultures derived from tumors arising from the limb and scapular regions in ten separate patients, and followed by cytogenetic analysis (Figure 2.7 and Table 2.3). Cytogenetic analysis revealed that the primary canine OSA cultures of naturally occurring primary OSA exhibited an increased number of metacentric chromosomes, as well as the eight established cell lines tested. Seven of the samples (OSA-2, OSA-4, OSA-7, OSA-8, OSA-9, OSA-10, and OSA-11) were with no increase of metacentric chromosomes, while three of the samples (OSA-1, OSA-3, and OSA-5) had increased numbers of metacentric chromosomes. FISH with a PNA telomere probe showed that the cell cultures with increased metacentric chromosomes exhibited predominantly Rb^{-}, Robertsonian translocation with no telomere signal in centromeres (Figure 2.7). The numbers of telomere fusions in the primary cultures were small with dominant ITS, interstitial telomeric sequence.

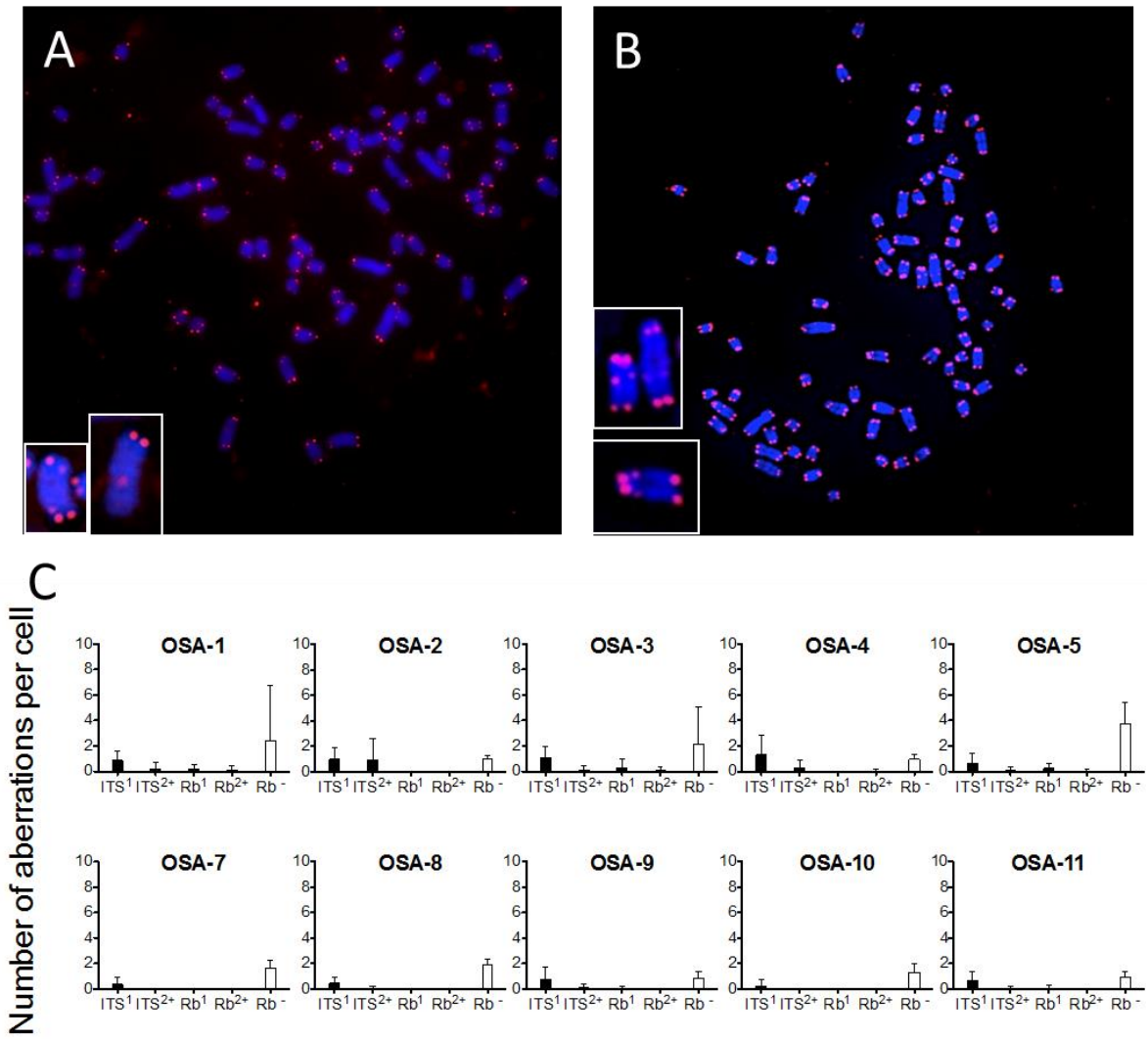

Figure 2.7: *Primary canine OSA cell cultures and telomere fusions.* Representative FISH images of the two primary canine OSA cell cultures' metaphase chromosomes hybridized with probes against telomeres; OSA-1 (A), the sample originated from the limb, OSA-2 (B), the sample originated from the scapula. Note the abnormal telomere signals in the magnification box. Blue represents DNA staining by DAPI and red represents a telomere signal by Cy3. (C) The number of telomere aberrations per each metaphase cell. Error bars indicate the standard error of the means.

Table 2.3: Sum of telomere abnormalities in 10 primary canine OSA cell cultures.

	OSA-1	OSA-2	OSA-3	OSA-4	OSA-5	OSA-7	OSA-8	OSA-9	OSA-10	OSA-11
No. of Chromosomes*	96.5 ±31.6	76.8 ±6.25	73.6 ±9.47	71.9 ±8.86	115.2 ±4.02	66.5 12.9±	83.2 ±25.4	74.8 20.5±	74.9 ±10.3	82.7 ±23.0
No. of Metacentric***	11.54 ±6.8	1.00 ±0.29	1.80 ±2.63	1.68 ±3.14	8.16 ±2.58	1.70 ±0.51	2.0 ±1.01	0.92 ±0.53	1.89 ±1.01	1.16 ±0.42
Sum of Telomere Abnormalities**	1.30 ±1.0	1.87 ±2.3	1.50 ±1.25	1.60 ±1.87	0.97 ±0.96	0.37 ±0.56	0.47 ±0.51	0.87 ±1.08	0.23 ±0.50	0.77 ±0.76

*Mean ± SD of chromosome number per cell from more than 100 metaphases.
**Mean ± SD of metacentrics per cell from more than 50 metaphases.
***Sum of four types of telomere abnormalities ± SD per cell from more than 30 cells.

Effects of Long-Term Culture on Canine OSA Cells

To understand the chromosome instability observed during long passage culture in canine OSA cells, we examined telomere fusions with time in culture in one primary canine OSA culture (OSA-2) and the results are summarized in Table 2.4. The OSA-2 was telomerase positive and with no increase metacentric chromosomes at the lowest passage (average 1.00 per cell) (Figure 2.7). We maintained the cells over a period of 235 days (18 passage cultures). As shown in the cell growth curve (Figure 2.8a), the primary canine OSA culture entered slow growth phase at the 9th passage. Post slow phase canine OSA cells grew as fast as the same speed or more than that before the slow phase (Figure 2.8a). Prior to the slow growth phase, the OSA cells started changing the total chromosome number, however, maintained the number of diploidy or tetraploidy (Figure 2.8c). In the 10th passage at the slow phase, canine OSA culture sporadically exhibited metacentric chromosomes (average 2.5 per cell), which showed a significant increase compared to the passage 3 ($p<0.05$). Approximately 40% of metaphases (most have less than 100 chromosome per cell) in the 10th passage showed increased number of metacentric chromosomes and ranged up to ten. As shown the value M in Figure 2.8c, the metacentric chromosomes accumulated rapidly after the 10th passage (12.6 and 17.6 per cell, at passage 14 and 18, respectively) and coincided with exhibiting variable chromosome numbers (Figure 2.8c). FISH with a PNA telomere probe revealed that the metacentric chromosomes increased at the 10 passage exhibited no or weak telomere signals at the involved centromeric regions (Figure 2.9). We scored the abnormal telomere FISH signals, including a complete loss of signals at the end of chromosomes in the passages (Figure 2.9c). As the passage number increased from 5 to 10, the number of Rb^- translocations and loss of telomere signals at the ends

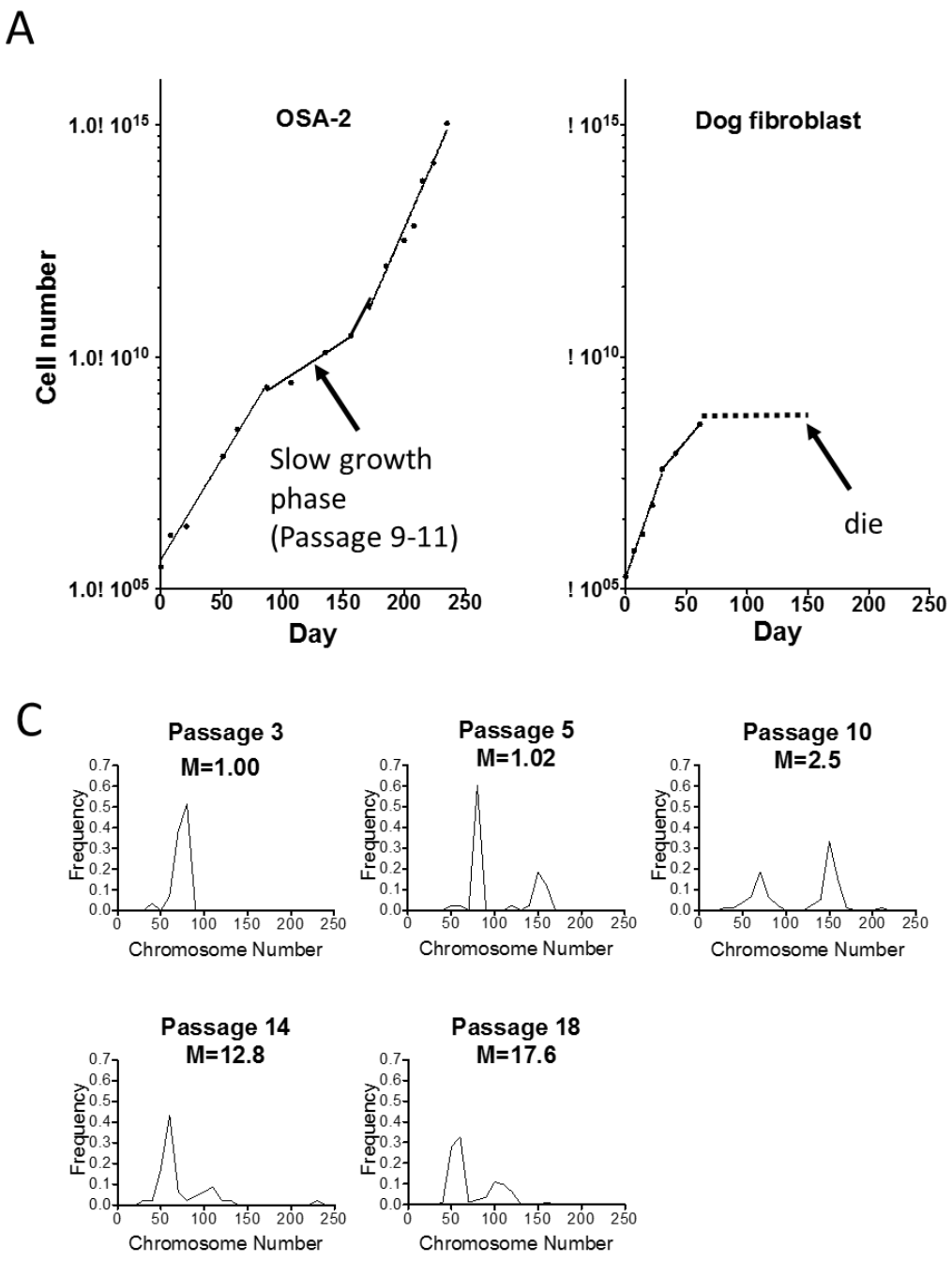

Figure 2.8: *Primary OSA culture growth curves and chromosome numbers over passage culture.* (A, B) Growth curves for the growth curves for primary OSA culture (A) showing the three growth phases; the first fast growth, the slow growth and followed by the fast growth. Normal canine fibroblast culture stopped growing at 12th passage (B). The line for each phase was fitted by exponential growth equation. The dash line of the dog fibroblasts expressed stopped growth after passage 12th. (C) The change of distribution of chromosome number over passage culture. M: Mean of metacentric chromosomes per cell.

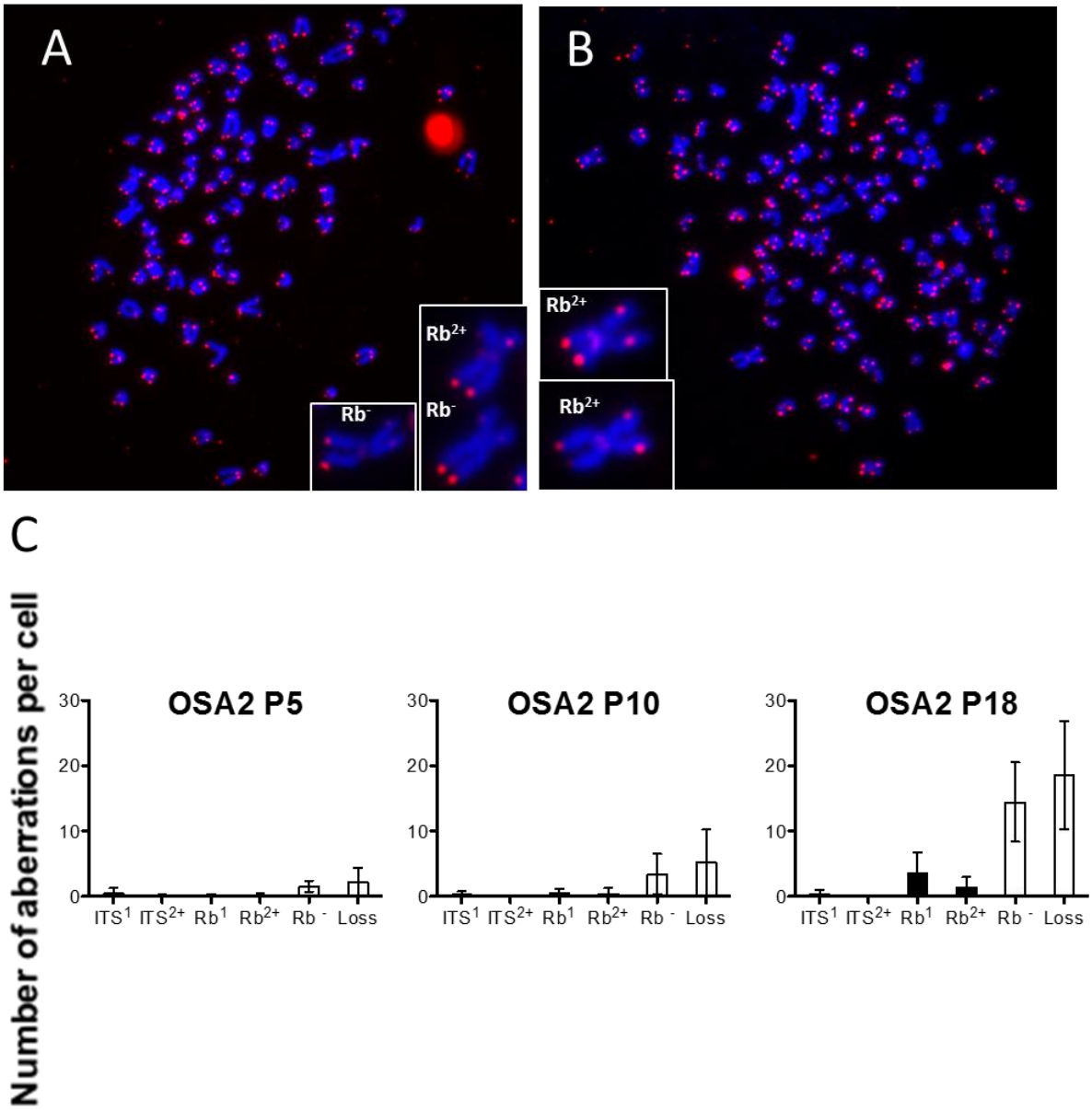

Figure 2.9: *Telomere abnormalities in primary canine OSA cell cultures over passage culture.* Representative FISH images of the 10th passage (A) and 18th passage (B) cultures' metaphase chromosomes hybridized with probes against telomeres. Note the abnormal telomere signals in the magnification box. Blue represents DNA staining by DAPI and red represents a telomere signal by Cy3. (C) The number of telomere aberrations including loss of signals (Loss) per each metaphase cell. Error bars indicate the standard error of the means.

Table 2.4: Chromosomal changes and telomere aberrations in primary cell cultures over passage.

Source of cells		Passage	No of chromosome per cell[a]	No of metacentric chromosomes per cell[b]	Sum of telomere abnormalities[c]
Dog	Primary OSA	3	73/75	1.00 ± 0.29	1.87 ± 2.30
		5	102/78	1.02 ± 1.10	0.67 ± 0.92
		10	116/145	2.50 ± 2.65*	1.33 ± 1.49
		18	74/59	17.6 ± 8.13*	5.38 ± 4.40*
	Normal skin fibroblast	5	85/78	2.19 ± 0.64	0.21 ± 0.52
		11[d]	69/65	1.80 ± 0.97	0.57 ± 0.86
Mouse	B6 ATM+/+ skin fibroblast	2	81/73	0.23 ± 0.42	0.37 ± 0.62
		31	67/66	0.31 ± 0.51	0.20 ± 0.48
	B6 ATM -/- skin fibroblast	2	89/79	0.21 ± 0.47	0.23 ± 0.43
		30	96/75	0.18 ± 0.44	0.23 ± 0.43
	BALB ATM+/+ skin fibroblast	2	61/50	0.32 ± 0.55	0.48 ± 0.69
		30	73/80	0.16 ± 0.37	0.54 ± 0.64
	BALB ATM -/- skin fibroblast	3	82/77	0.36 ± 0.48	0.15 ± 0.46
		30	79/69	0.20 ± 0.45	0.30 ± 0.60

[a] Mean/Median of chromosome number per cell from more than 50 metaphases.
[b] Mean ± SD of metacentrics per cell from more than 50 metaphases.
[c] Sum of four types of telomere abnormalities ± SD per cell from more than 27 cells.
[d] Stop growing at passage 12th.*=$p<0.05$ versus the lowest passage for each culture. Non parametric Kruskal-Wallis test for the primary OSA culture and unpaired two tailed t-test with Welch's correction for primary canine fibroblast and mouse fibroblast cells were uses.

per cell were significantly increased ($p<0.05$). From passage 10 to passage 18, increased numbers of Rb^{1} and Rb^{2+} furions, Rb^{-} translocations, and loss of telomere signals were observed.

Effects of Long-Term Culture on Normal Canine Skin Fibroblasts

In the 5th passage of the normal canine skin fibroblast cell culture, a majority of the cells (71%) showed a normal chromosomal complement (78 including two X chromosomes). Until the 12th passage the cells grew steadily, and then stopped growing during the 12th passage (Figure 2.8b). Although the decrease of the total number of chromosomes (median 65) was observed in the 11th passage, the number of metacentric chromosomes per cell did not increase (Table 2.4). In the FISH analysis, metaphase cells in the 11th passage showed decreased overall fluorescence intensity for telomeres compared to that from the 5th passage cells. However, frequency of absence of telomere fluorescence signals at the end of chromosomes didn't significantly increased with the passage time ($p=0.43$) (Figure 2.10). The sum of four types of telomere aberrations (ITS^{1}, ITS^{2+}, Rb^{1} and Rb^{2+}) were 0.22 and 0.53, in the 5th and 11th passages, respectively, showing no significant difference ($p=0.10$) (Table 2.4). The cells didn't grow or die after the 11th passage with a continuous fresh medium supply twice every week for two months.

Effects of Long-Term Culture on Non-Cancerous Mouse Cells

Furthermore, given that primary mouse fibroblast cultures derived from normal and ATM gene deficient mice were available, we investigated the long time culture effects on telomere abnormalities in these cells. Four mouse primary fibroblast cultures: B6 ATM+/+, B6 ATM-/-, BALB/c ATM+/+ and BALB/c ATM-/- were cultured till passage 30. Mutation in ATM gene is known to cause chromosome instability, and BALB/c is known to exhibit DNA-PKcs

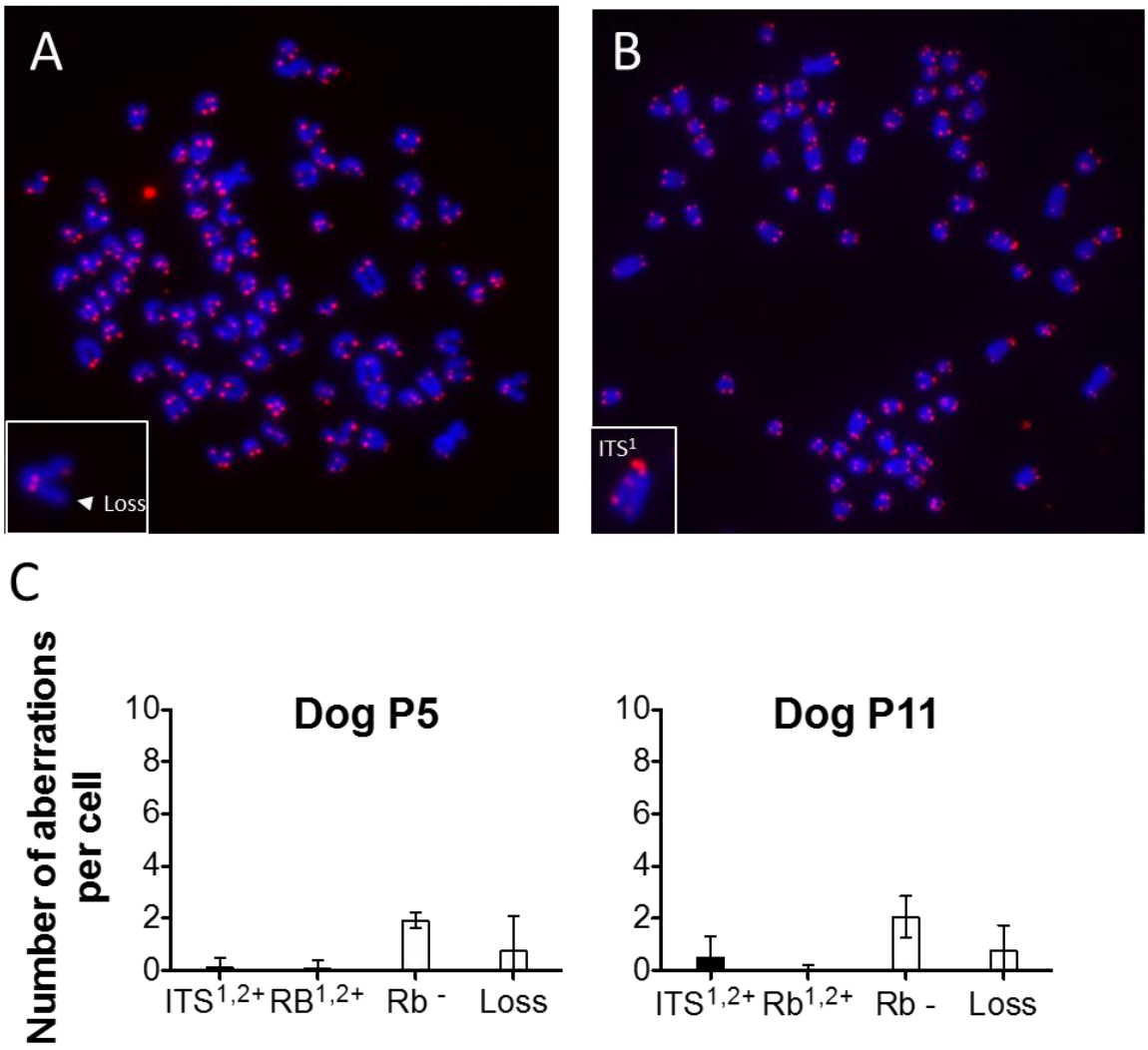

Figure 2.10: *Telomere abnormalities in a primary normal canine fibroblast culture from skin over passage culture.* Representative FISH images of the 5th passage (A) and 11 passage (B) cultures' metaphase chromosomes hybridized with probes against telomeres. Note the abnormal telomere signals in the magnification box. Blue represents DNA staining by DAPI and red represents a telomere signal by Cy3. (C) The number of telomere aberrations including ITS combined with ITS^1 and ITS^{2+}, Rb combined with Rb^1 and Rb^2, Rb^- and loss of signals (Loss) per each metaphase cell in passage 5 and passage 11. Error bars indicate the standard error of the means.

polymorphism, which might affect telomere function (Williams et al., 2009). However, no increase of metacentric chromosomes in either ATM+/+ or ATM-/- primary mouse fibroblast cells in the two different strain backgrounds were observed over 30 passage cultures (Table 2.4). The telomere aberration rates were not significantly higher in the highest passage cultures compared to those in the lowest passage cultures (Figure 2.11). BALB/c ATM+/+ showed the highest telomere aberrations (0.54 per cell) and loss of telomere signals (2.6 per cell) at the 30th passage. The telomere aberrations per cells were not significantly different between the lowest and highest passage cultures in all mouse primary fibroblasts in this study. We tested the radiosensitivity and ATM knockout allele in the 30th passage cultures to confirm their phenotypes (Figure 2.12). The two fibroblast cultures with ATM homozygous mouse skin fibroblast cultures (B6 ATM-/-, BALB/c ATM-/-) were more sensitive to gamma-ray than its wild type cultures. ATM genotyping confirmed the wild type ATM allele and ATM knockout allele were retained in each 30th passage cultures.

Discussion

Despite variable chromosome numbers, proliferation rates, and radiosensitivites, all eight canine OSA cell lines displayed increased numbers of metacentric chromosomes and exhibited numerous telomere aberrations, including interstitial telomeric signals and telomere fusions (telomere signals at the point of fusion, in this case in the centromeric regions of Robertsonian translocated chromosomes). Based on observations in ten primary OSA cell cultures, of increased metacentric chromosomes, no telomere signals were present at the involved centromeric regions. Furthermore, we observed that metacentric chromosome frequencies and telomere fusions

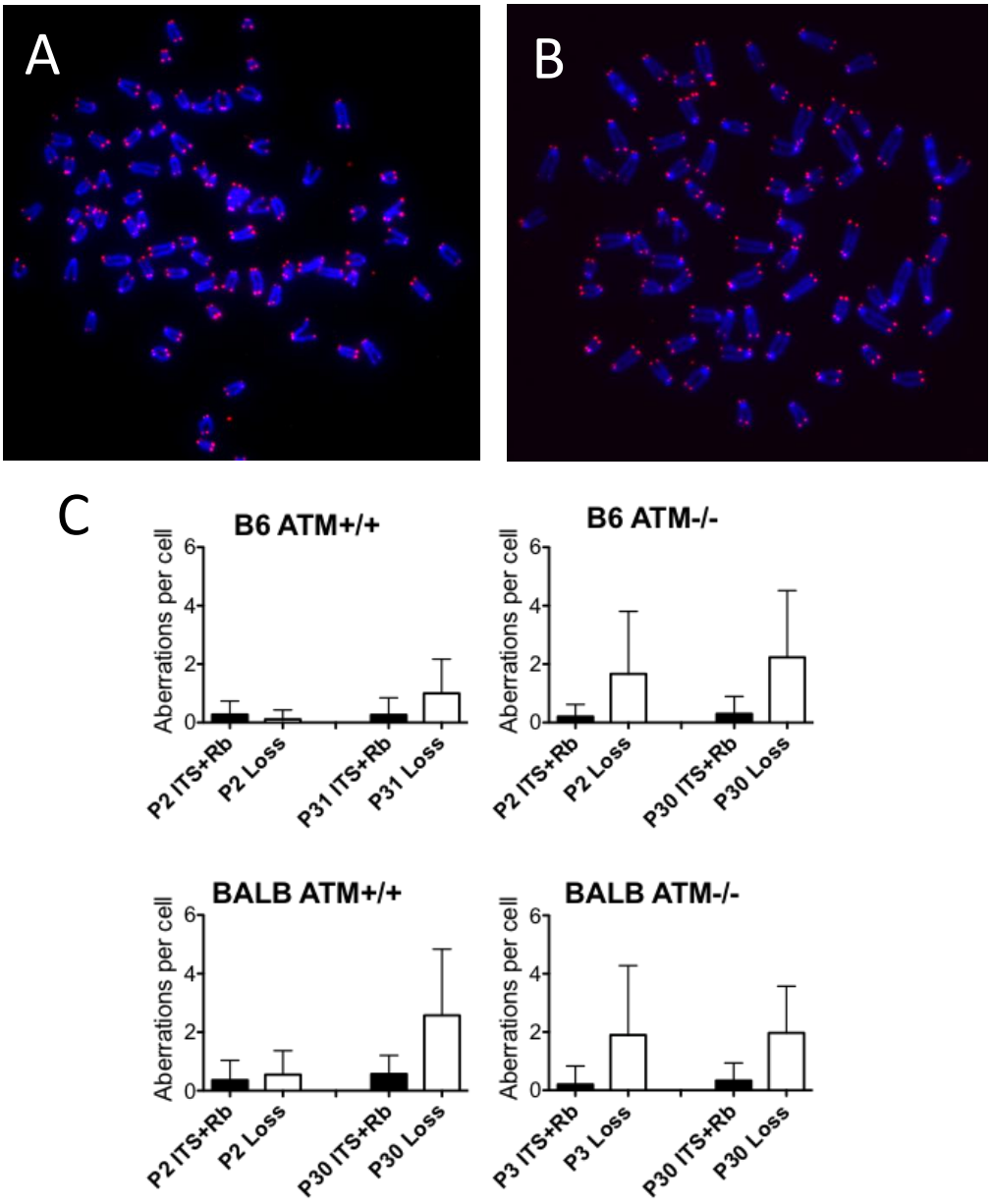

Figure 2.11: *Telomere abnormalities in primary skin fibroblast cultures from two mouse strains with and without ATM homozygous mutation.* Representative FISH images from BALB/c ATM-/- fibroblasts of the 3th passage (A) and 30th passage (B) cultures' metaphase chromosomes hybridized with probes against telomeres. Blue represents DNA staining by DAPI and red represents a telomere signal by Cy3. (C) The number of telomere aberrations including ITS combined with ITS^{1} and ITS^{2+}, Rb combined with Rb^{1} and Rb^{2}, Rb^{-} and loss of signals (Loss) per each metaphase cell in the lowest and highest passage in our analysis. Error bars indicate the standard error of the means.

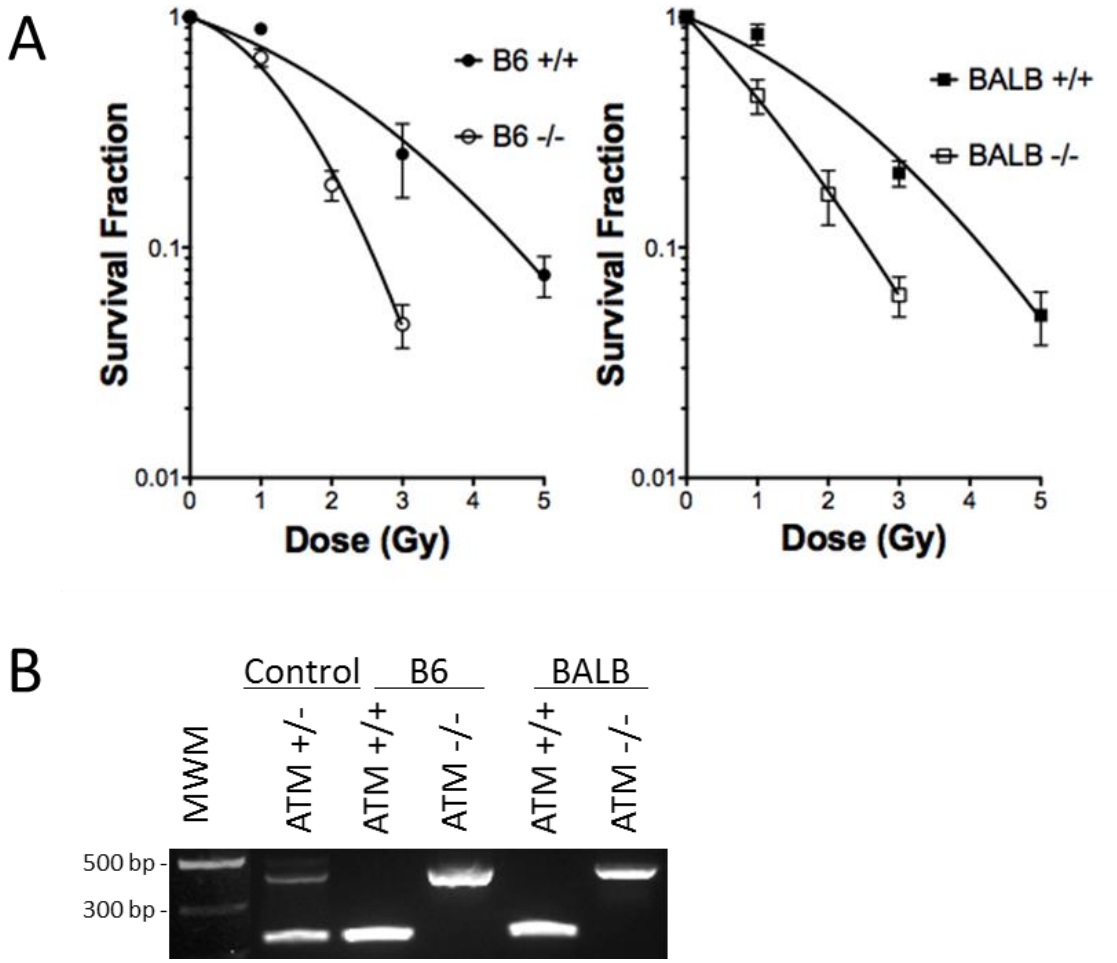

Figure 2.12: *Phenotype analysis of mouse fibroblast cell cultures at passage 30.* (A) Radiation induced survival curves. The curve with black circles indicate B6 ATM+/+, the white circle indicates B6 ATM-/-, the black square indicate BALB/c ATM+/+, and the white square indicate BALB/c ATM-/-. Experiments were carried out three times and error bars indicate the standard error of the means. (B) Genotyping of wild-type ATM allele and ATM knockout allele by PCR. ATM heterozygous mutation was used as control both wild type ATM allele (161 bp) and ATM knockout allele (441 bp). MWM: DNA molecular weight marker.

increased with increasing passage in an OSA culture, but not in non-cancerous canine fibroblasts or DNA repair deficient mouse fibroblasts.

As observed previously in published studies using canine OSA cells (Thomas et al., 2009), the eight canine OSA cells examined in this study possessed chaotic karyotypes that comprised a wide range of both chromosome numbers and abnormal structures (Figure 2.1 and Table 2.1). Aneuploidy, hyperploidy, and hypodiploidy of canine OSA from direct tissue biopsies has also been reported (Taylor et al., 1975, Mayr et al., 1991). In the previous study utilizing 25 radiation-induced canine OSA samples and six spontaneous canine OSA, chromosome numbers presented with predominant ranges of 45 to 55 and 90 to 105 (Taylor et al., 1975). Furthermore, ranges of 10–15 and 20–30 abnormal metacentric chromosomes were observed in these cell lines. Our results with the chromosome analysis showed the established canine OSA cell line to have remarkably different karyotypes that were clearly distinguishable from normal canine cell lines, confirming previous findings (Table 2.1). Chromosome number instabilities were different among the eight canine OSA cell lines. Cell lines with bimodal peaks representing chromosome numbers displayed a wide range of chromosome numbers from cell to cell. Metacentric chromosomes have been shown to be a centric fusion for canine OSA cells (Taylor et al., 1975, Mayr et al., 1991), and our results support this work. The frequencies of metacentric chromosomes in our eight canine OSA cell lines varied from higher to lower relative to findings of previous studies, suggesting a potential sub-classification of canine OSA using the number of metacentric chromosomes.

Our results showed that most of the cellular characteristics we tested were not uniform among canine OSA cell lines. Several studies have addressed the high resistance canine OSA cells have towards radiation (Dernell, 2007). In a previous study, the mean SF2 was relatively high (0.62), and the mean SF2 did not differ significantly among the four cell lines tested at these

radiation doses (Fitzpatrick et al., 2008). Contrary to these findings, we found both radioresistant and highly radiosensitive cell lines (Figure 2.2). In addition, other studies in human tumor cell lines showed that cells with multiple copies of chromosomes tended to be resistant to ionizing radiation (IR) (Schwartz et al., 1999). However, we didn't observe this trend. The cell lines Grey and Hughes were shown to be the most sensitive to IR while their average chromosome number were the highest among the eight cell lines. The cell proliferation rates were vastly different in the cell lines, which is consistent with a previous report (Legare et al., 2011). We did not find any correlation between radiation sensitivities and cellular proliferation rates (Table 2.1), and the eight OSA cell lines utilized varied in terms of chromosome numbers, radiosensitivity and cell proliferation. Additionally, for the three radioresistant canine OSA cell lines, exposure to heavy ions yielded decreased cell survival compared to gamma-rays, resulting in high RBE values for the heavy ions (Figure 2.3). In contrast, the radiosensitive canine OSA cell line, Grey showed more similar cell survival and smaller RBE values compared to the radioresistant cell lines. The response of Grey to high LET was similar to the DNA repair deficiency cell lines in previous human and rodent studies (Cartwright et al., 2015). Studies suggested that the effectiveness of high LET depends on the cellular repair capacity because high LET causes non-repairable DSBs for which kind of lesions that normal DSB repair system seems not be effective (Loucas and Geard, 1994, George et al., 2001).

Perhaps the most important finding in the current study was the demonstration that telomere fusions are a potential causative factor regarding genomic instability in canine OSA (Figure 2.4). It is widely supported that telomere dysfunction could possibly play a causal role in early carcinogenesis through instigating a bridge-breakage fusion type chromosomal instability, leading to the promotion of neoplastic transformation (Murnane, 2012). Furthermore, recent

studies have shown that telomere fusions are present in the early stages of several human cancers. Although metacentric chromosomes have been shown and hypothesized to be a result from telomere fusions in SV-40 transfected canine cells (Reimann et al., 1994), our study identifies telomere fusion as a novel chromosome dysfunction in canine OSA cells.

We found that different types of telomere fusions including ITS and Rb were present in the canine OSA cell lines (Figure 2.5). Through counting metacentric chromosomes and telomere abnormalities, we found further chaotic karyotypes among the eight canine OSA cell lines. Interestingly, telomere signals at the centromere region of metacentric chromosomes were not present in all cells with metacentric chromosomes except sex chromosomes. We observed that telomere signals at fusion points were less than twice the strength of telomere signals at the chromosome ends (Table 2.2). These results may support previous studies reporting that telomere shortening leads to telomere fusions, which was also previously described in breast cancer (Bailey and Murnane, 2006, Desmaze et al., 2003, Tanaka et al., 2012). However, there are other possibilities such as centric fusions between two DSBs or telocentric fusions between a telomere and a DSB, resulting in loss or less of telomere signals at fusion points (Bailey and Cornforth, 2007, Murata et al., 2007). Isochromosomes that result from a duplication of a single chromosome arm have been considered as a possible model for Robertsonian translocation (Shaffer and Lupski, 2000). However, identical lengths of both arms in metacentric chromosome were not always in the case of the metacentric chromosome found in canine OSA in the current study. The interstitial telomere signals with both chromatids (categorized ITS^{2+} in this study) may result in telomere-DSB fusion between uncapped telomere and a chromosome break, or tail-to-tail telomere fusions, which could be distinguished using the chromosome orientation FISH (CO-FISH) (Goodwin and Meyne, 1993). Furthermore, interstitial telomere signals were also found located at a single

chromatid (categorized ITS[1] in this study). As the origin of interstitial telomere signals, chromatid breaks induced by replication fork stalling leading to chromosome healing possibly by telomere capture or chromosome fusions of uncapped telomeres has been proposed as the mechanism of origin of ITSs (Bodvarsdottir et al., 2012, Bolzan and Bianchi, 2006). Furthermore, high frequency of ITSs have been reported in BRCA2 heterozygous cells, suggesting that ITSs may result from insufficient DSB repair (Bodvarsdottir et al., 2012). Since canine cancer cell lines exhibit variable number of ITSs, the identification of the mechanisms that could partially be responsible by the CO-FISH and centromere staining (Hayden and Willard, 2012), will provide further understanding of the telomere aberrations.

Western blotting analysis suggested that these eight cell lines have different levels of the DNA repair protein DNA-PKcs (Figure 2.6b). DNA-PKcs is one of telomere maintenance proteins preventing telomere fusion and also known to mediate NHEJ (Bailey et al., 1999). We observed high expression of DNA-PKcs in D17 cells and low expression in Vogel cells. D17 cells showed highly chaotic karyotypes and high amounts of telomere fusion. Our results suggested that the reduction of DNA-PKcs is not always the cause of telomere fusion in canine OSA cell lines. Other proteins, many of which are commonly associated with DNA repair, are also required for effective telomere protection (Bailey and Murnane, 2006, Verdun and Karlseder, 2007). Altered function of other telomere maintenance proteins including TRF2, RAP1, and POT1 might also be related to telomere fusions in canine OSA (van Steensel et al., 1998, Sarthy et al., 2009, Hockemeyer et al., 2006).

We observed colocalization of phosphorylated histone H2AX (γ-H2AX) and telomere signals in interphase cells as TIFs (Figure 2.6a). Nuclear foci of γ-H2AX are sensitive markers for DNA DSBs (Rogakou et al., 1998). Previous studies have shown that dysfunctional telomeres seen

in TRF2 deficient cells, different cultured tumor cell lines and senescence cells become associated with DNA damage response factors, such as γ-H2AX (Takai et al., 2003, Nakamura et al., 2009, Herbig et al., 2004). Our results support the idea that the cellular response to telomere dysfunction is controlled by DNA damage repair proteins (d'Adda di Fagagna et al., 2003). However, the exact contribution of DNA repair pathways to telomere fusions in canine OSA is still unclear. Previous studies have shown the mechanistic basis of fusion involving DNA repair pathways in human cells (Capper et al., 2007). Inhibition of TRF2 function results in telomere fusion events that are dependent on factors involved in NHEJ (Smogorzewska et al., 2002, Celli and de Lange, 2005). However, telomere fusions have been observed in the absence of components of NHEJ in human cells (Baumann and Cech, 2000, Heacock et al., 2004, Maser et al., 2007). Therefore, it will be important to investigate the molecular and cellular processes responsible for the generation of the fusion junctions in canine OSA cells.

As we described above, we were unable to find any correlations between telomere fusions and other characteristics associated with cytogenetic analysis, radiosensitivity, and DNA damage. The eight canine OSA cell lines utilized in our study, which all exhibited altered telomere signals, were all from cells which were telomerase positive somewhat contrary to a previous study describing 27% of canine OSA samples presenting as telomerase negative (Figure 2.6c) (Kow et al., 2008). These results suggest the requirement of further exploration regarding telomere fusion in telomerase negative canine OSA cells using a larger number of cell lines than the current study.

We confirmed that the end-to-end chromosome fusion events also occurred in short-term cultures from ten canine OSA clinical samples (Figure 2.7 and Table 2.3). Based on the observation of telomere aberrations in these primary cultures, we are reasonably certain that we are indeed working with an in vivo situation and not just genomic alteration due to prolonged culture. In the

ten primary OSA cell cultures tested, frequency distribution plots for the four types of telomere abnormalities observed is less than in the eight canine OSA cell lines. The metacentric chromosomes elevated in the primary cultures had no detectable telomere signals in the involved centrometic regions by the FISH analysis (categorized as Rb^- in this study) (Figure 2.7). Absence of telomere signals in primary cultures may indicate that telomeric DNA is relatively shortened before fusion, as reported in human cancer (Tanaka et al., 2012). However, as discussed above, there are other mechanism forming the metacentric chromosomes without telomere signals in the centromeric regions, such as centric fusions resulted from DSBs. Therefore, we can not conclude that telomere shortening is the mechanism of telomere fusion in canine OSA cell lines in our study.

The observation of telomere fusions in primary canine OSA culture indicated that telomere fusions in established canine OSA cell lines might be enhanced by long passages. Our results of long term culture supported the idea. Long term culture effects have been well characterized in human cell cultures (Romanov et al., 2001). In the current study, the number of metacentric chromosomes was increased with the passage numbers only in the canine OSA cell culture but not non-cancerous canine and mouse cells (Table 2.4). Furthermore, telomere signals at the involved centromeric regions became more obvious in the later passage (Figure 2.9). Our results suggest that telomere dysfunction in the canine OSA cells contributes to further increase in end-to-end chromosome fusion events with time in culture. As with human normal fibroblasts, canine primary fibroblasts exhibited a limited number of cell divisions (Figure 2.10). This could be explained by the senescence well described in human and rodent cells, where telomere shortening triggers cell cycle arrest through both p53-p21 and p16-RB pathways (Campisi, 2005, Kuilman et al., 2010). However, it is also known that cells escape from the p53 or p16 pathway, resulting in further cell proliferation and, ultimately, a telomere shortening crisis characterized by gross chromosomal

abnormalities emerges (Romanov et al., 2001). This crisis phase can be overcome through telomerase reactivation, such as seen in cancer cells or in immortalized cells (Kim et al., 1994, Shay and Wright, 2011). The timing of the increase of metacentric chromosomes at the slow growth phase in canine primary OSA culture seems to occur at a state similar to telomere-based crisis. Since the canine OSA culture utilized in the long passage study was already telomerase positive at the lowest passage, further studies with measurement of telomerase activity level and telomere length over passage culture in telomere positive and negative canine OSA may provide further understanding of telomere dysfunction in canine OSA cells. Chronic oxidative stress in culture or replication stress might offer possibilities that enhance telomere fusions in canine OSA culture. Oxidative stress is known to shorten telomeres (von Zglinicki, 2002). Telomere fusions might be consequence of increased cell growth; replication stress is known to cause genomic instability (Mazouzi et al., 2014). We also utilized mouse cells, where the all chromosomes are acrocentric as in dogs, derived from wild-type and ATM knockout mice, to study the long term effects in telomere dysfunction. We assumed the ATM homozygous mutations in DNA-PKcs polymorphism background increased the metacentric chromosomes resulted from telomere dysfunction, considering the roles of the ATM and DNA-PKcs in the telomere maintenance (Williams et al., 2009, Hande et al., 2001). However, our results suggested that telomere dysfunction in cells with ATM homozygous mutations and DNA-PKcs polymorphism might not contribute to the further increase in the end-to-end chromosome fusion events over long term culture, likely due to their unique telomere features in mice, such as its longer telomere length than humans and dogs, and unlimited telomerase activity (Todaro and Green, 1963).

The increase of metacentric chromosomes characterized in this study have been shown for other various tumors, such as transmissible sarcoma, hemangiopericytoma,

hemangioendothelioma, spindle-cell sarcoma, mammary carcinoma, and cutaneous mast cell tumors in dogs (Mayr et al., 1992, Mayr et al., 1994, Stone et al., 1991, Fujinaga et al., 1989). Molecular studies of canine cancer tissue not only for canine OSA but also other tumors will be necessary to determine whether telomeric fusions of canine chromosomes frequently occur *in vivo*. In human study, telomere fusions have been confirmed increasing in several cancers using the PCR based methods (Tanaka et al., 2012). However, the PCR based methods to detect telomere fusions are not available for dogs because of the absence of the sequence information of canine chromosome ends which the primers are based on (NCBI, website). The detection of telomere fusions in canine tissue is likely to become available with future improvements in sequence techniques at repetitive DNA regions in dogs.

In conclusion, we tested eight canine OSA cell lines that have different karyotypes, radiation sensitivity, and proliferation rates for cytogenetic analysis. All of the cell lines tested showed telomere fusions and the characteristics was observed in primary cell cultures. Our results suggest that the occurrence of telomere dysfunction may be a highly frequent genomic aberration event in canine cancer. The unique telomere aberrations might be a significant diagnostic marker and potential treatment target proceeding further research for canine tumors. Therefore, it will be important to investigate the presence in the canine cancer tissues, telomere fusions in telomerase negative canine OSA cell lines, as well as the translational potential for clinical applications.

REFERENCES

ALBERTSON, D. G., COLLINS, C., MCCORMICK, F. & GRAY, J. W. 2003. Chromosome aberrations in solid tumors. *Nat Genet,* 34**,** 369-76.

BAILEY, S. M. 2008. Telomeres and double-strand breaks - all's well that "ends" well. *Radiat Res,* 169**,** 1-7.

BAILEY, S. M. & CORNFORTH, M. N. 2007. Telomeres and DNA double-strand breaks: ever the twain shall meet? *Cell Mol Life Sci,* 64**,** 2956-64.

BAILEY, S. M., MEYNE, J., CHEN, D. J., KURIMASA, A., LI, G. C., LEHNERT, B. E. & GOODWIN, E. H. 1999. DNA double-strand break repair proteins are required to cap the ends of mammalian chromosomes. *Proc Natl Acad Sci U S A,* 96**,** 14899-904.

BAILEY, S. M. & MURNANE, J. P. 2006. Telomeres, chromosome instability and cancer. *Nucleic Acids Res,* 34**,** 2408-17.

BAKHOUM, S. F. & COMPTON, D. A. 2012. Chromosomal instability and cancer: a complex relationship with therapeutic potential. *J Clin Invest,* 122**,** 1138-43.

BARLOW, C., HIROTSUNE, S., PAYLOR, R., LIYANAGE, M., ECKHAUS, M., COLLINS, F., SHILOH, Y., CRAWLEY, J. N., RIED, T., TAGLE, D. & WYNSHAW-BORIS, A. 1996. Atm-deficient mice: a paradigm of ataxia telangiectasia. *Cell,* 86**,** 159-71.

BAUMANN, P. & CECH, T. R. 2000. Protection of telomeres by the Ku protein in fission yeast. *Mol Biol Cell,* 11**,** 3265-75.

BODVARSDOTTIR, S. K., STEINARSDOTTIR, M., BJARNASON, H. & EYFJORD, J. E. 2012. Dysfunctional telomeres in human BRCA2 mutated breast tumors and cell lines. *Mutat Res,* 729**,** 90-9.

BOLZAN, A. D. & BIANCHI, M. S. 2006. Telomeres, interstitial telomeric repeat sequences, and chromosomal aberrations. *Mutat Res,* 612**,** 189-214.

CAMPISI, J. 2005. Senescent cells, tumor suppression, and organismal aging: good citizens, bad neighbors. *Cell,* 120**,** 513-22.

CAPPER, R., BRITT-COMPTON, B., TANKIMANOVA, M., ROWSON, J., LETSOLO, B., MAN, S., HAUGHTON, M. & BAIRD, D. M. 2007. The nature of telomere fusion and a definition of the critical telomere length in human cells. *Genes Dev,* 21**,** 2495-508.

CARTWRIGHT, I. M., BELL, J. J., MAEDA, J., GENET, M. D., ROMERO, A., FUJII, Y., FUJIMORI, A., KITAMUTA, H., KAMADA, T., CHEN, D. J. & KATO, T. A. 2015. Effects of targeted phosphorylation site mutations in the DNA-PKcs phosphorylation domain on low and high LET radiation sensitivity. *Oncol Lett,* 9**,** 1621-1627.

CATALAN, J., AUFFRAY, J. C., PELLESTOR, BRITTON-DAVIDIAN. 2000. Spontaneous occurrence of Robertsonian fuion involving chromosome 19 by single whole-arm reciprocal translocation (WART) in wild-derived house mice. *Chromosome Research 8.7*:593-601

CELLI, G. B. & DE LANGE, T. 2005. DNA processing is not required for ATM-mediated telomere damage response after TRF2 deletion. *Nat Cell Biol,* 7**,** 712-8.

CORNFORTH, M. N. & BEDFORD, J. S. 1985. On the nature of a defect in cells from individuals with ataxia-telangiectasia. *Science,* 227**,** 1589-91.

D'ADDA DI FAGAGNA, F., REAPER, P. M., CLAY-FARRACE, L., FIEGLER, H., CARR, P., VON ZGLINICKI, T., SARETZKI, G., CARTER, N. P. & JACKSON, S. P. 2003. A DNA damage checkpoint response in telomere-initiated senescence. *Nature,* 426**,** 194-8.

DERNELL WS, EHRHARDT NP, STAW RC, VAIL DM. 2007. Tumor of the skeletal system. In: Withrow SJ, Vail DM, editors. St Louis, MO:Saunders. 540-582m,

DESMAZE, C., SORIA, J. C., FREULET-MARRIERE, M. A., MATHIEU, N. & SABATIER, L. 2003. Telomere-driven genomic instability in cancer cells. *Cancer Lett,* 194**,** 173-82.

FITZPATRICK, C. L., FARESE, J. P., MILNER, R. J., SALUTE, M. E., RAJON, D. A., MORRIS, C. G., BOVA, F. J., LURIE, D. M. & SIEMANN, D. W. 2008. Intrinsic radiosensitivity and repair of sublethal radiation-induced damage in canine osteosarcoma cell lines. *Am J Vet Res,* 69**,** 1197-202.

FRIAS, C., PAMPALONA, J., GENESCA, A. & TUSELL, L. 2012. Telomere dysfunction and genome instability. *Front Biosci (Landmark Ed),* 17**,** 2181-96.

FUJII, Y., YURKON, C. R., MAEDA, J., GENET, S. C., KUBOTA, N., FUJIMORI, A., MORI, T., MARUO, K. & KATO, T. A. 2013. Comparative study of radioresistance between feline cells and human cells. *Radiat Res,* 180**,** 70-7.

FUJINAGA, T., YAMASHITA, M., YOSHIDA, M. C., MIZUNO, S., OKAMOTO, Y., TAJIMA, M. & OTOMO, K. 1989. Chromosome analysis of canine transmissible sarcoma cells. *Zentralbl Veterinarmed A,* 36**,** 481-9.

GARAGNA, S., MARZILIANO, N., ZUCCOTTI, M., SEARLE, J. B., CAPANNA, E. & REDI, C. A. 2001. Pericentromeric organization at the fusion point of mouse Robertsonian translocation chromosomes. *Proc Natl Acad Sci U S A,* 98**,** 171-5.

GEORGE, K., WU, H., WILLINGHAM, V., FURUSAWA, Y., KAWATA, T. & CUCINOTTA, F. A. 2001. High- and low-LET induced chromosome damage in human lymphocytes: a time-course of aberrations in metaphase and interphase. *Int J Radiat Biol,* 77**,** 175-83.

GESHI, M., SAKAGUCHI, M., YONAI, M., NAGAI, T., SUZUKI, O. & HANADA, H. 1996. Effects of the 7 21 Robertsonian translocation on fertilization rates and preimplantation development of bovine oocytes in vitro. *Theriogenology,* 46**,** 893-7.

GOODWIN, E. & MEYNE, J. 1993. Strand-specific FISH reveals orientation of chromosome 18 alphoid DNA. *Cytogenet Cell Genet,* 63**,** 126-7.

HANDE, M. P., BALAJEE, A. S., TCHIRKOV, A., WYNSHAW-BORIS, A. & LANSDORP, P. M. 2001. Extra-chromosomal telomeric DNA in cells from Atm(-/-) mice and patients with ataxia-telangiectasia. *Hum Mol Genet,* 10**,** 519-28.

HAYDEN, K. E. & WILLARD, H. F. 2012. Composition and organization of active centromere sequences in complex genomes. *BMC Genomics,* 13**,** 324.

HEACOCK, M., SPANGLER, E., RIHA, K., PUIZINA, J. & SHIPPEN, D. E. 2004. Molecular analysis of telomere fusions in Arabidopsis: multiple pathways for chromosome end-joining. *EMBO J,* 23**,** 2304-13.

HERBIG, U., JOBLING, W. A., CHEN, B. P., CHEN, D. J. & SEDIVY, J. M. 2004. Telomere shortening triggers senescence of human cells through a pathway involving ATM, p53, and p21(CIP1), but not p16(INK4a). *Mol Cell,* 14**,** 501-13.

HOCKEMEYER, D., DANIELS, J. P., TAKAI, H. & DE LANGE, T. 2006. Recent expansion of the telomeric complex in rodents: Two distinct POT1 proteins protect mouse telomeres. *Cell,* 126**,** 63-77.

JAFFE, N. 2009. Osteosarcoma: review of the past, impact on the future. The American experience. *Cancer Treat Res,* 152**,** 239-62.

KAMADA, T., TSUJII, H., TSUJI, H., YANAGI, T., MIZOE, J. E., MIYAMOTO, T., KATO, H., YAMADA, S., MORITA, S., YOSHIKAWA, K., KANDATSU, S. & TATEISHI, A. 2002. Efficacy and safety of carbon ion radiotherapy in bone and soft tissue sarcomas. *J Clin Oncol,* 20**,** 4466-71.

KIM, N. W., PIATYSZEK, M. A., PROWSE, K. R., HARLEY, C. B., WEST, M. D., HO, P. L., COVIELLO, G. M., WRIGHT, W. E., WEINRICH, S. L. & SHAY, J. W. 1994. Specific association of human telomerase activity with immortal cells and cancer. *Science,* 266**,** 2011-5.

KOJIS, T. L., GATTI, R. A. & SPARKES, R. S. 1991. The cytogenetics of ataxia telangiectasia. *Cancer Genet Cytogenet,* 56**,** 143-56.

KOW, K., THAMM, D. H., TERRY, J., GRUNERUD, K., BAILEY, S. M., WITHROW, S. J. & LANA, S. E. 2008. Impact of telomerase status on canine osteosarcoma patients. *J Vet Intern Med,* 22**,** 1366-72.

KUILMAN, T., MICHALOGLOU, C., MOOI, W. J. & PEEPER, D. S. 2010. The essence of senescence. *Genes Dev,* 24**,** 2463-79.

LEGARE, M. E., BUSH, J., ASHLEY, A. K., KATO, T. & HANNEMAN, W. H. 2011. Cellular and phenotypic characterization of canine osteosarcoma cell lines. *J Cancer,* 2**,** 262-70.

LIAO, M. J., YIN, C., BARLOW, C., WYNSHAW-BORIS, A. & VAN DYKE, T. 1999. Atm is dispensable for p53 apoptosis and tumor suppression triggered by cell cycle dysfunction. *Mol Cell Biol,* 19**,** 3095-102.

LIN, T. T., LETSOLO, B. T., JONES, R. E., ROWSON, J., PRATT, G., HEWAMANA, S., FEGAN, C., PEPPER, C. & BAIRD, D. M. 2010. Telomere dysfunction and fusion during the progression of chronic lymphocytic leukemia: evidence for a telomere crisis. *Blood,* 116**,** 1899-907.

LITHNER, F. & PONTEN, J. 1966. Bovine fibroblasts in long-term tissue culture: chromosome studies. *Int J Cancer,* 1**,** 579-88.

LOUCAS, B. D. & GEARD, C. R. 1994. Kinetics of chromosome rejoining in normal human fibroblasts after exposure to low- and high-LET radiations. *Radiat Res,* 138**,** 352-60.

MASER, R. S., WONG, K. K., SAHIN, E., XIA, H., NAYLOR, M., HEDBERG, H. M., ARTANDI, S. E. & DEPINHO, R. A. 2007. DNA-dependent protein kinase catalytic subunit is not required for dysfunctional telomere fusion and checkpoint response in the telomerase-deficient mouse. *Mol Cell Biol,* 27**,** 2253-65.

MAYR, B., ESCHBORN, U., LOUPAL, G. & SCHLEGER, W. 1991. Characterisation of complex karyotype changes in two canine bone tumours. *Res Vet Sci,* 51**,** 341-3.

MAYR, B., KRAMBERGER-KAPLAN, E., LOUPAL, G. & SCHLEGER, W. 1992. Analysis of complex cytogenetic alterations in three canine mammary sarcomas. *Res Vet Sci,* 53**,** 205-11.

MAYR, B., REIFINGER, M., WEISSENBOCK, H., SCHLEGER, W. & EISENMENGER, E. 1994. Cytogenetic analyses of four solid tumours in dogs. *Res Vet Sci,* 57**,** 88-95.

MAZOUZI, A., VELIMEZI, G. & LOIZOU, J. I. 2014. DNA replication stress: causes, resolution and disease. *Exp Cell Res,* 329**,** 85-93.

MUELLER, F., FUCHS, B. & KASER-HOTZ, B. 2007. Comparative biology of human and canine osteosarcoma. *Anticancer Res,* 27**,** 155-64.

MURATA, K., HANZAWA, K., KASAI, F., TAKEUCHI, M., ECHIGOYA, T. & YASUMOTO, S. 2007. Robertsonian translocation as a result of telomere shortening during replicative senescence and immortalization of bovine oviduct epithelial cells. *In Vitro Cell Dev Biol Anim,* 43**,** 235-44.

MURNANE, J. P. 2012. Telomere dysfunction and chromosome instability. *Mutat Res,* 730**,** 28-36.

NACHMAN, M. W. & SEARLE, J. B. 1995. Why is the house mouse karyotype so variable? *Trends Ecol Evol,* 10**,** 397-402.

NAKAMURA, A. J., REDON, C. E., BONNER, W. M. & SEDELNIKOVA, O. A. 2009. Telomere-dependent and telomere-independent origins of endogenous DNA damage in tumor cells. *Aging (Albany NY),* 1**,** 212-8.

PAOLONI, M. & KHANNA, C. 2008. Translation of new cancer treatments from pet dogs to humans. *Nat Rev Cancer,* 8**,** 147-56.

RANKIN, K. S., STARKEY, M., LUNEC, J., GERRAND, C. H., MURPHY, S. & BISWAS, S. 2012. Of dogs and men: comparative biology as a tool for the discovery of novel biomarkers and drug development targets in osteosarcoma. *Pediatr Blood Cancer,* 58**,** 327-33.

REIMANN, N., NOLTE, I., BARTNITZKE, S. & BULLERDIEK, J. 1999. Re: Sit, DNA, sit: cancer genetics going to the dogs. *J Natl Cancer Inst,* 91**,** 1688-9.

REIMANN, N., ROGALLA, P., KAZMIERCZAK, B., BONK, U., NOLTE, I., GRZONKA, T., BARTNITZKE, S. & BULLERDIEK, J. 1994. Evidence that metacentric and submetacentric chromosomes in canine tumors can result from telomeric fusions. *Cytogenet Cell Genet,* 67**,** 81-5.

ROGAKOU, E. P., PILCH, D. R., ORR, A. H., IVANOVA, V. S. & BONNER, W. M. 1998. DNA double-stranded breaks induce histone H2AX phosphorylation on serine 139. *J Biol Chem,* 273**,** 5858-68.

ROMANOV, S. R., KOZAKIEWICZ, B. K., HcOLST, C. R., STAMPFER, M. R., HAUPT, L. M. & TLSTY, T. D. 2001. Normal human mammary epithelial cells spontaneously escape senescence and acquire genomic changes. *Nature,* 409**,** 633-7.

SARTHY, J., BAE, N. S., SCRAFFORD, J. & BAUMANN, P. 2009. Human RAP1 inhibits non-homologous end joining at telomeres. *EMBO J,* 28**,** 3390-9.

SCHWARTZ, J. L., MURNANE, J. & WEICHSELBAUM, R. R. 1999. The contribution of DNA ploidy to radiation sensitivity in human tumour cell lines. *Br J Cancer,* 79**,** 744-7.

SHAFFER, L. G. & LUPSKI, J. R. 2000. Molecular mechanisms for chromosomal rearrangements in humans. *Annu Rev Genet,* 34, 297-329.

SHAY, J. W. & WRIGHT, W. E. 2011. Role of telomeres and telomerase in cancer. *Semin Cancer Biol,* 21**,** 349-53.

SHILOH, Y. 2001. ATM and ATR: networking cellular responses to DNA damage. *Curr Opin Genet Dev,* 11**,** 71-7.

SMOGORZEWSKA, A., KARLSEDER, J., HOLTGREVE-GREZ, H., JAUCH, A. & DE LANGE, T. 2002. DNA ligase IV-dependent NHEJ of deprotected mammalian telomeres in G1 and G2. *Curr Biol,* 12**,** 1635-44.

STONE, D. M., JACKY, P. B. & PRIEUR, D. J. 1991. Cytogenetic evaluation of four canine mast cell tumors. *Cancer Genet Cytogenet,* 53**,** 105-12.

STORCHOVA, Z. & PELLMAN, D. 2004. From polyploidy to aneuploidy, genome instability and cancer. *Nat Rev Mol Cell Biol,* 5**,** 45-54.

SUZUKI, M., KASE, Y., YAMAGUCHI, H., KANAI, T. & ANDO, K. 2000. Relative biological effectiveness for cell-killing effect on various human cell lines irradiated with heavy-ion medical accelerator in Chiba (HIMAC) carbon-ion beams. *Int J Radiat Oncol Biol Phys,* 48**,** 241-50.

TAKAI, H., SMOGORZEWSKA, A. & DE LANGE, T. 2003. DNA damage foci at dysfunctional telomeres. *Curr Biol,* 13**,** 1549-56.

TANAKA, H., ABE, S., HUDA, N., TU, L., BEAM, M. J., GRIMES, B. & GILLEY, D. 2012. Telomere fusions in early human breast carcinoma. *Proc Natl Acad Sci U S A,* 109**,** 14098-103.

TAYLOR, N., SHIFRINE, M., WOLF, H. G. & TROMMERSHAUSEN-SMITH, A. 1975. Canine osteosarcoma karyotypes from an original tumor, its metastasis, and tumor cells in tissue culture. *Transplant Proc,* 7**,** 485-93.

THOMAS, R., WANG, H. J., TSAI, P. C., LANGFORD, C. F., FOSMIRE, S. P., JUBALA, C. M., GETZY, D. M., CUTTER, G. R., MODIANO, J. F. & BREEN, M. 2009. Influence of genetic background on tumor karyotypes: evidence for breed-associated cytogenetic aberrations in canine appendicular osteosarcoma. *Chromosome Res,* 17**,** 365-77.

TODARO, G. J. & GREEN, H. 1963. Quantitative studies of the growth of mouse embryo cells in culture and their development into established lines. *J Cell Biol,* 17**,** 299-313.

VAIL, D. M. & MACEWEN, E. G. 2000. Spontaneously occurring tumors of companion animals as models for human cancer. *Cancer Invest,* 18**,** 781-92.

VAN GENT, D. C., HOEIJMAKERS, J. H. & KANAAR, R. 2001. Chromosomal stability and the DNA double-stranded break connection. *Nat Rev Genet,* 2**,** 196-206.

VAN STEENSEL, B., SMOGORZEWSKA, A. & DE LANGE, T. 1998. TRF2 protects human telomeres from end-to-end fusions. *Cell,* 92**,** 401-13.

VERDUN, R. E. & KARLSEDER, J. 2007. Replication and protection of telomeres. *Nature,* 447**,** 924-31.

VON ZGLINICKI, T. 2002. Oxidative stress shortens telomeres. *Trends Biochem Sci,* 27**,** 339-44.

WILLIAMS, E. S., KRINGLER, R., PONNAIYA, B., HARDT, T., SCHROCK, E., LEES-MILLER, S., MEEK, K., ULLRICH, R. & BAILEY, S. M. 2009. Telomere dysfunction and DNA-PKcs deficiency: characterization and consequence. *Cancer Res,* 69, 2100-7.

CHAPTER 3

CHARACTERIZATION OF RADIOSENSITIVITY SIGNATURES IN CANINE CANCER CELL LINES

Summary

Radiatiosensitivity signatures are critical for evaluating individual response to radiation therapy. A human cancer cell line panel, the NCI-60, has been utilized to develop informative markers of radiosensitivity in cancer regardless of tumor tissue type. Spontaneous cancers in dogs are considered unique and underused resources for cancer research. In this study, we investigated radiosensitivity signatures in a novel canine cancer cell panel. A canine cancer cell line panel, called ACC30, was recently developed along with microarray gene expression data at the FACC of Colorado State University. We used 27 canine cell lines derived from ten tumor types from the ACC30 panel. First, radiosensitivity was determined using a clonogenic assay for adherent cell cultures, or a limiting dilution assay for suspension cell cultures. The 27 cell lines had varying radiosensitivities regardless of tumor type (survival fraction at 2 Gy, SF2= 0.17–0.94). Based on the basic cellular characteristics analyzed in this study, there was a statistically significant correlation between radiosensitivity and plating efficiency. Next, we selected the five most radiosensitive cell lines as the radiosensitive group and the five most radioresistant cell lines as the radioresistant group. Then we evaluated known parameters for the relationship with the level of cell killing by IR, including IR-induced DNA DSB repair and apoptosis in the radiosensitive group as compared to the radioresistant group. These parameters could partially explain the difference of radiosensitivity in the canine cancer cell lines. Further, we investigated a possible common radiosensitivity signature using the basal gene expression profiling of the ACC panel for

approximately 18,000 genes. Three hundred fourteen genes were identified as being differentially expressed between the radiosensitive and radioresistant groups based on the SF2 and SF5 comparisons. Gene set enrichment analysis was used to inform potential pathways and functions involving the differentially expressed genes and, indeed, several biological processes including cell-matrix adhesion and apoptosis were related to radiosensitivity in the canine cancer cell lines. In support of our findings, cell adhesion was one of the signatures previously identified in the human microarray analysis. Together, our results suggest that cell adhesion related genes, rather than the more commonly regarded radiosensitivity associated apoptosis and DNA repair related genes, may provide the most beneficial prediction of radiosensitivity.

Introduction

Radiation therapy is one of the most important treatment methods for cancer in humans and pet dogs (Delaney et al., 2005, McEntee, 2006). The radiation response for the same type of tumor can vary in different patients. Therefore, identification of predictive biomarkers of radiotherapy response is a crucial step towards personalized therapy (Begg, 2009, Torres-Roca and Stevens, 2008). Despite numerous studies for the development of predictive assays, none have become routine in the clinic. Such studies have suggested that differences in intrinsic radiosensitivity exist and understanding the mechanisms could significantly impact practice for personalized radiotherapy (Torres-Roca and Stevens, 2008, Begg, 2009).

Intrinsic radiosensitivities measured by *in vitro* colony formation assays are expressed as SF2, the fraction of cells surviving a single 2 Gy dose of irradiation. The dose of 2 Gy is commonly used as a dose per fraction in clinical radiotherapy in humans. The SF2 in humans has been shown to predict tumor response *in vivo* in previous studies (West et al., 1997, Bjork-Eriksson et al.,

2000). Colony formation assays can detect IR-induced reproductive cell death, including mitotic cell death as a result of unrepaired DSBs and chromosome aberrations, as well as apoptosis and other types of cell death (Hall, 2006). In mitotic cell death, cells fail to undergo successful division due to persistent DNA damage. This results in genomic loss and eventually cell death. Mitotic cell death is thought to be the major mechanisms of death by IR, and apoptosis after irradiation could account for a fraction of the total clonogenic cell kill (Dewey et al., 1995).

Repair of DNA DSBs is known as one of the most important elements that determines intrinsic radiosensitivity (Schwartz, 1998, West et al., 1997). There are two major DNA DSBs repair pathways: NHEJ and HR. NHEJ is the dominant pathway in mammalian cells, and is active in the G1, S and G2 phase of the cell cycle (Thompson, 2012). Studies have shown that mutations in genes associated with NHEJ increase sensitivity to radiation (Thacker and Zdzienicka, 2004). On the other hand, HR becomes active during S/G2 phases of the cell cycle and its deficiency induces mild sensitization to radiation (Thompson, 2012). There are other DNA repair pathways that potentially contribute to IR-induced DNA damage repair, such as the Fanconi Anemia (FA) pathway. The loss of this pathway results in a moderate sensitive phenotype to IR, which is less severe than HR mutants (Duckworth-Rysiecki and Taylor, 1985, Niedernhofer et al., 2005). In many studies, the intrinsic radiosensitivity of a tumor cell has been defined by different factors; DNA break induction and repair, chromosome aberrations, and others, such as apoptosis frequency (Begg, 2009, Torres-Roca and Stevens, 2008). However, inconsistent correlations with cell survival have been reported in the measurement of these parameters.

Intrinsic radiosensitivity results from genetic alterations in the cellular response to radiation, which is frequently found in cancer cells (Begg, 2009, Pawlik and Keyomarsi, 2004). A study on molecular genetic events related to radiosensitivity has been the focus of many research

projects. An association between radioresistance and the expression of genes involved in various radiation response pathways, including DNA repair, apoptosis, growth factor, signal transduction, cell cycle and hypoxia has been observed (Ogawa et al., 2007). This has the potential to lead to the identification of gene regulatory pathways that result in the development of radiosensitivity predictive assays, but studies so far have been unable to validate their clinical importance. Consequently there is interest in deriving a gene signature with the advent of the microarray technology, which permits simultaneous analysis of the expression levels of thousands of genes (Ogawa et al., 2007). Recently, it was hypothesized that the gene signature identified in a population of cell lines with diverse tumor types will be more robust and general (Hall et al., 2014). In a study using the NCI-60 cell line panel which represents nine human tumor types, gene expression profiling identified cell adhesion molecular interacted with the integrin signaling pathway as the common radiosensitivity signature regardless of tumor type (Kim et al., 2012).

Although the use of microarray analysis for radiosensitivity has not yet reached any significant impact at the clinical level for cancer patients, the technology is promising for a better understanding of the molecular events implicated in radiation sensitivity. Recently, the canine cancer cell line panel (ACC30) has been developed, with associated microarray-based gene expression data. The gene expression profiling has been utilized for developing a predictive assay for response to doxorubicin in canine cancer (Fowles et al., 2014). Compared to the human cell lines in the NCI-60 panel, the canine cell lines have not been as fully characterized. Along with the basic cellular characterization and the biological endpoints of radiation response, genome-wide studies of the novel canine cancer panel may provide a framework for further elucidating profiles for prediction of radiotherapy response for dogs and prospectively for humans as well.

We aimed to test the hypothesis that identification of the determinants of response to IR in diverse canine cancer cell lines would provide additional information, some specific to dogs, and some potentially supplementing those reported for human cancer. To test the hypothesis, we examined the intrinsic radiosensitivity of 27 canine cancer cell lines in the ACC30 panel. Each cell line was characterized by a combination of data representing cell cycle distribution, cellular doubling time, chromosome number, metacentric chromosome frequency, DNA ploidy pattern and plating efficiency. The known parameters including DNA DSB repair efficiency and apoptosis following exposure were evaluated between radiosensitive and radioresistant cell lines. To identify a radiosensitive gene signature and explain related signaling pathways, microarray data of their basal gene expression patterns between radiosensitive and radioresistant cell lines in the ACC30 panel were analyzed.

Materials and Methods

Cell Culture

The 27 canine tumor cell lines were kindly supplied by FACC of Colorado State University (Fort Collins, CO, USA) (Table 3.1). Adhesive tumor cell lines were grown in Minimum Essential Medium (MEM/EBSS, Thermo Fisher Scientific, Waltham, MA) supplemented with 10% fetal bovine serum (FBS; Sigma-Aldrich, St Louis, MO), 1% MEM vitamins, non-essential amino acids, sodium pyruvate, penicillin, streptomycin and fungizone. Suspension tumor cells were grown in RPMI 1640 medium (Gibco Life Technologies) supplemented with the same as the MEM. Cell lines were maintained at 37°C in a humidified incubator with 95% air and 5% CO_2.

Cell Proliferation

In order to determine the doubling times of the cell lines, cells were plated at different concentrations in 30 mm culture dishes. Cells were incubated at 37°C. The number of cells was counted every 24 hours by Coulter counter (Beckman Coulter, Brea, CA). Cellular doubling times were calculated by GraphPad Prism 5 software (Graph Pad Software, LaJolla, CA) with the following formula;

$$Y(t) = A \times e^{K \times t}, Doubling\ time = 0.6932/K$$

Where A is initial number of cells and Y(t) is the number of cells at time t. At least three independent experiments were carried out.

Chromosome Number

Cells were cultured with 0.1 mg/mL colcemid (GIBCO, Invitrogen, Carlsbad, CA) for 6 hours in order to harvest metaphase chromosomes. Samples were treated in hypotonic 75 mM KCl solution for 20 minutes at 37°C and fixed in 3:1 (methanol: acetic acid) fixation solution three times. Spread metaphase chromosomes were stained with Giemsa solution, and the chromosome number was observed under a BX51 microscope (Olympus, Tokyo, Japan). A minimum of 100 metaphase cells were analyzed to count chromosomes per cell. At least 50 metaphase cells were analyzed to count metacentric chromosomes per cell.

Cell Cycle Analysis

Cell cultures at 60% to 70% confluence were fixed in 70% ethanol at -20°C more than overnight. Cells were then centrifuged at 1,500 rpm for 5 minutes and washed once with PBS. Cells were then resuspended in 1 mL of staining solution (20 μg/mL propidium iodide, 0.1% TritonX-100, 500 μg/mL RNase A) and stained for 30 minutes at room temperature. Analysis was

done by FACSCalibur (Becton-Dickinson) and Cell Quest Pro program (BD Bioscience, Franklin Lakes, NJ). Three independent experiments with each cell line were carried out. Ploidy was estimated as the DNA content of G1 cells in the tumor cells normalized to diploid Chinese hamster ovary cells.

Irradiation

Log phase cultures were irradiated with different doses of ^{137}Cs gamma-rays using a J.L. Shepherd Model Mark I-68 6000Ci 137Cs irradiator, delivered at approximately 2.5 Gy/min at room temperature.

Cell Survival Assay for Adhesive Cultures

Radiosensitivity was measured by clonogenic assay for nonsuspension cell lines. Randomly dividing cells in T-12.5 flasks were irradiated, trypsinized and plated in triplicate onto 100 mm or 60 mm culture dishes at appropriate cell density. After incubating for 1–2 weeks to allow colony formation, colonies were rinsed with 0.9% NaCl, fixed with 100% ethanol and stained by 0.1% crystal violet. Each colony consisting of more than 50 cells was scored as a survivor. For each dose point, the number of positive colonies obtained from three dishes was averaged. Survival fraction (SF) was estimated by the following formula:

SF= (number of colonies formed) / (number of cells seeded × PE of the control group)

Plating efficiency (PE) was calculated as the ratio between colonies observed and number of cells plated. At least three independent experiments were carried out, then survival curves were drawn using linear-quadratic regression equations with Graph Pad Prism 5 software (Graph Pad Software). The survival fraction at 2 Gy radiation (SF2) and the survival fraction at 5 Gy radiation

(SF5) were obtained by interpolation of cell survival as estimates of the intrinsic radiosensitivity of each cell line.

Cell Survival Assay for Suspension Cultures

Since lymphoma and mast cell tumor cell lines are grown in suspension in media and their colonies are not measureable by the regular colony formation assay, a limiting dilution assay was used (Furth et al., 1981). Cells were plated in 96-well microtiter plates at densities of 1-200 cells per well at two or three cell densities per dose point. After irradiation the plates were incubated at 37°C for 2-3 weeks before scoring as negative or positive for growth based on microscopic examination (i.e. wells in which cell growth had occurred are positive). Based on the Poisson distribution, PE was calculated with following formula:

$$\mathrm{PE} = -\frac{\ln\left(Xs/Ns\right)}{S}$$

Where S is the cell number plated, Xs is the number of wells that had no colony growth, and Ns is the total number of wells scored. Survival fraction was calculated as ratio of PE of irradiated cells divided by PE of control cells and. At least three independent experiments were carried out, then survival curves were drawn using linear-quadratic regression equations with Graph Pad Prism 5 software (Graph Pad Software). The survival fraction at 2 Gy (SF2) and the survival fraction at 5 Gy (SF5) were calculated from the survival curves.

Analysis of Apoptosis

Apoptosis induction by IR was assessed using the terminal deoxynucleotidyl transferase (TdT)-mediated deoxyuridine triphosphate nick end-labeling (TUNEL) assay. Log phase growing cells cultured in 60 mm culture dishes were irradiated with 0 Gy or 5 Gy gamma-rays. After 48 hours of incubation, the cells were placed by means of cytocentrifugation (Cytospin, USA; 600

rpm speed for 4 minutes) on poly-D-lysine (Sigma-Aldrich) -coated slides. The slides were rinsed in PBS and fixed with 4% paraformaldehyde for one hour at room temperature. After the slides were washed three times with PBS, they were transferred into ice-cold 70% ethanol for 30 minutes. Following three washes with PBS, the slides were permeabilized with 0.5%Triton-X 100 and 0.1%SDS in PBS for 15 minutes on ice. For the positive control, a slide was treated with DNase (Sigma-Aldrich) before the TdT reaction. The cells were washed three times with PBS and incubated in 25 μL of the reaction mixture containing 1.5 mM $CoCl_2$, 12.5 U TdT, 1 mM 5-Bromo-2'-deoxyuridine-5'-triphosphate in TdT buffer (Br-dUTP, Sigma-Aldrich: the others, Roche, Indianapolis, IN) for 4 hours at 37°C in the dark. The reaction was stopped by PBS wash, and the cells were blocked in PBS with 10% goat serum overnight at 4°C. The slides were incubated with a mouse monoclonal BrdU antibody in 10% goat serum with PBS for one hour at 37°C. The cells were then washed three times with PBS, followed by incubation for one hour at 37°C with Alexa 488 Fluor-conjugated goat anti-mouse antibody (Molecular probes). Finally, the cells were counterstained with DAPI, and visualized by an Olympus BX51 equipped with a cooled CCD Exi Aqua camera (Q-imaging). Approximately 1000 nuclei from each slide were counted, and TUNEL positive frequencies were calculated. Apoptosis ratios were also determined by scoring DAPI staining cells with fragmented nuclear morphology.

G2 Chromosomal Assay

Gamma-ray-induced chromosomal aberrations during G2 phase of the cell cycle were measured as previously described (Parshad 1983). Log phase growing cells in T-25 culture flasks at 50 to 80% confluence were irradiated with 0 Gy or 0.5 Gy gamma-rays. After irradiation, the cells were incubated for 30 minutes, and then 0.1 μg/mL of Colcemid (Gibco) was added for one hour at 37°C in the incubator. The chromosome samples post 1.5 hours of irradiation were prepared

as described in chromosome number section. Although the cell populations were asynchronous, metaphase cells fixed at 1.5 hours after irradiation would presumably be in G2 at the time of gamma-irradiation. The interval of approximately 30 minutes after irradiation before Colcemid addition would allow cells in metaphase or prophase at the time of irradiation to complete mitosis and be in interphase by the time of fixation of cells. Chromatid-type aberrations (breaks and gaps) in 100 metaphase cells were scored for two separate experiments. Breaks are defined as discontinuities in the chromatids more than one chromatid wide. Gaps are defined as discontinuities less than the width of a chromatid. Abnormalities were expressed as the total number of chromatid breaks and gaps per 1,000 chromosomes as used in a canine study (Thamm et al., 2013).

Phosphorylated-H2AX in G1-Irradiated cells

We carried out the assay with cells synchronized and maintained in G1 during irradiation using the isoleucine deprivation method (Tobey and Ley, 1971). This was done because non-irradiated cells in S-phase have much higher levels of γ-H2AX foci, and also because the number of foci per cell depend on DNA content (MacPhail et al., 2003). Cells were cultured for 24 hours on plastic chamber slides to get 50% confluence and washed with PBS once. The normal growth medium was replaced twice in 1.5 doubling times with isoleucine-deficient MEM containing 5% 3×dialyzed FBS to synchronize the cells in the G1 phase. After G1 synchronization and exposure to 0 Gy or 1 Gy of gamma-rays, cells were incubated with 5-ethynyl-20-deoxyuridine (EdU) for 30 minutes (either immediately or after 5.5-hour incubation for repair). EdU-labeling was used to judge G1 synchronization; EdU specifically labels S phase cells (Limsirichaikul et al., 2009). The cells were then washed in PBS and fixed in 4% paraformaldehyde for 15 minutes. Following a second wash with PBS, cells were permeabilized with 0.5% Triton-X 100 and 0.1% SDS in PBS

for 10 minutes. EdU was first stained with the Click-iT® EdU Alexa Fluor1 488 Cell Proliferation Assay Kit (Molecular Probes, Invitrogen, OR, USA) (Salic 2008, Buck 2008). The slides were incubated with the Click-iT® EdU reaction cocktail prepared according to the manufacturer's instructions at room temperature in the dark for 1 hour. Slides were washed three times in PBS, fixed in 4% paraformaldehyde and blocked in PBS with 10% goat serum overnight at 4°C. Following overnight incubation, the cells were incubated with a mouse monoclonal phosphorylated histone H2AX antibody (Ser139) (γ-H2AX) (Millipore, Billerica, MA) in 10% goat serum with PBS for one hour at 37°C. The cells were then washed three times for 10 minutes each in PBS, followed by incubation for 1 hour at 37°C with Alexa 594 Fluor-conjugated goat anti-mouse antibody (Molecular Probes, Eugene, OR). The cells were mounted in a solution with DAPI containing slow fade (Invitrogen) after four times washes with PBS. Digital images were captured using a Zeiss Axioskop motorized Z-stage Microscope (Carl Zeiss, Jena, Germany) with CoolSnapHQ2 (Photometrics, Tucson, AZ) and Metamorph software (Molecular Devices, Sunnyvale, CA). Images were taken with one micron thickness and stacked by Metamorph Software. The pictures were then later used to count γ-H2AX foci per cell. Three independent experiments were carried out and numbers of the γ-H2AX were counted for a minimum of 50 EdU staining negative cells for each sample in each experiment.

Western Blotting

Cells were lysed with M-PER Mammalian Protein Extraction Reagent (Thermo Fisher Scientific) and protease inhibitors, Halt Protease Inhibitor Cocktail Kit (Thermo Fisher Scientific). Protein extracts (20 μg per sample) were size-fractionated on NuPage® 4–12% Bis-Tris gels (Invitrogen), electro-transferred to nitrocellulose membranes (Bio-Rad) in buffer (25 mM Tris, 192 mM glycine, 20% (v/v) methanol, and 0.01% SDS) at a current density of 3.0 mA/cm2 for 16

hours at 4°C. The filters were blocked with Tris-bufferd saline with 0.05% Tween 20 containing 2% (w/v) skim milk, and reacted with a primary antibody for 2 hours at room temperature, followed by an incubation with a secondary antibody for 1 hour at room temperature. The immunoreactive signals were detected using SuperSignal Western Blotting Detection Kit (Thermo Fisher Scientific) and a ChemiDocTM XRS+System (Bio-Rad). Protein expression from band strength was analyzed by Image Lab software (Bio-Rad). The primary antibodies used in this study were the mouse anti-DNA-PKcs monoclonal antibody (Ab-4; Neomarkers, Fremonti, CA) (1:100), the rabbit anti-RAD51 polyclonal antibody (H-92; Santa Cruz Biotechnology, Inc., Santa Cruz, CA) (1:100), the rabbit anti-FANCD2 polyclonal antibody (NB100-182; Novus Biologicals, Littleton CO) (1:1,000), and the mouse monoclonal beta-actin (Abcam 8226; Abcam, Cambridge, MA) (1:3,000). The secondary antibodies were goat anti-mouse IgG HRP conjugated antibody (1:10,000) (Santa Cruz Biotechnology, Inc., Santa Cruz, CA) and goat anti-rabbit IgG HRP conjugated antibody (1:10,000) (Cell signaling, Boston MA). Each expression band was estimated from molecular weight of each protein and the band detected in human cancer cell line A549.

Immunocytochemistry

Cells cultured in 60 mm culture dishes for at least 24 hours were fixed, permeabilized and immunostained as in the section of phosphorylated-H2AX in G1 irradiated cells. The primary antibodies were the same for the western blotting (see in the Western blotting section). The secondary antibodies were Alexa 594 Fluor-conjugated goat anti-mouse antibody (Molecular Probes, Eugene, OR) and Alexa 488 Fluor-conjugated goat anti-rabbit antibody (Molecular Probes).

Identification of Differentially Expressed Genes

The basal gene expression profiles of the canine tumor cell lines were from Affymetrix GeneChip Canine Genome 2.0 arrays, obtained from the study by FACC. The data had been previously preprocessed using Robust Multichip Average (RMA) algorithm, and the expression values were log-transformed with a base of 2 for the data analysis, yielding a set of 18030 genes for downstream analysis. We applied the Pathway Studio 7.0 software (Ariadne Genomics, Inc., Rockvilee, MD, USA) to identify genes that were expressed significantly differently between the radiosensitive and radioresistant groups. Differences in expression between the sensitive group versus the resistant group were calculated using an unpaired t-test. The Benjamini-Hochberg false discovery rate was used for multiple testing corrections (Benjamini 1995). An absolute log ratio greater than 1 with a p-value less than 0.05 was used for the statistical significance. A heat map for the identified 314 genes was made using MultiExperiment Viewer (MeV) v 4.9 (Saeed et al., 2006). The significantly differentially expressed genes were imported into the Protein Analysis Through Evolutionary Relationships (PANTHER) 9.0 software (Mi et al., 2010) and visualized as pie charts showing the number of genes in each functional classification category and were compared against the number of genes in that representation of PANTHER classification categories.

Gene Set Enrichment Analysis

Functional analysis was performed by examining the enrichment for differentially expressed genes for Gene Ontology (GO) biological processes in the Pathway Studio 7.0 software and by the Database for Annotation, Visualization and Integrated Discovery (DAVID) 6.7 (Ashburner et al., 2000, Dennis et al., 2003, Kruse and Stewart, 2007). Fisher's exact p-value was used for the ranking. Since the 314 genes were significantly enriched in 268 functions of the

biological process in the Gene ontology (GO) as cut off level $p<0.05$ by the Pathway Studio 7.0 software, we used the DAVID to confirm the significant levels of each functions and generated the table in the results. Gene ontology (GO) is a system widely used for gene expression profiling including radiosensitivity (Dennis et al., 2003). It provides a shared vocabulary (ontology) of defined terms to represent specific gene product properties. Ingenuity Pathway Analysis (IPA) software v 8.6 (Ingenuity System, Redwod City, CA) was used to define canonical pathways specifically enriched in the sets of genes. We used this software based on a previous study of the NCI-60 (Kim et al., 2012). In this test, the p-value was measured to decide the likelihood that the association between genes and a given pathway was due to random chance using Fisher's exact test. The Benjamini-Hochberg method of multiple testing was used for correction (Benjamini et al., 2001).

Statistical Analysis

For statistical analysis, GraphPad Prism 5 software (Graph Pad Software) was used. The D'Agostino-Pearson test was used to determine if the values have a normal distribution. Differences with a P value of less than 0.05 were considered statistically significant. Correlations of SF2 and other parameters were determined by Pearson test. Statistical comparisons of mean values in the G2 chromosome assay (among each cell line) and the γ-H2AX assay (control vs 6 hours following 1 Gy) were performed using Kruskal-Wallis test followed by Dunn's multiple comparison test. Statistical comparison of mean values in the SF2/SF5 (radioresistant group vs radiosensitive group) and in the apoptosis assay (0 Gy vs 5 Gy) was performed using unpaired two tailed t-test.

Results

Clonogenic Survival Following Exposure to Gamma-Radiation

The study design is in Figure 3.1. We irradiated each of the 27 canine cancer cell lines in the ACC30 panel with 0, 1, 3 or 5 Gy of gamma-rays and measured colony formation. Their survival curves are shown in Figure 3.2. SF2 and SF5 values that were calculated from the survival curve, as well as plating efficiency, are reported in Table 3.1. These data represent the range of canine tumor cell radiosensitivities across different tumor types. The SF2 ranged from 0.17 to 0.94, and the SF5 ranged from 0.009 to 0.69. The plating efficiency of these cell lines also demonstrated a wide variation and ranged from 3% to 68%. The radiosensitivity of the three canine OSA cell lines (D17, Moresco and Gracie) measured by clonogenic assay was consistent with those that have been described in Chapter 2, Figure 2.2. Therefore, the data of the basic cellular characteristics (e.g. doubling time, chromosome analysis) shown in Chapter 2 were also used for the analysis in this Chapter. One of the canine OSA cell lines, Abrams, showed a more resistant phenotype to gamma-rays in this study compared to the result in the Chapter 2. Therefore, the experiments of all the other basic characteristics in this study for Abrams were examined again.

Basic Characterization of Canine Cancer Cell Lines

Each cell line was characterized by a combination of data representing cellular doubling time, cell cycle distribution, ploidy pattern, chromosome number, and metacentric chromosome frequency, with the data summarized in Table 3.1 and Table 3.2. The doubling times of each cell line ranged from 15 hours (CML-6M, CTAC) to 40 hours (STSA-1), showing wide variation among the cell lines. We measured the cell cycle distribution of each cell line by flow cytometry. The percentage of cells in each phase of the cell cycle ranged from 39.3% (CLBL1) to 69.6% (BR)

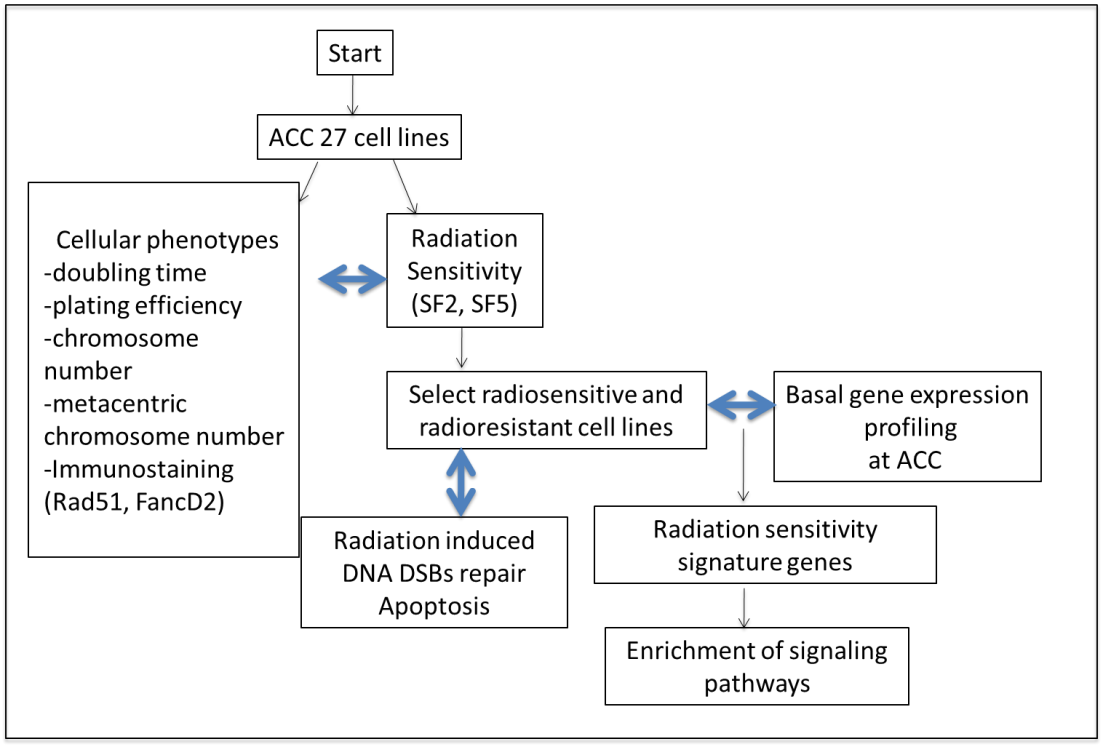

Figure 3.1: *Study scheme of analysis.*

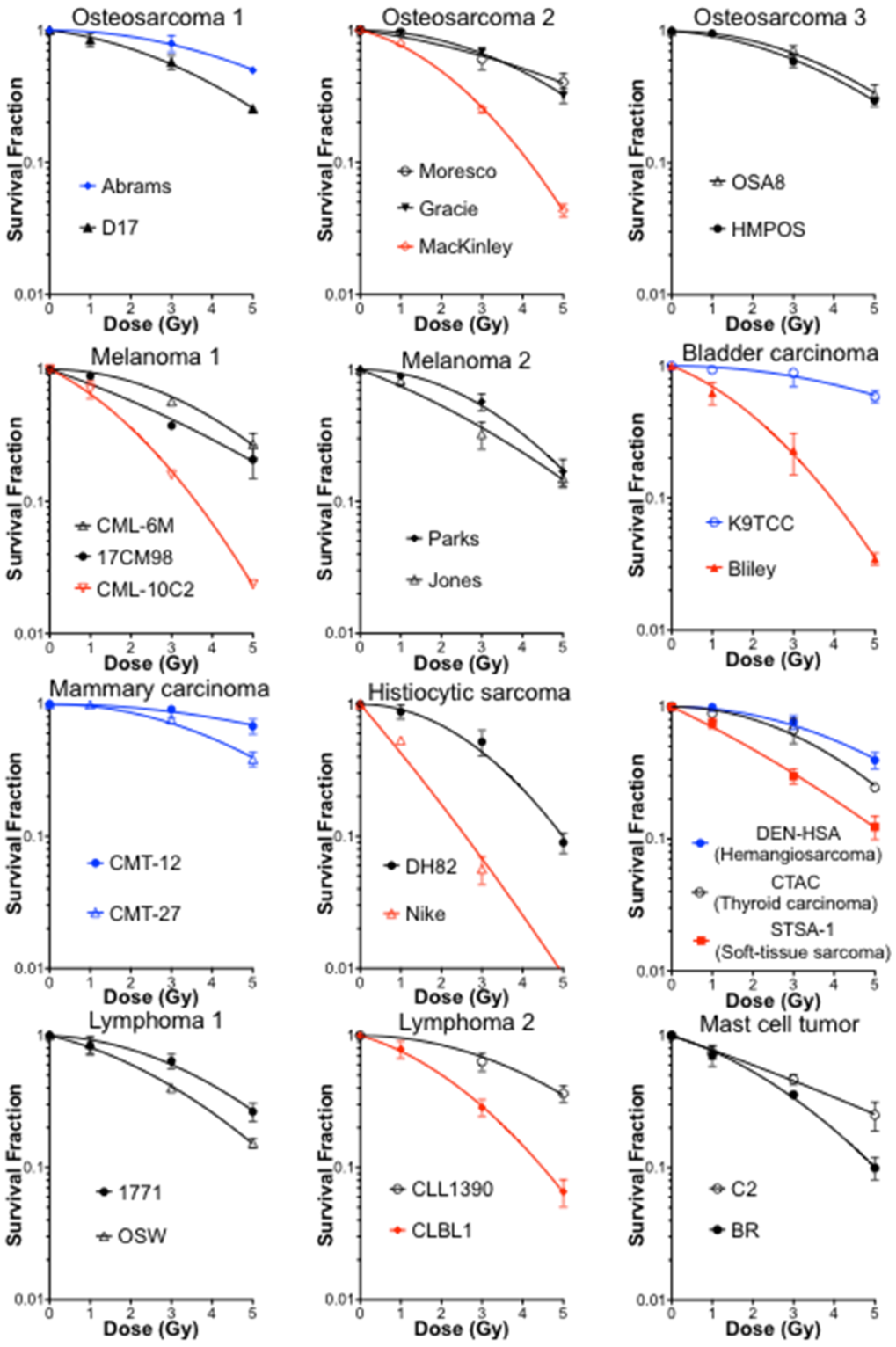

Figure 3.2: *Radiation induced survival curves in 27 canine cancer cell lines from various tumors in the ACC30 panel.* Experiments were carried out at least three times and error bars indicate the standard error of the means. We selected the most radiosensitive cell lines (red curves) and the most radioresistant cell lines (blue curves) for the following analysis.

Table 3.1: Characteristics and radiation survival of cell lines used in this study

Cell line	Type	Doubling time (hour)	PE	SF2	SF5	Cell cycle distribution (%)		
						G1	S	G2/M
D17*	OSA	22	0.35	0.70	0.258	43.3	28.1	28.5
Abrams	OSA	19	0.49	0.896	0.503	49.0	36.8	14.4
Moresco*	OSA	22	0.21	0.81	0.398	67.5	28.3	4.20
Gracie*	OSA	19	0.18	0.84	0.324	44.4	38.6	17.0
MacKinley*	OSA	28	0.18	0.49	0.043	40.2	47.7	12.1
HMPOS	OSA	20	0.24	0.776	0.295	52.7	35.4	12.0
OSA8	OSA	21	0.36	0.829	0.339	67.5	22.8	9.83
17CM98	Melanoma	22	0.22	0.577	0.201	62.0	22.7	15.3
CML-6M	Melanoma	15	0.65	0.809	0.266	51.9	34.3	13.8
CML-10C2	Melanoma	21	0.17	0.360	0.023	50.7	32.2	17.1
Jones	Melanoma	14	0.68	0.532	0.146	55.0	33.5	11.5
Parks	Melanoma	30	0.18	0.755	0.173	42.3	17.3	29.9
CMT-12	Breast	19	0.51	0.943	0.692	37.7	39.4	22.9
CMT-27	Breast	18	0.55	0.861	0.394	42.1	35.2	22.8
DEN-HSA	HSA	16	0.47	0.870	0.403	47.7	36.5	15.7
K9TCC	Bladder	18	0.61	0.921	0.600	46.7	37.4	15.9
Bliley	Bladder	20	0.16	0.418	0.035	55.1	28.7	16.2
DH82	Histiocytic	26	0.38	0.690	0.099	45.8	31.7	22.6
Nike	Histiocytic	25	0.16	0.174	0.009	42.1	37.9	20.0
STSA-1	Soft-tissue	40	0.23	0.503	0.122	42.3	27.8	29.9
CTAC	Thyroid	15	0.60	0.801	0.253	53.2	36.7	10.2
1771	Lymphoid	24	0.65	0.782	0.270	66.2	28.5	5.38
OSW	Lymphoid	16	0.43	0.603	0.151	56.2	36.6	7.28
CLBL1	Lymphoid	19	0.41	0.504	0.065	39.3	50.1	10.5
CLL1390	Lymphoid	37	0.55	0.847	0.354	62.6	33.6	3.74
C2	Mast cell	21	0.44	0.599	0.254	64.7	27.1	8.18
BR	Mast cell	36	0.03	0.533	0.101	69.6	28.9	1.52

Abbreviations: OSA, osteosarcoma; HSA, hemangiosarcoma; PE, plating efficiency; SF2, survival fraction at 2 Gy; SF5, survival fraction at 5 Gy. *Data from the CHAPTER 2.

Table 3.2. Characteristics of chromosome number of cell lines used in this study

Cell line	Type	Ploidy pattern	No. of chromosomes/cell Mean±SD	No. of metacentric chromosomes/cell Mean±SD (%*)
D17*	OSA	Triploid	79.1±25.4	43.2±14.2 (54%)
Abrams	OSA	Triploid	107.5±21.0	15.8±3.56 (15%)
Moresco*	OSA	Triploid	82.4±15.9	30.9±4.9 (38%)
Gracie*	OSA	Diploid	74.3±4.8	4.3±2.5 (5.8%)
MacKinley*	OSA	Diploid	58.2±5.1	15.7±3.2 (27%)
HMPOS	OSA	Triploid	84.3±10.6	29.2±2.90 (35%)
OSA8	OSA	Triploid	94.5±6.70	14.3±1.57 (15%)
17CM98	Melanoma	Tetraploid	155.2±28.5	2.40±1.01 (1.5%)
CML-6M	Melanoma	Diploid	78.6±5.24	2.03±0.65 (2.6%)
CML-10C2	Melanoma	Aneuploid (2-3)	105.2±16.6	6.67±1.27 (6.3%)
Jones	Melanoma	Aneuploid (2-3)	81.0±3.61	1.99±0.45 (2.5%)
Parks	Melanoma	Aneuploid (2-3)	73.66±11.5	2.82±1.28 (3.8%)
CMT-12	Breast	Tetraploid	120.6±20.3	15.6±2.38 (13%)
CMT-27	Breast	Diploid	76.1±20.5	10.2±2.91 (13%)
DEN-HSA	HSA	Aneuploid (2-3)	76.9±6.67	5.27±0.95 (6.9%)
K9TCC	Bladder	Diploid	77.3±14.3	8.12±1.36 (11%)
Bliley	Bladder	Tetraploid	145.3±31.8	5.21±1.73 (3.6%)
DH82	Histiocytic	Triploid	72.2±13.4	28.2±6.20 (39%)
Nike	Histiocytic	Aneuploid (2-3)	64.4±102	19.5±4.77 (30%)
STSA-1	Soft-tissue	Diploid	60.5±12.1	15.5±1.70 (26%)
CTAC	Thyroid	Aneuploid (2-3)	81.1±13.4	7.80±2.00 (9.6%)
1771	Lymphoid	Diploid	56.6±3.02	19.5±3.23 (34%)
OSW	Lymphoid	Diploid	73.6±2.56	1.92±0.87 (2.6%)
CLBL1	Lymphoid	Diploid	73.1±15.2	4.73±1.09 (6.5%)
CLL1390	Lymphoid	Triploid	142.7±29.2	4.47±1.46 (4.8%)
C2	Mast cell	Triploid	94.0±9.39	15.8±1.95 (17%)
BR	Mast cell	Aneuploid (1-2)	73.5±7.05	3.35±0.94 (4.5%)

Abbreviations: OSA, osteosarcoma; HSA, hemangiosarcoma.

*Frequencies of metacentric chromosome.

for G1 phase, from 17.3% (Parks) to 50.1% (CLBL1) for S phase, and from 1.52% (BR) to 29.9% (Parks and STSA-1) for G2/M phase. These cell lines displayed variable average numbers of chromosomes, ranging from 57 (1771) to 155 (17CM98). The canine cancer cell lines in the ACC 30 panel showed increased numbers of metacentric chromosomes resulting from Robertsonian translocation events, with the exception of two cell lines (Jones and OSW). Frequencies of metacentric chromosomes varied among cell lines from less than two, the normal karyotype, to 43.2 (D17) per cell. All cell lines had greater than the diploid amount of DNA. We found overall agreements between abnormal ploidy and increased chromosome numbers, but not always. Nike, for example, had a smaller number of chromosome per cell with 64.4, but the ploidy pattern was between diploidy and triploidy. We evaluated correlations between the variable cellular characteristics and the radiosensitivity. In these cell lines, there was no significant correlation of SF2 with S-phase fraction, doubling time, chromosome number, or number of metacentric chromosomes, while there was a statistically significant correlation between SF2 and plating efficiency (r^2=0.26, p=0.008, Pearson test) (Figure 3.3).

Selection of Radiosensitive and Radioresistant Groups

The canine cancer cell lines in the ACC30 panel were ranked by the radiosensitivity parameters, SF2 or SF5, and sensitive or resistant lines for each parameter were defined by cutting the groups at discontinuities in the data (Figure 3.4). The sensitive or resistant groups comprised 5-6 cell lines. The radioresistant group selected for microarray analysis displayed SF2 values from 0.17 to 0.50. The radiosensitive group exhibited SF2 values above 0.86. The difference of tumor cell radiosensitivity was better seen when the radiosensitivity of tumor cells was expressed as survival fractions at the higher dose (SF5). The cell lines in the two groups based on the SF5 comparison were slightly different from those based on the SF2 comparison. The survival fractions

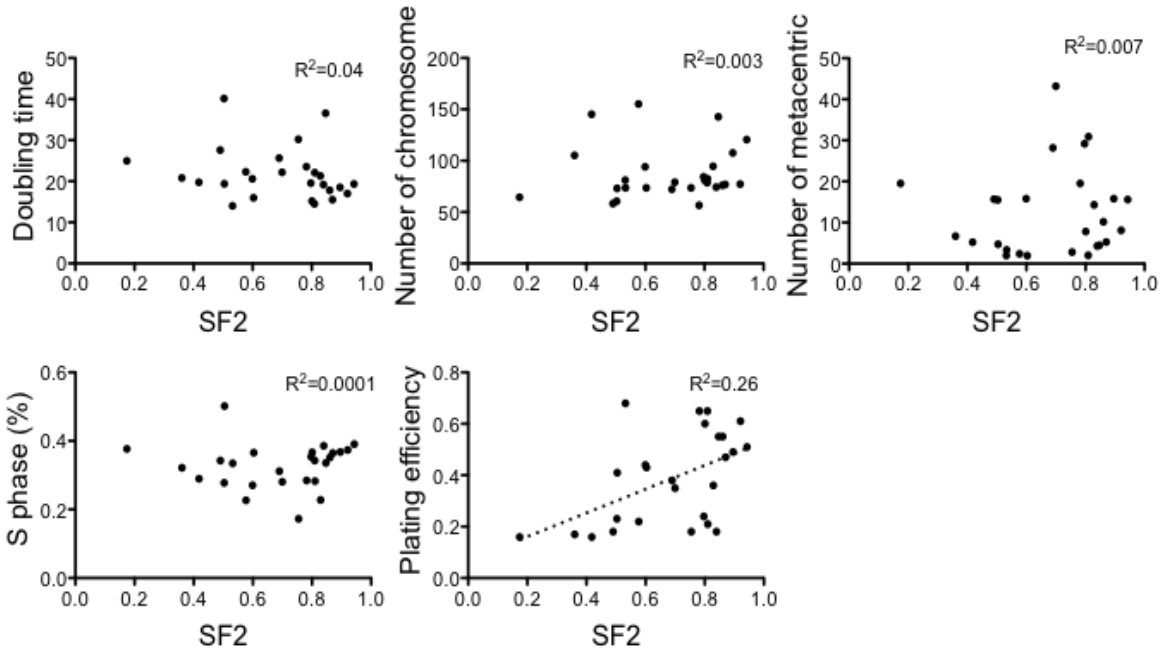

Figure 3.3: *Plots of the cellular characteristics as a function of the SF2 values in each cell line.* Each dot represents a cell line. The correlations were assessed using the Pearson test. The lines were fitted by a least-squares method.

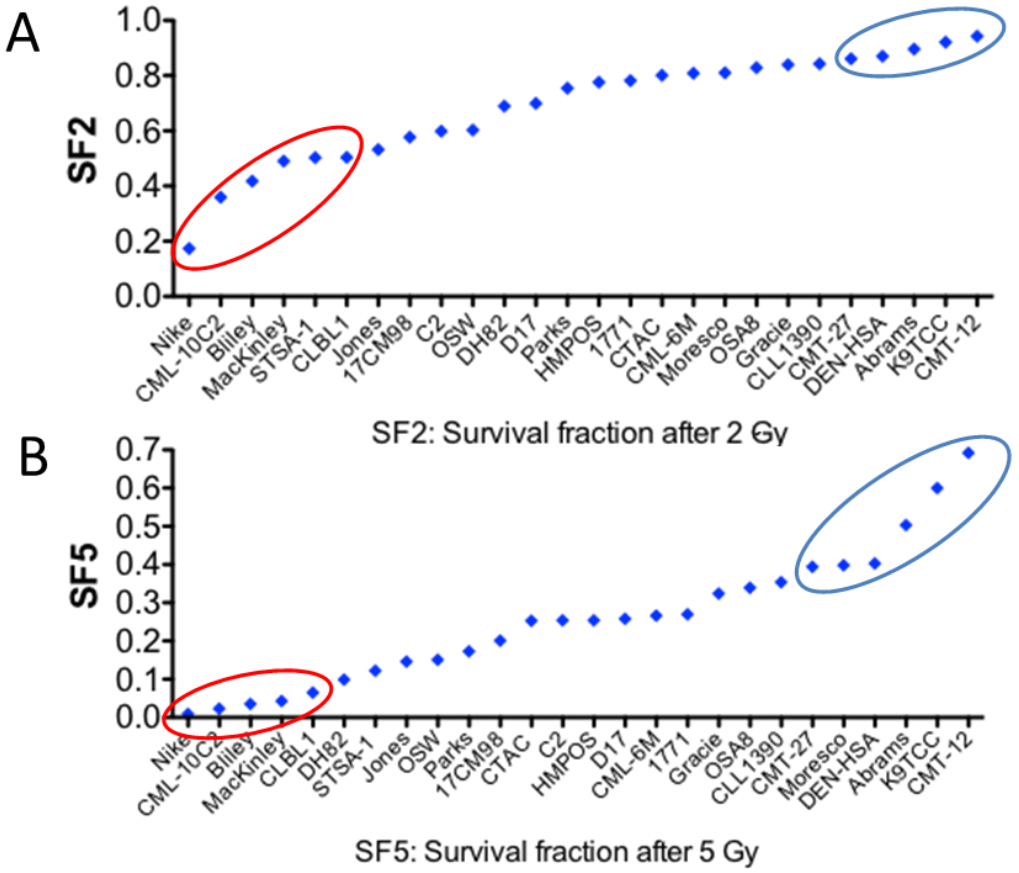

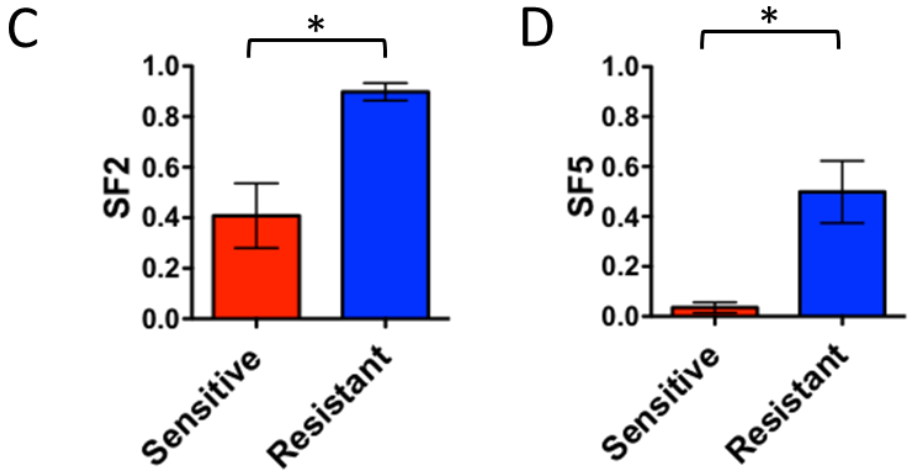

Figure 3.4: *The measured SF2 and SF5 of 27 canine cell lines. 27 cell lines are ranked based on SF2 (A) and SF5 (B*). Red circle: radiosensitive group, blue circle: radioresistant group. (C, D) Comparison between the mean values of two groups based on the SF2 (C) or SF5 (D). Error bars indicate standard deviation. * $p<0.0001$ versus sensitive and resistant group (unpaired two tailed t-test).

between two groups of cell lines based on either the SF2 or SF5 comparison were statistically different ($p<0.001$) (Figure 3.4c).

Relationship between Intrinsic Radiosensitivity and DNA DSBs in G1-irradiatied Cells

To examine whether the response of cells to DNA DSBs correlates with radiosensitivity in the canine cancer cell lines, we used γ-H2AX assay in the five most radioresistant and five most radiosensitive cell lines selected from SF2 ranking. We measured the number of γ-H2AX foci after 1 Gy gamma irradiation in G1-phase synchronized cells following 30-min or 6-hour repair time (Figure 3.5). In the isoleucine deficient media to synchronize cells in G1, most of DEN-HSA cells died after a 24-hour incubation, and CMT-12 cell line was not synchronized in the media. Therefore, we couldn't use these two cell lines for this analysis. The other cell lines showed G1 synchronization with less than 16% in the S-phase in the isoleucine deficient media for 1.5 times doubling time. In some cells not in the S phase with 0 Gy treatment, large numbers of endogenous γ-H2AX foci were observed in all of the canine cancer cells. We excluded cells with high levels of foci outside of IR-induced distribution from the analysis to detect the residual levels of foci induced by IR. Based on the analysis without cells with high levels of endogenous γ-H2AX foci numbers, 1 Gy of gamma-rays induced significantly higher levels of γ-H2AX foci after 30 min irradiation in all cell lines utilized in this analysis ($p>0.05$ vs 0 Gy, not shown in the figure) (Figure 3.5). At the 30 minutes after irradiation, the median number of γ-H2AX foci was dependent on the DNA content of each cell line. Furthermore, the radiosensitive CML-10C2, Nike, STSA-1 and MacKinley showed that the numbers of γ-H2AX after 6 hour following 1 Gy irradiation were still significantly higher compared to their control levels. On the other hand, all three of the radioresistant cell lines and one radiosensitive cell line, Bliley, didn't show significant differences between control cells and cells with 6 hours following irradiation.

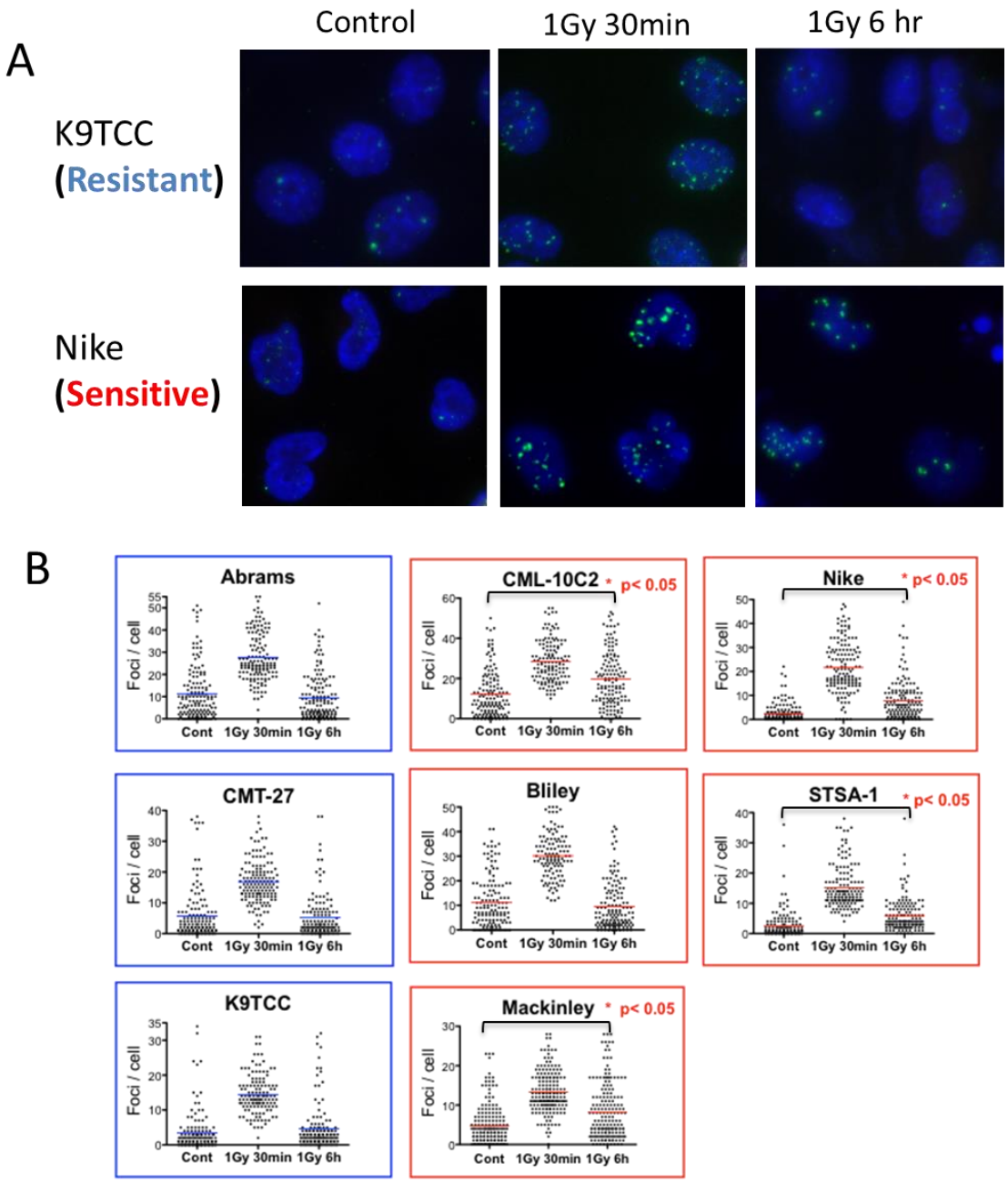

Figure 3.5: *Phosphorylated-H2AX in G1 irradiated cells of radioresistant and radiosensitive groups in the ACC30 panel.* Cells were synchronized in G1 using isoleucine deficient media and then irradiated with 1 Gy of gamma-rays. Following 30 min or 6 hr incubation time, cells were stained with γ-H2AX immunocytochemistry. (A) Examples of γ-H2AX foci (green) in nuclear DAPI (blue) staining in control, 1Gy followed by 30 min incubation and 1 Gy followed by 6 hr incubation in EdU negative cells. B) Quantitative analysis of gamma-H2AX foci per cell. The pooled date from three independent experiments scoring 50 cells in each experiment are shown. The bar indicates mean. Statistical significances are shown for only control versus 6 h after 1 Gy (nonparametric Kruskal-Wallis test).

Relationship between Intrinsic Radiosensitivity and Chromosomal Damage in G2-irradiated Cells

To determine whether the differences in intrinsic radiation sensitivity were because of chromosome damage resulting from DSBs, the number of chromatid breaks and gaps due to radiation exposure were measured. The cells of the radioresistant and radiosensitive groups were irradiated in G2 phase and following 1.5 hour repair time prepared for chromosome analysis (Figure 3.6). We measured the aberrations at 1.5 hours post irradiation because previous work had suggested that G2-phase delay is minimal when cells are analyzed within 2 hours of irradiation (Parshad et al., 1983). However, we observed a different effect on irradiation on the percentage of irradiated cells relative to non-irradiated cells entering metaphase among the cell lines (Figure 3.6c). The G2-delay effects can be dose dependent (Walters and Petersen, 1968), therefore, we used a lower dose of 0.5 Gy than the other assays in this study. Since the 10 cell lines showed a statistically different number of chromatid breaks and gaps in non-irradiated control cells among the cell lines ($p<0.05$, Kruskal-Wallis test) (Figure 3.6d), the induced number of breaks and gaps by 0.5 Gy were calculated and shown in the Figure 3.6e. The mean frequency of chromatid breaks and gaps per 1000 chromosome induced by 0.5 Gy of gamma-rays ranged from 14.7 (CMT-27) to 34.2 (CML-10C2). Some of the radiosensitive cell lines, such as CML-10C2, had a significant deference versus most radioresistant cell lines, but not all of them ($p>0.05$, CML-10C2 vs Abrams). The results expressed as the levels of chromatid aberrations per cell also showed similar results. A comparison of the IR induced G2 chromosome aberrations with the SF2 values showed no significant correlation ($R^2=0.27$, Pearson test) (Figure 3.6f).

Relationship between Intrinsic Radiosensitivity and Apoptosis Frequency in Irradiated Cells

The five radioresistant cell lines and the five radiosensitive cell lines were also assessed for apoptosis at 48 hour post-irradiation (0 Gy and 5 Gy). The percentage of apoptotic cells for

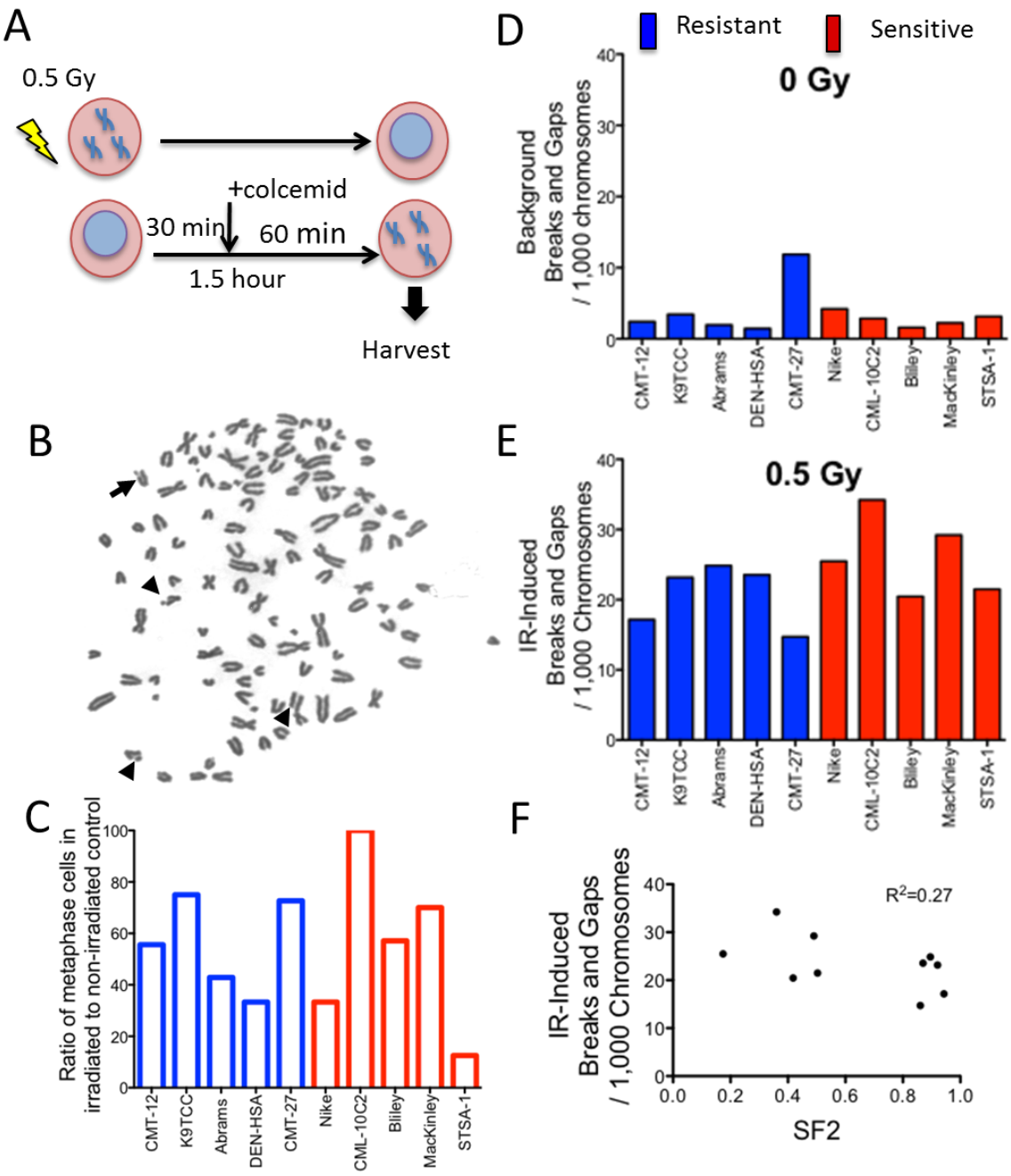

Figure 3.6: *G2 chromosome assay in the radioresistant and radiosensitive canine cancer cell lines.* (A) The scheme of G2 chromosome assay. (B) Example of a metaphase spread (DEN-HSA) after 0.5 Gy gamma-irradiation. Chromatid breaks (arrowheads) and gaps (arrow) were counted. (C) Influence of irradiation on progression of G2 cells into metaphase. Results counting 300 cells. (D, E) Incidence of chromatid breaks and gaps. Since spontaneous levels (C) were significantly different between the cell lines ($p<0.001$, Kruskal Wallis test), chromatid breaks and gaps following 0.5 Gy of gamma-rays were shown based on the IR-induced levels (D). Two independent 50 metaphase cells were counted. (F) Correlation between total aberration and SF2. Correlation was tested by Pearson test.

each cell line of 0 Gy or 5 Gy is shown in Figure 3.7. Apoptotic cells were counted by TUNEL staining and DAPI stating and reported separately. DNase treatment was used as a positive control representing the highly apoptotic cells (>90%) (Figure 3.7a). Although apoptosis was seen in all control cultures ranging 0.1-3.4% by TUNEL staining and 0.37-3.3% by DAPI staining of the cells, depending on the cell line, there was no significant difference between the cell lines. The percentage of apoptotic cells increased significantly with 5 Gy irradiation in Abrams, Nike, and CML-10C2 by DAPI staining relative to 0 Gy samples ($p<0.05$, unpaired t-tests) (Figure 3.7c). Using the measurement of apoptotic cells by TUNEL assay, similar results to these by DAPI staining were observed. A significant increase of apoptosis frequency by IR were observed in one (Abrams) out of the five radioresistant cell lines and in three (Nike, CML-10C2 and MacKinley) out of the five radiosensitive cell lines (Figure 3.7d).

Protein Expression of DNA Repair pathway in Radiosensitive and Radioresistant Groups

Since DNA DSB repair pathways are closely related to cell killing by IR, we studied the protein status of the major pathways in the canine cancer cells. We focused on the two major NHEJ and HR in the DSB repair and FA pathway, which possibly contributes to DNA damage repair for irradiation. Protein expression of major players in each pathway, DNA-PKcs in NHEJ, RAD51 in HR and FANCD2 in FA pathway were detected by western blotting in the radioresistant and radiosensitive groups (Figure 3.8). The expression of DNA-PKcs, FANCD2 and RAD51 were not uniform among the cell lines, and there was no clear trend between the expression levels in the two groups as shown in Figure 3.8b. The expression of the three proteins in the canine cancer cells were overall higher than those in normal dog fibroblasts. We observed less expression of DNA-PKcs proteins in Nike (1.4 fold of normal) and the highest expression in STSA-1 (5.4 fold of normal). For the FANCD2 protein, the lowest expression was in DEN-HSA (0.8 fold of normal)

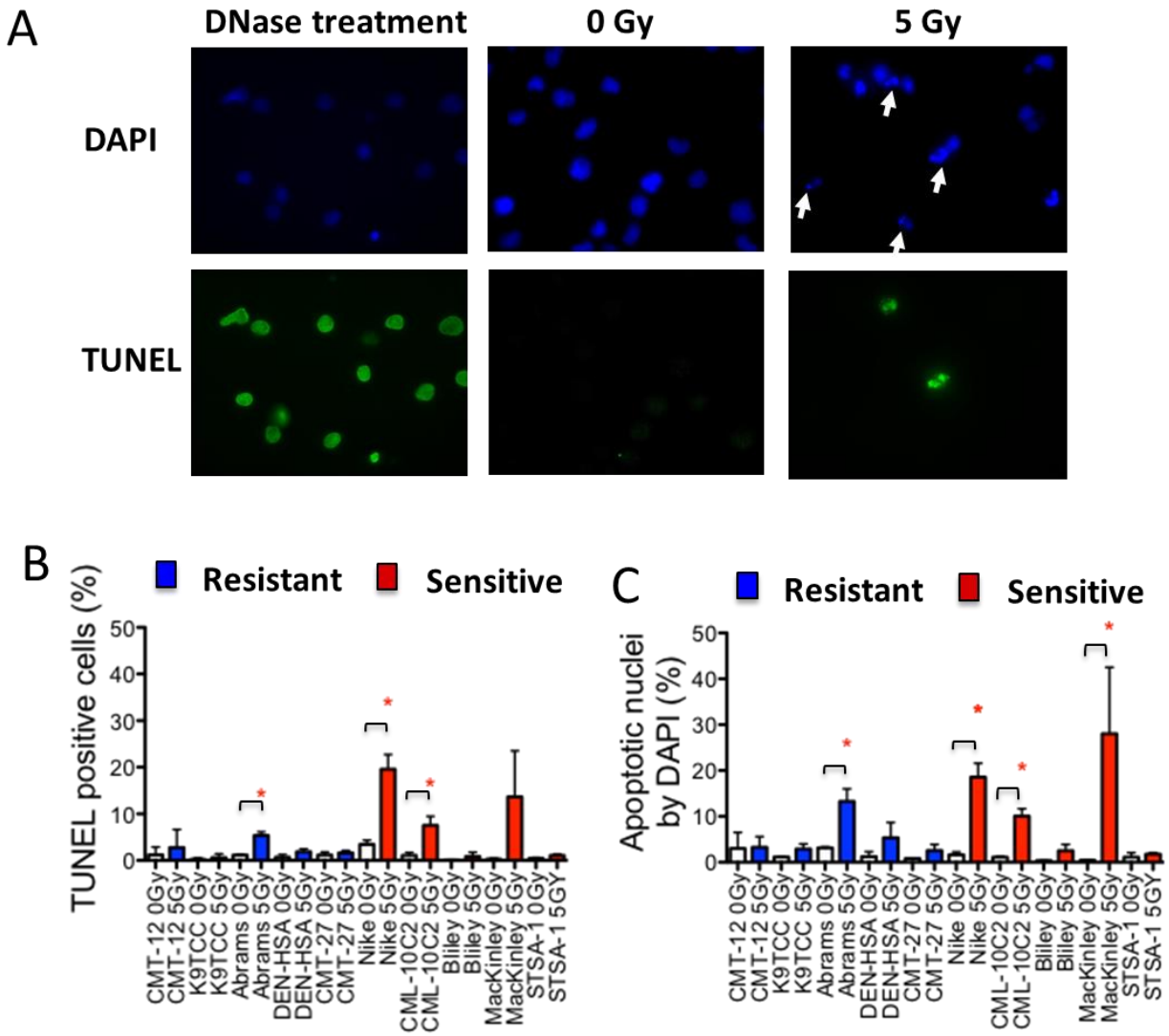

Figure 3.7: *Radiation-induced apoptosis in the radioresistant and radiosensitive canine cancer cell lines.* (A) Representative immunofluorescence images of Nike cell line. TUNEL positive cells were induced by DNase treatment as a positive control. Cells from irradiated cells with 0 Gy and 5Gy of gamma-rays were collected by cytospin on slides 48 hour after irradiation. We counted TUNEL positive cells and apoptotic nuclei by DAPI staining (arrows) separately. (B, C) IR-induced apoptosis cells using TUNEL staining (B) and DAPI staining (C). 1000 cells were counted in two independent experiments. Error bars represent standard deviation. *, $p<0.05$ versus 0 Gy and 5 Gy for each cell line (unpaired two tailed t-test).

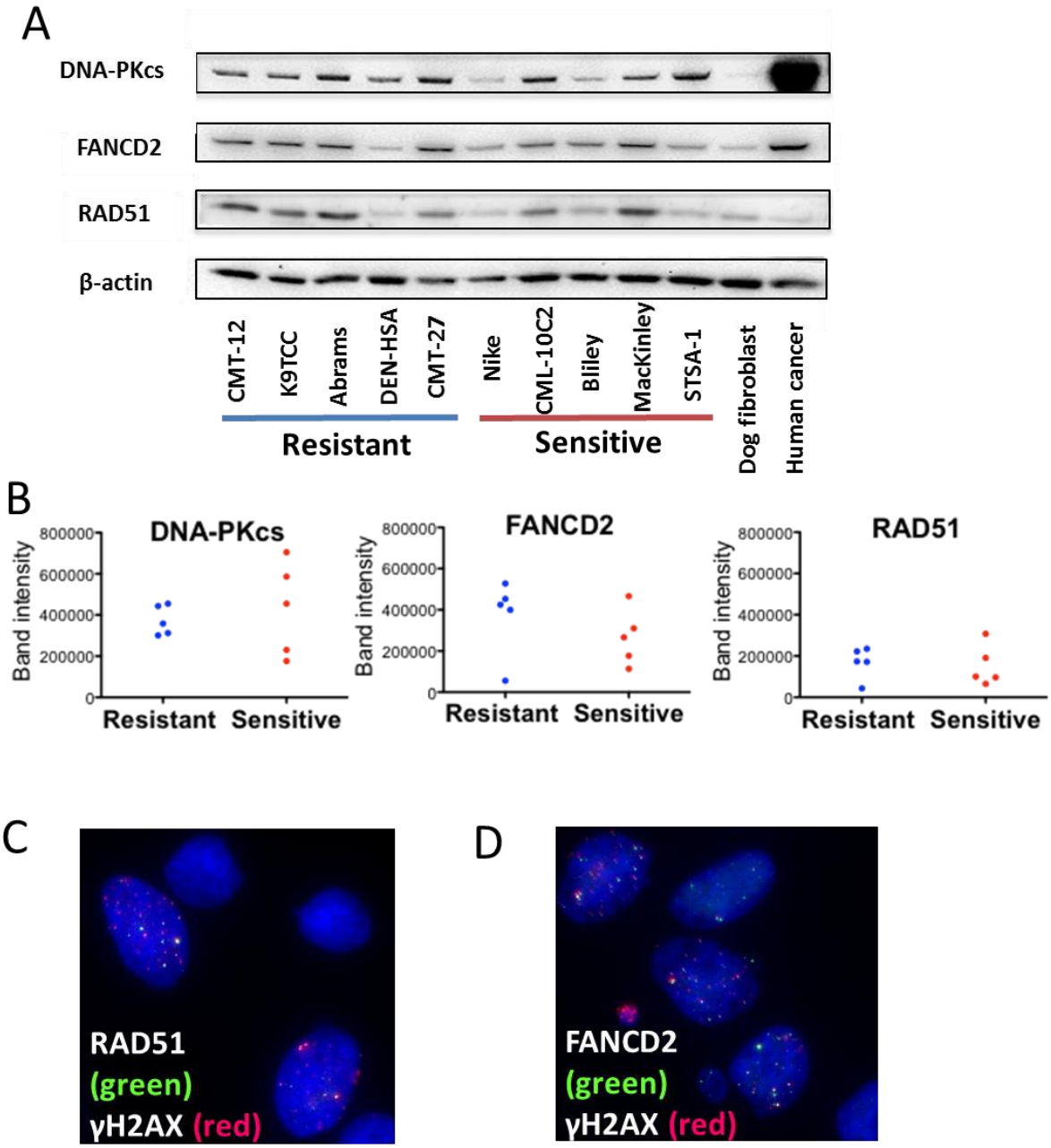

Figure 3.8: *Basal expressions of DNA repair proteins in the radioresistant and radiosensitive canine cancer cell lines.* (A) Western blot analysis of DNA-PKcs (460 kDa), FANCD2 (165 kDa) and RAD51 (37 kDa). β-actin (42 kDa) expression was used as a control. Each expression band was estimated from molecular weight. (B) Band intensity of western blot. (C, D) Representative images for RAD51 foci (C) and FANCD2 foci (D) co-localized with gamma-H2AX.

and the highest expression was in CMT-27 (7.2 fold of normal). For the RAD51 protein, the lowest expression in DEN-HSA (0.4 fold of normal) and the highest expression was in MacKinley (3.0 fold of normal). When compared between the canine and the human cancer cell line (A549), the expression levels of DNA-PKcs in STSA-1, which showed the highest expression of the canine cell lines, were 10 times less than that of A549.

We also observed the foci of RAD51 and FANCD2 as functionally co-localized with γ-H2AX on the replication stress without irradiation in all 27 cell lines (Figure 3.8c). Another advantage for testing RAD51 and FANCD2 was that these protein foci formations require other upstream proteins, such as five RAD 51 paralog proteins and eight Fanconi anemia proteins (Moldovan and D'Andrea, 2009, van Veelen et al., 2005, Bogliolo et al., 2007). Therefore, detecting foci formation enabled us to screen for the presence of these upstream proteins in all the 27 canine cancer cell lines in the ACC30 panel. We observed functional foci of RAD51 and FANCD2 in all of the cell lines.

Selection of Differentially Expressed Genes between Radiosensitive and Radioresistant Groups

We performed microarray analysis of gene expression profiling over 18,000 genes between the six most radiosensitive and the five most radioresistant canine cancer cell lines based on the SF2 comparison (Figure 3.4a). Using the Pathway Studio software, we identified a total of 566 genes that were differentially expressed between the two groups; 387 transcriptswere increased and 179 were decreased in the radiosensitive group compared with the radioresistant group. We also analyzed differentially expressed genes, depending on the SF5 comparison (Figure 3.4b). Overlapping significantly differently expressed genes were found for the analysis using SF2 the SF5 comparison (Figure 3.9). We assumed that the significant genes would be in the shared genes of SF2 and SF5. Therefore, the 314 genes commonly upregulated and downregulated in both SF2

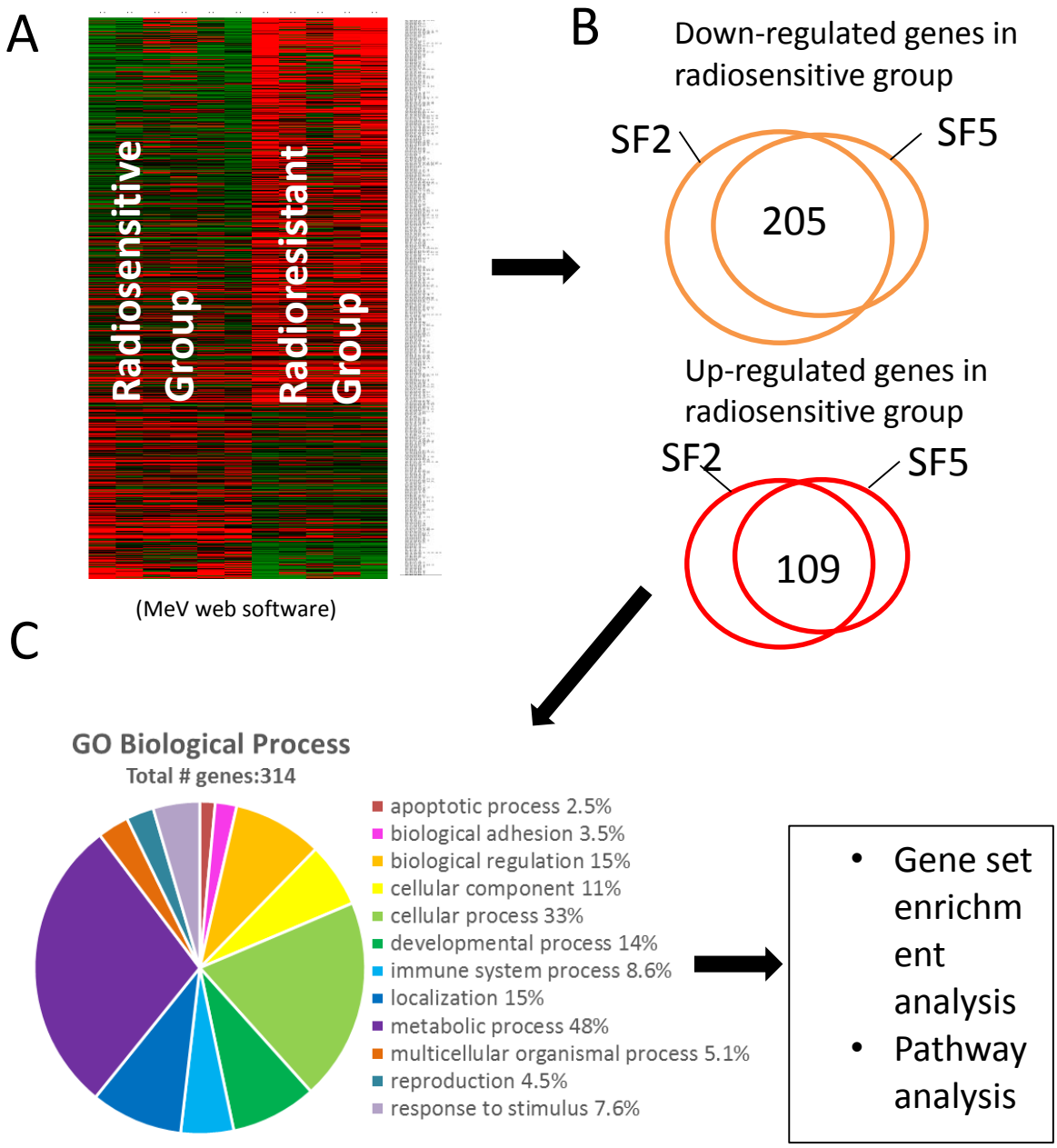

Figure 3.9: *Flowchart of microarray analysis*. (A) Differentially expressed transcripts in radiosensitive and radioresistant cell lines in the heat map generated by MeV (website). Up-regulated genes are shown in red and down regulated genes are shown in green. (B) The 341 genes were selected based on both SF2 and SF5 comparison. (C) Functional classification of the 314 genes. The genes were classified into different biological processes of gene ontology (GO) terms using PANTHER (software). Category name and % of gene hit against total gene numbers were shown.

and SF5 comparison were used for gene set enrichment analysis (Supplementary Table 1 and 2). Among them, the top upregulated and downregulated genes and previously reported genes were shown in the Table 3.3. Several genes in the list have a common functions related to cell junction and adhesion such as EPCAM (Epithelial adhesion molecule) and ITGB6 (integrin beta 6). Almost no known radiation related genes were in the list, except a DNA damage related gene GADD45B. The fraction of the genes in the different biological processes of the total identified genes was shown (Figure 3.9c). The genes grouped under metabolic process (48.1%) and cellular process (38.1%) were prominent.

Functional Gene Enrichment Analysis and Pathway Analysis

To explain the enriched biological processes of radiosensitivity, a gene set functional study using the 314 differentially expressed transcripts was generated using the DAVID (Dennis et al., 2003). The genes enriched in the biological processes included cell-matrix adhesion and apoptosis (Table 3.4). To identify signaling pathways related to radiosensitivity, statistical ranking with canonical pathways was performed using IPA as the human NCI-60 study (Table 3.5) (Kim et al., 2012). Overrepresented pathways were adhesion related pathways including the epithelial adhesion junction signaling and integrin signaling. In addition, death receptor signaling which is related to apoptosis important to radiosensitivity was also identified.

Discussion

This study explored a common radiosensitivity signature regardless of tumor type in canine cancer for potential biomarkers of cellular radioresistance. In the radiosensitive and radioresistant groups based on the colony formation assay, IR-induced DNA DSB repair and IR-induced

Table 3.3. List of top genes and previous reported genes in our differentially expressed genes.

Down-regulated genes in radiosensitive cells		
Gene symbol	Log ratio	Description
EPCAM*	-5.84	Epithelial cell adhesion molecule
SPINK5*	-5.18	Serine protease inhibitor
F3	-4.72	Coagulation factor III
NPNT*	-4.63	Nephronectin
EDN1	-4.36	Endothelin 1, produce by endothelial
ANK3*	-4.35	Ankyrins 3, membrane-cytoskeleton linker
TCEAL8	-4.10	Transcription elongation factor
MAL2	-4.02	Machinery of polarized transport
GSTT1	-4.00	Glutathione S-transferase
MAP7	-4.00	Microtubule-associated protein 7
PTGES	-3.94	Prostaglandin E synthase
(Previously reported gene in our gene list)		
ITGB6	-3.21	Integrin beta 6
GADD45B	-2.02	Growth arrest and DNA damage inducible beta

Up-regulated genes in radiosensitive cells		
Gene symbol	Log ratio	Description
CELF2	4.74	RNA binding proteins
PKIB	4.27	cAMP-dependent protein kinase inhibitor family
RGS1	4.15	Regulator of G-protein signaling 1
SASH1	4.04	SAM and SH3 domain containing 1
GUCY1B3	3.83	Soluble guanylate cyclase
MEF2C	3.50	Transcription factor in myogenesis
ZEB2	3.30	Transcriptional repressor
GPC3	3.07	Cell surface heparan sulfate proteoglycan
LRAT	3.01	Lecithin retinol acyltransferase
NSD1	3.00	Nuclear receptor
SPP2*	2.82	Secreted phosphoprotein
(Previously reported gene in our gene list)		
IQGAP2	2.73	IQ motif containing GTPase activating protein 2**

*Adhesion related molecule genes

**Previously reported genes based on gene expression profiling of human cancers (Kim. et al., 2012)

Table 3.4: Analysis of the 314 gene that differentially expressed between radiosensitive and radioresistant groups by DAVID.

GO Term	p-value *
Cell-matrix adhesion	0.0037
Protein tetramerization	0.0039
Cell-substrate adhesion	0.0059
Cytoskeleton organization	0.0063
Negative regulation of cytokine-mediated signaling pathway	0.0072
Protein homotetramerization	0.0089
Microtubule-based process	0.010
Positive regulation of protein kinase B signaling cascade	0.014
Post-Golgi vesicle-mediated transport	0.016
Actin filament-based process	0.020
Regulation of cell morphogenesis	0.022
Golgi vesicle transport	0.022
Apoptosis	0.023
Negative regulation of response to stimulus	0.026
Programmed cell death	0.026
Enzyme linked receptor protein signaling pathway	0.028
Regulation of cytokine-mediated signaling pathway	0.028
Cell death	0.031
Regulation of protein kinase B signaling cascade	0.032
Death	0.033
Transmembrane receptor protein tyrosine kinase signaling pathway	0.034
Actin cytoskeleton organization	0.035
Protein processing	0.039
Platelet-derived growth factor receptor signaling pathway	0.039
Actin polymerization or depolymerization	0.039
Ribonucleoside metabolic process	0.041
Coenzyme metabolic process	0.043
Regulation of developmental growth	0.043
Positive regulation of cell size	0.045

*Fisher exact test

Table 3.5: Top canonical pathway identified from the Ingenuity Pathway Analysis library of canonical pathways that are most significant to the 314 genes.

Term	p-value *
Epithelial Adherens Junction Signaling	0.0016
Valine Degradation I	0.0023
Integrin Signaling	0.0034
Remodeling of Epithelial Adherens Junctions	0.0035
Rac Signaling	0.0048
Role of Oct4 in Mammalian Embryonic Stem Cell Pluripotency	0.0049
Actin Cytoskeleton Signaling	0.0055
Signaling by Rho Family GTPases	0.0089
Actin Nucleation by ARP-WASP Complex	0.0098
Regulation of Actin-based Motility by Rho	0.012
Death Receptor Signaling	0.012
ERK5 Signaling	0.015
L-cysteine Degradation II	0.015
Sulfite Oxidation IV	0.015
Guanosine Nucleotides Degradation III	0.016
Ephrin Receptor Signaling	0.016
Urate Biosynthesis/Inosine 5 phosphate Degradation	0.018
Clathrin-mediated Endocytosis Signaling	0.022
Caveolar-mediated endocytosis Signaling	0.022
RAR Activation	0.025
Adenosine Nucleotides Degradation II	0.026
Role of RIG1-like Receptors in Antiviral Innate Immunity	0.030
All-trans-decaprenyl Diphosphate Biosynthesis	0.030
Cysteine Biosynthesis/Homocysteine Degradation	0.030
Germ Cell-Sertoli Cell Junction Signaling	0.033
Punne Nucleotides Degradation II (Aerobic)	0.035
RhoA Signaling	0.037
Cdc42 Signaling	0.040
Tyrosine Biosynthesis IV	0.044
4-aminobutyrate Degradation I	0.044
N-acety/glucosamine Degradation I	0.044
Virus Entry via Endocytic Pathways	0.045
Hereditary Breast Cancer Signaling	0.045
RhoGDI Signaling	0.046

* Fisher's exact test

apoptosis frequency were not always related to radiosensitivity (Figure 3.5 and Figure 3.7). Using a microarray analysis, we compared basal gene expressions between the two groups. Cell adhesion related genes, rather than the more commonly regarded radiosensitivity associated DNA repair genes, were identified as the radiosensitivity signature genes (Table 3.4 and Table 3.5).

In support of our findings, cell adhesion was one of the signatures previously identified in the human microarray analysis (Kim et al., 2012). Using pathway analysis, we showed that several enriched signaling pathways related to radiosensitivity including the integrin signaling pathway, which was also identified as a function of radiosensitivity signature in the human NCI-60 study (Kim et al., 2012) (Table 3.5). Cell adhesion mediated radioresistance has been previously proposed as an integrin-mediated pathway (Sandfort et al., 2007, Makrilia et al., 2009). The interaction with the extracellular matrix causes anti-apoptotic signals via downstream effectors including ILK (integrin-linked kinase). ILK was upregulated in radiosensitive cell lines in our study, which was consistent with the previous studies (Monferran et al., 2008, Sandfort et al., 2007). ILK is a strong anti-survival mediator that enhances radiation sensitivity in a variety of human tumor cell lines (Cordes, 2004).

Of the several genes in the identified genes linked with cell-adhesion, we noticed integrin beta 6 (ITGB6), which is similar to integrin beta 5 (ITGB5), found in the radiosensitivity signature in the previous study using the human NCI-60 panel (Kim et al., 2012). Integrins are heterodimetric glycoprotein receptors of alpha and beta-subunits and are known to regulate several signal transductions (Desgrosellier and Cheresh, 2010). They directly bind to the extracellular matrix and contribute to proliferation, survival and invasion in cancer. Integrin beta 1 has been progressively studied in human oncology because its targeting has demonstrated strong potential to sensitize cancer cells to conventional radiotherapies and chemotherapies (Park et al., 2008). It has also been

reported that silencing ITGB3 and ITGB5 reduces survival after IR in cancer cells (Monferran et al., 2008). Like the other integrins, it has been suggested that ITGB6 could serve as a prognostic indicator with high levels of expression correlating with poor patient prognosis in several human carcinomas (Hazelbag et al., 2007, Zhang et al., 2008). Although we couldn't find common mechanisms to make tumor cells radioresistant, our results suggest that the cell adhesion molecules could explain a common radiosensitivity signature representing the population with diverse tumor types.

In order to understand parameters that might contribute to intrinsic radiosensitivity, we evaluated the relationships of cellular radiosensitivity with basic cellular characteristics in the ACC30. The canine cancer cell lines in the ACC30 have been developed and utilized for cancer research, but have not been as fully characterized as human cell lines. We observed a wide variation in radiosensitivity and cellular characteristics in the ACC30 panel. In our study, we didn't find a correlation between chromosome number, S-phase fraction, and doubling time (Figure 3.3). Previously, the largest number of chromosomes has been found in some of radioresistant human cancer cells (Schwartz et al., 1999). It is possible that such lines can better tolerate chromosome loss because of a greater degree of genomic redundancy (Revell, 1983). However, this is not a consistent observation in human cancer cell lines (West et al., 1995). Since S-phase cells are known to the most radioresistant in the cell cycle, fraction of S-phase in cell population is possible a parameter of radiosensitivity in cancer. However, some human studies have not shown correlations (Schwartz, 1992) and some have shown (Bush and McMillan, 1993). In human studies, cell proliferation rates are known as one of the important parameters mainly in tissues *in vivo* (Torres-Roca and Stevens, 2008, Hall et al., 2014). Therefore, based on the uncertainty of these parameters, our results in canine cancer cell lines agreed with the human studies. In contrast, plating efficiency

of the cells in the ACC30 panel showed mild correlation with the radiosensitivity in our study (Figure 3.3). The parameter has not been discussed in depth in previous papers, except where one report noted that resistant cells had better plating efficiencies (Schwartz, 1992) and another study reported no correlation (Hall et al., 2014). However, some cell lines with low plating efficiency in the ACC30 panel (Moresco, Gracie and Parks) showed radioresistant phenotype, therefore, plating efficiency was not always related to radioresistance (Table 3.1 and Figure 3.3). We need to evaluate the plating efficiency in the other panel of dogs to confirm whether this is a more prominent feature in dogs.

The DSB repair is an obvious candidate marker for radiation response because DSBs are considered the most critical DNA damage by IR. In normal cells, both slower overall rates of DSB rejoining and higher levels of residual breaks are associated with more radiosensitive phenotypes (Schwartz, 1998). In this study, we used the γ-H2AX assay which is known as a sensitive method to measure DSBs (Rogakou et al., 1998). In G1-synchronized cells, the high levels of residual γ-H2AX foci were associated with the four out of the five radiosensitive canine cancer cell lines, but not with one cell line, Bliley (Figure 3.5). In human cancer cell lines, the relationship of residual levels of γ-H2AX or rates of its disappearance to clonogenic cell survival in cancer cells has been studied by several investigators, and correlations were found in some studies (Banath et al., 2004, Taneja et al., 2004), but not all (Mahrhofer et al., 2006). This discrepancy might be due to the high endogenous γ-H2AX foci in cancer cells relative to normal cells as previously observed (Yu et al., 2006) and also observed in canine cancer cells. These high endogenous γ-H2AX foci in non-irradiated cells were not in the S-phase. We decided to exclude these cells with foci numbers outside of the distribution induced by IR because the high back ground level possibly hides the γ-H2AX foci change by repair. The development of protocols to better cut out high level of

endogenous γ-H2AX foci may help the analysis to explore DNA DSB repair as a robust parameter to determine responses of tumor cells to radiation. Furthermore, levels of γ-H2AX foci after low dose rate irradiation may reveal the DNA DSB rejoining defect in radiosensitive cells which could not be shown by acute dose rate irradiation, such as Bliley in this study. Previous studies with low dose rate irradiation have shown better discrimination in radiation response in cells from individuals and mice who are mildly hypersensitive to IR, such as ATM heterozygotes, compared to acute dose irradiation (Kato et al., 2006a, Kato et al., 2006b). However, we used the assay only with a single dose of 1 Gy instead of low dose rate irradiation in this study. This is because the low dose rate experiment required a longer time for G1 synchronization in isoleucine deficient media than the acute dose rate experiment, which induced toxicity in canine cancer cell lines. The toxicity was not a problem in non-cancerous human cells in the previous study (Kato et al., 2006a), but was limiting to the γ-H2AX assay with acute dose rate irradiation in canine cancer cell lines.

In contrast to the γ-H2AX analysis, the G2 chromosome assay didn't show more unrepaired chromosome damages in the radiosensitive group compared to radioresistant group in this study (Figure 3.6). However, we cannot conclude that DNA DSB repair efficiency in G2 phase does not contribute to the canine tumor cell radiosensitivity differences due to the limitations in our study. The dose used in our study (0.5 Gy) might not be enough to induce detectable changes between the two groups. Furthermore, it is also possibly due to the higher levels of the IR-induced chromatid breaks and gaps observed in canine cancer cells might mask the relatively small changes caused by different radiosensitivity. In the canine cancer cells, there were almost 10 times higher levels of IR-induced chromatid breaks previously reported in normal dogs (2/1000 chromosome by 1 Gy) (Thamm et al., 2013). This difference between normal and cancer cells observed in our results was consistent with the previous human studies using normal and cancer cell lines (Parshad

1984). G2 chromosome assays have been known as a sensitive assay to detect differences of radiosensitivity between cancer prone and normal cells (Scott, 2004), however, this approach might be not easy to detect radiosensitivity for tumor cells. In fact, there are only few papers describing the intrinsic radiosensitivity by G2 chromosome assays for human tumor cells (Schwartz, 1992).

The investigation of proteins involved in DNA DSB repair pathway by western blotting analysis showed that canine cancer cell lines have different levels of expression of DNA-PKcs, RAD51 and FANCD2, which were higher than the levels in normal canine fibroblasts (Figure 3.8). However, the basal expression levels were not associated with their radiosensitivity. The results suggest that dysregulation of the proteins involved in the DNA damage pathway is present in canine cancer cell lines. This result agreed with the failure in previous studies to predict radiation response in cancer using expression of a single proteins (Ogawa et al., 2007). In human studies, the protein expression of DNA damage response including DNA-PKcs has shown conflicting results with high expression associated with both good and poor outcomes following radiotherapy (Beskow et al., 2009). The determinants of radiation response in cancer cells are probably more than one protein or pathway (Torres-Roca and Stevens, 2008). In addition, the expression of DNA-PKcs, which is a main player in NHEJ, was lower in the canine samples than those in human. This is might be because the antibody directed against human DNA-PKcs has low reactivity with canine DNA-PKcs. Moreover, in a previous study, it has been shown that the kinase activity of this protein measured by the [γ-^{32}P] ATP kinase assay is also 13-fold lower in canine than in human fibroblasts (Meek et al., 2001). Therefore, not only kinase activity, but also the protein function might be necessary to understand the contribution of NHEJ in DNA DSB repair in dogs.

Apoptosis has been studied as an important element that determines radioresponsiveness of cancer cells. However, its correlations with radiosensitivity have been variable in previous human studies (Begg, 2009). In our study, the percentage of cells that underwent apoptosis at 48 hours following 5 Gy differed considerably between the canine cancer cell lines. However, the apoptosis frequency didn't distinguish two groups, suggesting incomplete parameters like in human cancer. We measured apoptosis frequency only at 48 hours following radiation, based on the previous human studies (Dunne et al., 2003); thus, this is a limitation in our study. This is because the time of IR-induced apoptosis is possibly cell line dependent, further research will be needed to characterize the parameter fully. In the pathways identified as contributing to radiosensitivity signature in the gene expression profiling, death receptor signaling is one of the numerous signaling pathways involved in apoptosis via tumor necrosis factor-alpha (TNF-α) (Zhou et al., 2003). It has been suggested that the death receptor signaling pathway might account for the late apoptosis observed after IR treatment in breast cancer cells (Luce et al., 2009). However, there are no previous studies showing death signaling pathway as a radiosensitivity signature in microarray analysis. Furthermore, based on our results that IR-induced increases in apoptosis were only significant three out of the five radiosensitive cell lines, the contribution of apoptosis to radiosensitivity among tumor cell lines will still be necessary to be determined.

Several studies have reported possible radiosensitivity predictive genes using microarray analysis in the NCI-60 panel (Kim et al., 2012). However, the human studies have not shown any common genes among the studies. We identified 314 genes common between SF2 and SF5. Almost no known radiation related genes were in the differentially expressed gene list. GADD45B (Growth arrest and DNA damage inducible beta) is well known as a DNA damage response gene that increases following stressful conditions, and deficiency in this gene sensitizes cells to radiation

(Liebermann and Hoffman, 2008). In this study, GADD45B was downregulated in radiosensitive cell lines, consistent with the explanation. Of the genes identified in this study, some genes were previously reported in the NCI-60 (Kim et al., 2012). IQGAP2, IQ motif containing GTPase activation protein 2, was upregulated in our study which is also found in the NCI-60. This IQGAP2 is known to interact with several signaling molecules in order to regulate cell morphology and motility, and associates with calmodulin (Atcheson et al., 2011). However, there are no previous reports showing relationship between the gene and radiationsensitivity.

Our results support the involvement of adhesion molecules in radioresistance. There is a concern in this statement because adhesion related molecules could be related to plating efficiency. The expression differences may only be because cell lines in radiosensitive group have low plating efficiencies relative to resistant groups in the ACC30 panel. Moreover, mRNA expression of these adhesion-related molecules has not been investigated in both this study and the previous human study. We need further research about the relationship between adhesion molecules and radiosensitivity in canine cancer cell lines to confirm the significance in the radiosensitivity mechanism. Another concern is that cell origin could have introduced bias in analysis, especially because the resistant group contained more carcinomas than the sensitive group in this study. The significant genes, such as ITGB6 (Breuss et al., 1995) and EPCAM are also proteins expressed in epithelial tumor cells. On the other hand, the expressions of EPCAM in the radioresistant cell lines except carcinomas were also high relative to radiosensitive cell lines. The NCI-60 study didn't show the correlation between radiosensitivity and plating efficiency. However, we need to adjust the effects of plating efficiency through comparing the radiosensitive and radioresistant groups with the similar plating efficiency to better understanding the mechanisms underlying radiosensitivity in canine cancer cell lines.

In summary, our results suggest that the cell adhesion related genes, rather than the more commonly regarded radiosensitivity associated apoptosis and DNA repair related genes, may provide the most beneficial radiosensitivity biomarkers for predicting individual response to radiotherapy, regardless of tumor type.

REFERENCES

ASHBURNER, M., BALL, C. A., BLAKE, J. A., BOTSTEIN, D., BUTLER, H., CHERRY, J. M., DAVIS, A. P., DOLINSKI, K., DWIGHT, S. S., EPPIG, J. T., HARRIS, M. A., HILL, D. P., ISSEL-TARVER, L., KASARSKIS, A., LEWIS, S., MATESE, J. C., RICHARDSON, J. E., RINGWALD, M., RUBIN, G. M. & SHERLOCK, G. 2000. Gene ontology: tool for the unification of biology. The Gene Ontology Consortium. *Nat Genet,* 25**,** 25-9.

ATCHESON, E., HAMILTON, E., PATHMANATHAN, S., GREER, B., HARRIOTT, P. & TIMSON, D. J. 2011. IQ-motif selectivity in human IQGAP2 and IQGAP3: binding of calmodulin and myosin essential light chain. *Biosci Rep,* 31**,** 371-9.

BANATH, J. P., MACPHAIL, S. H. & OLIVE, P. L. 2004. Radiation sensitivity, H2AX phosphorylation, and kinetics of repair of DNA strand breaks in irradiated cervical cancer cell lines. *Cancer Res,* 64**,** 7144-9.

BEGG, A. C. 2009. Predicting response to radiotherapy: evolutions and revolutions. *Int J Radiat Biol,* 85**,** 825-36.

BENJAMINI, Y., DRAI, D., ELMER, G., KAFKAFI, N. & GOLANI, I. 2001. Controlling the false discovery rate in behavior genetics research. *Behav Brain Res,* 125**,** 279-84.

BESKOW, C., SKINKUNIENE, A., HOLGERSSON, B., NILSSON, B., LEWENSOHON, R., KANTER, L., & VIKTORSSON, K. 2009. Radioresistant cervival cancer shows upregulation of the NHEJ proteins DNA-PKcs, Ku70 and Ku86. *British journal of cancer, 101-5,* 816-821

BJORK-ERIKSSON, T., WEST, C., KARLSSON, E. & MERCKE, C. 2000. Tumor radiosensitivity (SF2) is a prognostic factor for local control in head and neck cancers. *Int J Radiat Oncol Biol Phys,* 46**,** 13-9.

BOGLIOLO, M., LYAKHOVICH, A., CALLEN, E., CASTELLA, M., CAPPELLI, E., RAMIREZ, M. J., CREUS, A., MARCOS, R., KALB, R., NEVELING, K., SCHINDLER, D. & SURRALLES, J. 2007. Histone H2AX and Fanconi anemia FANCD2 function in the same pathway to maintain chromosome stability. *EMBO J,* 26**,** 1340-51.

BREUSS, J. M., GALLO, J., DELISSER, H. M., KLIMANSKAYA, I. V., FOLKESSON, H. G., PITTET, J. F., NISHIMURA, S. L., ALDAPE, K., LANDERS, D. V., CARPENTER, W. & ET AL. 1995. Expression of the beta 6 integrin subunit in development, neoplasia and tissue repair suggests a role in epithelial remodeling. *J Cell Sci,* 108 (Pt 6)**,** 2241-51.

BUSH, C. & MCMILLAN, T. J. 1993. Micronucleus formation in human tumour cells: lack of correlation with radiosensitivity. *Br J Cancer,* 67**,** 102-6.

CORDES, N. 2004. Overexpression of hyperactive integrin-linked kinase leads to increased cellular radiosensitivity. *Cancer Res,* 64**,** 5683-92.

DELANEY, G., JACOB, S., FEATHERSTONE, C. & BARTON, M. 2005. The role of radiotherapy in cancer treatment: estimating optimal utilization from a review of evidence-based clinical guidelines. *Cancer,* 104**,** 1129-37.

DENNIS, G., JR., SHERMAN, B. T., HOSACK, D. A., YANG, J., GAO, W., LANE, H. C. & LEMPICKI, R. A. 2003. DAVID: Database for Annotation, Visualization, and Integrated Discovery. *Genome Biol,* 4**,** P3.

DESGROSELLIER, J. S. & CHERESH, D. A. 2010. Integrins in cancer: biological implications and therapeutic opportunities. *Nat Rev Cancer,* 10**,** 9-22.

DEWEY, W. C., LING, C. C. & MEYN, R. E. 1995. Radiation-induced apoptosis: relevance to radiotherapy. *Int J Radiat Oncol Biol Phys,* 33**,** 781-96.

DUNNE, A. L., PRICE, M. E., MOTHERSILL, C., MCKEOWN, S. R., ROBSON, T. & HIRST, D. G. 2003. Relationship between clonogenic radiosensitivity, radiation-induced apoptosis and DNA damage/repair in human colon cancer cells. *Br J Cancer,* 89**,** 2277-83.

FOWLES, S 2014, "Canine COXEN: cross-species genomic applications for predicting chemosensitivity in dogs", in 15 th Annual Research Day at the Colorado State University

FURTH, E. E., THILLY, W. G., PENMAN, B. W., LIBER, H. L. & RAND, W. M. 1981. Quantitative assay for mutation in diploid human lymphoblasts using microtiter plates. *Anal Biochem,* 110**,** 1-8.

GROSSE, N., VAN LOON, B. & ROHRER BLEY, C. 2014. DNA damage response and DNA repair - dog as a model? *BMC Cancer,* 14**,** 203.

Hall, E. J., Giaccia, A. J. (2006). *Radiobiology for the Radiologist Sixth Edition*. Philadelphia, PA: Lippincott Williams and Wilkins.

HALL, J. S., IYPE, R., SENRA, J., TAYLOR, J., ARMENOULT, L., OGUEJIOFOR, K., LI, Y., STRATFORD, I., STERN, P. L., O'CONNOR, M. J., MILLER, C. J. & WEST, C. M. 2014. Investigation of radiosensitivity gene signatures in cancer cell lines. *PLoS One,* 9**,** e86329.

HAZELBAG, S., KENTER, G. G., GORTER, A., DREEF, E. J., KOOPMAN, L. A., VIOLETTE, S. M., WEINREB, P. H. & FLEUREN, G. J. 2007. Overexpression of the alpha v beta 6 integrin in cervical squamous cell carcinoma is a prognostic factor for decreased survival. *J Pathol,* 212**,** 316-24.

KATO, T. A., NAGASAWA, H., WEIL, M. M., GENIK, P. C., LITTLE, J. B. & BEDFORD, J. S. 2006a. gamma-H2AX foci after low-dose-rate irradiation reveal atm haploinsufficiency in mice. *Radiat Res,* 166**,** 47-54.

KATO, T. A., NAGASAWA, H., WEIL, M. M., LITTLE, J. B. & BEDFORD, J. S. 2006b. Levels of gamma-H2AX Foci after low-dose-rate irradiation reveal a DNA DSB rejoining defect in cells from human ATM heterozygotes in two at families and in another apparently normal individual. *Radiat Res,* 166**,** 443-53.

KIM, H. S., KIM, S. C., KIM, S. J., PARK, C. H., JEUNG, H. C., KIM, Y. B., AHN, J. B., CHUNG, H. C. & RHA, S. Y. 2012. Identification of a radiosensitivity signature using integrative metaanalysis of published microarray data for NCI-60 cancer cells. *BMC Genomics,* 13**,** 348.

KOW, K., THAMM, D. H., TERRY, J., GRUNERUD, K., BAILEY, S. M., WITHROW, S. J. & LANA, S. E. 2008. Impact of telomerase status on canine osteosarcoma patients. *J Vet Intern Med,* 22**,** 1366-72.

KRUSE, J. J. & STEWART, F. A. 2007. Gene expression arrays as a tool to unravel mechanisms of normal tissue radiation injury and prediction of response. *World J Gastroenterol,* 13**,** 2669-74.

LIEBERMANN, D. A. & HOFFMAN, B. 2008. Gadd45 in stress signaling. *J Mol Signal,* 3**,** 15.

LIMSIRICHAIKUL, S., NIIMI, A., FAWCETT, H., LEHMANN, A., YAMASHITA, S. & OGI, T. 2009. A rapid non-radioactive technique for measurement of repair synthesis in primary human fibroblasts by incorporation of ethynyl deoxyuridine (EdU). *Nucleic Acids Res,* 37**,** e31.

LUCE, A., COURTIN, A., LEVALOIS, C., ALTMEYER-MOREL, S., ROMEO, P. H., CHEVILLARD, S. & LEBEAU, J. 2009. Death receptor pathways mediate targeted and non-targeted effects of ionizing radiations in breast cancer cells. *Carcinogenesis,* 30**,** 432-9.

MACEWEN, E. G. 1990. Spontaneous tumors in dogs and cats: models for the study of cancer biology and treatment. *Cancer Metastasis Rev,* 9**,** 125-36.

MACPHAIL, S. H., BANATH, J. P., YU, T. Y., CHU, E. H., LAMBUR, H. & OLIVE, P. L. 2003. Expression of phosphorylated histone H2AX in cultured cell lines following exposure to X-rays. *Int J Radiat Biol,* 79**,** 351-8.

MAHRHOFER, H., BURGER, S., OPPITZ, U., FLENTJE, M. & DJUZENOVA, C. S. 2006. Radiation induced DNA damage and damage repair in human tumor and fibroblast cell lines assessed by histone H2AX phosphorylation. *Int J Radiat Oncol Biol Phys,* 64**,** 573-80.

MAKRILIA, N., KOLLIAS, A., MANOLOPOULOS, L. & SYRIGOS, K. 2009. Cell adhesion molecules: role and clinical significance in cancer. *Cancer Invest,* 27**,** 1023-37.

MCENTEE, M. C. 2006. Veterinary radiation therapy: review and current state of the art. *J Am Anim Hosp Assoc,* 42**,** 94-109.

MEEK, K., KIENKER, L., DALLAS, C., WANG, W., DARK, M. J., VENTA, P. J., HUIE, M. L., HIRSCHHORN, R. & BELL, T. 2001. SCID in Jack Russell terriers: a new animal model of DNA-PKcs deficiency. *J Immunol,* 167**,** 2142-50.

MI, H., DONG, Q., MURUGANUJAN, A., GAUDET, P., LEWIS, S. & THOMAS, P. D. 2010. PANTHER version 7: improved phylogenetic trees, orthologs and collaboration with the Gene Ontology Consortium. *Nucleic Acids Res,* 38**,** D204-10.

MLADENOV, E., MAGIN, S., & ILiaks, G. 2013. DNA double-strand break repair as determinant of cellular radiosensitivity to killing and target in radiation therapy. *Frontiers in oncology, 3.*

MOLDOVAN, G. L. & D'ANDREA, A. D. 2009. FANCD2 hurdles the DNA interstrand crosslink. *Cell,* 139**,** 1222-4.

MONFERRAN, S., SKULI, N., DELMAS, C., FAVRE, G., BONNET, J., COHEN-JONATHAN-MOYAL, E. & TOULAS, C. 2008. Alphavbeta3 and alphavbeta5 integrins control glioma cell response to ionising radiation through ILK and RhoB. *Int J Cancer,* 123**,** 357-64.

OGAWA, K., MURAYAMA, S. & MORI, M. 2007. Predicting the tumor response to radiotherapy using microarray analysis (Review). *Oncol Rep,* 18**,** 1243-8.

PARK, C. C., ZHANG, H. J., YAO, E. S., PARK, C. J. & BISSELL, M. J. 2008. Beta1 integrin inhibition dramatically enhances radiotherapy efficacy in human breast cancer xenografts. *Cancer Res,* 68**,** 4398-405.

PARSHAD, R., SANFORD, K. K. & JONES, G. M. 1983. Chromatid damage after G2 phase x-irradiation of cells from cancer-prone individuals implicates deficiency in DNA repair. *Proc Natl Acad Sci U S A,* 80**,** 5612-6.

PAWLIK, T. M. & KEYOMARSI, K. 2004. Role of cell cycle in mediating sensitivity to radiotherapy. *Int J Radiat Oncol Biol Phys,* 59**,** 928-42.

ROGAKOU, E. P., PILCH, D. R., ORR, A. H., IVANOVA, V. S. & BONNER, W. M. 1998. DNA double-stranded breaks induce histone H2AX phosphorylation on serine 139. *J Biol Chem,* 273**,** 5858-68.

SAEED, A. I., BHAGABATI, N. K., BRAISTED, J. C., LIANG, W., SHAROV, V., HOWE, E. A., LI, J., THIAGARAJAN, M., WHITE, J. A. & QUACKENBUSH, J. 2006. TM4 microarray software suite. *Methods Enzymol,* 411**,** 134-93.

SANDFORT, V., KOCH, U. & CORDES, N. 2007. Cell adhesion-mediated radioresistance revisited. *Int J Radiat Biol,* 83**,** 727-32.

SCHWARTZ, J. L. 1992. The radiosensitivity of the chromosomes of the cells of human squamous cell carcinoma cell lines. *Radiat Res,* 129**,** 96-101.

SCHWARTZ, J. L. 1998. Alterations in chromosome structure and variations in the inherent radiation sensitivity of human cells. *Radiat Res,* 149**,** 319-24.

SCHWARTZ, J. L., MURNANE, J. & WEICHSELBAUM, R. R. 1999. The contribution of DNA ploidy to radiation sensitivity in human tumour cell lines. *Br J Cancer,* 79**,** 744-7.

SCOTT, D. 2004. Chromosomal radiosensitivity and low penetrance predisposition to cancer. *Cytogenet Genome Res,* 104**,** 365-70.

SCOTT, D. & EVANS, H. J. 1967. X-ray-induced chromosomal aberrations in vicia faba: changes in response during the cell cycle. *Mutat Res,* 4**,** 579-99.

TANEJA, N., DAVIS, M., CHOY, J. S., BECKETT, M. A., SINGH, R., KRON, S. J. & WEICHSELBAUM, R. R. 2004. Histone H2AX phosphorylation as a predictor of radiosensitivity and target for radiotherapy. *J Biol Chem,* 279**,** 2273-80.

THACKER, J. & ZDZIENICKA, M. Z. 2004. The XRCC genes: expanding roles in DNA double-strand break repair. *DNA Repair (Amst),* 3**,** 1081-90.

THAMM, D. H., GRUNERUD, K. K., ROSE, B. J., VAIL, D. M. & BAILEY, S. M. 2013. DNA repair deficiency as a susceptibility marker for spontaneous lymphoma in golden retriever dogs: a case-control study. *PLoS One,* 8**,** e69192.

THOMPSON, L. H. 2012. Recognition, signaling, and repair of DNA double-strand breaks produced by ionizing radiation in mammalian cells: the molecular choreography. *Mutat Res,* 751**,** 158-246.

TOBEY, R. A. & LEY, K. D. 1971. Isoleucine-mediated regulation of genome repliction in various mammalian cell lines. *Cancer Res,* 31**,** 46-51.

TORRES-ROCA, J. F. & STEVENS, C. W. 2008. Predicting response to clinical radiotherapy: past, present, and future directions. *Cancer Control,* 15**,** 151-6.

VAN VEELEN, L. R., ESSERS, J., VAN DE RAKT, M. W., ODIJK, H., PASTINK, A., ZDZIENICKA, M. Z., PAULUSMA, C. C. & KANAAR, R. 2005. Ionizing radiation-induced foci formation of mammalian Rad51 and Rad54 depends on the Rad51 paralogs, but not on Rad52. *Mutat Res,* 574**,** 34-49.

WALTERS, R. A. & PETERSEN, D. F. 1968. Radiosensitivity of mammalian cells. II. Radiation effects on macromolecular synthesis. *Biophys J,* 8**,** 1487-504.

WEST, C. M., DAVIDSON, S. E., BURT, P. A. & HUNTER, R. D. 1995. The intrinsic radiosensitivity of cervical carcinoma: correlations with clinical data. *Int J Radiat Oncol Biol Phys,* 31**,** 841-6.

WEST, C. M., DAVIDSON, S. E., ROBERTS, S. A. & HUNTER, R. D. 1997. The independence of intrinsic radiosensitivity as a prognostic factor for patient response to radiotherapy of carcinoma of the cervix. *Br J Cancer,* 76**,** 1184-90.

YU, T., MACPHAIL, S. H., BANATH, J. P., KLOKOV, D. & OLIVE, P. L. 2006. Endogenous expression of phosphorylated histone H2AX in tumors in relation to DNA double-strand breaks and genomic instability. *DNA Repair (Amst),* 5**,** 935-46.

ZHANG, Z. Y., XU, K. S., WANG, J. S., YANG, G. Y., WANG, W., WANG, J. Y., NIU, W. B., LIU, E. Y., MI, Y. T. & NIU, J. 2008. Integrin alphanvbeta6 acts as a prognostic indicator in gastric carcinoma. *Clin Oncol (R Coll Radiol),* 20**,** 61-6.

ZHOU, L., YUAN, R. & SERGGIO, L. 2003. Molecular mechanisms of irradiation-induced apoptosis. *Front Biosci,* 8**,** d9-19.

CHAPTER 4

CONCLUSIONS AND DISCUSSION

General conclusions

This dissertation characterized canine cancer cells using sets of canine cancer cell lines. Compared to human studies, canine cancer cell lines have not been fully characterized. Characterization of large number of canine cancer cell lines will provide a better understanding of underlying canine cancer biology and reveal common features which might have a potential to improve clinical management, such as the development of novel therapeutic targets and identification of therapy sensitivity markers for dogs, with a translational relevance for humans.

In Chapter 2 we explored chromosome aberrations and telomere dysfunction using a set of canine OSA cell lines. Chromosome aberrations are known as a hallmark of cancer (Albertson et al., 2003), and malignant canine cell lines from a variety of canine tumors (including OSA) have been reported to exhibit metacentric chromosomes (Reimann et al., 1999). Telomeres play an important role in chromosome integrity and dysfunction has been reported in human cancer (Tanaka et al., 2012). In the set of canine OSA cell lines, the cell lines showed variable chromosome numbers, proliferation rates and radiosensitivities. In the variety of the cell lines, metacentric chromosomes with telomere fusions were common characteristics of canine OSA cell lines. Furthermore, in the primary canine OSA cultures, the telomere aberrations were fewer but telomere dysfunction contributed to an increased number of metacentric chromosomes in the long term cultures. This characteristic was in primary canine OSA cells, but not in the non-cancerous cells even with telomere dysfunction. These finding suggests that telomere fusions occur

frequently in canine OSA and might be a significant diagnostic marker and potential treatment target contingent with further research for canine tumors.

In Chapter 3 we investigated radiosensitivity signatures in the ACC30 panel of canine cancer cell lines in many cancer types. Radiosensitivity signatures are a central goal for developing methods to evaluate individual response to radiation therapy (Begg, 2009). The underlying mechanisms of radiosensitivity in canine cancer cells attributed to DNA DSB repair and apoptosis frequency were uncommon features in radiosensitive cell lines. Plating efficiency, one of the basic cellular characteristics and dysregulated cell adhesion molecules identified from gene expression profiling, was associated with radiosensitivity in the ACC30 panel. These findings suggest that the cell adhesion related genes, rather than the more commonly regarded radiosensitivity associated apoptosis and DNA repair related genes, may provide the most beneficial radiosensitivity biomarkers for predicting individual response to radiotherapy, regardless of tumor type.

Discussion

The findings in this dissertation improved the understanding of chromosome aberrations, telomere dysfunction, and radiosenstivity signatures in canine cancer. The strategy of using large numbers of canine cell lines provided a better understanding of these characteristics. In the first part of the dissertation, we focused on canine OSA because of its high mortality. Unlike canine OSA, other sets of many cancer types were characterized to identify radiosensitivity signatures in the latter part of the dissertation. In current human studies, telomere fusions have been reported in the several tumor types and evaluated for their contributions to the development of specific cancers (Tanaka et al., 2012, Lin et al., 2010). Gene-expression profiling of a heterogeneous set of human cancer cell lines has been used to identify patterns of gene expression that correlate with responses

to drugs or radiation *in vitro* (Kim et al., 2012, van's Veer and Bernards, 2008). It has also been hypothesized that robust and general radiosensitivity signatures obtained from cell lines regardless tumor type might improve the development of predictive assays for radiotherapy response in human patients (Hall et al., 2014). Therefore, we assumed similar situations between human and canine cancer biology in these characteristics.

Metacentric chromosomes have been reported to increase over the evolution of rodents and cows as seen in their species-specific normal karyotypes (Nachman and Searle, 1995, Geshi et al., 1996). We found that telomere fusions contribute to the aberrant metacentric chromosomes in canine OSA cell lines. Telomere fusions have been known to result from either excessive telomere shortening or the loss of end capping function in human studies (Bailey and Murnane, 2006). This might be enhanced by other factors related to long term culture, such as further increased telomerase activity, oxidative stress and replication stress. *In vitro* culture environment differs from *in vivo* condition in that the oxygen concentration is higher and, in such conditions, cells show a higher reactive oxygen species which can shorten telomere and damage telomeric DNA (Goto et al., 1993, von Zglinicki, 2002, Mazouzi et al., 2014). In the current study, the slow growth phase observed in the long term culture of primary OSA may result from DNA damage response on dysfunctional telomeres, and the damage response may be stabilized through telomere fusions, allowing cells for further growth. We couldn't determine the mechanisms underlying telomere fusions in canine OSA cell lines, but different chromosome shapes might contribute to telomere fusions. Studies in mammalian cells have suggested that p-arm telomeres are shorter than q-arm telomeres (Hemann et al., 2001, Perner et al., 2003). In a mice study, most of the chromosome fusion events involved the fusion of two chromosomal p-arms with the shorter telomeres (Hemann et al., 2001). Therefore, although we didn't evaluate a difference in telomere length between p-

and q-arm telomeres in canine chromosomes, telomere fusions may be due to the shorter telomeres in p-arm chromosomes. Humans only have 10 acrocentric chromosomes out of 46 chromosomes, while normal karyotypes in dogs only consist only of acrocentric autosomes. Although the telomere fusions have been found in several types of human cancer, the biological and clinical significances are likely different in human and canine cancer.

One of the main findings in Chapter 3 was that expression of adhesion related molecules might be a radiosensitivity signature in canine cancer. This was consistent with the previous ideas, that cellular adhesion mediated radioresistance can occur through anti-apoptotic signals when integrin interacts with the extracellular matrix (Sandfort et al., 2007). In support of our findings, cell adhesion related molecules interacting with integrin signaling pathway were one of the signatures previously identified in the human microarray analysis (Kim et al., 2012). However, there is a concern because adhesion related molecules would be related to low plating efficiency, which was the other characteristic in the radiosensitive cell lines in the ACC30 panel. The cell lines with high plating efficiency might be associated with high population of cancer stem cells, which is also known as a possible radioresistant mechanism for cancer (Bao et al., 2006). However, we didn't observed stem cell related genes, such as Oct3/4 and Sox2 (Schoenhals et al., 2009), in the differentially expressed gene list in the current study. In addition, the resistant group contained more carcinomas than the sensitive group in our study. The cell or tissue types included in the radiosensitive and radioresistant cell lines could have introduced bias in analysis.

We showed that the DNA DSB repair detected by γ-H2AX and the apoptosis frequency were incomplete parameters for prediction of radiosensitivity, which was consistent with some of the human cancer studies (Mahrhofer et al., 2006). Repair of DNA DSBs is known as one of the most important elements that determines intrinsic radiosensitivity (Schwartz, 1998), For the DNA

DSB repair and apoptotic frequency, we used only a single dose of irradiation and analyzed minimum time points following irradiation. Therefore, it is possible that we needed more experiments to detect the differences in the radiosensitivity. The assays to detect DSBs might not be easy for tumor cells even with DNA DSB repair dysregulation. G2 chromosomal assay and γ-H2AX have been developed based on normal cells, which are likely to have small numbers of mutations in the radiation response pathways. However, cancer has been known as a disease resulting from multiple genetic alterations. Among the multiple changes in tumors, DSB assay would be affected by many factors involved in the radiation response. Therefore, the single assay, such as γ-H2AX and G2 chromosomal aberrations may not detect the radiosensitivities in tumor cell lines. On the other hand, the adhesion molecules might be possible to detect the differences in radiosensitivity as a common signature regarding a population of heterogeneous tumors.

Future directions

Further studies will seek to understand the biological and clinical significance of telomere fusions in canine cancer. Molecular studies of canine cancer tissue, canine OSA and other tumors, will be necessary to determine whether telomere fusions frequently occur *in vivo*. In human studies, telomere fusions have been confirmed in several cancers using PCR based methods (Tanaka et al., 2012). However, the PCR based methods are not available for dogs because of the absence of the sequence information at the ends of canine chromosome that the primers are based on. The detection of telomere fusions in canine tissue is likely to become available with future improvements in sequence techniques at repetitive DNA regions in dogs.

The relationship between telomere fusions and telomerase are sparse in our study because all of the canine OSA cell lines used were telomerase positive. Human studies have shown that the

frequency of telomere fusions was telomerase activity independent (Tanaka et al., 2014). Since a previous study described 27% of canine OSA samples presenting as telomerase negative (Kow et al., 2008), further exploration regarding telomere fusion should be done with telomerase negative canine OSA cells. Furthermore, studies that measure telomerase activity level and telomere length over passage culture in telomerase positive and negative canine OSA may provide further understanding of telomere dysfunction in canine OSA cells. Telomere fusions might be a significant diagnostic marker or potential treatment target proceeding further research for canine tumors.

In our investigations of radiosensitivity signatures in canine cancer, the adhesion related molecular genes were based on the microarray analysis. Their significance as potential markers should to be confirmed by mRNA expressions using real time RT-PCR, compering DNA sequences, and protein expression. Moreover, silencing each gene with specific siRNA and investigating the effect on radiation survival in tumor cells will show the role of the gene in radiosensitivity in canine cancer. A panel showing the similar plating efficiency between radiosensitive and radioresistant groups could reveal whether the plating efficiency is a more prominent feature in dogs. Potentially, a gene expression model could be developed from selected genes to predict intrinsic tumor radiosensitivity and evaluate the model to predict treatment response in canine patients.

REFERENCES

ALBERTSON, D. G., COLLINS, C., MCCORMICK, F. & GRAY, J. W. 2003. Chromosome aberrations in solid tumors. *Nat Genet,* 34**,** 369-76.

BAILEY, S. M. & MURNANE, J. P. 2006. Telomeres, chromosome instability and cancer. *Nucleic Acids Res,* 34**,** 2408-17.

BAO, S., WU, Q., MCLENDON, R. E., HAO, Y., SHI, Q., HJELMELAND, A. B., DEWHIRST, M. W., BIGNER, D. D. & RICH, J. N. 2006. Glioma stem cells promote radioresistance by preferential activation of the DNA damage response. *Nature,* 444, 756-60.

BEGG, A. C. 2009. Predicting response to radiotherapy: evolutions and revolutions. *Int J Radiat Biol,* 85**,** 825-36.

GESHI, M., SAKAGUCHI, M., YONAI, M., NAGAI, T., SUZUKI, O. & HANADA, H. 1996. Effects of the 7 21 Robertsonian translocation on fertilization rates and preimplantation development of bovine oocytes in vitro. *Theriogenology,* 46**,** 893-7.

GOTO, Y., NODA, Y., MORI, T. & NAKANO, M. 1993. Increased generation of reactive oxygene species in embryos cultured in vitro. *Free Radic Biol Med,* 15, 69-75.

HALL, J. S., IYPE, R., SENRA, J., TAYLOR, J., ARMENOULT, L., OGUEJIOFOR, K., LI, Y., STRATFORD, I., STERN, P. L., O'CONNOR, M. J., MILLER, C. J. & WEST, C. M. 2014. Investigation of radiosensitivity gene signatures in cancer cell lines. *PLoS One,* 9**,** e86329.

HEMANN, M. T., STRONG, M. A., HAO, L. Y. & GREIDER, C. W. 2001. The shortest telomere, not average telomere length, is critical for cell viability and chromosome stability. *Cell,* 1007, 67-77.

KIM, H. S., KIM, S. C., KIM, S. J., PARK, C. H., JEUNG, H. C., KIM, Y. B., AHN, J. B., CHUNG, H. C. & RHA, S. Y. 2012. Identification of a radiosensitivity signature using integrative metaanalysis of published microarray data for NCI-60 cancer cells. *BMC Genomics,* 13**,** 348.

KOW, K., THAMM, D. H., TERRY, J., GRUNERUD, K., BAILEY, S. M., WITHROW, S. J. & LANA, S. E. 2008. Impact of telomerase status on canine osteosarcoma patients. *J Vet Intern Med,* 22**,** 1366-72.

LIN, T. T., LETSOLO, B. T., JONES, R. E., ROWSON, J., PRATT, G., HEWAMANA, S., FEGAN, C., PEPPER, C. & BAIRD, D. M. 2010. Telomere dysfunction and fusion during the progression of chronic lymphocytic leukemia: evidence for a telomere crisis. *Blood,* 116**,** 1899-907.

MAHRHOFER, H., BURGER, S., OPPITZ, U., FLENTJE, M. & DJUZENOVA, C. S. 2006. Radiation induced DNA damage and damage repair in human tumor and fibroblast cell

lines assessed by histone H2AX phosphorylation. *Int J Radiat Oncol Biol Phys,* 64**,** 573-80.

MAZOUZI, A., VELIMEZI, G. & LOIZOU, J. I. 2014. DNA replication stress: causes, resolution and disease. *Exp Cell Res,* 329**,** 85-93.

NACHMAN, M. W. & SEARLE, J. B. 1995. Why is the house mouse karyotype so variable? *Trends Ecol Evol,* 10**,** 397-402.

PERNER, S., BRUDERLEIN, S., HASEL, C., WAIBEL, I., HOLDENRIED, A., CILOGLU, N., CHOPURIAN, H., NIELSEN, K. V., PLESCH, A., HOGEL, J. & MOLLER, P. 2003. Quantifying telomere lengths of human individual chromosome arms by centromere-calibrated fluorescence in situ hybrization and degital imaging. *Am J Pathol,* 163, 1751-6.

REIMANN, N., NOLTE, I., BARTNITZKE, S. & BULLERDIEK, J. 1999. Re: Sit, DNA, sit: cancer genetics going to the dogs. *J Natl Cancer Inst,* 91**,** 1688-9.

SANDFORT, V., KOCH, U. & CORDES, N. 2007. Cell adhesion-mediated radioresistance revisited. *Int J Radiat Biol,* 83**,** 727-32.

SCHOENHALS, M., KASSAMBARA, A., DE VOS, J., HOSE, D., MOREAUX, J. & KLEIN, B. 2009. Embryonic stem cell markers expression in cancers. *Biochem Biophys Res Commun,* 383, 157-62.

SCHWARTZ, J. L. 1998. Alterations in chromosome structure and variations in the inherent radiation sensitivity of human cells. *Radiat Res,* 149**,** 319-24.

TANAKA, H., ABE, S., HUDA, N., TU, L., BEAM, M. J., GRIMES, B. & GILLEY, D. 2012. Telomere fusions in early human breast carcinoma. *Proc Natl Acad Sci U S A,* 109**,** 14098-103.

TANAKA, H., BEAM, M. J. & CARUANA, K. 2014. The presence of telomere fusion in sporadic colon cancer independently of disease stage, TP53/KRAS mutation status, mean telomere length, and telomerase activity. *Neoplasia,* 16**,** 814-23

VAN'T VEER, L. J. & BERNARDS, R. 2008. Enabling personalized cancer medicine through analysis of gene-expression patterns. *Nature,* 452, 564-70.

VON ZGLINICKI, T. 2002. Oxidative stress shortens telomeres. *Trends Biochem Sci,* 27**,** 339-44.

APPENDIX

Supplementary Table 1: Down regulated genes in radiosensitive cells of the ACC panel.

Gene symbol	Log ratio	Gene name
EPCAM	-5.84	epithelial cell adhesion molecule
SPINK5	-5.18	serine peptidase inhibitor, Kazal type 5
F3	-4.72	coagulation factor III (thromboplastin, tissue factor)
NPNT	-4.63	nephronectin
EDN1	-4.36	endothelin 1
ANK3	-4.35	ankyrin 3, node of Ranvier (ankyrin G)
TCEAL8	-4.10	transcription elongation factor A (SII)-like 8
MAL2	-4.02	mal, T-cell differentiation protein 2
GSTT1	-4.00	glutathione S-transferase theta 1
MAP7	-4.00	microtubule-associated protein 7
SAA1	-3.94	serum amyloid A1
PTGES	-4.10	prostaglandin E synthase
NIPAL1	-3.87	NIPA-like domain containing 1
CDS1	-3.78	CDP-diacylglycerol synthase (phosphatidate cytidylyltransferase) 1
BEX4	-3.65	brain expressed, X-linked 4
AGRN	-3.65	agrin
C1S	-3.62	complement component 1, s subcomponent
MOB3B	-3.57	MOB3B kinase activator 3B
PCBD1	-3.52	pterin-4 alpha-carbinolamine dehydratase/dimerization cofactor of hepatocyte nuclear factor 1 alpha
MYO5B	-3.47	myosin VB
IRX5	-3.33	iroquois homeobox 5
GPRC5C	-3.26	G protein-coupled receptor, family C, group 5, member C
ITGB6	-3.21	integrin, beta 6
ELOVL7	-3.21	ELOVL family member 7, elongation of long chain fatty acids (yeast)
MT1H	-3.12	metallothionein 1H
FCGRT	-2.98	Fc fragment of IgG, receptor, transporter, alpha
UPF3B	-2.94	UPF3 regulator of nonsense transcripts homolog B (yeast)
NXN	-2.93	nucleoredoxin
ESRP1	-2.93	epithelial splicing regulatory protein 1
THBS3	-2.83	thrombospondin 3
TSPAN13	-2.82	tetraspanin 13
RHPN2	-2.76	rhophilin, Rho GTPase binding protein 2
CCL20	-2.72	chemokine (C-C motif) ligand 20
LMO7	-2.64	LIM domain 7
CXADR	-2.59	coxsackie virus and adenovirus receptor pseudogene 2
FGFBP1	-2.58	fibroblast growth factor binding protein 1
Ccnjl	-2.55	cyclin J-like
DGAT2	-2.54	diacylglycerol O-acyltransferase homolog 2 (mouse)
CYBRD1	-2.52	cytochrome b reductase 1

KRT15	-2.51	keratin 15
DDO	-2.50	D-aspartate oxidase
SLC39A8	-2.49	solute carrier family 39 (zinc transporter), member 8
SNX7	-2.48	sorting nexin 7
PI3	-2.47	peptidase inhibitor 3, skin-derived
Spink6	-2.46	serine peptidase inhibitor, Kazal type 6
RHBDL2	-2.44	rhomboid, veinlet-like 2 (Drosophila)
DNAJC22	-2.35	DnaJ (Hsp40) homolog, subfamily C, member 22
FBLN5	-2.31	fibulin 5
EMC9	-2.29	EM membrane protein complex subunit 9
STAP2	-2.28	signal transducing adaptor family member 2
SELENBP1	-2.24	selenium binding protein 1
GRHL1	-2.24	grainyhead-like 1 (Drosophila)
GRHL3	-2.33	grainyhead-like 3 (Drosophila)
Anxa9	-2.23	annexin A9
WASL	-2.21	Wiskott-Aldrich syndrome-like
CASK	-2.19	calcium/calmodulin-dependent serine protein kinase (MAGUK family)
ARMCX5	-2.18	armadillo repeat containing, X-linked 5
SGMS2	-2.17	sphingomyelin synthase 2
CTPS2	-2.17	CTP synthase II
TMEM56	-2.16	transmembrane protein 56
ARID5B	-2.09	AT rich interactive domain 5B (MRF1-like)
GNMT	-2.09	glycine N-methyltransferase
TUBA4A	-2.09	tubulin, alpha 4a
EFNA1	-2.08	ephrin-A1
GDPD1	-2.04	glycerophosphodiester phosphodiesterase domain containing 1
SLC6A8	-2.03	solute carrier family 6 (neurotransmitter transporter, creatine), member 8
AKAP9	-2.02	A kinase (PRKA) anchor protein (yotiao) 9
CYB561	-2.00	cytochrome b-561
GADD45B	-2.00	growth arrest and DNA-damage-inducible, beta
SEC14L2	-1.98	SEC14-like 2 (S. cerevisiae)
TDRD7	-1.97	tudor domain containing 7
MAP2	-1.97	microtubule-associated protein 2
CCDC113	-1.96	coiled-coil domain containing 113
TMEM54	-1.95	transmembrane protein 54
SMTNL2	-1.95	smoothelin-like 2
TLCD1	-1.92	TLC domain containing 1
ASB9	-1.92	ankyrin repeat and SOCS box-containing 9
B4GALNT 4	-1.89	beta-1,4-N-acetyl-galactosaminyl transferase 4
Irx3	-1.89	iroquois homeobox 3
LY6E	-1.85	lymphocyte antigen 6 complex, locus E
GRB7	-1.85	growth factor receptor-bound protein 7
IRX2	-1.84	iroquois homeobox 2

NR2F6	-1.83	nuclear receptor subfamily 2, group F, member 6
EPB41L1	-1.82	erythrocyte membrane protein band 4.1-like 1
SPAG1	-1.79	sperm associated antigen 1
EPB41L4B	-1.76	erythrocyte membrane protein band 4.1 like 4B
TTL	-1.76	tubulin tyrosine ligase
SPG21	-1.76	spastic paraplegia 21 (autosomal recessive, Mast syndrome)
SSX2IP	-1.75	synovial sarcoma, X breakpoint 2 interacting protein
IFIH1	-1.73	interferon induced with helicase C domain 1
WDR60	-1.72	WD repeat domain 60
PPARA	-1.71	peroxisome proliferator-activated receptor alpha
ZNF182	-1.70	zinc finger protein 182
LIMK2	-1.69	LIM domain kinase 2
SERINC5	-1.69	serine incorporator 5
HSD17B6	-1.68	hydroxysteroid (17-beta) dehydrogenase 6 homolog (mouse)
MARVELD 2	-1.68	MARVEL domain containing 2
KLHL24	-1.65	kelch-like 24 (Drosophila)
C1R	-1.65	complement component 1, r subcomponent
SUOX	-1.64	sulfite oxidase
MNS1	-1.64	meiosis-specific nuclear structural 1
VANGL1	-1.64	vang-like 1 (van gogh, Drosophila)
ITGA7	-1.62	integrin, alpha 7
PANK1	-1.62	pantothenate kinase 1
DNPEP	-1.61	aspartyl aminopeptidase
CYP27A1	-1.60	cytochrome P450, family 27, subfamily A, polypeptide 1
TMEM67	-1.59	transmembrane protein 67
TAX1BP1	-1.59	Tax1 (human T-cell leukemia virus type I) binding protein 1
IFI6	-1.56	interferon, alpha-inducible protein 6
SLK	-1.54	STE20-like kinase (yeast)
NDUFA4L2	-1.53	NADH dehydrogenase (ubiquinone)1α sub あ complex,4-like 2
TMEM25	-1.52	transmembrane protein 25
KIAA1407	-1.52	protein-coding gene
VSIG10	-1.51	Hypothetical protein FLJ20674
Nt5c2	-1.51	5'-nucleotidase, cytosolic II
PSTPIP2	-1.50	proline-serine-threonine phosphatase interacting protein 2
SSH3	-1.49	slingshot homolog 3 (Drosophila)
TMEM138	-1.48	transmembrane protein 138
FAM108C1	-1.48	family with sequence similarity 108, member C1
RBPMS	-1.48	RNA binding protein with multiple splicing
LRRC34	-1.48	leucine rich repeat containing 34
KBTBD6	-1.47	kelch repeat and BTB (POZ) domain containing 6
DHX29	-1.47	DEAH (Asp-Glu-Ala-His) box polypeptide 29
Tctn1	-1.47	tectonic family member 1
MFN1	-1.47	mitofusin 1
TM2D2	-1.46	TM2 domain containing 2
MORN2	-1.46	MORN repeat containing 2

HDAC11	-1.45	histone deacetylase 11
HDAC8	-1.45	histone deacetylase 8
WASF1	-1.44	WAS protein family, member 1
TMED4	-1.44	transmembrane emp24 protein transport domain containing 4
CSTF3	-1.42	cleavage stimulation factor, 3' pre-RNA, subunit 3, 77kDa
KLHL11	-1.42	kelch-like 11 (Drosophila)
BSPRY	-1.42	B-box and SPRY domain containing
PRR15L	-1.40	ATPase family, AAA domain containing 4
IFT140	-1.39	intraflagellar transport 140 homolog (Chlamydomonas)
TCTEX1D2	-1.38	Tctex1 domain containing 2
ARMC9	-1.37	armadillo repeat containing 9
PTPRF	-1.37	protein tyrosine phosphatase, receptor type, F
Sh3bgrl2	-1.36	SH3 domain binding glutamic acid-rich protein like 2
RBKS	-1.36	ribokinase
MTERF	-1.35	mitochondrial transcription termination factor
RBM41	-1.35	RNA binding motif protein 41
SHFM1	-1.35	split hand/foot malformation (ectrodactyly) type 1
IFT74	-1.35	intraflagellar transport 74 homolog (Chlamydomonas)
PSTK	-1.33	phosphoseryl-tRNA kinase
MXI1	-1.33	MAX interactor 1
Slc35f2	-1.32	solute carrier family 35, member F2
TM2D1	-1.31	TM2 domain containing 1
NDUFB5	-1.31	NADH dehydrogenase (ubiquinone) 1ß subcomplex 5
ALDH5A1	-1.30	aldehyde dehydrogenase 5 family, member A1
IL6ST	-1.29	interleukin 6 signal transducer (oncostatin M receptor)
NFE2L3	-1.29	nuclear factor (erythroid-derived 2)-like 3
CAMSAP3	-1.29	glycogen synthase kinase 3 ß
USP20	-1.28	ubiquitin specific peptidase 20
TMED5	-1.28	transmembrane emp24 protein transport domain containing 5
CTNNBL1	-1.26	catenin, beta like 1
TTC14	-1.25	tetratricopeptide repeat domain 14
LETM2	-1.25	leucine zipper-EF-hand containing transmembrane protein 2
SLC25A14	-1.24	solute carrier family 25, member 14
OPA1	-1.24	optic atrophy 1 (autosomal dominant)
SFXN1	-1.24	sideroflexin 1
FGD6	-1.24	FYVE, RhoGEF and PH domain containing 6
IKBKB	-1.24	inhibitor of κ light polypeptide gene enhancer in B-cells, kinase beta
KIF1C	-1.23	kinesin family member 1C
FBXO21	-1.22	F-box protein 21
KLHL7	-1.22	kelch-like 7 (Drosophila)
HIBCH	-1.21	3-hydroxyisobutyryl-Coenzyme A hydrolase
ITSN1	-1.21	intersectin 1 (SH3 domain protein)
SORT1	-1.20	sortilin 1
HDHD3	-1.20	haloacid dehalogenase-like hydrolase domain containing 3
Ccdc151	-1.20	coiled-coil domain containing 151

RP2	-1.20	retinitis pigmentosa 2 (X-linked recessive)
OPTN	-1.19	optineurin
CTH	-1.18	cystathionase (cystathionine gamma-lyase)
TM9SF3	-1.18	transmembrane 9 superfamily member 3
DYNC2H1	-1.18	dynein, cytoplasmic 2, heavy chain 1
WDR34	-1.18	WD repeat domain 34
PCGF6	-1.16	polycomb group ring finger 6
DFFB	-1.17	DNA fragmentation factor, 40kDa, beta polypeptide
AMDHD2	-1.16	amidohydrolase domain containing 2
TBC1D8B	-1.16	TBC1 domain family, member 8B (with GRAM domain)
NDUFS1	-1.15	NADH dehydrogenase (ubiquinone) Fe-S protein 1, 75kDa
YIPF1	-1.13	Yip1 domain family, member 1
SLC46A2	-1.13	solute carrier family 46, member 2
SLC35B3	-1.13	solute carrier family 35, member B3
SNX25	-1.12	sorting nexin 25
ECHS1	-1.11	enoyl Coenzyme A hydratase, short chain, 1, mitochondrial
CHFR	-1.10	checkpoint with forkhead and ring finger domains
ANKRD10	-1.09	ankyrin repeat domain 10
CHRNB1	-1.09	cholinergic receptor, nicotinic, beta 1 (muscle)
DBT	-1.09	dihydrolipoamide branched chain transacylase E2
CETN2	-1.08	centrin, EF-hand protein, 2
RAB11FIP2	-1.07	RAB11 family interacting protein 2 (class I)
PTPLB	-1.07	protein tyrosine phosphatase-like (proline instead of catalytic arginine), member b
WDR31	-1.06	WD repeat domain 31
AZI1	-1.05	5-azacytidine induced 1
FARS2	-1.04	phenylalanyl-tRNA synthetase 2, mitochondrial
Nudt7	-1.04	nudix (nucleoside diphosphate linked moiety X)-type motif 7
ADAM9	-1.04	ADAM metallopeptidase domain 9 (meltrin gamma)
NAT14	-1.02	N-acetyltransferase 14 (GCN5-related, putative)
PDSS2	-1.02	prenyl (decaprenyl) diphosphate synthase, subunit 2
ZFYVE21	-1.02	zinc finger, FYVE domain containing 21
RB1CC1	-1.01	RB1-inducible coiled-coil 1
KDM5B	-1.00	lysine (K)-specific demethylase 5B

Supplementary Table 2: Up regulated genes in radiosensitive cells of the ACC panel.

Gene symbol	Log ratio	Gene name
CELF2	4.74	CUG triplet repeat, RNA binding protein 2
PKIB	4.27	protein kinase (cAMP-dependent, catalytic) inhibitor beta
RGS1	4.15	regulator of G-protein signaling 1
SASH1	4.04	SAM and SH3 domain containing 1
GUCY1B3	3.83	guanylate cyclase 1, soluble, beta 3
MEF2C	3.50	myocyte enhancer factor 2C
ZEB2	3.30	zinc finger E-box binding homeobox 2
GPC3	3.07	glypican 3
LRAT	3.01	lecithin retinol acyltransferase
NSD1	3.00	nuclear receptor binding SET domain protein 1
SPP2	2.82	secreted phosphoprotein 2, 24kDa
EMP3	2.77	epithelial membrane protein 3
IQGAP2	2.73	IQ motif containing GTPase activating protein 2
DOCK10	2.72	dedicator of cytokinesis 10
NCF2	2.67	neutrophil cytosolic factor 2
EYA2	2.62	eyes absent homolog 2 (Drosophila)
SYNE3	2.50	spectrin repeat containing, nuclear envelope family member 3
MILR1	2.45	mast cell immunoglobulin-like receptor 1
WDFY4	2.37	WDFY family member 4
SMOC2	2.31	SPARC related modular calcium binding 2
DENND5B	2.14	DENN/MADD domain containing 5B
JAZF1	1.98	JAZF zinc finger 1
DYNC1I1	1.97	dynein, cytoplasmic 1, intermediate chain 1
COTL1	1.90	coactosin-like 1 (Dictyostelium)
NT5E	1.87	5'-nucleotidase, ecto (CD73)
MYO1E	1.85	myosin IE
CD83	1.85	CD83 molecule
FMNL3	1.68	formin-like 3
CAP1	1.63	CAP, adenylate cyclase-associated protein 1 (yeast)
AP1S2	1.61	adaptor-related protein complex 1, sigma 2 subunit pseudogene
CDCA4	1.60	cell division cycle associated 4
BNIP2	1.58	BCL2/adenovirus E1B 19kDa interacting protein 2
EIF3B	1.57	eukaryotic translation initiation factor3, subunit B
CRIP1	1.54	cysteine-rich protein 1 (intestinal)
PPP2R5D	1.54	protein phosphatase 2, regulatory subunit B', delta isoform
NOMO2	1.52	NODAL modulator 2
CITED2	1.52	Cbp/p300-interacting transactivator, with Glu/Asp-rich carboxy-terminal domain2
SLC7A1	1.50	solute carrier family 7 (cationic amino acid transporter, y+ system), member 1
RCC2	1.45	regulator of chromosome condensation 2
TXNDC16	1.44	thioredoxin domain containing 16

ILK	1.43	integrin-linked kinase
IQGAP1	1.42	IQ motif containing GTPase activating protein 1
WHSC1	1.41	Wolf-Hirschhorn syndrome candidate 1
ERGIC1	1.41	endoplasmic reticulum-golgi intermediate compartment (ERGIC) 1
BIN1	1.40	bridging integrator 1
CSK	1.39	c-src tyrosine kinase
PPP3CC	1.39	protein phosphatase 3 (formerly 2B), catalytic subunit, gamma isoform
TBC1D1	1.36	TBC1 (tre-2/USP6, BUB2, cdc16) domain family, member 1
ZNF384	1.34	zinc finger protein 384
MAPRE2	1.31	microtubule-associated protein, RP/EB family, member 2
STK10	1.31	serine/threonine kinase 10
EMC1	1.31	EM membrane protein complex subunit 1
HNRNPUL 1	1.30	heterogeneous nuclear ribonucleoprotein U-like 1
ZG16B	1.30	zymogen granule protein 16 homolog B (rat)
USP24	1.29	ubiquitin specific peptidase 24
WIPF1	1.29	WAS/WASL interacting protein family, member 1
TMEM41B	1.29	transmembrane protein 41B
TATDN2	1.28	TatD DNase domain containing 2
STX7	1.27	syntaxin 7
ACTB	1.26	actin, beta
MORC1	1.26	MORC family CW-type zinc finger 1
Tiparp	1.25	TCDD-inducible poly(ADP-ribose) polymerase
RPL22L1	1.24	ribosomal protein L22-like 1
SH3KBP1	1.24	SH3-domain kinase binding protein 1
AP1M1	1.23	adaptor-related protein complex 1, mu 1 subunit
TLE4	1.2	transducin-like enhancer of split 4 (E(sp1) homolog, Drosophila)
EP300	1.22	E1A binding protein p300
LANCL1	1.22	LanC lantibiotic synthetase component C-like 1 (bacterial)
ARAP1	1.22	ArfGAP with RhoGAP domain, ankyrin repeat and PH domain 1
SLC41A2	1.22	solute carrier family 41, member 2
N4BP2L1	1.22	NEDD4 binding protein 2-like 1
OAF	1.22	OAF homolog (Drosophila)
STMN1	1.21	stathmin 1
CBFB	1.21	core-binding factor, beta subunit
MAP7D3	1.21	MAP7 domain containing 3
MGAT1	1.20	mannosyl (alpha-1,3-)-glycoprotein beta-1,2-N-acetylglucosaminyltransferase
NCSTN	1.20	nicastrin
CDCA8	1.18	cell division cycle associated 8
EXOSC10	1.16	exosome component 10
RSPH9	1.16	radial spoke head 9 homolog (Chlamydomonas)
STARD7	1.14	StAR-related lipid transfer (START) domain containing 7
WDR1	1.13	WD repeat domain 1
GATAD2A	1.13	GATA zinc finger domain containing 2A

RPS6KA5	1.12	ribosomal protein S6 kinase, 90kDa, polypeptide 5
ASAP1	1.12	ArfGAP with SH3 domain, ankyrin repeat and PH domain 1
EMC10	1.11	ER membrane protein complex subunit 10
NCAPH2	1.11	non-SMC condensin II complex, subunit H2
TP53I3	1.11	tumor protein p53 inducible protein 3
COPS7B	1.11	COP9 constitutive photomorphogenic homolog subunit 7B (Arabidopsis)
MOB3A	1.10	MOB kinase activator 3A
MCM5	1.10	minichromosome maintenance complex component 5
Ppp2r5c	1.10	protein phosphatase 2, regulatory subunit B', gamma isoform
ACTR2	1.10	ARP2 actin-related protein 2 homolog (yeast)
UTP11L	1.10	UTP11-like, U3 small nucleolar ribonucleoprotein, (yeast)
SULF2	1.10	sulfatase 2
IRAK3	1.09	interleukin-1 receptor-associated kinase 3
PARP8	1.09	poly (ADP-ribose) polymerase family, member 8
Ncapg	1.09	non-SMC condensin I complex, subunit G
TMEM2	1.09	transmembrane protein 25
TMPO	1.08	thymopoietin
STK24	1.08	serine/threonine kinase 24 (STE20 homolog, yeast)
LARP1	1.07	La ribonucleoprotein domain family, member 1
UBL3	1.06	ubiquitin-like 3
Mnda	1.05	myeloid cell nuclear differentiation antigen
RNF114	1.05	ring finger protein 114
ZNF362	1.03	zinc finger protein 362
SPRYD3	1.03	SPRY domain containing 3
NID2	1.02	nidogen 2 (osteonidogen)
Rcc1	1.02	regulator of chromosome condensation 1; SNHG3-RCC1 readthrough transcript

LIST OF ABBREVIATIONS

(Listed in alphabetical order)

ATM	Ataxia Telangiectasia Mutated
ALT	Alternative lengthening of Telomeres
BACs	Bacterial Artificial Chromosomes
bp	base pairs
BRCA	Breast Cancer Susceptibility Gene
BrdU	Bromodeoxyuridine
CO-FISH	Chromosome Orientation FISH
CGH	Comparative Genomic Hybridization
CLL	Chronic Lymphocytic Leukemia
DAPI	4,6-diamidino-2-phenylindole
DNA	Deoxyribose Nucleic Acid
DNA-PK	DNA Dependent Protein Kinase
DNA-PKcs	DNA Dependent Protein Kinase Catalytic Subunit
DSB	Double Strand Break

MeV	Mega electron Volt
FA	Fanconi Anemia
FBS	Fetal Bovine Serum
FISH	Fluorescence in situ hybridization
Gy	Gray
HSA	Hemangiosarcoma
HR	Homologous Recombination
IR	Ionizing Radiation
ICL	Interstrand DNA Crosslink
IdU	Iododeoxyuridine
ITS	Interstitial Telomeric Sequence
LET	Linear Energy Transfer
Mb	Megabase
mFISH	Multicolor FISH
NBS	Nijmegen Breakage Syndrome
NHEJ	Non-homologous End-joining
OSA	Osteosarcoma

PE	Plating Efficiency
PNA	Peptide Nucleic Acid
RBE	Relative Biological Effect
RPA	Replication Protein A
RT-PCR	Reverse Transcription Polymerase Chain Reaction
SF2	Survival Fraction at 2 Gy
SKY	Spectral Karyotyping
SSB	Single Strand Break
SSC	Saline-Sodium-Citrate
SSB	Single Strand Break
TIFs	Telomere-dysfunction Induced Focus
TRAP	Telomeric Repeat Amplification Protocol